Geologic Excursions in Northern California
San Francisco to the Sierra Nevada

CALIFORNIA
DEPARTMENT
OF CONSERVATION
Division of Mines and Geology

Special Publication 109

DIVISION OF MINES AND GEOLOGY
JAMES F. DAVIS
STATE GEOLOGIST

Field Trip Guidebook for the Joint Meeting of the Geological Society of America Cordilleran Section and the Seismological Society of America, San Francisco, California, March 1991. This guidebook is available for purchase from the Division of Mines and Geology.

Cover Photograph: View looking northward across the Marin Headlands from the south tower of the Golden Gate Bridge.
Photograph by Doris Sloan, UCB.

Special Publication 109

GEOLOGIC EXCURSIONS IN NORTHERN CALIFORNIA: San Francisco to the Sierra Nevada

Editors

DORIS SLOAN
University of California, Berkeley

and

DAVID L. WAGNER
Division of Mines and Geology

California Department of Conservation
DIVISION OF MINES AND GEOLOGY
1416 Ninth Street, Room 1341
Sacramento, CA 95814

GEOLOGIC EXCURSIONS IN NORTHERN CALIFORNIA

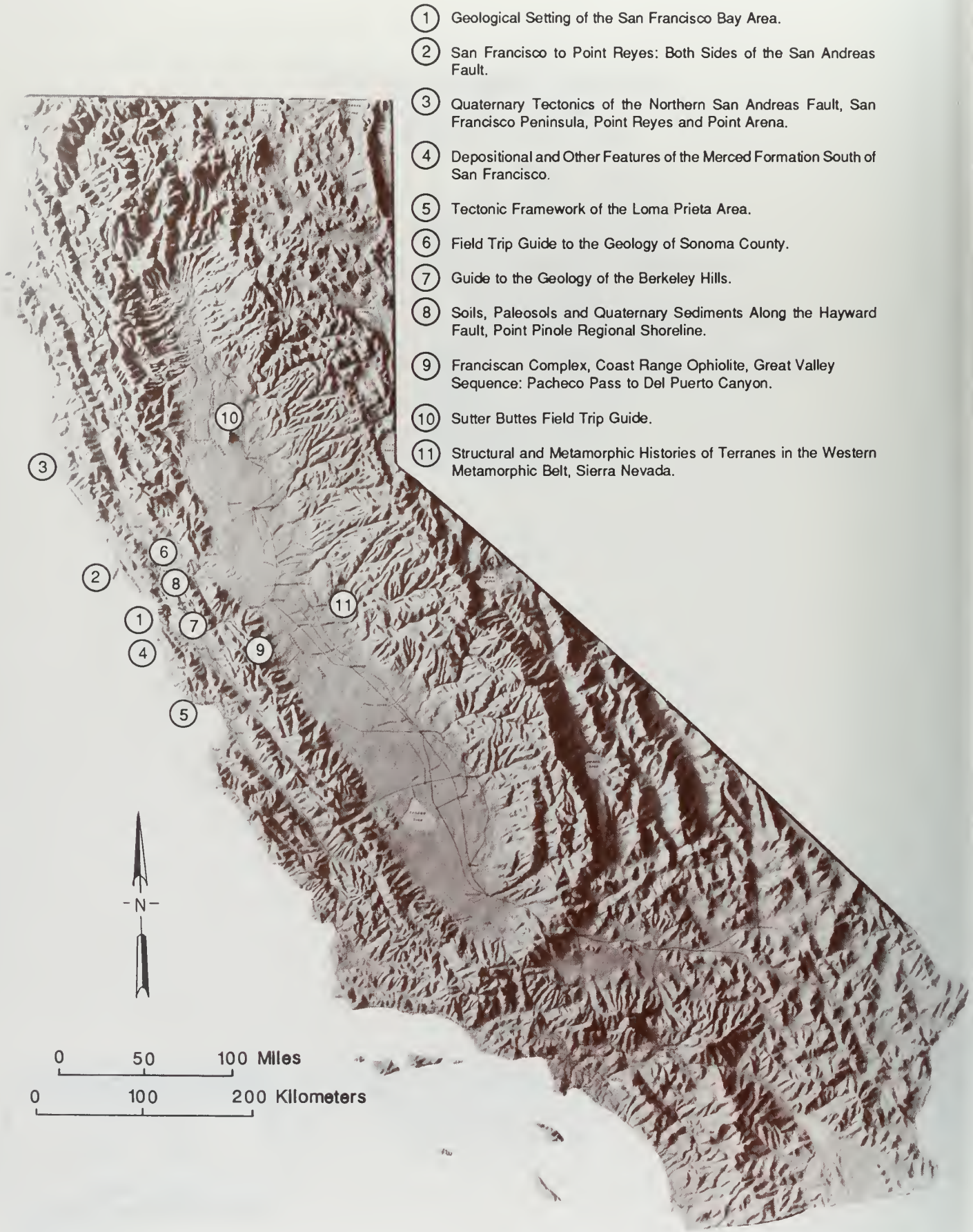

Table of Contents

Preface

Special Publication 109 contains guides and explanatory text for 11 field trips conducted before and after the 87th Annual Meeting of the Cordilleran Section of the Geological Society of America (GSA) and the Seismological Society of America, held in San Francisco, March 25-27, 1991. The meeting was hosted by the Department of Geosciences, San Francisco State University.

In the past, meetings of the Geological Society of America have provided impetus for the Division of Mines and Geology to release publications describing the geology of California. The Division published Bulletin 170, Geology of Southern California, in conjunction with the 1954 GSA meeting held in Los Angeles. Bulletin 190, Geology of Northern California, was published in conjunction with the 1966 GSA meeting held in San Francisco. Bulletin 190 contained guides for seven field trips in the Bay area, the northern Coast Ranges, the Sacramento Valley and the Sierra Nevada. Now, 25 years later, the guides in this volume cover much of the same ground, but the geology is interpreted from a profoundly different perspective. Plate tectonic theory, developed in the late 1960s and early 1970s, radically altered interpretions of the geology and tectonics of California. It is interesting, however, that the San Andreas fault is the subject of two field trips in this volume as it was in Bulletin 190.

This volume was planned by the Technical Committee of the 87th Annual Meeting and organized by a subcommittee consisting of M.C. Blake, Doris Sloan, and D.L. Wagner. Twenty-eight authors, representing government (12), universities (12), and industry (4) contributed to Special Publication 109. These authors met tight deadlines and endured sometimes painful cuts in their manuscripts to fit within the available space. For this, and the graceful acceptance of editorial changes, the editors are grateful.

The editors would like to extend special thanks to many groups and individuals who made this publication possible. Much of the editorial work was done using facilities at the University of California, Berkeley. Special thanks go to Don Bain and Anneke Vonk of the Geography Computing Center and to Yvonne Norpchen and Jere Lipps of the Museum of Paleontology. We appreciate the cooperation and fine work of Charlie Scribner and the people at University of California Printing Services. Thanks also go to Joseph Ziony, James Davis, William Guerard, Robert Streitz and Steve Newton-Reed of the Division of Mines and Geology (DMG). The DMG Publications unit performed superbly under great pressure. We are grateful to Carol Allen, Ed Foster, Louise Huckaby, Debbie Maldonado, Ross Martin, Cynthia Pridmore, Joy Sullivan, Lena Tabilio, Jeff Tambert, Peggy Walker, and Jim Williams.

DORIS SLOAN and DAVID L. WAGNER, Editors

Introduction to the Tectonic History of Northern California

M.C. Blake, Jr.

The advent of plate tectonics in the late 1960s had an enormous impact on the interpretation of California geology. The concepts of sea-floor spreading, subduction, forearc basins, arc-related magmatism, and transform faulting were applied to the formerly enigmatic and contradictory relationships of the Franciscan Complex, the Great Valley sequence, the Salinian block, and the Sierra Nevada batholith. Application of plate-tectonic models to northern California made it the type example of an active continental margin. The following simplified tectonic history of this region is excerpted from various sources.

Until recently it was thought that, throughout most of the Jurassic, northern California consisted of one or more active island arcs that lay to the west of the continental margin. Near the close of the Jurassic, during the Nevadan orogeny, these arcs and associated slices of oceanic crust and upper mantle (ophiolite) were accreted to the continent along the steeply-dipping fault zones of the Sierran Foothills. The active margin then jumped westward, trapping a fragment of Middle Jurassic oceanic crust (Coast Range ophiolite). Franciscan rocks consisting of Jurassic oceanic basalt and radiolarian chert plus overlying continent-derived trench sediments (largely graywacke) were then subducted eastward beneath the Coast Range ophiolite and its sedimentary cover (Great Valley sequence) along the Coast Range thrust and related paleosubduction zones. Farther east, deeply subducted oceanic rocks were partially melted and rose to form calc-alkaline volcanoes and underlying granitic batholiths of the central Sierra Nevada. Radiometric dating of Sierran granitic rocks suggested that this process was more or less continuous from about 125 to 80 Ma. The locus of volcanism and plutonism then shifted eastward, implying that there was a flattening of the subduction zone. By Miocene time, the East Pacific Rise had arrived at the subduction zone and strike-slip (transform) faulting of the San Andreas system was initiated. Initially, transform segments were probably offshore, but later the faulting moved inboard and translated a large fragment of the continental margin, the Salinian block, northward, some 195 mi (310 km). Transform faulting and attendant damaging earthquakes continue at the present time.

Although its simplicity is appealing, this history fails to explain many geologic relationships that have been described in recent years. During several of the field trips, the emphasis will be on these conflicting data. In the Sierra Nevada (Trip 11), detailed structural and isotopic studies indicate that development of "Nevadan" cleavage and metamorphism along the Foothills suture zones was taking place at the same time as deposition of the older part of the Great Valley sequence and early high P/T metamorphism of the Franciscan Complex (~146-123 Ma). To the west, in the Diablo Range (Trip 9), we will see evidence that the Coast Range ophiolite was the site of a volcanic arc during the latest Jurassic and that the well-exposed low-angle fault that forms the present boundary between Franciscan metagraywacke and overlying Coast Range ophiolite (Coast Range thrust), is probably a normal fault, formed during uplift of the Franciscan subduction complex. Farther west, in the Santa Cruz Mountains near Loma Prieta (Trip 5), and in Marin County (Trip 2), paleontologic and paleomagnetic data indicate that Franciscan terranes east of the San Andreas fault have been translated northward from near-equatorial latitudes, requiring that large-scale transform faulting took place prior to the development of the San Andreas system. Trip 2 also presents evidence that the Salinian block has been offset about 90 mi (150 km) in the last 10-15 my by the San Gregorio fault. Trip 7, in the

East Bay Hills, suggests that during the last 5 my, there have been both large-scale strike-slip and thrust faulting along the Hayward, Calaveras, and other active faults in the region. Trips 1, 3, 4, 5, and 8 emphasize the Quaternary tectonics of the San Andreas transform system and its role in recent sedimentation. Trips 6 and 10 emphasize Neogene and Quaternary volcanism, thought by some to be related to passage of the triple junction rather than to subduction.

Thus, nearly every manifestation of plate tectonics can be seen in northern California, and the geologic features described in this guidebook provide an excellent introduction to the geologic and tectonic history of the region.

Geological Setting of the San Francisco Bay Area

Raymond Sullivan and Jon S. Galehouse[1]

INTRODUCTION

The Franciscan Complex in the northern Coast Ranges, east of the San Andreas fault, has been divided into the northwest-trending Coastal, Central, and Eastern tectonic belts (Irwin, 1960). Most of the Franciscan rocks in the area of this field trip are part of the Central belt, which as a whole is a tectonic melange with most of the rocks of Late Jurassic to Early Cretaceous age. The melange probably formed within an accretionary wedge at the junction of one or more Pacific oceanic plates (the Kula and/or Farallon plates) with the western North American plate margin. Many of the larger blocks within the Central belt melange have been given separate terrane names. The terranes are mostly gently dipping thrust sheets that trend northwesterly and dip northeasterly.

The Salinian block occurs west of the San Andreas fault and is mainly a mosaic of Cretaceous calc-alkaline plutons and older high-T metamorphic rocks that originated south of their present location. There is some debate about the distance of travel of the Salinian block along the strike-slip systems (Page, 1989). Salinian plutons are similar in age, mineralogy, and chemistry to those along the crest of the Sierra Nevada. They may represent, therefore, a slice from the southern Sierra Nevada that has been transported northerly some 195 mi (315 km) since Eocene time. However, Paleocene turbidites that were deposited on Salinian basement give paleomagnetic evidence of some 1550 mi (2500 km) of northward displacement (Champion and others, 1984).

In general, the Franciscan and Salinian basement complexes are unconformably overlain by various sequences of Cenozoic deposits. These include a thick early Tertiary sequence that accumulated in deep marine basins and a thick late Tertiary sequence of predominantly diatomaceous beds that accumulated in sediment-starved basins.

On this field trip, we will first view a subsidence area along the San Francisco Bay margin. Then we will look at the terrane setting of San Francisco. We will then view Tertiary sections at two stops along the coast south of the City. Lastly, we will focus on the geological hazards along the San Andreas fault on the San Francisco Peninsula and along the Hayward fault in the East Bay (Fig. 1). Details of the geology between stops can be found in Sullivan and Galehouse (1990).

STOP 1 - SOUTH OF MARKET SUBSIDENCE AREA

The effects of subsidence on structures located on the filled ground South of Market is best seen on Shipley and Clara streets between Fifth and Sixth streets. Bedrock contour maps show that a Pleistocene valley at a depth of over 195 ft (60 m) underlies the South of Market area and has been filled with a sequence of Pleistocene and Holocene deposits of fluvial and dune sand and Bay mud (Schlocker, 1974).

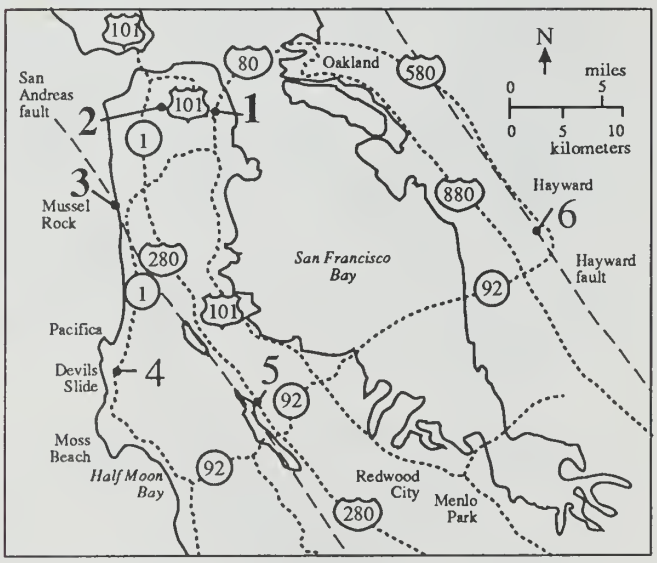

Figure 1. Route map of the trip.

[1]Department of Geosciences, San Francisco State University, San Francisco, CA 94132

Prior to the Gold Rush, the South of Market area was a marshland along the margins of the Bay. Inland from the marsh was a large belt of sand dunes that covered more than half the City. Hills composed of Franciscan bedrock protruded above the dune field. Streams flowed down the east side of these hills and meandered across the marshland before entering the Bay. The main stream in the South of Market area had its source in the highlands of Pacific Heights and Nob Hill. This stream entered the marshland near the Civic Center and flowed into San Francisco Bay in the vicinity of Fourth and Bryant streets (Fig. 2). In order to make these areas suitable for building, Bay mud was covered by artificial fill composed of dune sand, quarry rubble, and garbage. These old unengineered artificial fills are extremely unstable when severely shaken during a strong tremor and often result in differential settlement and lateral spreading of the ground (Youd and Hoose, 1978). Because the water table is very close to the surface, the liquefaction potential is high in the South of Market area.

The 1900 census recorded that the South of Market area was second only to Chinatown in population density. These two areas of the City had the greatest loss of life during the 1906 tremor. The exact number will never be known because the casualties were poorly recorded, but may have totaled more than two thousand. Hansen and Condon (1989) dramatically describe the destruction from the tremor and the fires that followed soon after. Eyewitnesses report that fires broke out in restaurants, laundries, and boarding houses throughout the South of Market area within minutes after the early morning earthquake. The fires quickly spread with no means at hand to halt the inferno. By early afternoon, the South of Market area was engulfed by a single massive fire.

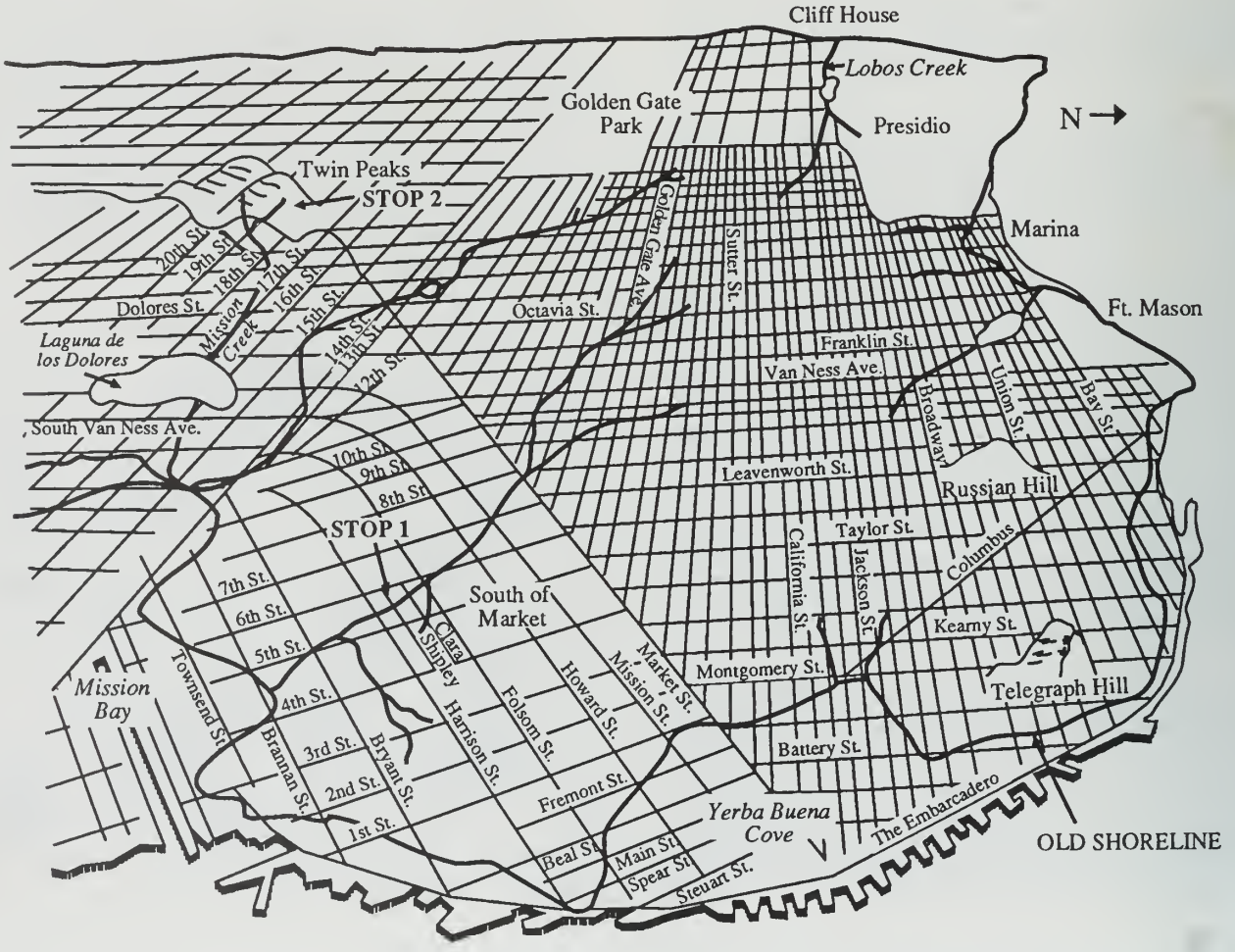

Figure 2. Schematic map showing the approximate location of old shoreline and creeks in San Francisco.

Most of the buildings, therefore, in the South of Market area date back to the reconstruction period following the 1906 tremor. The area is of geologic interest because of the widespread effects of slow settlement of structures built on filled ground (Wahrhaftig, 1966). Because of this continuing subsidence, main roads and utilities have had to be raised periodically in order to maintain them at "official" grade level. Small side alleys were built up at less frequent intervals and often are not level with the main streets but meet at a steep slope as seen at the intersection of Seventh and Natoma streets. As a result, doors and garage entrances are often two to three feet below street level. Some of the buildings have been deformed by differential settling and are no longer upright, but lean toward a neighboring structure.

The South of Market area was once again the site of widespread damage during the Loma Prieta earthquake. Most of the damaged structures were located in the old filled marshland of Mission Bay where the water table is very close to the surface. The greatest damage was found in the area between Fifth and Eighth streets and Mission and Townsend streets. In this area buildings settled as much as a foot following the tremor. In the vicinity of the old creek bed at Shipley and Harrison streets between Fifth and Sixth streets, water flooded some of the basements of the buildings and had to be pumped out. The preliminary Modified Mercalli intensity rating for the South of Market area and the Marina district was IX, whereas the rest of the City was assigned a value of VI or VII (Plafker and Galloway, 1989).

STOP 2 - CORONA HEIGHTS

The second stop in the City is at the Josephine Randall Junior Museum in the Corona Heights district. The museum is accessed off Roosevelt Way at its intersection with Museum Way. Corona Heights provides a spectacular view of the City, San Francisco Bay, and the East Bay Hills.

Much of the western North American plate is an amalgamation of dozens of small tectonostratigraphic terranes that are fault-bounded and characterized by geologic histories that are different from that of their neighbors. Blake and others (1984) differentiated 17 separate terranes in the San Francisco Bay region. The city of San Francisco is comprised of four different terranes (Fig. 3) that are all part of the Central tectonic belt of the Franciscan Complex that was emplaced before the inception of the modern San Andreas fault.

This location on Corona Heights was once the site of a brick works and quarry in Franciscan rocks of the Marin Headlands terrane. In the early morning of 18 April 1906, the residents of this area were rudely awakened by the violent shaking and the sight of the brick works on fire. Many residents thought that a volcano had erupted on Corona Heights. Damage was widespread, particularly in the vicinity of the Mission. The greatest destruction in the district occurred in apartment houses and residences located on the filled land of former Lake Dolores and along old Mission Creek (Fig. 2). The old Mission church survived the tremor and fire, which eventually reached the Mission District on the third day after the quake, when the firestorm suddenly turned southwestward. The Mission fire was eventually stopped in the vicinity of Dolores Street, and many old Victorians can still be observed nestled among the homes below Corona Heights.

The exposures behind the tennis courts below the Junior Museum show highly weathered pillow basalts. Their convex-upward margins indicate that the sequence is right side up. Cherts behind the Junior Museum overlie the pillow basalts, and cherts exposed below along States Street underlie these basalts. These relationships suggest that the basalts represent renewed submarine volcanism in an area of the seafloor where chert (radiolarian ooze) was accumulating. Basalts of the Franciscan Complex are usually slightly metamorphosed and are commonly called "greenstone." Because basalts only comprise about ten percent of the Franciscan (Bailey and others, 1964), most of the oceanic crust that encountered the western North American continent was probably subducted.

The rocks exposed in the quarry adjacent to the Museum are a typical sequence of radiolarian chert within one of the slices of the Marin Headlands terrane. These siliceous rocks owe their red, brown, and green color to the presence of iron. The sequence is usually made up of several hundred thin beds of chert, a few inches in thickness, with shale partings. Radiolarians in the chert

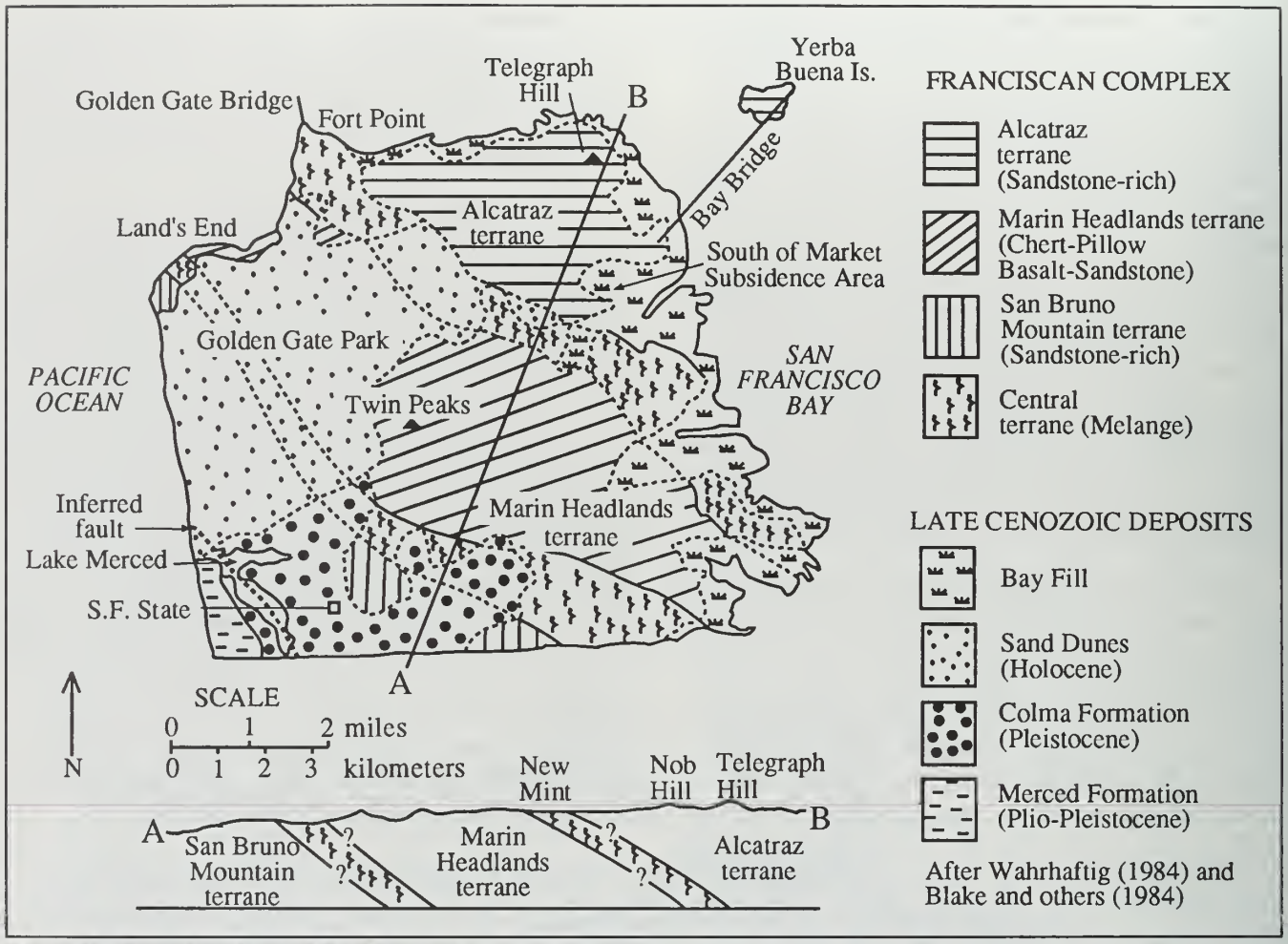

Figure 3. General geology of San Francisco.

can often be seen with a hand lens. The chert displays the small-scale chevron folding which is commonly seen in these units and is probably related to the larger fold structures. Some recumbent folding is present behind the northwest corner of the Museum. Numerous small fractures and faults are also common throughout the chert beds in the quarry face. Although chert is abundant here, it comprises only about one percent of the entire Franciscan Complex (Bailey and others, 1964). Several detailed studies of chert within the Marin Headlands terrane (Blake, 1984) indicate that it is the diagenetic product of radiolarian ooze accumulation over a wide region of the Mesozoic Pacific Ocean. Most of the chert originated south of here and probably moved northward on previously-existing oceanic plates.

STOP 3 - MUSSEL ROCK

Mussel Rock is located in Daly City, about 3 mi (5 km) south of San Francisco. Take Manor Drive exit off Hwy. 1 and follow Palmetto Ave. to Westline Drive. On a clear day the Mussel Rock area presents a spectacular view of the northern California coastline. The main scarp of the San Andreas fault forms the southwest-facing slope about 2000 ft (600 m) north of Mussel Rock.

The view to the north is the Marin Peninsula made up of Franciscan rocks on the edge of the North American plate. The Marin Peninsula is bounded on the west by the San Andreas fault which separates it from the Point Reyes Peninsula composed of granitic rocks of the Salinian block. The Farallon Islands are also part of the Salinian block and can be seen on the clearest of days at a distance of 19 mi (31 km) offshore, close to the

edge of the continental shelf. Two offshore Cenozoic basins on the Salinian block have been considered for petroleum exploration. West of Point Reyes is the Bodega Bay Basin which is separated from the southern Santa Cruz Basin by the Farallon Ridge. The Tertiary sequences in these basins include siliceous shales of the Monterey Formation. The only drilling to date took place between 1963 and 1967 when Shell Oil drilled 12 exploratory wells in the offshore basins.

The cliff exposures to the northwest of Mussel Rock contain the type section of the Merced Formation of Pleistocene age, possibly late Pliocene in the lowest part. The formation is about 5900 ft (1800 m) thick, and detailed studies by Clifton and Hunter (1987) have shown that the succession is made up predominantly of upward shallowing (regressive) sequences.

The hills immediately to the southeast of Mussel Rock are of Franciscan rocks of the Permanente terrane, which consists largely of greenstone and graywacke with minor amounts of chert, limestone, and serpentinite. The prominent headland to the south is Montara Mountain which is composed of granitic rocks of the Salinian block. The Pilarcitos fault runs along San Pedro Valley on the north side of the mountain and goes out to the ocean near Point San Pedro. The Pilarcitos fault is a formerly active but presently inactive branch of the San Andreas fault.

This coastal zone is an example of an area where rapid urban development took place in the post-World War II years without an adequate study of the geological hazards (Sullivan, 1975). Although the coastline here is flanked by steep and treacherous cliffs, it became the location at the beginning of this century of the Ocean Shore

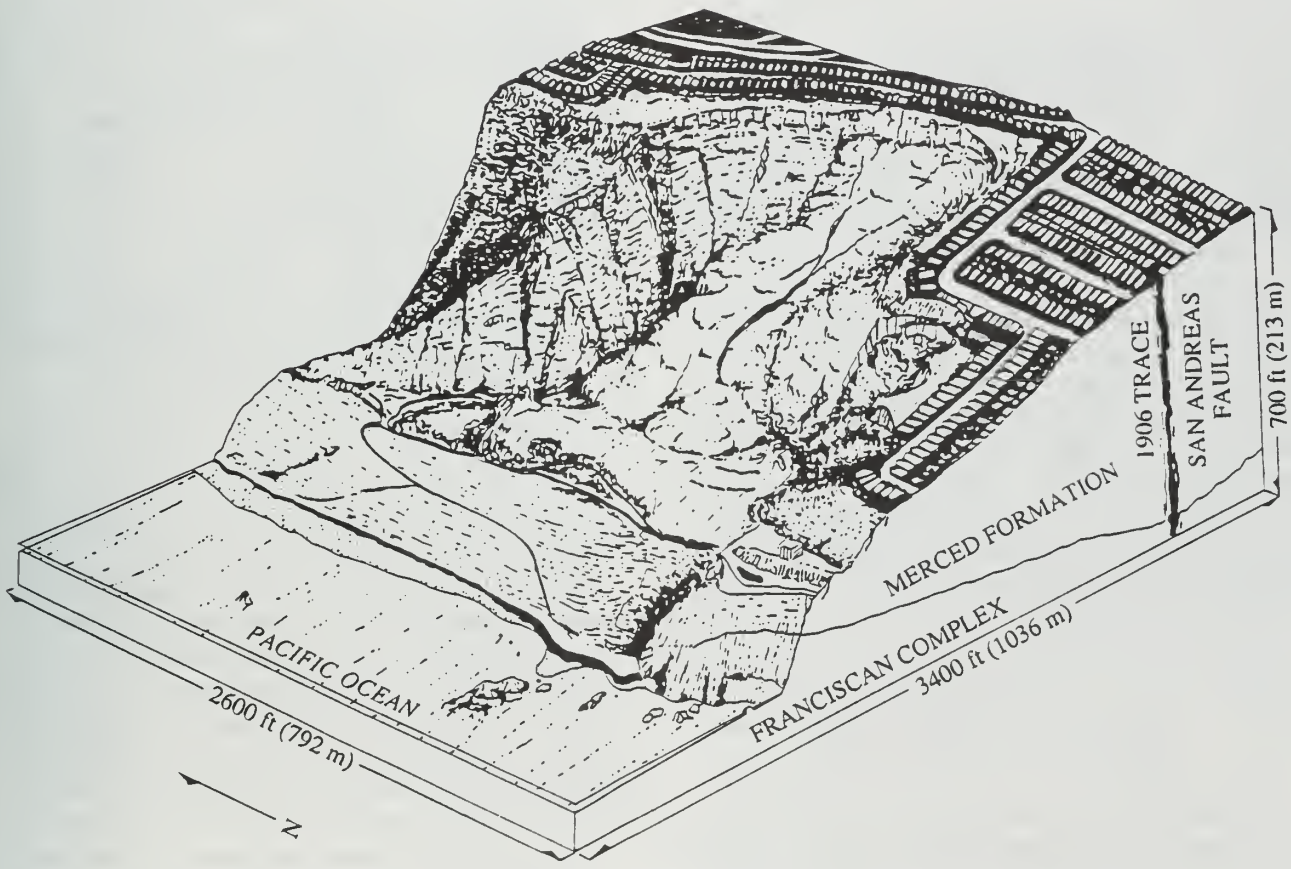

Figure 4. Block diagram showing the urban development and active landside within the San Andreas fault zone at Mussel Rock, Daly City, California (after Smelser, 1987).

Railway that was in operation until 1920. The railroad bed in this area became the site of a coastal highway (Hwy. 1) in the 1930s until its closure in 1957 due to landslide damage from the nearby M 5.3 earthquake. Housing developments expanded into this area between the late 1950s and early 1970s. The homes that can be seen above the cliffs date from this period. The effects of the 1957 earthquake on the Bay area have been described by Bonilla (1959) and Steinbrugge and others (1959). The epicenter of the M 5.3 quake was in the vicinity of Mussel Rock, and the maximum intensity was MM VI or VII. The greatest damage was to single family, wood frame homes of this area that were under construction at the time.

The main landslide at Mussel Rock (Fig. 4) involves approximately 9 million cubic yards of unconsolidated material from the Merced Formation (Smelser, 1987). It is primarily a rotational slump with numerous small slumps and shallow debris flows. A sanitary landfill operation was located in the landslide depression developed in the San Andreas fault zone and directly above the beach. This garbage dump operated until 1979 when it was abandoned, and the landfill site was regraded for open space.The toe and slope of the main slide are largely covered with this landfill material which in many places is broken by cracks. Methane gas from the decomposition of the garbage can be detected near many of the cracks.

Homes of the Westlake development fringe the steep cliff that marks the head of the slide. Slumping and erosion have caused rapid retreat of the cliff line, which has endangered many of the perimeter homes. More than a dozen homes (11 of these between 1965 and 1972) have been removed in this area and several more homes have been condemned or threatened by the landslide. Virtually no damage occurred in this area due to the Loma Prieta earthquake.

STOP 4 - PALEOCENE SEQUENCE IN THE DEVILS SLIDE AREA

The Paleocene strata exposed near Devils Slide along Hwy. 1 represent a stratigraphically isolated unit, bounded to the north by the Pilarcitos fault and the Franciscan Complex and resting nonconformably upon Montara granitic rocks to the south (Fig. 5). The section has been severely faulted and folded, attesting to the traumatic tectonic history of the Salinian block within which it resides. This unnamed Paleocene formation is best exposed in the beach cliffs of Shelter Cove in Pacifica and along Hwy. 1 near Devils Slide. It has a total thickness of approximately 3800 ft (1160 m) (Brabb and Pampeyan, 1983). The strata consist of a turbidite sequence that has been informally subdivided by Morgan (1981) into (1) a lower turbidite unit, (2) a conglomerate unit, (3) an upper turbidite unit, and (4) a basal turbidite unit. The section has no known stratigraphic top.

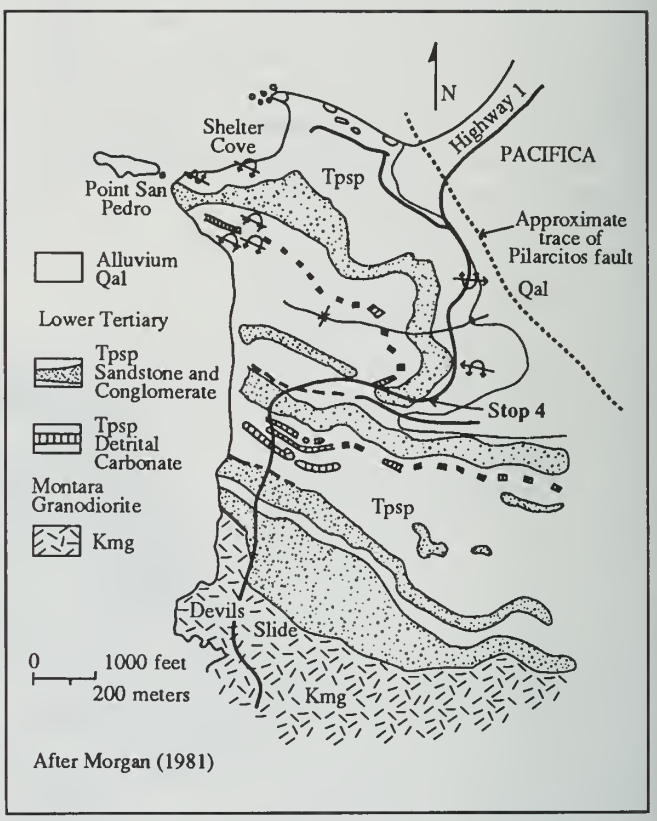

Figure 5. General geology of the Devils Slide area.

Interbedded turbidite sandstone and shale of the lower turbidite unit best exposed at Shelter Cove is overlain by a conglomerate-filled channel in the roadcut exposure where we will stop along Hwy. 1. The conglomerate consists of an overall thinning- and fining-upward succession of internally channelized conglomerate, massive sandstone, turbidites, and silty shale. Clast composition of the conglomerate includes granitic material with affinities to Montara granitic rocks, as well as typical Salinian terrane silicic metavolcanics, chert, and quartzite. The petrography of the

conglomerate differs substantially from the thin, fine-grained sandstones of the underlying lower turbidite unit. Because of these compositional differences, Morgan (1981) interpreted the succession as representing a distinct depositional sequence in the history of the Devils Slide section. In contrast, Nilsen and Yount (1981) believe the underlying turbidites to be overbank deposits of a submarine channel, and interpret the conglomerate to be the infill of a channel within a normal depositional sequence.

Interbedded turbidite sandstone and shale with thin-bedded, fine-grained detrital dolomite turbidites compose the upper turbidite unit along Hwy. 1 south of the submarine channel locality. The upper turbidite sequence is highly folded and faulted, and most of the beds are overturned. The carbonate turbidites, which occur as fine-grained, bronze-weathering beds, are stratigraphically above the boulder-filled channel.

South of the carbonate turbidites, the basal turbidite unit is exposed in sections along Hwy. 1. This sequence consists of shale and thin sandstone beds. The exact age and stratigraphic relationships of this unit with the other three are unknown, but these sandstones are compositionally similar to those of the lower and upper turbidite sandstones. Although highly faulted, the basal turbidite unit apparently lies nonconformably above Montara granitic rocks. This relationship suggests a paleogeography similar to the modern continental borderland basin setting in southern California.

This section of Hwy. 1 is located approximately 330-490 ft (100-150 m) above the ocean along the edge of precipitous sea cliffs known as Devils Slide. The Ocean Shore Railway ran through the Devils Slide area from 1908 to 1920. High maintenance costs associated with keeping the line open through this unstable area did much to deplete the financial resources of the company, and the tracks were removed in 1920. Since the present highway was built in 1937, there has been a long history of closures due to landslides and rocks falling onto the road, subsidence of the road grade, and erosion of the road bed. A deep-seated failure surface has its head at a scarp which is more than 33 ft (10 m) high and about 2130 ft (650 m) long. The scarp is about 1000 ft (300 m) above sea level. The failure surface is more than 330 ft (100 m) below the present road bed and its toe is near sea level (Heyes, 1984).

The unstable nature of Devils Slide, the proximity of the San Andreas fault, and the likelihood of a large earthquake in this area have necessitated the evaluation of a number of proposals to seek alternate routes for this important stretch of highway. These include either a bypass around the Devils Slide area on one of a number of alternate routes farther inland or a marine disposal alternative, involving massive removal and disposal of slide material into the ocean at the base of the cliff. The highway alignment would then be shifted inland. Extensive debate and controversy involving ecological, geological, political, and demographic issues have stalled the project. About $50 million in federal funds has been set aside, awaiting a judicial decision regarding which alternative will be chosen. Meanwhile, the road is being monitored for movement, and horizontal drainage wells and rockfall fences minimally mitigate some of the slope instabilities.

STOP 5 - SAN ANDREAS FAULT AT CRYSTAL SPRINGS DAM

The San Andreas fault system strikes from about N35°W to N40°W across the San Francisco Bay region and separates the relatively rapid northwesterly moving Pacific plate from the more slowly moving North American plate. The San Andreas fault transform system extends southeastward for about 745 mi (1200 km) from the Mendocino triple junction off the northern California coast near Cape Mendocino to the head of the Gulf of California. The present San Andreas fault system came into existence about 29 Ma when the Pacific-Farallon spreading center came into contact (near our present border with Mexico) with a subduction zone that had bounded the western edge of the North American plate through Mesozoic and Paleogene time. About 205 mi (330 km) of right slip has occurred thus far along the present fault system.

Crystal Springs Reservoir is the main storage basin for Hetch Hetchy water from the western slopes of the Sierra Nevada north of Yosemite Valley. This system is owned and operated by the city of San Francisco and supplies water to the City and to many of the communities on the San

Francisco Peninsula. The 1640 ft (500 m) wide reservoir lies within the San Andreas rift valley, and the 1906 fault trace runs parallel to and near the middle of the valley.

When the Crystal Springs Reservoir Dam was completed in 1890, it was one of the largest concrete dams in the world. It is about 145 ft (44 m) high, 600 ft (183 m) long, and has the capacity to impound 58,000 acre-feet of water. The dam is built of interlocking concrete blocks and its foundation is highly fractured graywacke (broken formation) of the Franciscan Complex. Even though the 1906 rupture trace is only about 985 ft (300 m) west of the crest of the dam, it suffered no damage in the 1906 earthquake. Failure of the Crystal Springs Reservoir Dam today would endanger over 70,000 people who live downstream.

The San Andreas rift valley at this location is situated in the Central terrane of the Franciscan Complex (Blake and others, 1984). Note that the linearity of the rift valley runs parallel to and near the crest of the drainage divide between the Pacific Ocean and San Francisco Bay. Stream valleys are usually more perpendicular than parallel to ridge crests. In this case, however, faulting has broken up the rocks and allowed streams to cut valleys along the linear brecciated zone. Reservoirs along fault zones are common in California because valleys suitable for water storage were created in this manner (Schlocker, 1969).

This presently locked portion of the San Andreas fault had surface displacement in the M 8.3 San Francisco earthquake of 18 April 1906. This segment extends some 280 mi (450 km) from near San Juan Bautista northwestward to the Cape Mendocino area. In general, the amount of surface slip in 1906 was greater north of San Francisco than it was to the south. The portion of the fault on the San Francisco Peninsula had about 6.5-10 ft (2-3 m) of surface displacement in 1906. The slip was almost entirely a horizontal right slip as indicated by offset cultural features and horizontal slickensides (Lawson, 1908). The Loma Prieta earthquake occurred along the southernmost 25-30 mi (40-50 km) of the 280-mi (450-km) length that broke in 1906. No surface displacement occurred along the Peninsula segment of the fault which is northwest of the 1989 aftershock zone.

The Working Group on California Earthquake Probabilities (1990) estimated that the chance of a M 7 or greater earthquake on the Peninsula segment of the San Andreas fault is about one in four within the next 30 years.

STOP 6 - HAYWARD FAULT IN THE CITY OF HAYWARD

The northwesterly-trending Hayward fault extends for more than 50 mi (80 km) in the East Bay portion of the San Francisco Bay area. This creeping fault consists of a northerly segment from San Pablo Bay to San Leandro that was probably the site of an approximate M 6.8 earthquake in 1836 and a southerly segment from San Leandro to Fremont that was the site of an approximate M 6.8 earthquake in 1868 that produced surface rupture.

The Working Group on California Earthquake Probabilities (1990) estimated that each segment of the Hayward fault has about one chance in four of producing a M 7 earthquake or larger within the next 30 years. They also suggested that if both segments of the Hayward fault slip during the same seismic event, the magnitude could reach about 7.5.

The southern segment of the Hayward fault runs right through the city of Hayward. At our stop along D Street between Mission Street and Main Street there are two actively creeping traces of the Hayward fault. Galehouse and others (1989) have been monitoring the creep rate at five sites along the Hayward fault, including this one, for more than ten years and have determined that the creep rate is presently about 0.2 in/yr (4.5 to 5 mm/yr) (Fig. 6). This is about half the Holocene slip rate of 0.4 in/yr (9 mm/yr) that Lienkaemper and Borchardt (1990) have determined from trench investigations along the southern segment of the Hayward fault in Union City. Lienkaemper and Borchardt (1990) estimate that enough strain has already accumulated that another 1868-type earthquake could occur at any time.

At our stop on D Street we can see curb offsets and *en echelon* cracks that precisely locate the two presently creeping traces of the Hayward fault in the city of Hayward.

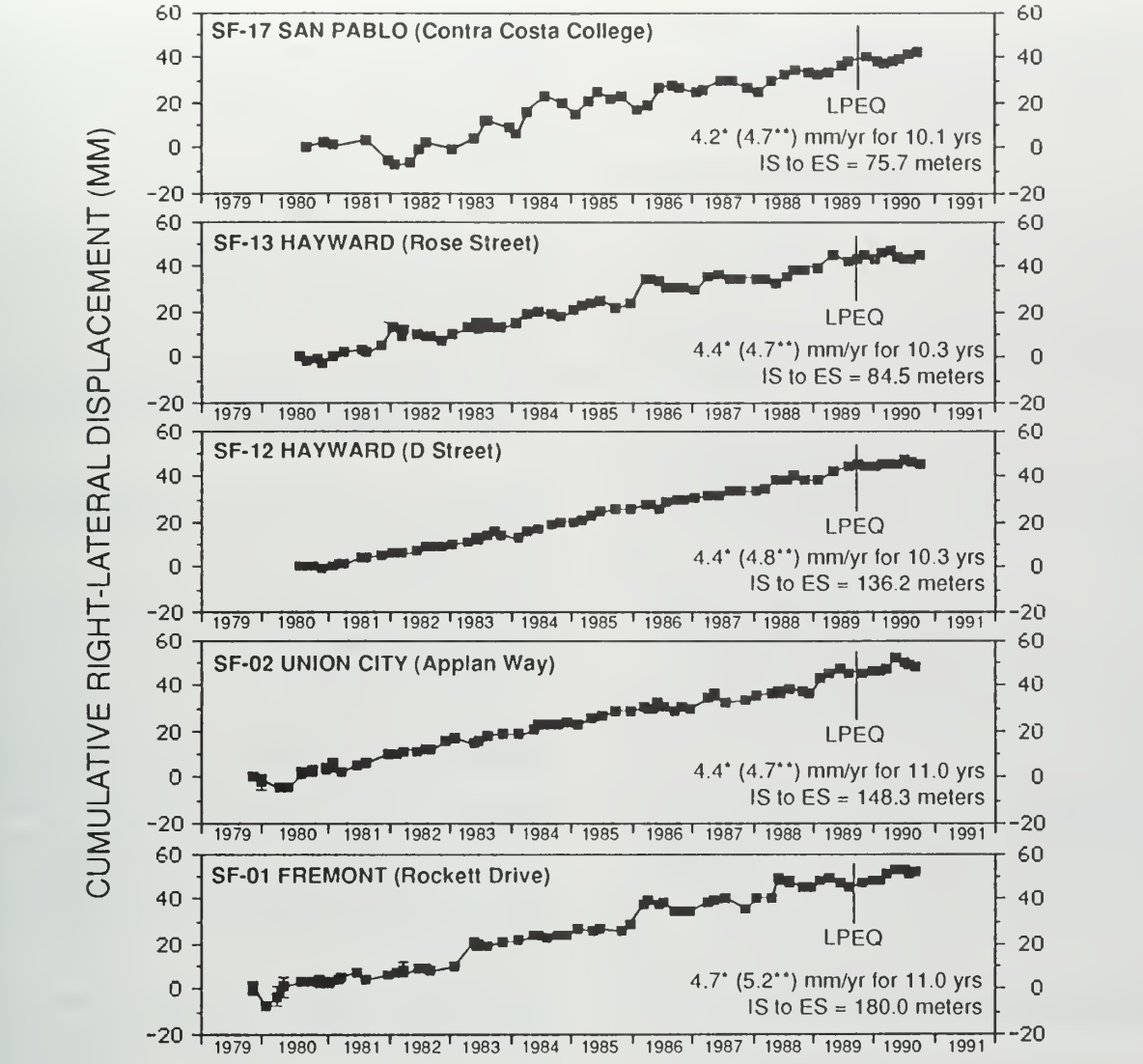

Figure 6. Hayward fault displacement from 1979-1990 (updated from Galehouse and others, 1989).

ACKNOWLEDGEMENTS

We would like to thank Karen Grove, Raymond Pestrong, and Lisa White, who are faculty members with us at San Francisco State University. They assisted us in the preparation of an original, more detailed, version of this field guide that was prepared for the June 1990 annual meeting of the AAPG in San Francisco. We also wish to acknowledge the help we received from Scott Morgan of Exxon Production Research who provided information on the Paloecene section at Devils Slide. Gary Palmer and Pamela Nishikawa of the Graphics Department at San Francisco State University gave us invaluable assistance in drafting the figures and laying out the manuscript.

REFERENCES CITED

Bailey, E.H., Irwin, W.P., and Jones, D.L., 1964, Franciscan and related rocks and their significance in the geology of western California: *California Division of Mines and Geology Bulletin 183*, 177p.

Blake, M.C., Jr., ed., 1984, *Franciscan geology of northern California:* Pacific Section, Society of Economic Paleontologists and Mineralogists, v. 43, 254p.

Blake, M.C., Jr., Howell, D.G., and Jayko, A.S., 1984, Tectonostratigraphic terranes of the San Francisco Bay region: *in* Blake, M.C., Jr., ed., *Franciscan geology of northern California,* Pacific Section, Society of Economic Paleontologists and Mineralogists, v. 43, p. 5-22.

Bonilla, M.G., 1959, Geologic observations in the epicentral area of the San Francisco earthquake of March 22, 1957, *in* Oakeshott, G.B., ed., San Francisco earthquake of March 22, 1957*: California Division of Mines and Geology Special Report 57*, p. 25-37.

Brabb, E.E., and Pampeyan, E.H., 1983, Geologic map of San Mateo County, California: *U.S. Geological Survey Miscellaneous Investigations Series Map I-1257-A*, scale 1:62,500.

Champion, D.E., Howell, D.G., and Gromme, C.S., 1984, Paleomagnetic and geologic data indicating 2500 km of northward displacement for the Salinian and related terranes, California: *Journal of Geophysical Research*, v. 89, p. 7736-7752.

Clifton, H.E., and Hunter, R.E., 1987, The Merced Formation and related beds—a mile-thick succession of late Cenozoic coastal and shelf deposits in the sea-cliffs of San Francisco, California: Hill, M.L., ed., *Cordilleran Section of the Geological Society of America Centennial Field Guide Volume 1*, p. 257-262.

Galehouse, J.S., Baker, F.B., Graves, O., and Hoyt, T., 1989, San Francisco Bay region fault creep rates measured by theodolite, *in* Sylvester, A.G., and Crowell, J.C., eds., *The San Andreas transform belt:* Field Trip Guidebook T 309, 28th International Geological Congress, American Geophysical Union, Washington, D.C., p. 45-48.

Hansen, G., and Condon, E., 1989, *Denial of Disaster:* Cameron and Company, San Francisco, California, 160p.

Heyes, D.G., 1984, *Engineering geology of the Devils Slide, San Mateo County, California*: 35th Annual Highway Geology Symposium Field Trip Guidebook, San Jose State University, p. 14-41.

Irwin, W.P., 1960, Geologic reconnaissance of the northern Coast Ranges and Klamath Mountains, California: *California Division of Mines and Geology Bulletin 179*, 79p.

Lawson, A.C., 1908, The California earthquake of April 18, 1906; Report of the State Earthquake Investigation Commission: *Carnegie Institution of Washington Publication 87*, v. 1, 451p.

Lienkaemper, J.J., and Borchardt, G., 1990, Holocene slip rate, historic creep rate, and the potential for large earthquakes on the Hayward fault, California (abs.): *EOS, Transactions,* American Geophysical Union, v. 71, no. 43, p. 1645.

Morgan, S.R., 1981, General geology of the strata at Point San Pedro, San Mateo County, California, *in* Frizzell, V., ed., *Upper Cretaceous and Paleocene turbidites, central California coast:* Pacific Section, Society of Economic Paleontologists and Mineralogists, Field Trip 6, p. 13-19.

Nilsen, T.H., and Yount, J.C., 1981, Sedimentology of the Paleocene strata, Point San Pedro, California, *in* Frizzell, V., ed., *Upper Cretaceous and Paleocene turbidites, central California coast:* Pacific Section, Society of Economic Paleontologists and Mineralogists, Field Trip 6, p. 20-29.

Page, B.M., 1989, The Salinian block, *in* Wahrhaftig, C. and Sloan, D., eds., *Geology of San Francisco and vicinity:* Field Trip Guidebook T 105, 28th International Geological Congress, American Geophysical Union, Washington, D.C., p. 16-20.

Plafker, G., and Galloway, J.P., eds., 1989, Lessons learned from the Loma Prieta, California, earthquake of October 17, 1989: *U.S. Geological Survey Circular 1045*, 48p.

Schlocker, J., 1969, *Field Trip 3 - San Francisco Peninsula-Stanford Linear Accelerator Center*: 1969 Field Trips for National Meeting, Association of Engineering Geologists, San Francisco, p. C1-C17.

Schlocker, J., 1974, Geology of the San Francisco North quadrangle, California: *U.S. Geological Survey Professional Paper 782*, 109p.

Smelser, M.G., 1987, Geology of Mussel Rock landslide, San Mateo County: *California Geology*, v. 41, p. 59-66.

Steinbrugge, K.V., Bush, V.R., and Zacher, E.G., 1959, Damage to buildings and other structures by the San Francisco earthquake of March 22, 1957, *in* Oakeshott, G.B., ed., San Francisco earthquake of March, 22, 1957: *California Division of Mines and Geology Special Report 57*, p. 73-106.

Sullivan, R., 1975, Geological hazards along the coast south of San Francisco: *California Geology*, v. 28, p. 27-33.

Sullivan, R., and Galehouse, J.S., eds., 1990, *Geological setting of the San Francisco Bay area*: Field Trip Guidebook, American Association of Petroleum Geologists, Annual Meeting San Francisco, 82p.

Wahrhaftig, C., 1966, Geological nature walks in San Francisco and environs (Walk V), *in* Wahrhaftig, C., *A walker's guide to the geology of San Francisco:* Mineral Information Service, Special Supplement, California Division of Mines and Geology, p. S1-S17.

Wahrhaftig, C., 1984, *A streetcar to subduction and other plate tectonic trips by public transport in San Francisco,* revised edition, American Geophysical Union, Washington, D.C., 76p.

Working Group on California Earthquake Probabilities, 1990, Probabilities of large earthquakes in San Francisco Bay region, California: *U.S. Geological Survey Circular 1053*, 51p.

Youd, T.L., and Hoose, S.N., 1978, Historic ground failures in northern California triggered by earthquakes: *U.S. Geological Survey Professional Paper 993*, 177p.

San Francisco to Point Reyes: Both Sides of the San Andreas Fault[1]

Joseph C. Clark,[2] Clyde Wahrhaftig,[3] and Earl E. Brabb[3]

This field trip to Marin County visits the Franciscan Complex east of the San Andreas fault, and Salinian basement and its sedimentary cover on Point Reyes Peninsula west of the fault, stressing evidence for about 95 mi (150 km) of displacement on the San Gregorio fault.

THE FRANCISCAN OF MARIN COUNTY

The Franciscan Complex of northern California is an accretionary complex of oceanic origin and of Jurassic to Miocene age (mainly Jurassic and Cretaceous), that was accreted to western North America by combined subduction and transcurrent transport (cf. Blake and others, 1984). The Franciscan of Marin County consists mainly of an extensive melange matrix (often called the Central terrane) in which are embedded relatively coherent terranes ranging in age from early Jurassic to mid- or late Cretaceous. We visit two of the terranes, the Marin Headlands terrane (Stops 1-2 through 1-4, Fig. 1) and the Nicasio Reservoir terrane (Stop 2-5), pass within sight of others, and will stop at two localities in the melange (Stops 1-1 and 1-5).

The melange consists mainly of a tectonic stew of sandstone and shale that originated as turbidite deposits on the deep ocean floor from either the continent or volcanic arcs of the subduction zone. A lesser component of the stew is serpentinite as extensive slabs, but commonly as a melange itself. Embedded in the melange are blocks of sandstone, basalt, chert, limestone, and exotic rocks such as blueschist, eclogite, and amphibolite. The coherent terranes appear to be giant slabs, dipping mainly gently to the northeast, embedded in or separated by sheets of the melange.

The Marin Headlands terrane (Fig. 2) consists, at the base, of mid-ocean ridge basalt, mainly pillowed (Shervais, 1989), overlain by about 260 ft (80 m) of radiolarian chert 95-200 Ma old, with a 15-30 my gap at the J-K boundary marked by a brecciated zone; the chert is overlain by thick-bedded turbidites containing ammonites of mid-Cretaceous (Cenomanian and Albian) age (Wahrhaftig and Murchey, 1987). The radiolarian species and chemistry of the chert suggest an origin at near-equatorial latitudes (Murchey, 1984; Karl, 1984).

The Marin Headlands block of the Marin Headlands terrane consists of eight to 12 south-dipping thrust slices of chert, locally underlain by basalt and overlain by sandstone (Wahrhaftig, 1984). The orientation of minor asymmetric folds in chert and magnetic polarity in the basalt and chert suggests that the block was rotated more than 90° clockwise after accretion (Curry and others, 1984). A second block of the Marin Headlands terrane extends diagonally across San Francisco, from Lands End on the northwest through the Twin Peaks to Candlestick Point on the southeast.

The Nicasio Reservoir terrane (Fig. 2) consists largely of pillow basalt of tholeiitic or ocean-island affinity, with overlying radiolarian chert of Valanginian age and graywacke (Blake and others, 1984; Wright, 1984; Hagstrum, 1990). The Nicasio Reservoir terrane forms a series of rugged mountains in western Marin County, from the southwest end of Mt. Tamalpais northwestward to Black Mountain and Nicasio Reservoir. The rocks of Point Bonita and vicinity (shown on Fig. 2 as the Point Bonita block), the southernmost thrust slices of the Marin Headlands, are possibly related to the Nicasio Reservoir terrane (Stop 1-4).

---

[1] The stratigraphic nomenclature and age assignments used in this report may not necessarily conform to current usage by the U.S. Geological Survey.

[2] Geoscience Department, Indiana University of Pennsylvania, Indiana, PA 15705

[3] U.S. Geological Survey, 345 Middlefield Rd., Menlo Park, CA 94025

Other relatively coherent terranes that the field trip passes are the San Bruno Mountain terrane, which consists of graywacke turbidites with rather abundant detrital quartz and K-feldspar, a block of which lies along the west side of Bolinas Ridge between the Nicasio Reservoir terrane and the San Andreas fault; the Novato Quarry terrane, of arkosic turbidites and fossils of Late Cretaceous (Campanian) age, which makes up Big Rock Ridge north of our return route on Lucas Valley Rd. on the second day; and the Yolla Bolly terrane, composed mainly of metagraywacke with a pronounced schistosity caused by the flattening of clasts and high P/T metamorphic minerals, including lawsonite, jadeitic pyroxene, aragonite, and glaucophane.

GEOLOGY OF POINT REYES PENINSULA

The Point Reyes Peninsula is a triangular projection of the Marin County coast with an apex at Point Reyes and a base along Tomales Bay and the San Andreas rift valley (Fig. 3). Mesozoic granitic rocks of the Salinian block form its basement. Resting nonconformably upon this crystalline basement is a composite section of 14,340 ft (4370 m) of moderately deformed Tertiary marine sedimentary rocks that comprise three sequences, separated by unconformities. A complete superpositional section is not preserved, and good rock exposures are generally restricted to the sea cliffs. At five stops we will examine the granitic basement and Paleocene to Pliocene sedimentary rocks.

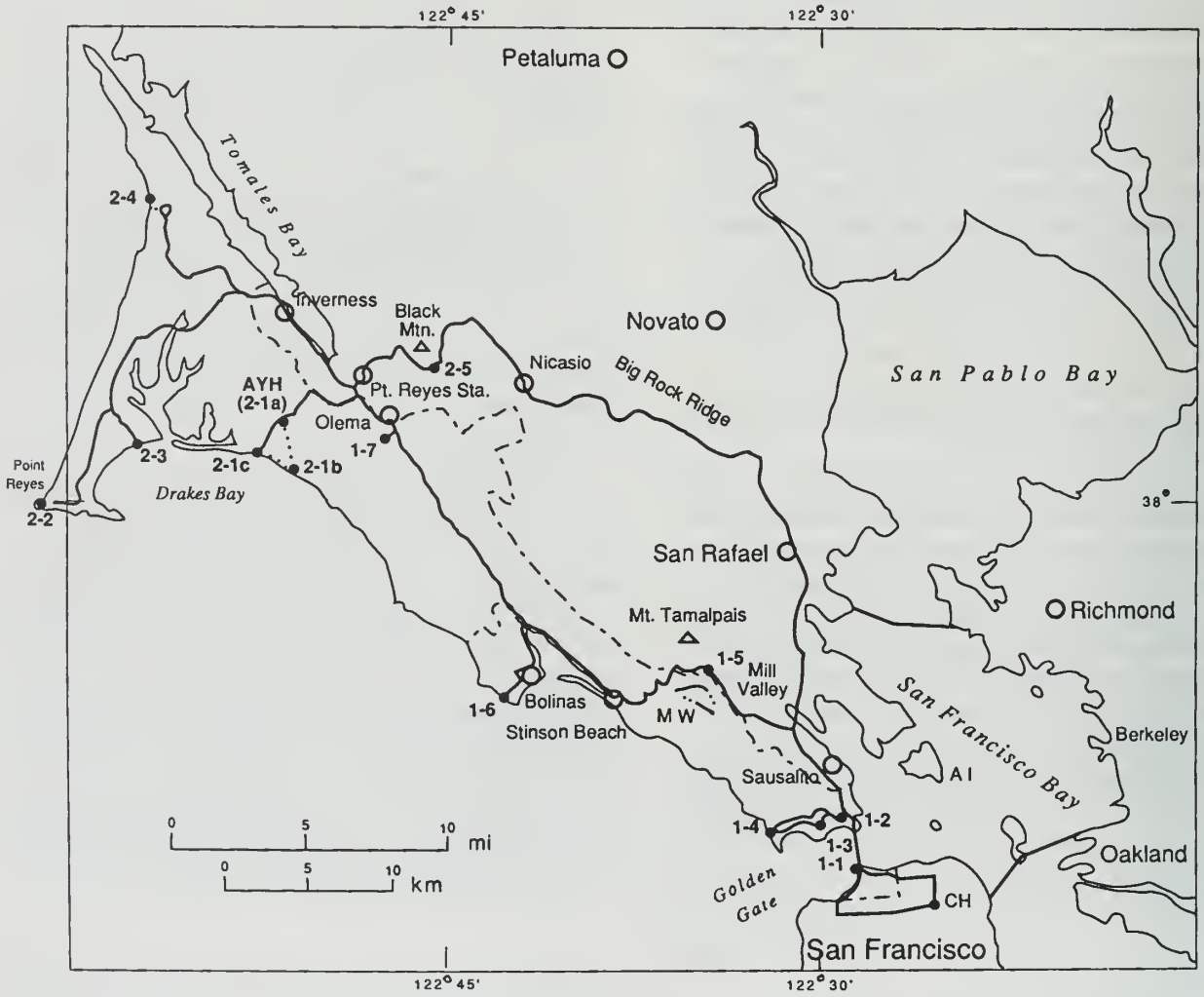

Figure 1. Map showing the field trip route and locations of stops. AI, Angel Island; AYH, Point Reyes AYH hostel; CH, Cathedral Hill Hotel; MW, Muir Woods.

Granitic basement: The basement of the Point Reyes Peninsula consists of three lithologically distinct granitic facies: (1) porphyritic granodiorite at the Point Reyes promontory; (2) granodiorite and granite that crop out along Inverness Ridge and are well exposed at Kehoe Beach (Stop 2-4); and (3) hornblende-biotite tonalite that forms Tomales Point to the north. The granodiorite-and-granite facies is biotitic and contains older metasedimentary inclusions of schist and gneiss, quartite, calc-hornfels, and marble (Ross, 1977). Dikes and masses of aplite and alaskite are locally abundant. Radiometric dating indicates that these granitic rocks probably crystallized about 100 Ma, during the Early Cretaceous (Ross, 1978).

Paleocene sedimentary sequence: The oldest Tertiary sedimentary rocks exposed on the Peninsula are interbedded conglomerate and sandstone of the Point Reyes Conglomerate of Galloway (1977), exposed only at Point Reyes (Stop 2-2) and resting depositionally upon the porphyritic granodiorite. It consists of 690 ft (210 m) of very thick, graded arkosic sandstone beds and very thick sandy conglomerate beds, locally channeled into underlying sandstone. These beds probably represent a northwesterly-trending, upper mid-fan channel complex (Clark and others, 1984) of bathyal depth and Paleocene age.

Middle and upper Miocene sedimentary sequence: This Neogene sequence is as much as 5280 ft (1610 m) thick and consists of a transgressive basal sandstone unit, the Laird Sandstone, and an overlying basinal siliceous unit, the Monterey Formation.

The arkosic Laird Sandstone crops out in a band on the southwest slope of Inverness Ridge, where it rests nonconformably upon granodiorite and granite and is overlain conformably by the Monterey Formation (Fig. 3). It is locally calcareous and in places is slightly bituminous. Its maximum thickness is 210 ft (64 m) at Kehoe Beach (Stop 2-4), where it is well exposed and yields a diverse megafossil fauna of middle Miocene age.

The Monterey Formation crops out southwest of the Laird Sandstone in a band narrowing northwest from the San Andreas fault to Kehoe Beach. The lower part is up to 490 ft (150 m) of

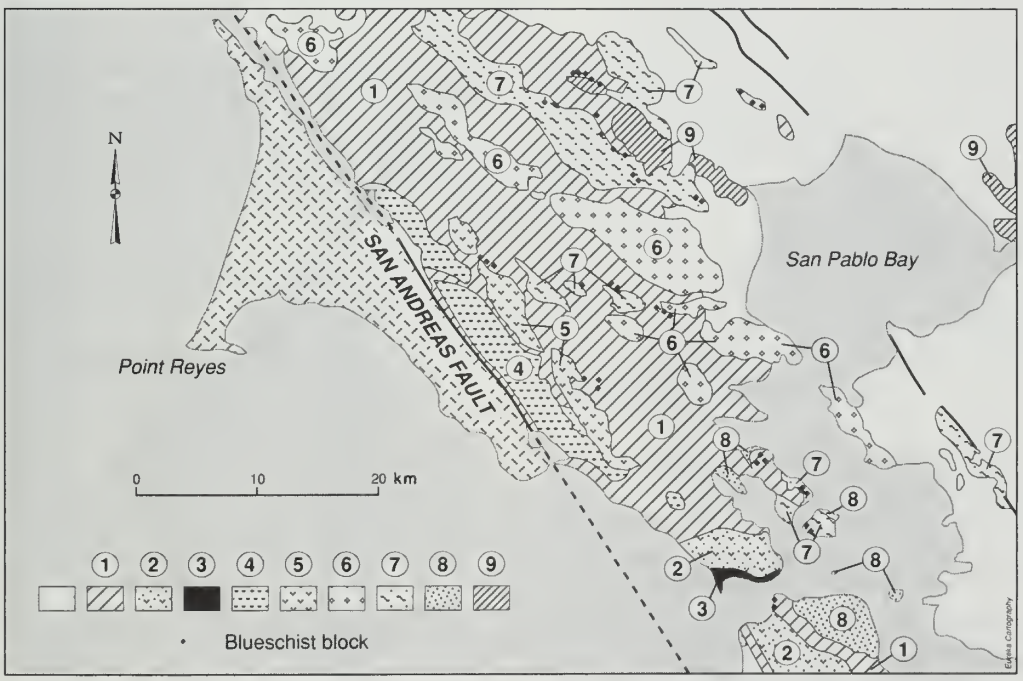

Figure 2. Map of tectonostratigraphic terranes of the Franciscan Complex in the area shown in Fig. 1. 1, Central terrane (melange); 2, Marin Headlands terrane; 3, Point Bonita block; 4, San Bruno Mountain terrane; 5, Nicasio Reservoir terrane; 6, Novato Quarry terrane; 7, Yolla Bolly terrane; 8, Alcatraz terrane; 9, Great Valley sequence. Blank land areas, Cenozoic cover. Area west of the San Andreas fault is Salinia. Modified from Blake and others, 1984, Fig. 2.

silty siliceous mudstone. Overlying it is locally contorted thin-bedded porcellanite and shale, which may be 1475 ft (450 m) thick. To the south, porcellanite and concretionary chert beds (Stop 2-1) form the upper part of the Monterey and are between 1475 ft (450 m) and 2950 ft (900 m) thick.

The Monterey Formation yields benthic foraminifers and diatoms diagnostic of Luisian and Mohnian (middle and late Miocene) age (Clark and others, 1984; White, 1990).

Upper Miocene to Pliocene sedimentary sequence: This Neogene sequence, 8200 ft (2500 m) thick (Fig. 4), rests unconformably on all older rocks of the Peninsula. It consists of a basal glauconitic sandstone unit, the Santa Margarita Sandstone, a siliceous mudstone unit, the Santa Cruz Mudstone, and an upper siltstone, mudstone, and sandstone unit, the Purisima Formation.

Clark and others (1984) applied these formation names from the Santa Cruz Mountains to the correlative units of this sequence at Point Reyes

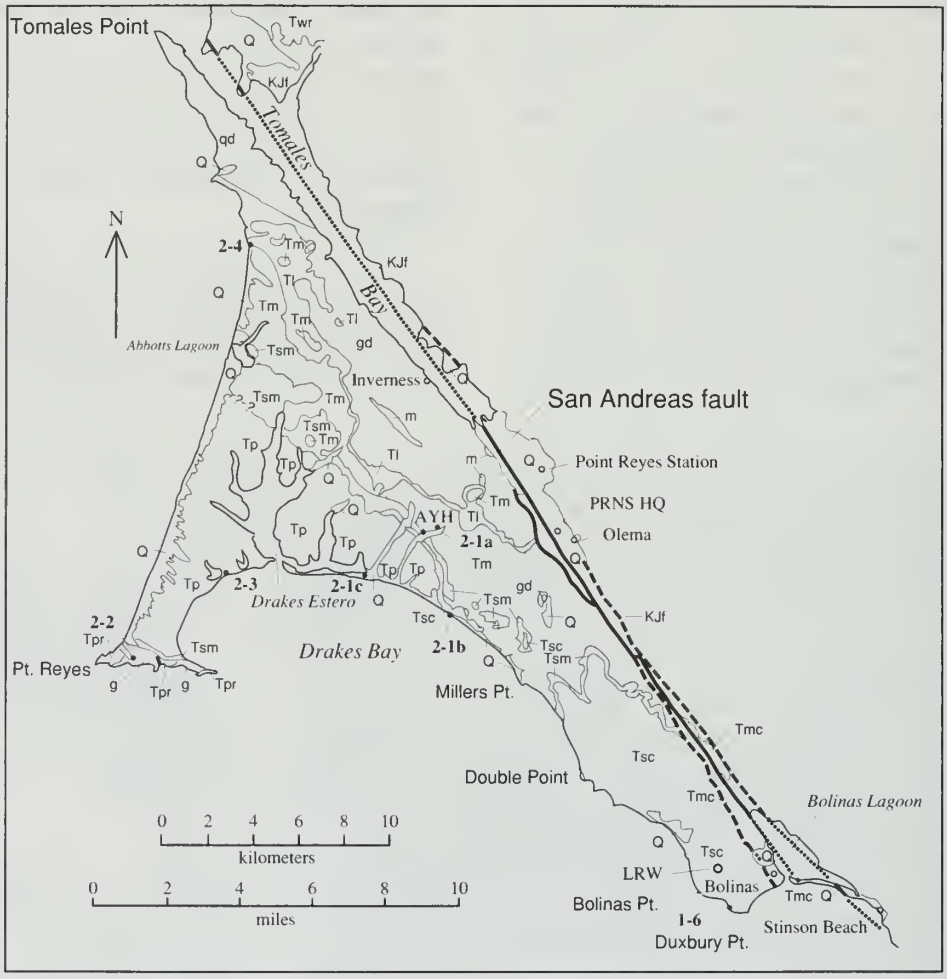

Figure 3. Generalized geologic map of Point Reyes Peninsula, showing location of Stops 1-6 and 2-1 through 2-4. Q, Quaternary deposits; Tmc, Merced Formation (Plio-Pleistocene); Twr, Wilson Ranch Formation; Tp, Purisima Formation (Drakes Bay Formation of Galloway, 1977 - Miocene-Pliocene); Tsc, Santa Cruz Mudstone (Miocene); Tsm, Santa Margarita Formation (Miocene); Tm, Monterey Formation (Miocene); Tl, Laird Sandstone (Miocene); Tpr, Point Reyes Conglomerate of Galloway, 1977 (Paleocene); qd, tonalite of Tomales Point; gd, granodiorite and granite of Inverness Ridge; g, porphyritic granite of Point Reyes; m, metamorphic rocks; KJf, Franciscan Complex (the latter five, Cretaceous and older). AYH, Pt. Reyes AYH hostel; LRW, Lockhhart R.C.A. No. 3 well; PRNS, Point Reyes National Seashore headquarters. From Clark and others, 1984.

because of the very similar stratigraphic relationships, lithologies, and fossil faunas and floras. Galloway (1977) had earlier assigned the beds that form the white cliffs at Drakes Bay to his Drakes Bay Formation and locally mapped a "basal glauconitic greensand" as a lower unit of his Drakes Bay Formation.

The Santa Margarita Sandstone contains 37 to 42 percent glauconite in south-central coastal exposures (Stop 2-1b), where it rests unconformably on siliceous beds of the Monterey and varies from 15 ft (5 m) to more than 65 ft (20 m) thick. Near the AYH hostel, at its base is 165 ft (50 m) of "clean" arkosic sandstone. To the southeast the Santa Margarita is highly bioturbated and bituminous.

The Santa Cruz Mudstone is sandy and glauconitic above the conformable contact with the Santa Margarita Sandstone (Stop 2-1) and grades upward into siliceous mudstone. This mudstone may be as thick as 6560 ft (2000 m) beneath Bolinas Mesa (Stop 1-6) and thins northward to a pinchout east of Drakes Estero (Figs. 3, 4). Sparse benthic foraminifers and diatoms from the Santa Cruz Mudstone near Bolinas Mesa are diagnostic of a late Miocene age (Clark and others, 1984).

On land the Purisima is confined to a broad synclinorium between Point Reyes and Inverness Ridge, where it is 1610 ft (490 m) thick. Best exposures are in the sea cliffs at Drakes Beach (Stop 2-3). It has yielded a diverse marine fauna and flora diagnostic of latest Miocene and Pliocene age (Galloway, 1977; Clark and others, 1984).

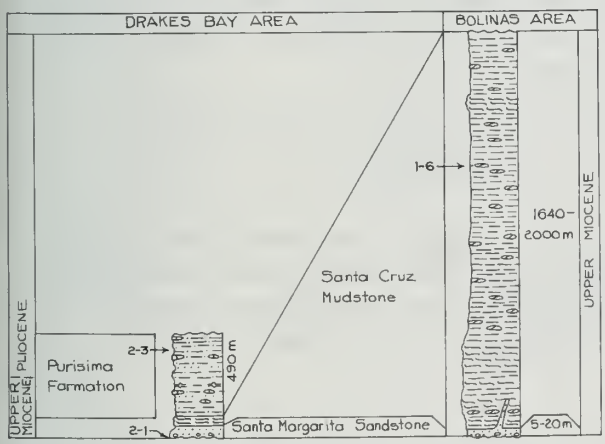

Figure 4. Upper Miocene to Pliocene sedimentary sequence of the Point Reyes Peninsula (modified after Clark and others, 1984).

The Purisima represents a shallow marine phase of the sequence that began with the Santa Margarita Sandstone. This transgression was followed by basinal deepening with 6560 ft (2000 m) of the Santa Cruz Mudstone deposited near Bolinas (Fig. 4). With basinal filling, the Purisima was deposited at inner neritic depths, and locally transgressed the granitic basement to the northwest. Much of the Purisima subsequently has been eroded from the Point Reyes Peninsula, and its top has been removed.

DISPLACEMENT AND MOVEMENT ON THE SAN GREGORIO FAULT

Detailed comparison of the Salinian basement and the overlying Tertiary sedimentary rock sequences of the Point Reyes Peninsula with correlative rocks in the Santa Cruz Mountains and the Monterey Bay region to the south (Clark and others, 1984) suggests about 95 mi (150 km) of right-slip displacement on the San Gregorio fault.

The porphyritic granodiorite of Point Reyes that also occurs as abundant clasts in the overlying Point Reyes Conglomerate of Galloway (1977) is strikingly similar to the porphyritic granodiorite of Monterey, which Ross (1978) states "is probably the most distinctive granitic unit in the central Salinian block." Restoration of 95 mi (150 km) of strike-slip along the San Gregorio fault juxtaposes not only the Point Reyes and Monterey granodiorite masses but also the similar Tomales and Ben Lomond hornblende-biotite tonalite masses (Fig. 5).

The Point Reyes Conglomerate of Galloway (1977) is very similar in lithology, paleocurrent direction, facies, and fauna to the Carmelo Formation that is exposed at Pt. Lobos (Clifton and Hill, 1987). Likewise, the Laird Sandstone and Monterey Formation of the Point Reyes Peninsula correlate lithologically and faunally with the basal transgressive sandstone (the Los Laureles Sandstone Member of the Monterey Formation of Bowen, 1965) and the type Monterey Formation to the south (Fig. 6).

The match of Cretaceous plutonics, and of Paleocene and middle and upper Miocene sequences of the Point Reyes and Monterey peninsulas suggests that the San Gregorio fault did not begin right-slip activity until between 12 and 11 Ma. Matching the thick Santa Cruz Mudstone sections of the Point Reyes Peninsula and Santa Cruz Mountains (Fig. 6) suggests about 45 mi (70 km) of this offset occurred in the last 6.5-6 Ma.

S.A. Graham (oral communication, 1988; Graham and Dickinson, 1978) points out that 95 mi (150 km) displacement places the granitic Farallon Islands south of the piercing point of the Sur-Nacimiento fault with the Hosgri fault; he consequently prefers a maximum displacement of 70 mi (115 km). However, the continuity of the San Gregorio with the Hosgri fault is still to be demonstrated.

A 95 mi (150 km) offset in 11 to 12 my gives an average slip rate of 0.5 in/yr (1.30 cm/yr), at the upper end of Weber and Lajoie's (1977) estimated Quaternary slip rate of 0.25-0.5 in/yr (0.63-1.30 cm/yr) for the still-active San Gregorio fault.

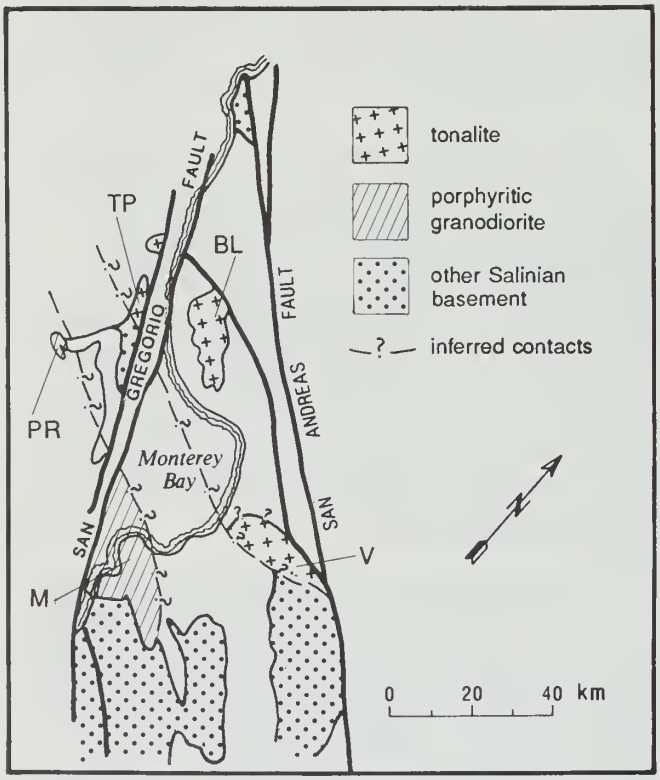

Figure 5. Generalized geologic map showing distribution of tonalites of Tomales Point (TP), Ben Lomond (BL), and Vergeles (V), and porphyritic granodiorites of Point Reyes (PR) and Monterey (M) after restoration of 95 mi (150 km) of right-slip on the San Gregorio fault. Modified after Clark and others, 1984.

FIELD TRIP, DAY 1

STOP 1-1 ABOVE BAKER BEACH

On Merchant Rd., 300 ft northwest of junction with Lincoln Blvd., Presidio of San Francisco.

Walk about 300 ft (100 m) north along Coastal Trail to a viewpoint southwest of the Golden Gate Bridge. The bedrock here is a serpentinite slab that dips gently northeast. The lower third of the bluff consists of melange with a matrix of shale and graywacke in which are embedded blocks of sandstone, basalt, chert, and amphibolite. Across the Golden Gate, the coherent thrust slices of the Marin Headlands block strike toward Stop 1-1, and dip 30°-45°SW. The structural discrepancy suggests a tectonic boundary beneath the Golden Gate.

Drive northeast 300 ft (100 m) on Merchant Rd., left at the bus stop on the west side of Hwy. 101, take the tunnel underneath Hwy. 101 and the toll plaza, and the next right to return to Hwy. 101 headed north across Golden Gate Bridge. On the north side of the bridge, take the Alexander Ave. off-ramp just beyond the view plaza, turn left at Alexander Ave., go beneath the freeway, and take the first right up the hill (Conzelman Rd.) into the Marin Headlands. Stop at Battery Spencer at top of hill and walk about 500 ft (160 m) back down Conzelman Rd. to look at folded chert on north side of road.

STOP 1-2 CHERT NEAR BATTERY SPENCER

In this excellent exposure of tightly folded radiolarian chert, the minor folds are vergent to the north; their hinge lines plunge about 25° to the west. Return to cars at Battery Spencer.

At the sharp bend in the road to the right at Battery Spencer is a complex of steep faults bringing basalt on the southwest against chert on the northeast. The roadcut west of Battery Spencer exposes dark green to black unweathered

pillow basalt that weathers orange-brown. The pillows are right-side-up. They are elongate and locally branching to the south, indicating that the sea floor fragment on which they accumulated sloped east before the 90° clockwise rotation. At the second sharp bend in the road, a slab of the basal manganiferous chert, about 200 Ma old and dipping to the southwest rests on the basalt with locally discordant contact.

Return to cars and drive west on Conzelman Rd. to Battery 129.

Doubly folded chert in roadcuts at the head of the valley west of Stop 1-2 are in the same chert body seen at the beginning of the stop. Keep left at the triangular intersection, which marks a body of sandstone. Between the intersection and Stop 1-3, the road passes several fault slices of tightly folded chert resting on basalt, in one case with basalt in fault contact over sandstone.

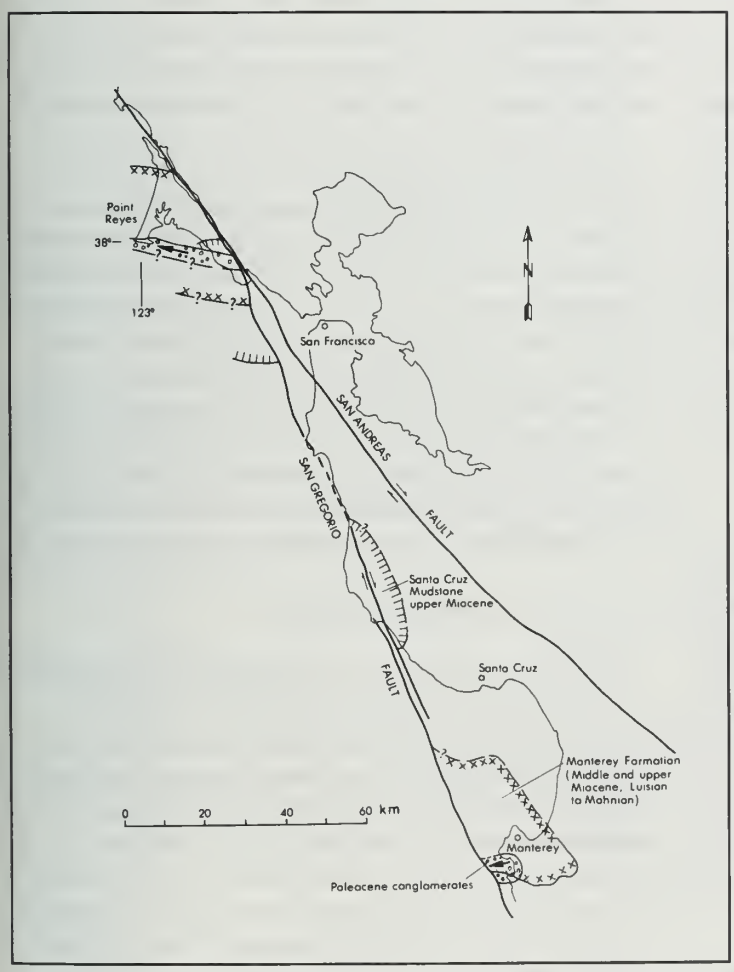

Figure 6. Distribution of offset Tertiary sequences of Point Reyes, Santa Cruz Mountains, and Monterey areas. Modified after Clark and others, 1984.

STOP 1-3 BATTERY 129

This is a classic viewpoint of the Golden Gate. At the east end of the parking area basal radiolarian chert rests on basalt. The prominent north-trending rocky ridge crest down the hill to the east is an exposure of chert in the second thrust sheet below the chert and basalt beside the parking area. Radiolarians from the near side (stratigraphic top) of the ridge crest are of Early Cretaceous age. The chert along the parking lot as far west as the nearest tunnel is of Early Jurassic age. The chert west of the first tunnel is of Middle to Late Jurassic age (Wahrhaftig and Murchey, 1987).

Continue west along Conzelman Rd. At 2 mi, turn right, then left in 15 yds, onto main road toward Pt. Bonita; continue west 0.3 mi along the north side of a wooded hill, and turn right into a large gravelled parking lot.

STOP 1-4 RODEO COVE

From the west side of the parking lot a trail leads about 1000 ft (300 m) west to the beach at the south end of Rodeo Cove. At the north end of the beach is an exposure of pillow basalt with pillow tops to the east. A pillow at the southwest corner of the exposure contains thin layers of basalt alternating with quartz-calcite rock that resulted from partial draining of the lava in the pillow and that were horizontal at the time the pillows erupted. They are now nearly vertical and strike north. Along the base of the seacliff east of the outcrop, the basalt is intruded by coarsely crystalline diabase, now deeply weathered, that makes up much of the seacliff. Around the rocky point a few feet north of the pillow-basalt outcrop is a small pocket beach in a reentrant eroded along a zone of melange and fault gouge trending northwesterly, which separates the diabase from pillow basalt in the seacliffs to the northeast.

The cliff at the south end of the beach is made of vesicular basaltic breccia, also

intruded by the diabase. The basaltic breccia dips gently east and rests on pillow basalt accessible only at low tide. Farther west along the base of the cliff, also accessible only at low tide, a layer of mixed red chert and pink limestone a few inches thick is interbedded with the basalt. The vesicular breccia, vesicles in some of the pillows, and pink limestone suggest that the basalt was erupted in much shallower water than the basalt in the thrust sheets at Stops 1-2 and 1-3 and farther north in the Marin Headlands. These features, and distinct differences between the geochemistry of this basalt and that of the main part of the headlands to the north (Shervais, 1989), justify recognizing a narrow belt along the north shore of the Golden Gate, including Point Bonita, as a fragment of a sea-mount terrane labelled the Pt. Bonita block on Fig. 2.

The exposures along the back of the beach are of angular pebble-size alluvium derived from local bedrock sources, with imbrication indicating deposition by west-flowing currents. This alluvium, and the deeply weathered bedrock on which it rests, indicate that the sea has never been higher against these hills than it is now, unlike those sections of the coast with marine terraces. The sand of the beach and of the Holocene dunes on the bluff-top behind it contains igneous minerals, indicating a source in the Sierra Nevada. They were brought through the site of the Golden Gate by the combined Sacramento-San Joaquin River during the ca. -400-ft (-120-m) low sea-level stand of the last glaciation, and were driven landward to form the dunes and the Potato Patch shoal (a submerged arcuate bar off the Golden Gate) as sea level rose.

Return to the parking lot. At the road, turn left and keep left past the Marin Headlands Visitor Center to the three-way intersection at the head of Rodeo Lagoon. Turn right (east) up Rodeo Valley, and right again at the next three-way intersection with a main road (at the west side of a military housing complex). The road goes uphill to a junction with Conzelman Rd. at a pass. Turn left at this junction onto Conzelman Rd., retracing your route east past Stop 1-2.

Where Conzelman Rd. joins the south-bound on-ramp to the Golden Gate Bridge, turn left "toward Eureka," go through the tunnel under the freeway, and immediately turn right onto the on-ramp to Hwy. 101 north. At about 3.5 mi, take the Hwy. 1 and Stinson Beach exit and follow Hwy. 1 and Panoramic Hwy. to Mountain Home, where Panoramic Hwy. leaves the ridge-crest drainage divide between Muir Woods and Mill Valley to contour along the south side of Mt. Tamalpais.

STOP 1-5 MOUNTAIN HOME

The parking lot is on the left (west) side of the road. The roadcut ahead exposes sheared sandstone and shale of the Franciscan melange, with phacoids of sandstone embedded in sheared shale. The view to the west is of Muir Woods National Monument.

Continue westward on Panoramic Hwy. Most roadcut exposures are of mixed shale and graywacke of the melange, but 2 mi beyond Stop 1-5, greenish exposures of serpentinite incorporated into melange are exposed in roadcuts, especially near Bootjack Campground and at Pantoll (the 4-way intersection at the highest point in the road).

Turn right onto Hwy. 1 into town of Stinson Beach and drive along the east shore of Bolinas Lagoon, at the north end of a graben-like structure probably related to the right offset of the San Andreas fault across the Gulf of the Farallones. Take the first road to the left (unmarked) at the head of the lagoon to Bolinas. We cross the active trace of the San Andreas fault, then turn left (south) along the west shore of the lagoon, keeping to the left. About 1.7 mi, turn right onto Mesa Rd., 0.5 mi farther, left onto Overlook Dr., and 0.4 mi farther, right onto Elm Rd. and continue to Agate Beach.

STOP 1-6 AGATE BEACH

Bolinas Mesa is an emergent marine terrace 130-200 ft (40-60 m) high cut in the siliceous beds of the Santa Cruz Mudstone. At Agate Beach (Figs. 3, 4) this mudstone is well exposed in the sea cliffs and wave-cut platform, where it is medium-bedded and laminated olive-gray to yellowish-gray siliceous mudstone. Silica content increases from 66.4 percent lower in the section to 74.5 percent here at Agate Beach to 79.0 percent higher in the section (Clark and others, 1984, Table 2). Orangish carbonate concretions are common elongate to the bedding.

This is the best-exposed and thickest section of the Santa Cruz Mudstone at Point Reyes, where 3410 ft (1040 m) of southwesterly-dipping beds are exposed between Bolinas and Duxbury Points. Resistant beds form southeasterly-striking shoals such as Duxbury Reef.

East of Duxbury Point, the section continues downward where there are extensive landslides at Bolinas, but the base is not exposed. About 1 mi (1.7 km) north of Agate Beach, the Lockhart R.C.A. No. 3-1 well is interpreted by Clark and others (1984) to have encountered 3375 ft (1029 m) of gently dipping Santa Cruz Mudstone and 65 ft (20 m) of Santa Margarita Sandstone above the siliceous Monterey Formation.

The Santa Cruz Mudstone here is locally bioturbated and contains a sparse but diverse mega- and microfossil assemblage including callianassid shrimp, echinoid spines and fragments, few pelecypod valves, and rare cetacean bones, arenaceous benthic foraminifers, and rarer calcareous foraminifers including *Bolivina obliqua*, diagnostic of a late Miocene ("Delmontian") age (Clark and others, 1984). A diatom flora from near Bolinas Point was assigned by John A. Barron (written communication, 1975, 1990) to the *Nitzchia reinholdii* zone, which he believes to be of late Miocene age.

Galloway (1977) assigned these siliceous beds at Bolinas Mesa to the Monterey Formation, and thus did not differentiate them from the more highly deformed porcelaneous and cherty Monterey beds that are exposed to the north at Stop 2-1 that are unconformable beneath the Santa Margarita Sandstone.

TRIP LOG DAY 2

From Agate Beach retrace route to Hwy. 1, turn left (north) and in 9.5 mi turn left onto Bear Valley Rd., then left again in 2 mi onto the road to Limantour Beach. In about 5.5 mi, turn left to the AYH hostel.

STOP 2-1 AYH, COAST CAMP

At Stop 2-1a, about 0.4 mi (0.6 km) northeast of the AYH, the Monterey Formation exposed in roadcuts consists of thin-bedded and laminated porcellanite and chert with several thin to medium interbeds of arkosic sand. The Monterey is locally contorted, but generally strikes N50°-60°W and dips 30°-50°SW.

The trail to Coast Camp beach (Stop 2-1b) is along a ridge southeast of the AYH, where the Santa Margarita Sandstone (generally not exposed) includes at its base as much as 165 ft (50 m) of "clean" slightly granular medium-grained biotitic arkose and several thin interbeds of slightly siliceous mudstone. The path passes several resistant strike exposures of slightly bituminous glauconitic sandstone of the upper Santa Margarita. The southwest-dipping siliceous Santa Cruz Mudstone, poorly exposed here, is estimated to be as thick as 72 ft (22 m), pinching out to the northwest. The overlying Purisima Formation, brownish fine-grained lithic sandstone, is exposed along the trail to the south.

At Stop 2-1b (Figs. 1, 3, 4) about 0.4 mi (0.7 km) east of Coast Campground, the Santa Margarita, which dips 14°NW, is unconformable on the Monterey, which dips 34°NE. The Monterey is thin-bedded dark yellowish-brown porcellanite with dark chert pods and a few dolomite interbeds. The porcellanite yields fish debris and fecal pellets. The stratigraphically diagnostic diatom *Coscinodiscus praeyabei* from a dolomite interbed about 36 ft (11 m) below the unconformity is reported by White (1990) to range from 14.7-13.4 Ma (Luisian-Mohnian).

The Santa Margarita is thin here and includes at its base a 3 ft (1 m) thick glauconitic conglomerate with abundant Monterey chert, few volcanic porphyry, and rare granitic pebbles and cobbles. About 15 ft (5 m) of interbedded glauconitic sandstone and siltstone are overlain by thin-bedded siliceous Santa Cruz Mudstone that contains few diatoms and radiolarians. The glauconitic sandstone has yielded a K-Ar date of 9.3 ± O.5 Ma (Galloway, 1977), which is late Miocene. Thus, the hiatus represented by this unconformity may be on the order of 4-5 my.

A marine terrace marks the east shore of Drakes Bay for most of the distance between Bolinas Lagoon and Limantour Spit. Bolinas Mesa, part of this terrace, stands 130-200 ft

(40-60 m) above sea level. The marine terrace is interrupted for a 4 mi (6.5 km) stretch from near Double Point to Millers Point by the landslide complex of the Lake Ranch area. Northward from Millers Point, the shoreline angle of this marine terrace descends northward from 100 ft (30 m) at Millers Point to sea level a short distance west of Coast Camp and Stop 2-1b. The alluvial cover passes beneath sea level near Stop 2-1c, and the Point Reyes Peninsula to the west displays a drowned topography.

From Stop 2-1c return on the Limantour Beach Rd. to Bear Valley Rd., turn left on Bear Valley Rd., left again onto Sir Francis Drake Hwy., and follow Sir Francis Drake Hwy. 21.4 mi to its end at the parking lot to the Point Reyes Lighthouse.

STOP 2-2 POINT REYES

The Salinian basement here (Fig. 7), exposed along the south side of the road east of the parking lot, is porphyritic granodiorite with euhedral K-feldspar phenocrysts that average 0.8-1.2 in (2-3 cm) and are as long as 2 in (5 cm). The granodiorite has 2-12 percent dark minerals, which are at least 4/5 biotite, the remainder hornblende, about 30 percent quartz, 25-35 percent K-feldspar, and the remainder plagioclase. Chemically it is about 70 percent SiO_2, 15 percent $A1_20_3$, 2.5 percent FeO, 2.8 percent CaO, 3.3 percent Na_20, and 3.4 per-cent K_20 (from Ross in Clark and others, 1984; Ross, 1984). Ross correlates this rock with porphyritic granodiorite on the Monterey Peninsula east of the San Gregorio fault (Fig. 5).

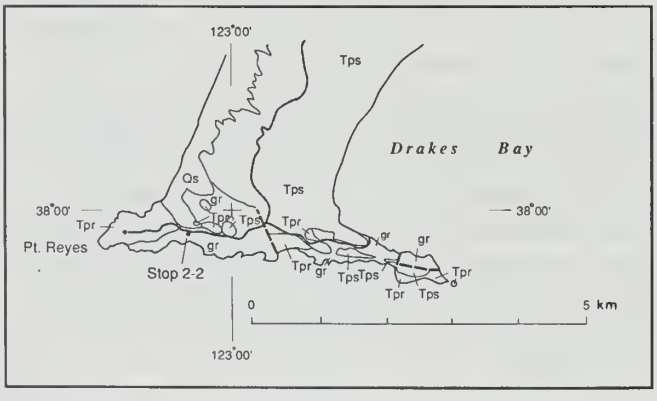

Figure 7. Geology of Point Reyes and vicinity, showing location of Stop 2-2. Qs, dune and beach sand; Tps, Purisima and Santa Margarita formations; Tpr, Point Reyes Conglomerate of Galloway, 1977; gr, porphyritic granodiorite of Point Reyes. From Galloway, 1977.

Resting unconformably upon this granodiorite is the Point Reyes Conglomerate of Galloway (1977). The northwest-dipping type section is well exposed along the steps leading to the lighthouse and consists of interbedded very thick graded arkosic sandstone and very thick sandy conglomerate, with conglomerate beds locally channeled into the sandstone. Porphyritic granodiorite boulders as long as 7-10 ft (2-3 m) are conspicuous. Clasts consist of 30-50 percent porphyritic granodiorite boulders, 30-40 percent well-rounded purple and black silicic volcanic porphyry pebbles and cobbles, and 10-20 percent light-colored quartzite pebbles, with lesser amounts of red chert and black and green volcanic pebbles.

This section displays thinning and fining upward cycles typical of channelized submarine fan deposits. Several channels trend northwesterly, and paleocurrent indicators suggest northwest-flowing currents. Siltstone rip-up clasts contain large specimens of the arenaceous foraminifer *Bathysiphon,* and a Paleocene arenaceous fauna from near the base of this lighthouse section is characteristic of bathyal depths. Clark and others (1984) believe that these beds are part of a northwesterly-trending, upper mid-fan channel complex that was derived from a porphyritic granodiorite and silicic volcanic or older conglomerate terrain to the southeast.

STOP 2-3 DRAKES BEACH

The Purisima Formation is beautifully exposed in the sea cliffs here (Figs. 3, 4). These light-colored rocks reminded Sir Francis Drake of the chalk cliffs of England when he landed here in 1579. Galloway (1977) designated these beds as the type section of his Drakes Bay Formation. Based on similarities in stratigraphy, lithology, and fauna, Clark and others (1984) correlated these beds with the Purisima Formation of the Santa Cruz Mountains to the south.

The Purisima is typically a thick- to very thick-bedded, light olive-gray siltstone that upon weathering becomes nodular and yellowish gray. Locally the siltstone is diatomaceous and includes

a few dark replacement chert pods. Spheroidal carbonate concretions, elongate as much as 7 ft (2 m) parallel to the bedding, form prominent discontinuous interbeds and locally contain cetacean bones. Several thick interbeds of light olive-gray, well-sorted, fine-to medium-grained lithic arkose appear "bluish" where fresh and are semifriable and commonly bioturbated.

Diatoms occur with radiolarians and siliceous sponge spicules. Cetacean bones are common, whereas pinniped bones are rare and include the remains of a primitive fur seal and a walrus. Mollusks and echinoids are also rare.

A diatom flora collected from the sea cliff section at Drakes Beach was assigned by John A. Barron to Subzone b of the *Nitzchia reinholdii* zone (Zone X in Clark and others, 1984). Repenning and Tedford (1977) believe that the pinniped fauna is diagnostic of a latest Miocene or Pliocene age, whereas the mollusk *Neptunea colmaensis* (Martin) occurs elsewhere in beds of Pliocene age. As much as 130 ft (40 m) of the Purisima at Drakes Bay falls within the latest Miocene, but the upper part that is not as well dated is considered by Clark and others (1984) to range into the Pliocene.

STOP 2-4 KEHOE BEACH

Trailhead is at mi 5.5 on the Pierce Point Rd. A safe turn-around for buses is 0.5 mi north.

At Kehoe Beach (Fig. 8), the Laird Sandstone rests nonconformably upon the granitic basement and is overlain conformably by Monterey Formation.

The Laird section is at its thickest, most fossiliferous and best-exposed at Kehoe Beach. This section will be designated as the stratotype (Clark, J.C., Brabb, E.E., and Link, M.H., in prep.). The lower 100 ft (30 m) is well exposed in cliffs along the axis of a syncline (Fig. 9). A complete measured section (Fig. 10), is about 210 ft (64 m) thick.

The Laird rests nonconformably on granitic basement and is conformably overlain here by Monterey Formation. At Kehoe Beach, its base contains a lag about 2-ft (0.6-m) thick, composed of boulders, pebbles, and sand that are weathered and partially cemented debris from the underlying granitic basement. This basal lag is interpreted as grus or regolith reworked by waves as the sea transgressed. At locality B2582, barnacle (probably *Notomegabalanus*, according to V.A. Zullo, written communication, 1990), mollusk (mostly pectens and *Ostrea* sp.), small echinoid, and bryozoan fragments occur in this sand-matrix-supported basal conglomerate.

Overlying the basal lag is thick-bedded, medium- to fine-grained arkosic sandstone with thick beds of coarse sandy, granule conglomerate. Some sandstone beds are laterally continuous. Granitic pebbles in several beds delineate crude graded bedding and parallel and cross stratification. Several carbonate-cemented and concretionary zones are up to 3.3 ft (1 m) thick. Individual

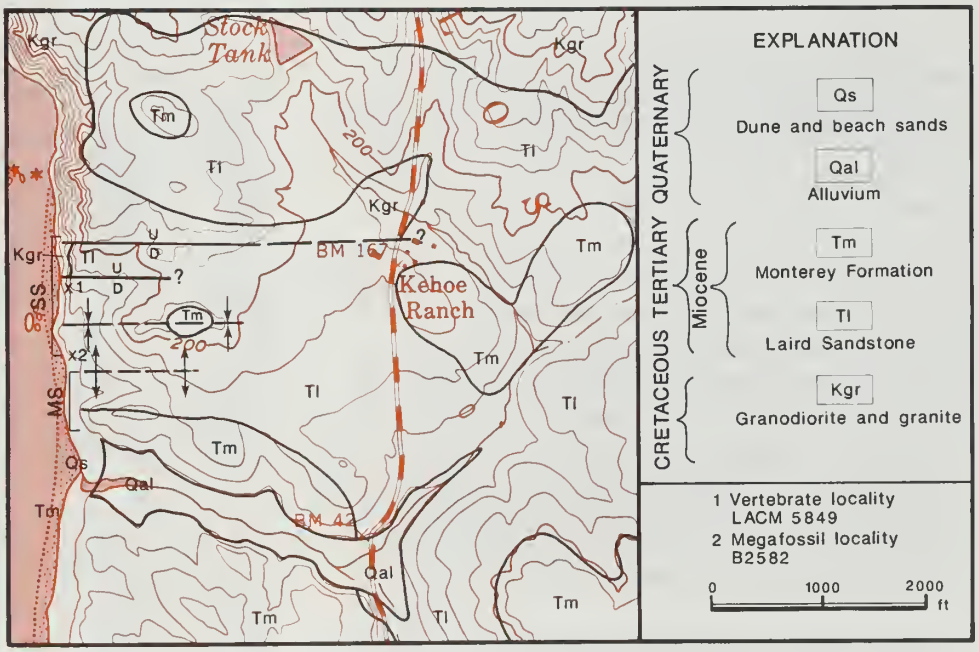

Figure 8. Geologic map of the Kehoe Beach area, showing fossil localities, sketch section (SS, Fig. 9), and measured section (MS, Fig. 10). Inland geology after Galloway, 1977. Base map from Tomales 7.5-minute quadrangle.

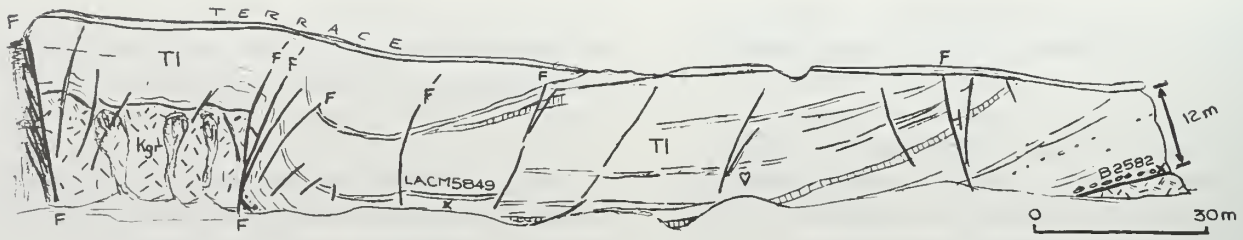

Figure 9. Sketch section of the northern part of the Kehoe Beach cliffs, looking east and showing the Laird Sandstone (Tl) in a syncline, which is faulted against a granitic basement (Kgr) horst and is truncated to the north by basement faults. F, faults; LACM5849, B2582, fossil localities; see Fig. 8 for location.

concretions are spherical, up to 1 ft (0.3 m) in diameter, and locally contain pebbles and fossils, including barnacles and rare desmostylian teeth.

Leptopecten andersoni (Arnold), identified by Judith Terry-Smith, from field locality B2582 (Fig. 9) is diagnostic of middle Miocene age, whereas the echinoids from this same locality identified by J. Wyatt Durham as *Astrodapsis brewerianus* (Rémond) and *A.* cf. *A. pabloensis* Kew (*in* Wahrhaftig, 1989) suggest a late middle to early late Miocene age. The desmostylian teeth from locality LACM5849 (Fig. 9) have recently been identified by Daryl P. Domning (written communication, 1990) as *Desmostylus* cf. *D. hesperus* Marsh, which is typically middle Miocene on the West Coast.

The Laird Sandstone at Kehoe Beach is transitional into the Monterey Formation, which consists of alternating thin-bedded and laminated micaceous siltstone and pinkish-gray siliceous mudstones, porcellanites, and fine-grained sandstones. The sandstone interbeds are 0.8-24 in (2-60 cm) thick, are graded, and contain parallel and cross laminae and mudstone intraclasts. Abundant fish scales and fragments and external molds of calcareous foraminifers occur in these finer-grained strata. This Laird-Monterey section records progressive deepening after transgression of the middle Miocene seas. The graded sandstone interbeds in the lower Monterey are interpreted by Clark and Link (1990) to be either distal storm deposits or thin clastic turbidities interbedded with slope and basinal deposits.

An excellent cliff-base outcrop of the crystalline basement about 655 ft (200 m) north of the southern fault in the cliff exposes an early coarse foliated hornblende-biotite granodiorite cut by a dark foliated dike, invaded in turn by a non-foliated complex of fine diorite, granodiorite, aplite, and pegmatite dikes (Fig. 11). The granitic basement of the cliffs is cut by numerous diversely oriented fractures and shear zones.

Return on Pierce Point Rd. and Sir Francis Drake Hwy. through Inverness, left on Hwy. 1 through town of Point Reyes Station, and at the northeast end of town, turn right onto the Point Reyes-Petaluma Rd. Turn left again 3.1 mi farther, at a T-intersection on far side of bridge, and 0.2 mi farther, park either in roadway on right on near side of bridge or cross road to park in flat on left. In either case, watch carefully for fast-moving traffic when slowing or crossing road.

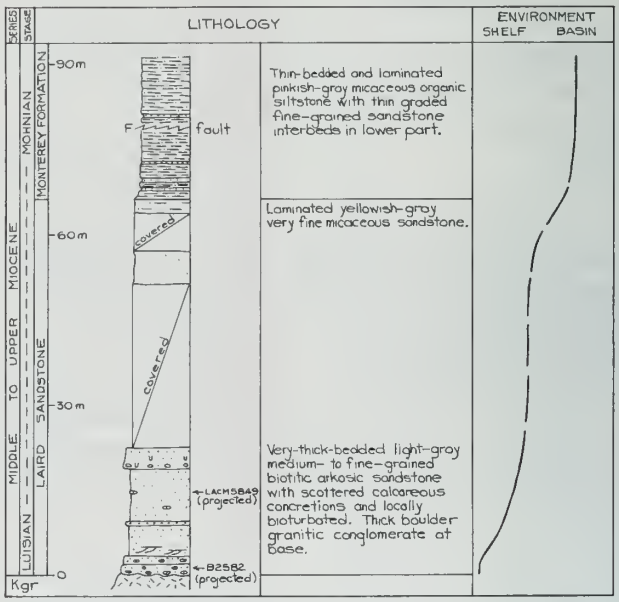

Figure 10. Laird Sandstone-Monterey Formation section on Kehoe Beach, measured by J.C. Clark, E.E. Brabb, and M.H. Link, 1985 and 1989 (see Fig. 8 for location).

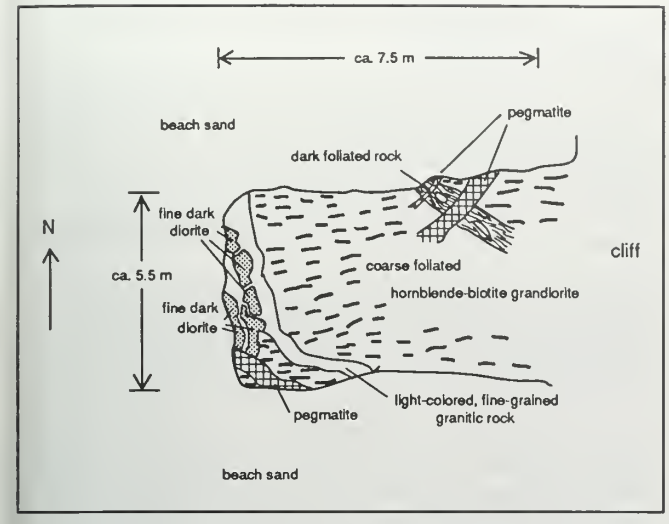

Figure 11. Field sketch map of exposure near north end of Kehoe Beach, showing cross-cutting relationships between several plutonic rocks. From Wahrhaftig, 1989, Fig. 38.

STOP 2-5 PILLOW BASALT OF NICASIO RESERVOIR TERRANE

The dark green basalt here is a spilite, containing albitized plagioclase phenocrysts and chlorite, pumpellyite, and laumontite, probably from reaction with seawater during or shortly after eruption (Cloos, 1990). Pillow dimensions and layering in chert suggest that the paleo-horizontal dips 45°NE on the average, and pillow tops are to the northeast (Gluskoter, 1968). Radiolarians indicate its age to be Early Cretaceous, Valanginian to Barremian (Murchey and Jones, 1984; Wright, 1984). Based on the 45° dip, the body of basalt containing these pillows is 4495 ft (1370 m) thick and the pillows are 1975 ft (600 m) above its base, which is probably tectonic. The body is broken by numerous faults, and the true thickness of the basalt is unknown. Amygdules (filled vesicles) are common in pillows in the eastern part of this mass. Paleomagnetic evidence suggests that the Nicasio Reservoir terrane has been displaced about 16°N and rotated about 86° clockwise since accretion (Hagstrum, 1990).

Continue northeast on the Pt. Reyes-Petaluma Rd. At 2.8 mi, turn right onto Nicasio Rd. Nicasio Valley and many surrounding hills are underlain by Franciscan melange. Isolated bedrock monuments are exotic blocks of chert, greenstone, hard massive sandstone, and metamorphics in a matrix of sheared and crushed shale and sandstone. When the sun is low, shadows on the hillsides bring out a rumpled topography caused by shallow earthflows.

One mile beyond Nicasio, turn left on Lucas Valley Rd., which continues through the melange. Serpentinite and sandstone are present in roadcut exposures. Six miles beyond Nicasio, the large rock, known as Big Rock, on the north side of the road at the summit, consists of eclogite. It is painted brown by the farmer to hide graffiti. Big Rock Ridge, the high mountain to the north, is K-feldspar-bearing sandstone of the Novato Quarry terrane of Late Cretaceous (Campanian) age.

In about 9.8 mi turn right onto Hwy. 101 to San Francisco. Roadcuts along the highway for the next 12 mi expose melange of the Central terrane.

REFERENCES CITED

Blake, M.C., Jr., Howell, D.G., and Jayko, A.S., 1984, Tectonostratigraphic terranes of the San Francisco Bay region, *in* Blake, M.C., Jr., ed., *Franciscan geology of northern California*: Pacific Section, Society of Economic Paleontologists and Mineralogists, v. 43, p. 5-22.

Bowen, O.E., Jr., 1965, Stratigraphy, structure, and oil possibilities in Monterey and Salinas quadrangles, California: American Association of Petroleum Geologists, Pacific Section, 40th Annual Meeting, Bakersfield, CA, p. 48-67.

Clark, J.C., Brabb, E.E., Greene, H.G., and Ross, D.C., 1984, Geology of Point Reyes peninsula and implications for San Gregorio fault history, *in* Crouch, J.K., and Bachman, S.B., eds., *Tectonics and sedimentation along the California margin*: Pacific Section, Society of Economic Paleontologists and Mineralogists, p. 67-86.

Clark, J.C., and Link, M.H., 1990, Lithology and stratigraphy of rocks exposed at Kehoe Beach, *in* Bilodeau, B.J., and Davis, S.O., eds., *Geologic guidebook to the Point Reyes area, northern California*: American Association of Petroleum Geologists, Pacific Section Guidebook No. 66, p. 30-34.

Clifton, H.E., and Hill, G.W., 1987, Paleocene submarine canyon fill, Point Lobos, California, *in* Hill, M.L., ed., *Cordilleran Section of the Geological Society of America Centennial Field Guide Volume 1*, p. 239-244.

Cloos, M., 1990, Nicasio pillow basalts: a fragment of a sea-mount accreted during Franciscan subduction, *in* Bilodeau, B.J., and Davis, S.O., eds., *Geologic guidebook to the Point Reyes area, northern California*: American Association of Petroleum Geologists, Pacific Section Guidebook No. 66, p. 9-16.

Curry, F.B., Cox, A., and Engebretson, D.C., 1984, Paleomagnetism of Franciscan rocks in the Marin Headlands, *in* Blake, M.C., Jr., ed., *Franciscan geology of northern California*: Pacific Section, Society of Economic Paleontologists and Mineralogists v. 43, p. 89-98.

Galloway, A.J., 1977, Geology of the Point Reyes Peninsula, Marin County, California: *California Division of Mines and Geology Bulletin 202*, 72p.

Gluskoter, H.J., 1969, Geology of a portion of western Marin County, California: *California Division Mines and Geology Map Sheet 11*, 1:48,000.

Graham, S.A., and Dickinson, W.R., 1978, Evidence for 115 kilometers of right slip on the San Gregorio-Hosgri fault trend: *Science*, v. 199, p. 179-181.

Hagstrum, J.T., 1990, Remagnetization and northward coastwise transport of Franciscan Complex rocks, northern California: a reinterpretation of the paleomagnetic data: *Tectonics*, v. 9, no. 5, p. 1221-1233.

Karl, S.M., 1984, Sedimentologic, diagenetic, and geochemical analysis of upper Mesozoic ribbon cherts from the Franciscan assemblage at the Marin Headlands, California, *in* Blake, M.C., Jr., ed., *Franciscan geology of northern California*: Pacific Section, Society of Economic Paleontologists and Mineralogists, v. 43, p. 71-88.

Murchey, Benita, 1984, Biostratigraphy and litho-stratigraphy of chert in the Franciscan complex, Marin Headlands, California, *in* Blake, M.C., Jr., ed., *Franciscan geology of northern California*, Pacific Section, Society of Economic Paleontologists and Mineralogists, v. 43, p. 51-70.

Murchey, B., and Jones, D.L., 1984, Age and significance of chert in the Franciscan Complex in the San Francisco Bay region, *in* Blake, M.C., Jr., ed., *Franciscan geology of northern California*: Pacific Section, Society of Economic Paleontologists and Mineralogists, v. 43, p. 23-30.

Repenning, C.A., and Tedford, R.H., 1977, Otarioid seals of the Neogene: *U.S. Geological Survey Professional Paper 992*, 93p.

Ross, D.C., 1977, Pre-intrusive metasedimentary rocks of the Salinian block, California —a tectonic dilemma, *in* Stewart, J.H., Stevens, C.H., and Fritsche, A.E., eds., *Paleozoic Paleogeography of the western United States*: Pacific Section, Society of Economic Paleontologists and Mineralogists, Pacific Coast Paleogeography Symposium 1, p. 371-380.

Ross, D.C., 1978, The Salinian block—A Mesozoic granitic orphan in the California Coast Ranges, *in* Howell, D.G., and McDougall, K.A., eds., *Mesozoic paleogeography of the western United States*: Pacific Section, Society of Economic Paleontologists and Mineralogists, Pacific Coast Paleogeography Symposium 2, p. 509-522.

Ross, D.C., 1984, Possible correlations of basement rocks across the San Andreas, San Gregorio-Hosgri, and Rinconada-Reliz-King City faults, California: *U.S. Geological Survey Professional Paper 1317*, 37p.

Shervais, J.V., 1989, Geochemistry of igneous rocks from Marin Headlands, *in* Wahrhaftig, C., and Sloan, D., eds., *Geology of San Francisco and vicinity*: 28th International Geological Congress Field Trip Guidebook T105, American Geophysical Union, p. 40-41.

Wahrhaftig, C., 1984, Structure of the Marin Headlands block, California: a progress report, *in* Blake, M.C., Jr., ed., *Franciscan geology of northern California*: Pacific Section, Society of Economic Paleontologists and Mineralogists, v. 43, p. 31-50.

Wahrhaftig, C., 1989, Stop 5, Kehoe Beach, *in* Wahrhaftig, C., and Sloan, D., eds., *Geology of San Francisco and vicinity*: 28th International Geological Congress Field Trip Guidebook T105, American Geophysical Union, p. 59-61.

Wahrhaftig, C., and Murchey, B., 1987, Marin Headlands, California: 100-million-year record of sea-floor transport and accretion: *in* Hill, M.L., ed., *Cordilleran Section of the Geological Society of America Centennial Field Guide Volume 1*, p. 263-268.

Weber, G.E., and Lajoie, K.R., 1977, Late Pleistocene and Holocene tectonics of the San Gregorio fault zone between Moss Beach and Point Año Nuevo, California (abs.): *Geological Society of America Abstracts with Programs*, v. 9, no. 4, p. 524.

White, L.D., 1990, Stratigraphy and paleooceanographic history of the Monterey Formation at Pt. Reyes and Pt. Año Nuevo, California, *in* Garrison, R.E., *Geology and tectonics of the central California coast region, San Francisco to Monterey*: American Association of Petroleum Geologists, Pacific Section Guidebook No. 67, p. 91-104.

Wright, R.H., 1984, Geology of the Nicasio Reservoir terrane, Marin County, California, *in* Blake, M.C., Jr., ed., *Franciscan geology of northern California*: Pacific Section, Society of Economic Paleontologists and Mineralogists, v. 43, p. 99-112.

Quaternary Tectonics of the Northern San Andreas Fault, San Francisco Peninsula, Point Reyes, and Point Arena, California

Carol Prentice,[1] Tina M. Niemi,[2] and N. Timothy Hall[3]

INTRODUCTION

The great San Francisco earthquake of April 18, 1906, was generated by rupture of the northern San Andreas fault (SAF). This field trip will visit sites where the effects of the 1906 earthquake are still visible, as well as sites where paleoseismic investigations have begun to characterize the prehistoric behavior of this portion of the SAF (Fig. 1). Many of these sites are on private land not readily accessible to the general public. Road log is at the end of the paper.

Probabilistic earthquake assessments depend largely on recurrence and slip-rate data gathered from analyses of geologic information about prehistoric fault behavior. Recent subsurface investigations at sites on the San Francisco Peninsula, near Olema, and near Point Arena have provided data on pre-1906 earthquakes, Holocene slip rate, and fault segmentation. While these studies have added significantly to the understanding of the recent behavior of the northern SAF, many questions remain, and more work is needed to understand this critical segment of the SAF.

STOP 1 - SAN ANDREAS DAM

The active strands of the SAF lie along the lower slopes of the northeast side of the rift valley, 200-400 ft (60-120 m)[4] east of the valley axis (Fig. 2). The knobby terrane with highly variable slopes east of the 1906 trace is developed on Franciscan melange (Brabb and Pampeyan, 1972), and contrasts strikingly with the steeper and more uniform slopes developed primarily on Franciscan greenstone and graywacke along the western margin of the rift valley.

San Andreas Dam is a 720-ft (220-m) long earthfill embankment built across the valley of the SAF zone. The original dam was constructed between 1868 and 1870 and was then raised in 1875 and 1928. Herman Schussler, Chief Engineer for the Spring Valley Water Company, published a folio 97 days after the 1906 earthquake that contained detailed maps of displaced cultural features and dozens of carefully annotated photographs showing the SAF (Schussler, 1906).

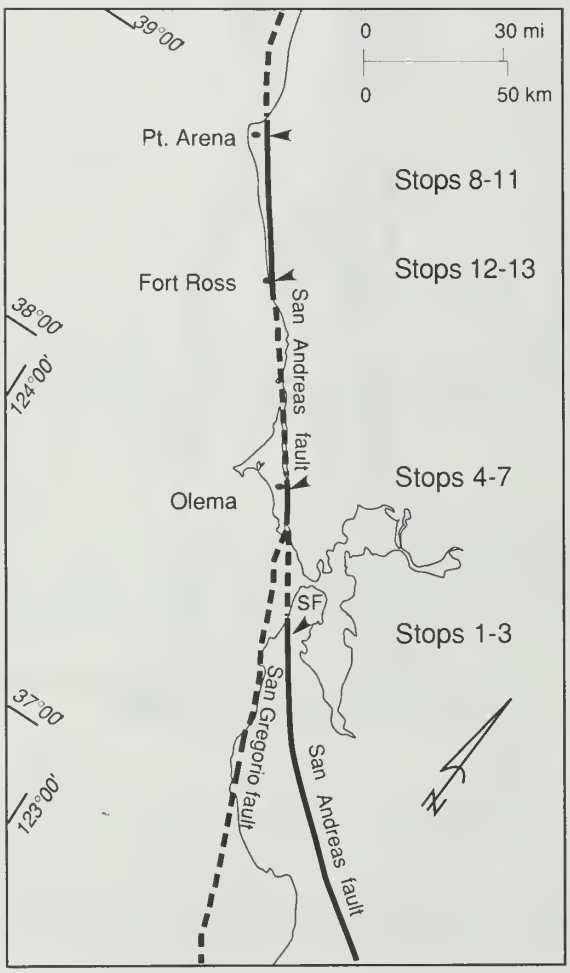

Figure 1. Map showing location of field trip Stops 1-13.

[1] U. S. Geological Survey, 345 Middlefield Rd. MS 977, Menlo Park, CA 94025
[2] Dept. of Geology, Stanford University, Stanford, CA 94305, and Earth Sciences Associates, Palo Alto, CA 94304
[3] Geomatrix Consultants, One Market Plaza, Spear Street Tower, Suite 717, San Francisco, CA 94105
[4] Most measurements in this paper were made in metric units; approximate English conversions included for convenience.

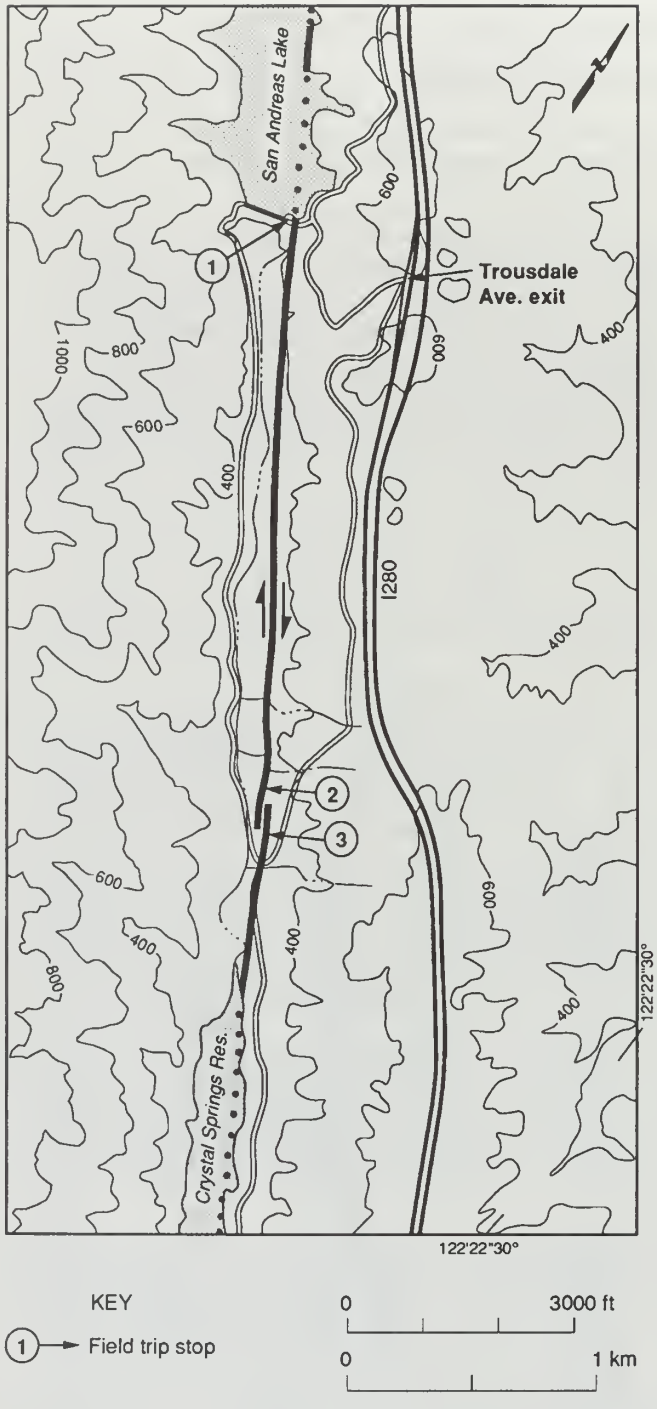

Figure 2. Topographic map of the SAF valley between San Andreas Dam and Lower Crystal Springs Reservoir. Field trip Stops 1-3 are marked.

The brick waste weir tunnel below San Andreas Dam was displaced right-laterally 9 ft (2.7 m).

The dam embankment did not fail, because shearing along the SAF was confined to a bedrock ridge that forms the eastern abutment of the dam. The internal geometry of this ridge was exposed in bulldozer cuts and trenches (Hall, 1984).

STOP 2 - OFFSET CYPRESS TREES AND RIGHT DEFLECTED CHANNEL

The best-preserved offset cultural features on the San Francisco Peninsula are a fence and a row of cypress trees near Crystal Springs Reservoir (Fig. 2). Here a right-lateral displacement of 9 ft (2.7 m) is still clearly visible. The 1906 trace of the SAF lies in a trough with a small closed depression. The SAF can be followed to the northwest where prior earthquakes have offset and deflected an incised stream between 170 and 285 ft (52-87 m). This deflection represents 19 to 32 seismic events comparable in slip to that of 1906, suggesting the active trace has not changed location for thousands of years.

STOP 3 - SLIP RATE STUDY ON PENINSULA SEGMENT OF THE SAF

Physiographic and stratigraphic evidence at this site were used to develop a geomorphic model from which Hall (1984) estimated a minimum late Holocene slip rate for the 1906 trace of the SAF of 0.5 in/yr (12 mm/yr). According to this model, deposition on a fan ponded behind a shutter ridge ceased either when slip on the fault removed the ridge from the path of the stream or when a flood added sufficient sediment to the surface of the fan to allow the stream to overtop the ridge. This event allowed the stream to incise a shorter, steeper channel straight across the fault. Deposition on the fan surface ceased at the time of this incision. After establishing its new channel, the stream has been dextrally offset approximately 44 ft (13.4 m) by slip on the SAF.

Estimating when the stream established its new straight channel across the fault is critical for calculating the rate of slip. In 1981, a conventional radiocarbon age of 1130 ± 160 yrs B.P. was determined for detrital charcoal collected between 6-18 in (15-45 cm) below the surface of the fan above a prominent stone line (Hall, 1984). In 1990, the trench was resampled, and seven AMS ^{14}C ages were determined for individual detrital

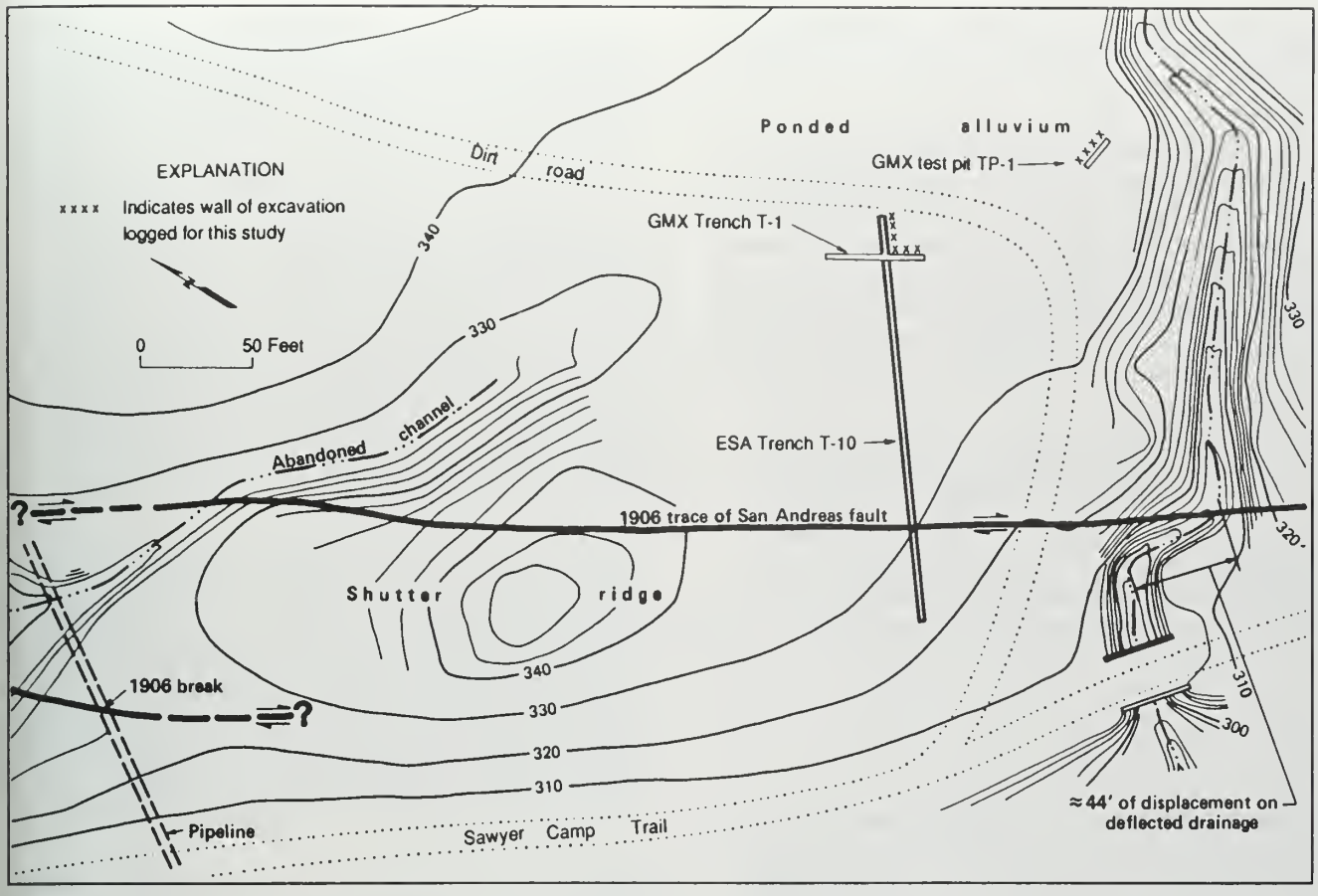

Figure 3. Map showing location of excavations for radiocarbon samples within alluvium ponded against the San Andreas fault, approximately 1.6 mi (2.6 km) south of San Andreas Dam (modified from Hall, 1984, Fig. 6). Location of Stop 3 shown on Fig. 2.

charcoal grains collected within the upper 12 in (30 cm) of the fan (Fig. 3). The AMS ages range from 1810 ± 50 to 2790 ± 60 radiocarbon yrs B.P. These ages are substantially older than the original value. By considering three probability distributions that might model the actual population of charcoal grain ages within the upper 12 in (30 cm) of the ponded alluvium, we estimate that the most likely difference between the youngest date of the set and the time of deposition is between 80-190 yrs. Applying this estimated correction to the youngest dendrochronologically corrected radiocarbon age (Stuvier and Pearson, 1986), the highest slip rate that can be derived from the new data is about 0.3 in/yr (8-9 mm/yr). This is significantly lower than geodetic estimates of modern strain accumulation on the San Francisco Peninsula (Prescott and others, 1981; Matsu'ura, and others, 1986). The model for the geomorphic evolution of this site may be incomplete or incorrect. Additional paleoseismic investigations on the peninsula segment of the SAF are required to resolve these apparent discrepancies.

STOP 4 - PT. REYES NATIONAL SEASHORE VISITOR CENTER

In Marin County, the SAF lies in a linear trough that extends from Bolinas Lagoon in the south to Tomales Bay in the north. In this area the SAF juxtaposes crystalline and sedimentary rocks of the Salinian block on the west with rocks of the Franciscan Complex on the east (Blake and others, 1974; Galloway, 1977). An estimated 195 mi (315 km) of right-lateral displacement occurred on the SAF since post-early Miocene time (Graham and others, 1989). Cumulative displacement of about 280 mi (455 km) of the Pt. Reyes Peninsula along the SAF system is estimated by adding 40-70 mi (70-115 km) of slip

on the San Gregorio fault since late Miocene time (Graham and Dickinson, 1978) to the SAF slip (Clark and others, 1984).

The Bear Valley Visitor Center of Pt. Reyes National Seashore is on the site of the Skinner Ranch. Here, the SAF lies along the southwest margin of a medial ridge in the fault valley that is underlain by late Pleistocene terrace deposits (Hall and Hughes, 1980). The northeast margin of this ridge has been eroded by the meanders of Olema Ck. during the late Holocene. After the 1906 earthquake, G.K. Gilbert mapped 14-16 ft (4.4 to 4.9 m) of right lateral slip from several offset features: a fence, bushes, a path, and the southeast corner of the cow barn on the Skinner Ranch (Lawson, 1908). Although none of these cultural features has survived, the sidehill bench of the 1906 fault trace and a reconstruction of both the barn and the offset fence can be seen along the Earthquake Trail (Hall, 1981).

STOP 5 - BOUCHER RANCH

After visiting the Skinner Ranch and the Payne Shafter Ranch (now the Vedanta Retreat), Gilbert followed the SAF to the southeast toward the Boucher Ranch. The SAF is marked by a linear series of sag ponds and has formed a broad sidehill bench between Olema Ck. on the east and the northeast-facing slope of Inverness Ridge on the west. The fault is also characterized by multiple subparallel traces. Using Gilbert's photographs and field descriptions, Hall and others (1986) mapped the traces of the SAF on a two-ft contour map of the Boucher Ranch site. Gilbert noted, "*Here for the first time I see features which might have been made by a similar fault 10 or 20 years ago. They are inflections of the surface quite similar to the ones recently made*" (Gilbert, 1907, p. 25-6). The multiplicity of fault strands in the Boucher Ranch area that may have been active at different times makes this an undesirable site for paleoseismic investigations.

STOP 6 - SLIP RATE STUDY AT VEDANTA RETREAT WIND GAP

At the Vedanta Retreat, Gilbert's descriptions and photographs of the 1906 rupture indicate that (1) the SAF is a single strand within a zone of secondary cracking 10-15 ft (3-4.5 m) wide, (2) local subsidence ponded water 28 in (70 cm) deep along the fault trace, and (3) the 1906 trace shifted from the base of the medial ridge to a sidehill bench southeast of a wind gap in the ridge.

The slip-rate study site is a wind gap cut across the medial ridge (Fig. 4). South of the wind gap, the 1906 trace lies high on the ridge and is marked by a linear sidehill bench and sag. At the gap, the 1906 trace steps 26 ft (8 m) to the left, creating a restraining geometry marked by thrust faults. Streams that formerly flowed eastward across the SAF through the wind gap, have been blocked by a slice of the ridge translated to the northwest along the fault. North of the wind gap this shutter ridge is buried below marsh deposits.

Subsurface information about fault characteristics and channel morphologies within the wind gap and in the marsh to the west was obtained by trenching. Before 1700 years ago, streams originating west of the fault, principally Gravel Ck., flowed eastward through the wind gap. Slip on the SAF has deflected this stream and diverted its drainage to the northwest by two processes: (1) lateral translation of a shutter ridge into the

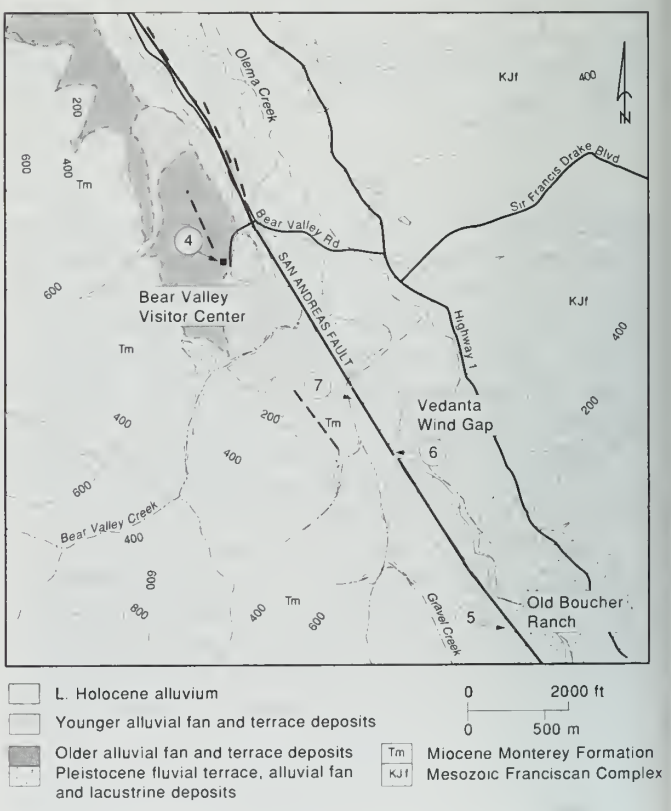

Figure 4. Map showing locations of Stops 4 through 7.

wind gap, and (2) development of a graben-like trough along the fault trace. Gravel Ck. later built an alluvial fan into the south end of the marsh and now reaches Olema Ck. by flowing through the water gap at the Vedanta Retreat barn, about 1640 ft (500 m) to the northwest.

Excavations east of the SAF at the north end of the wind gap exposed a distinctive channel deposit, 8-10 ft (2.5-3.0 m) wide, of wood debris and pebble-sized clasts derived from the Monterey Formation. This buried stream deposit represents the last narrow Gravel Ck. channel through the wind gap. West of the SAF and northwest of the wind gap, a channel of the same dimensions, lithology, and age has been identified in trenches (Fig. 5). Detrital organic material in the offset channel deposit has a weighted average, ^{13}C fractionation, and dendrochronologically calibrated age of 1790 ± 85 yrs B.P. (95% confidence level). These matching channel segments show 130 ± 11 ft (40.5 ± 3.5 m) of right separation, suggesting a minimum slip rate of about 1 in/yr (23 ± 3 mm/yr) for the segment of the SAF north of the junction with the San Gregorio fault.

STOP 7 - DOUGLAS FIR TREES

During excavation of trenches, we found well-preserved trees (Douglas fir, *Pseudotsuga menziesii*) buried at various depths in the Vedanta marsh. One tree fell across the SAF about 750 yrs ago and appears to have been offset by fault slip. These trees are potentially excellent piercing points for future slip-rate studies at this site. Additionally, their rings may contain a record of prehistoric seismic events. Slabs of the trees have been sent to Gordon Jacoby at the Tree-Ring Laboratory of the Lamont-Doherty Geological Observatory for tree ring analysis. Cores taken from living Douglas firs along this reach of the SAF show growth anomalies after 1906, suggesting earthquake damage and the possibility of establishing the dates of prehistoric earthquakes.

STOP 8 - SEA CLIFF EXPOSURE OF THRUST FAULT NEAR POINT ARENA

Exposures along the modern sea cliff northwest of the old Coast Guard LORAN station near Point Arena (Fig. 6) reveal two Quaternary thrust faults about 4 mi (7 km) from the SAF. The first of these exposures is illustrated in Fig. 7. Miocene bedrock has been thrust over deposits that overlie the lowest Pleistocene wave-cut platform. Several other exposures in this vicinity show similar relationships. Two nearby exposures show a thrust fault that soles into a bedding plane within the Miocene bedrock. Faulted terrace deposits are also exposed in a nearby sinkhole. These relationships indicate recent compression along the plate boundary in this area.

STOP 9 - OFFSET TREES AND EXCAVATION SITE

A row of trees that was offset in 1906 is still present less than 300 ft (100 m) northwest of the Skaramella ranch house (Fig. 8). This was the Fitch ranch at the time of the 1906 earthquake (Brown and Wolfe, 1972). Two fences in this area were measured after the earthquake and found to be offset 16 ft (5 m) (Lawson, 1908). However, the row of trees appears to be offset more than 5 m; whether this difference is the result of afterslip or is due to variation in amount of offset along

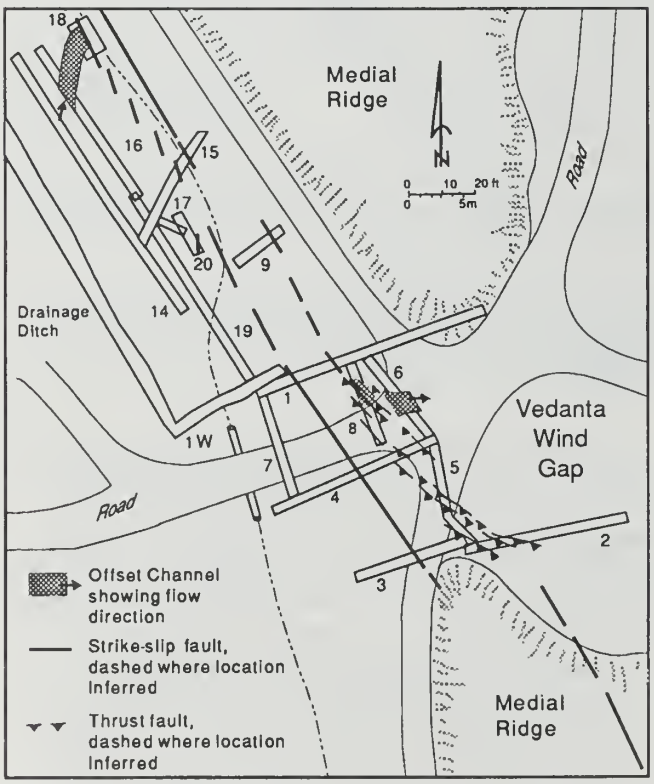

Figure 5. Map of Vedanta wind gap research site, Stop 6. Location shown on Fig. 4. Trenches are numbered 1-20.

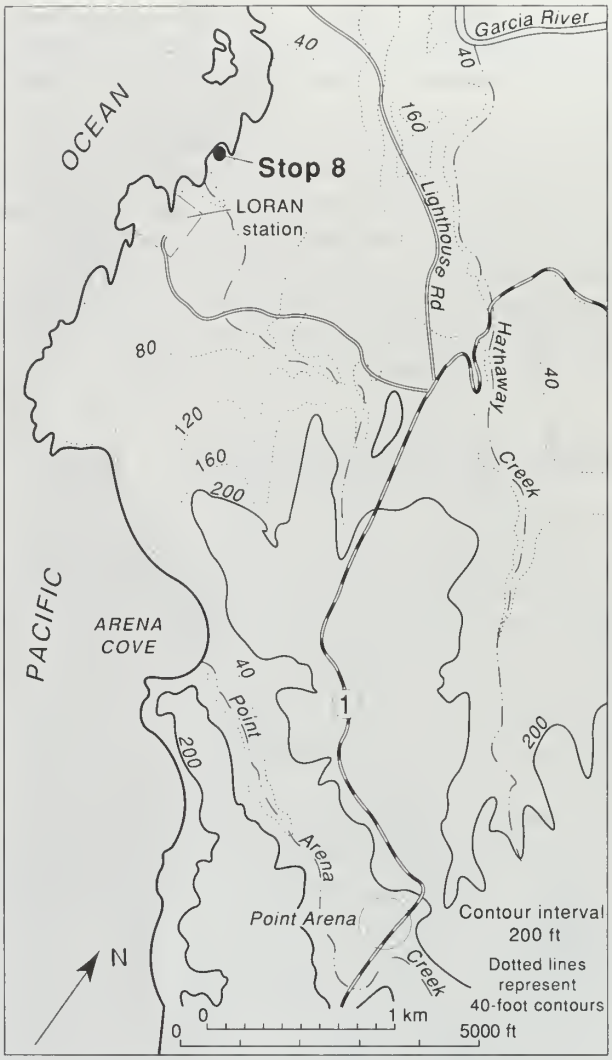

Figure 6. Portion of the Point Arena 7.5 minute quadrangle showing location of Stop 8.

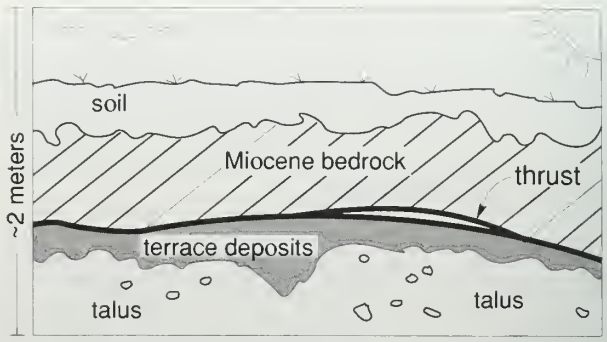

Figure 7. Line drawing made from a photograph showing Miocene bedrock thrust over Pleistocene marine terrace deposits exposed in the seacliff at Stop 8.

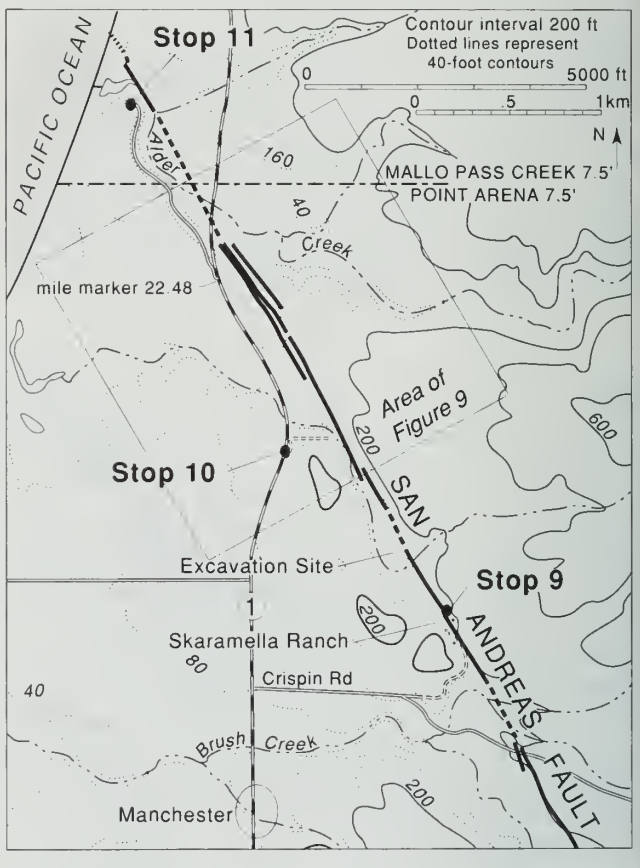

Figure 8. Portion of the Point Arena 7.5 minute quadrangle showing the locations of Stops 9 through 11.

strike is unknown. Because the original fences no longer exist, they cannot be used to resolve this question.

Approximately 1640 ft (500 m) northwest of the ranch house, a small ephemeral stream has built a fan across the SAF. Excavations into this fan across and parallel to the fault zone revealed stratigraphic information about the late Holocene history of the fault. Evidence suggests that at least five earthquakes have occurred here since the time of deposition of a unit that contains detrital charcoal with a dendrochronologically-corrected radiocarbon date of BC 90 to AD 210. The most recent of these is the 1906 event; the penultimate event occurred some time after AD 1530, most likely after AD 1635 (Prentice, 1989).

The excavations also revealed the presence of an offset, buried channel. The separation of the channel across the fault zone is about 210 ft (64 m). This represents a maximum for the amount of fault offset after the channel was cut. A more likely value for this offset is about 190 ft (58 m),

the value obtained by projecting the channel across the fault zone. The age of the channel fill (about 2350 to 2700 yrs B.P.) and the age of the material the channel was cut into (about 2350 to 2700 yrs B.P.) are indistinguishable. These data yield a maximum late Holocene slip rate of about 1 in/yr (25 ± 3 mm/yr), with a best estimate of about 23 ± 3 mm/yr (Prentice, 1989).

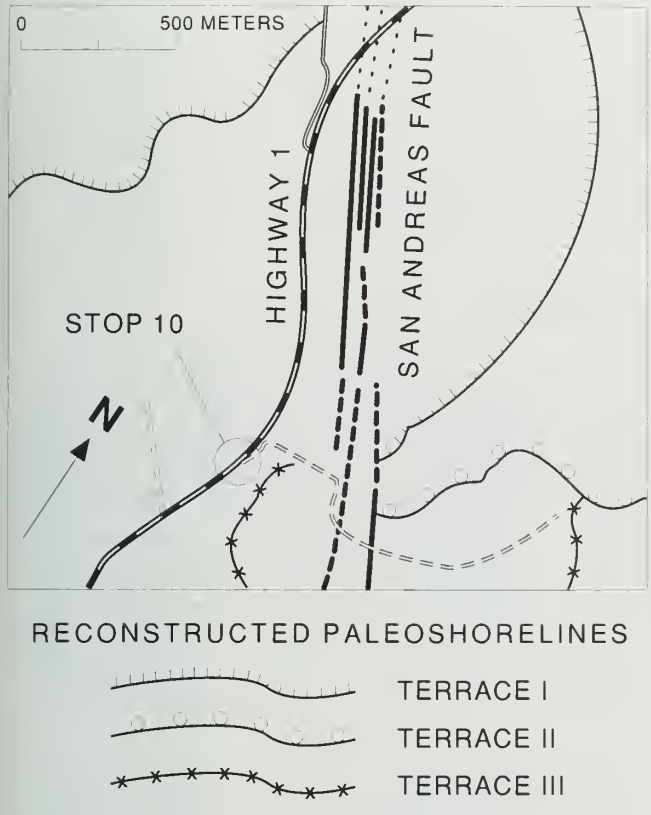

Figure 9. Map showing marine terrace risers offset by the SAF. Location shown by inset map in Fig. 8.

STOP 10 - OFFSET PALEO-SHORELINES

Two marine terrace risers that are truncated on the northeast side of the SAF are visible from this location (Fig. 9). A possible equivalent on the southwest side of the SAF shows a horizontal separation of 0.8-1.1 mi (1.3 to 1.8 km). An older marine terrace riser and its possible equivalent are separated by 1.4-2.0 mi (2.3 to 3.2 km). Estimates of the ages of these features (83,000 and 125,000 yrs, respectively) suggest slip rates of 16 to 22 mm/yr for the younger terrace riser and 18 to 26 mm/yr for the older feature (Prentice, 1989).

STOP 11 - ALDER CREEK

In 1906 the main road crossed Alder Ck. at this location. The wooden bridge that spanned the creek (and the SAF) was wrecked by the earthquake. The cement abutments now at this site are from a later bridge that replaced the destroyed bridge. This later bridge was abandoned when Highway 1 was rerouted to its present location. During low tide, a gouge zone is exposed along the southwest side of the creek downstream from the bridge site. The fault continues offshore northwest of the mouth of Alder Ck. (Curray and Nason, 1967).

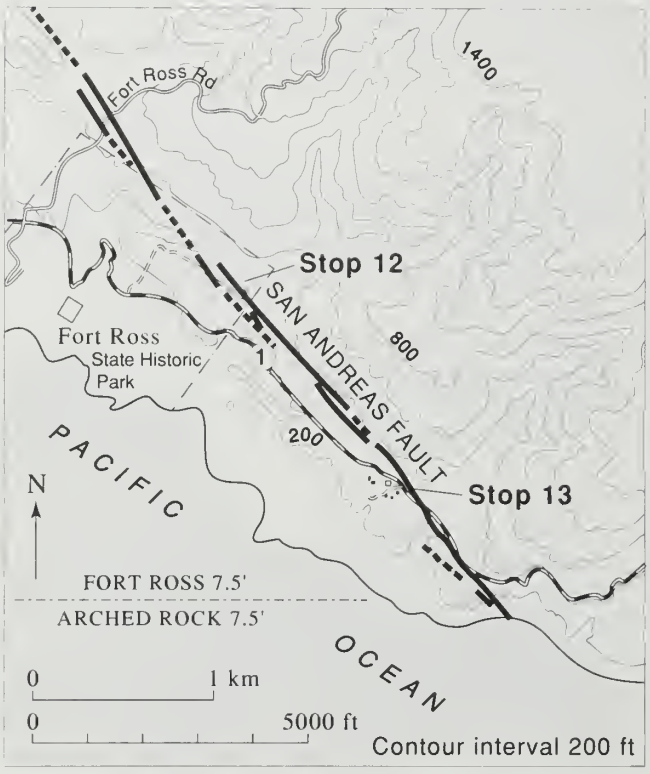

Figure 10. Part of the Fort Ross 7.5 minute quadrangle showing the locations of Stops 12 and 13.

STOP 12 - OFFSET FENCE AND RUSSIAN ROAD

Fig. 10 shows the location of an old picket fence that was offset as a result of the 1906 earthquake (Lawson, 1908). This offset is still evident today, though a new straight fence has been put in next to the old one. The old fence was surveyed by E.S. Larsen about a year after the earthquake (Fig. 11). The slip amounted to 12 ft

(3.7 m) distributed over a distance of 415 ft (127 m) (Lawson, 1908, p. 64). About 7.5 ft (2.3 m) of offset occurred at the fault trace. Less than 300 ft (100 m) to the southeast along the fault, the old Russian road leading to Fort Ross intersects the fault at a very low angle. Careful observation shows that this road is displaced about the same amount as the fence, suggesting that after the Russians established Fort Ross (1812), only one earthquake has offset this road.

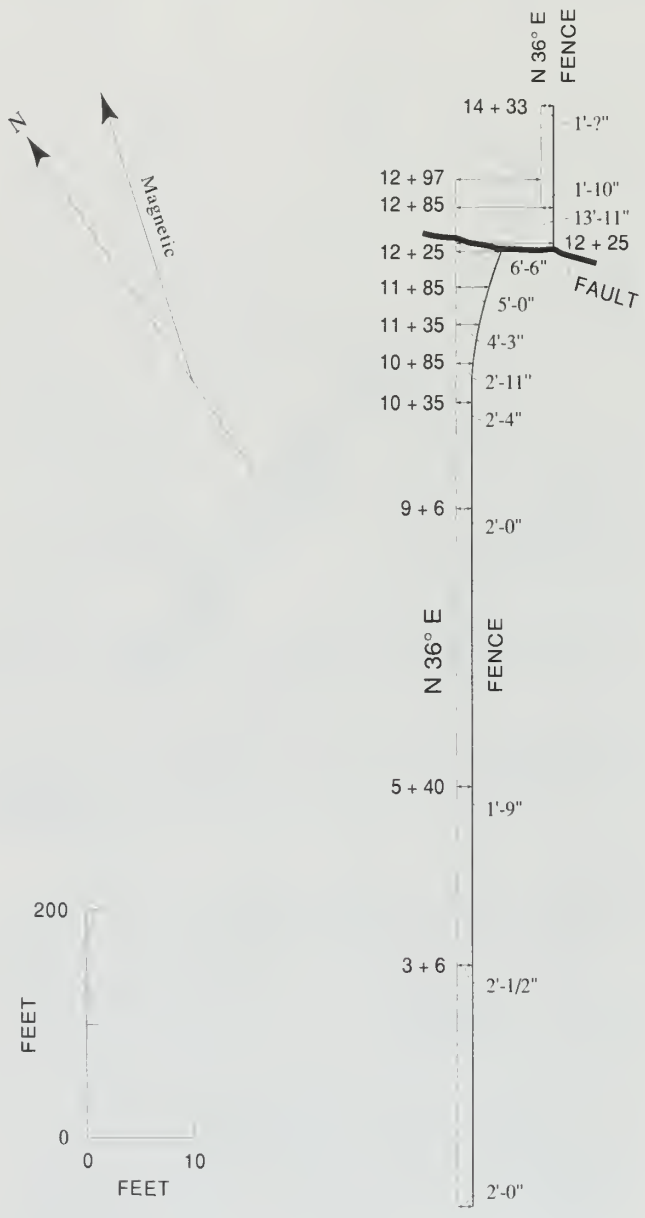

Figure 11. Offset fence at Stop 12. From Lawson, 1908.

STOP 13 - OFFSET STREAMS

A stream at Stop 13 (Figs. 10, 12) was reported by F.E. Matthes (in Lawson, 1908) to be offset about 12 ft (3.7 m) in 1906. Water ponded behind the scarp, as shown in the photograph on Plate 37 of the Lawson report. Although the stream cut through the scarp and drained the ponded water, this location is otherwise little changed since 1906. The stream is offset a total of about 23-26 ft (7-8 m), suggesting that at least two earthquakes have affected this channel. Mill Gulch, about 980 ft (300 m) southeast, is offset as much as 490 ft (150 m). Matthes made a detailed topographic map of this area, with contours at 5-ft intervals, showing the relationship of these and other features to the 1906 fault trace (Fig. 12).

ROAD LOG

Stops 1, 2, and 3. From the Cathedral Hill Hotel in San Francisco, take Van Ness Ave. south to Hwy. 101 south. Exit to Hwy. 280, travel south to the Trousdale Dr. exit. After coming off the exit ramp, turn right. **The San Francisco Water Department gate is locked, and special permission is required to drive through it to stops 1, 2, and 3.** (However, San Andreas Dam (Stop 1) is accessible by bicycle or foot via the Sawyer Camp Trail. The trail follows the fault valley between San Andreas and Crystal Springs dams.)

Stops 4, 5, 6, and 7. Take Hwy. 280 north from Trousdale Dr. to 19th Ave., and Hwy. 101 north across the Golden Gate Bridge to the Lucas Valley Rd. exit, 33 miles from the Trousdale onramp. Go west on Lucas Valley Rd. for 10.5 mi, turn right (north) on Nicasio Valley Rd.; turn left (west) after 4 mi onto Point Reyes-Petaluma Rd.; turn left (south) after 6 mi onto Hwy. 1; turn right (west) after 0.8 mi onto Sir Francis Drake Blvd.; turn left (south) after 0.7 mi onto Bear Valley Rd., and turn right (west) after 1.7 mi into Point Reyes National Seashore Visitor's Center for Stop 4.

From the Visitor's Center, turn right (south) onto Bear Valley Rd. After 0.8 mi, turn right onto Hwy. 1 (south). After 0.3 mi turn right (west) onto the driveway leading to the Vedanta Retreat. **This is private land and special permission is required to visit stops 5, 6, and 7.**

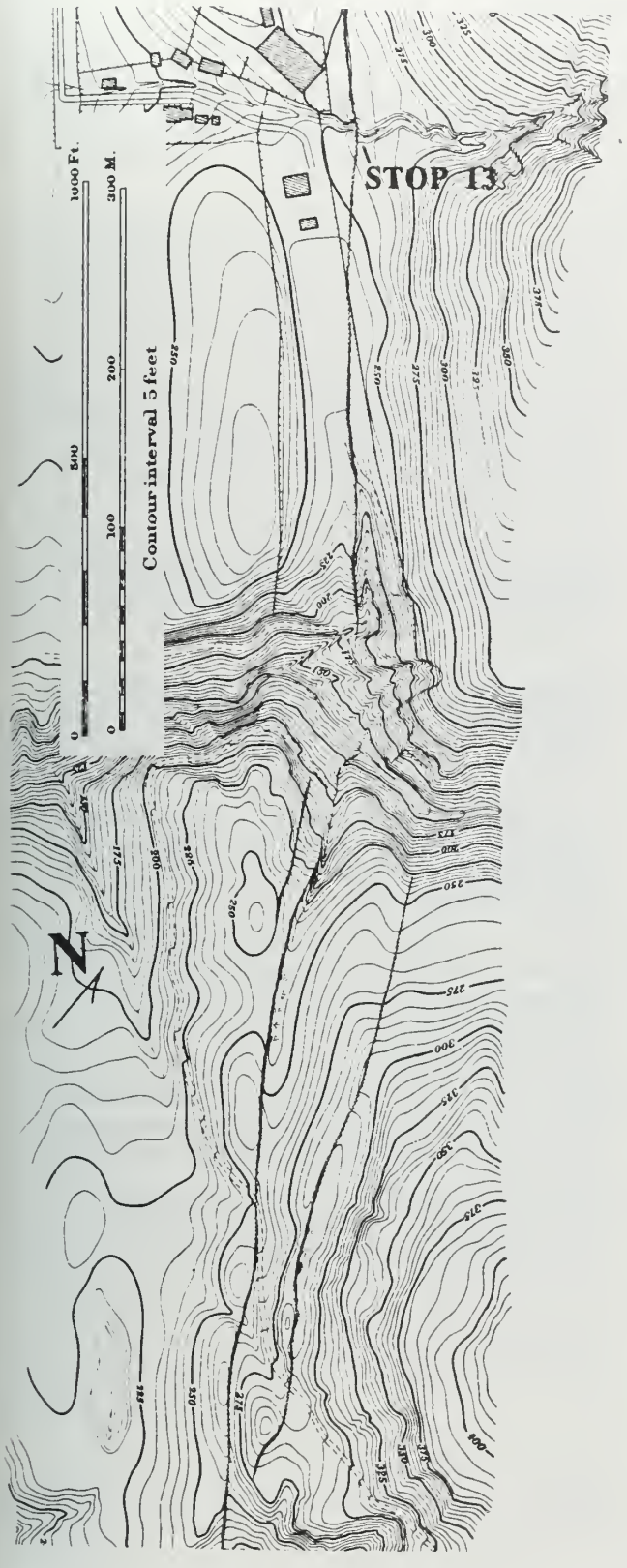

Figure 12. Map from Lawson, 1908, made by F.E. Matthes showing offset stream and ruptures (heavy lines) of the San Andreas fault near Stop 13. Location shown on Fig. 10.

Stops 8 through 13. Take Hwy. 1 north from Olema, though the towns of Bodega Bay, Jenner, and Gualala to Point Arena, about 100 mi. From the town of Point Arena, continue north on Hwy. 1 about 1.5 mi to a locked gate on the left (west) side of the highway about 100 ft (30 m) south of Lighthouse Rd. **This is private property and special permission is needed to go through the gate**. Follow the paved road toward the ocean to its end, about 1 mi. Walk 1000-1300 ft (300-400 m) north along the cliffs to the Stop 8 exposures.

Backtrack to the locked gate at Hwy. 1. Continue north on Hwy. 1 to Crispin Rd., 4.1 mi. Turn right (east) on Crispin Rd., continue 0.5 mi and bear left on the dirt driveway leading to the Skaramella Ranch. **This is private property and special permission is needed to visit the ranch**. Follow the driveway about 0.4 mi to the ranch house and Stop 9.

Backtrack to the intersection between Crispin Rd. and Hwy. 1. Continue north on Hwy. 1 for 0.8 mi to a dirt road on the right (east) side of the highway. Pull over at this turn off for Stop 10.

Continue north on Hwy. 1 for 0.6 mi to an unnamed paved road on the left (west) side of the highway at mile marker 22.48. Follow this road about 0.8 mi to its end at the mouth of Alder Creek for Stop 11.

Backtrack to Hwy. 1. Go south on Hwy. 1 about 49 mi to the turnoff to Fort Ross State Historic Park. From here continue south on Hwy. 1 for 0.8 mi to a locked gate on the left (east) side of the highway. **This is State Park land and special permission is required to go through the gate.** Follow the dirt road about 0.62 mi (1 km) to its end. This is Stop 12.

Backtrack to Hwy. 1 and continue south for 1.3 mi to the red barn on the right (west) side of the highway. Pull over here for Stop 13. **This is private property and special permission is needed to go through the gates.**

REFERENCES CITED

Blake, M.C., Jr., Bartow, J.A., Frizzell, V.A., Jr., Schlocker, J., Sorg, D., Wentworth, C.M., and Wright, R.H., 1974, Preliminary geologic map of Marin and San Francisco Counties and parts of Alameda, Contra Costa and Sonoma Counties, California: *U.S. Geological Survey Miscellaneous Field Studies Map MF-574*, scale 1:62,500.

Brabb, E.E., and Pampeyan, E., 1972, Preliminary geologic map of San Mateo County, California: *U.S. Geological Survey Miscellaneous Field Studies Map MF-328*, scale 1:62,500.

Brown, R.D., and Wolfe, E.W., 1972, Map showing recently active breaks along the San Andreas fault between Point Delgada and Bolinas Bay, California: *U.S. Geological Survey Miscellaneous Geologic Investigations Map I-692*, scale 1:24,000.

Clark, J.C., Brabb, E.E., Greene, H.G., and Ross, D.C., 1984, Geology of Point Reyes Peninsula and implications for San Gregorio fault history, *in* Crouch, J.K. , and Bachman, S.B., eds., *Tectonics and sedimentation along the California margin*: Pacific Section, Society of Economic Paleontologists and Mineralogists, v. 38, p. 67-86.

Curray, J.R., and Nason, R.D., 1967, San Andreas fault north of Point Arena, California: *Geological Society of America Bulletin*, v. 78, p. 413-418.

Galloway, A.J., 1977, Geology of Point Reyes Peninsula, Marin County, California: *California Division of Mines and Geology Bulletin 202*, 72p.

Gilbert, G.K., 1907, Notebook No. 110, Mar. 29, 1907.

Graham, S.A., and Dickinson, W.R., 1978, Apparent offsets of on-land geologic features across the San Gregorio-Hosgri fault trend, *in* Silver, E.A., and Normark, W.R., eds., San Gregorio-Hosgri fault zone, California: *California Division of Mines and Geology Special Report 137*, p. 13-23.

Graham, S.A., Stanley, R.G., Bent, J.V., and Carter, J.B., 1989, Oligocene and Miocene paleogeography of central California and displacement along the San Andreas fault: *Geological Society of America Bulletin*, v. 101, p. 711-730.

Hall, N.T., 1981, Stops 4, 5, 6, and 7, *in* Kleist, J.R., ed., *The Franciscan Complex and the San Andreas fault from the Golden Gate to Point Reyes, California*: Pacific Section, American Association of Petroleum Geologists, Field Trip Guidebook, p. 21-28.

Hall, N.T., 1984, Holocene history of the San Andreas fault between Crystal Springs Reservoir and San Andreas Dam, San Mateo County, California: *Bulletin Seismological Society of America*, v. 74, no. 1, p. 281-299.

Hall, N.T., and Hughes, D.A., 1980, Quaternary geology of the San Andreas fault zone, Point Reyes National Seashore, Marin County, California, *in* Studies of the San Andreas fault zone in northern California: *California Division of Mines and Geology Special Report 140*, p. 71-87.

Hall, N.T., Hay. E.A., and Cotton, W.R., 1986, *Investigation of the San Andreas fault and the 1906 earthquake, Marin County, California*: National Earthquake Hazards Reduction Program Final Tech. Rep. Contract # 14-08-0001-21242; 3 map sheets, scale 1:1200.

Lawson, A.C., Chairman, 1908, The California Earthquake of April 18, 1906; Report of the State Earthquake Investigation Commission: *Carnegie Institute of Washington Publication 87*, 451 p.

Matsu'ura, M., Jackson, D.D., and Cheng, A., 1986, Dislocation model for aseismic crustal deformation at Hollister, California: *Journal of Geophysical Research*, v. 91, no. B12, p. 12,661-12,674.

Prentice, C.S., 1989, *Earthquake geology of the northern San Andreas fault near Point Arena, California*: Ph.D. dissertation, California Institute of Technology, Pasadena, California, 252p.

Prescott, W.H., Lisowski, M., and Savage, J.C., 1981, Geodetic measurement of crustal deformation on the San Andreas, Hayward, and Calaveras faults near San Francisco, California: *Journal of Geophysical Research*, v. 86, p. 10853-10869.

Schussler, H., 1906, *The water supply of San Francisco, California, before, during, and after the earthquake of April 18, 1906:* M.B. Brown Press, New York, 103p.

Stuvier, M., and Pearson, G.W., 1986, High-precision calibration of the radiocarbon time scale, A.D. 1950-500 B.C.: *Radiocarbon*, v. 28, no. 2B, p. 805-838.

Depositional and Other Features of the Merced Formation in Sea Cliff Exposures South of San Francisco, California

H. Edward Clifton and Ralph E. Hunter[1]

INTRODUCTION

The sea cliffs south of San Francisco expose a mile-thick (1750-m) section that provides a nearly continuous record of coastal and shallow marine sedimentation through much of the Pleistocene. The exposures extend for about 3.8 miles (6 km) from the north end of Lake Merced to just north of Mussel Rock (Figs. 1, 2). The section can be reached from parking lots at either end of the exposures or by trails to the beach from Fort Funston (part of the Golden Gate National Recreation Area) or the western end of John Daly Blvd. (Fig. 2).

The section exposed here has been described in a number of field trip guidebooks and other publications. Hunter and others (1984) and Császár and others (1985) describe in detail the facies in the upper part of the section. The sedimentology of the complete section is discussed by Clifton and Hunter (1987), and Clifton and others (1988), and Clifton (1989), and its paleontology has been analyzed by Glen (1959) and Hall (1966).

The foregoing publications describe a number of features in this section that are likely to be of interest to sedimentologists, paleontologists, and geologists involved with studies of the region. The outcrops are so variable in their exposure, owing to landslides and seasonal fluctuations in the beach sand cover, that it is unlikely that all of the features can be seen in any one excursion. The sedimentologic observations in the literature cited above were based on repeated examinations of the section over an interval of about 10 years. This paper describes some of these features and their locations, with the goal of providing a focus for examination during any one excursion.

Typically, the exposures are best viewed during winter months when rain washes the outcrops clean and storm waves remove much of the covering beach sand. The visitor should beware of sudden rockfalls and cliff slumps which prevail during the rainy season.

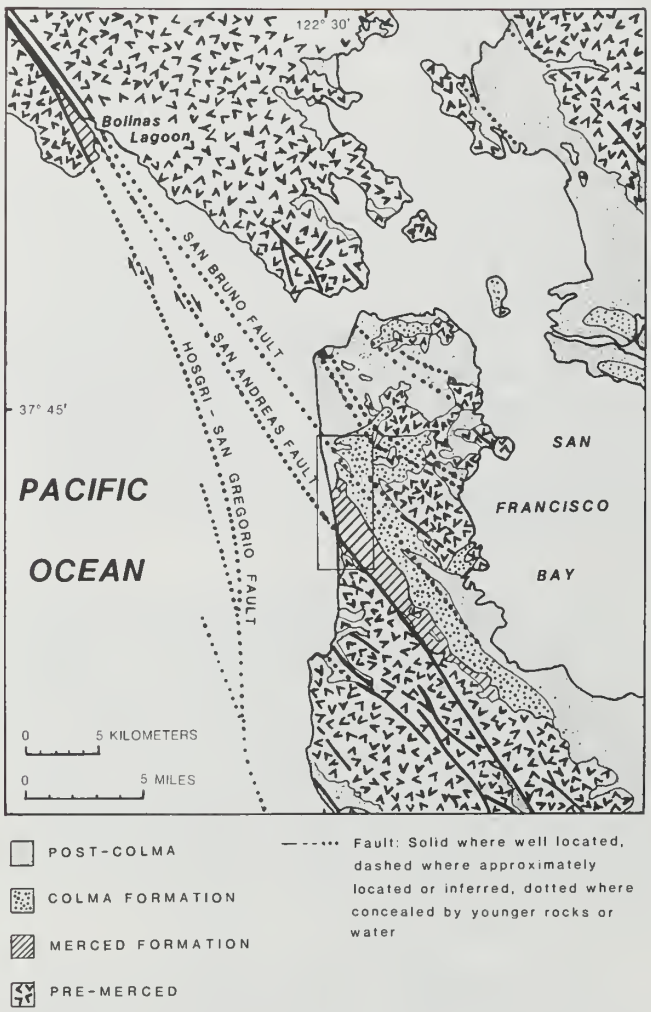

Figure 1. Index map showing generalized geology and distribution of the Merced and Colma formations (after Wagner and others, in press). Inset shows location of Fig. 2.

[1]U.S. Geological Survey, 345 Middlefield Road, Menlo Park, CA 94025

AGE AND GEOLOGIC SETTING

Most of the section is assigned to the Merced Formation, a unit of Pliocene (?) and Pleistocene age that fills a small fault-bounded trough across the San Francisco Peninsula (Fig. 1). The uppermost sequence Z (Figs. 3 and 4) is a thin sandy deposit that is assigned to the Colma Formation. Age data for these units are meager. Fossils in the Merced Formation suggest that, in the sea cliff exposures, the unit is entirely of Pleistocene age. A mineralogic change in the upper part of sequence P reflects a change in provenance from local rock sources dominated by the Franciscan Complex to more widespread sources dominated by rocks of the Sacramento-San Joaquin drainage basin (Hall, 1965, 1966). Tephrochronology in the San Joaquin basin indicates that this change occurred between 0.62 and 0.40 Ma (Sarna-Wojcicki and others, 1985). An ash bed near the top of sequence S has been identified as the informally named Rockland ash bed, which was deposited at 0.40 Ma (Sarna-Wojcicki and others, 1985). At the top of the section, the Colma Formation probably originated during one of the high stands of the sea in the interval between 0.07 and 0.13 Ma (Hunter and others, 1984).

The Merced and Colma Formations appear to have been deposited in a paralic setting. Merced facies were deposited in environments that range from shelf depths (33 ft, 100 m, or more according to Clifton, 1988) to eolian dune fields. Table 1 indicates identifying characteristics of the facies inferred to occur within the section. Crossbedding and gravel-filled gutter casts in the nearshore facies indicate that the shoreline trended between north and northwest during deposition of the Merced (Chiocci and Clifton, in press).

The strata accumulated in a relatively small structural basin that probably developed between a set of the strike-slip faults that prevail in this part of the California Coast Range. No evidence exists within the sediment exposed in the sea cliff section for deposition within a topographic trough; rather, the sediment appears to have accumulated in an open-coast setting. Although the San Andreas fault currently bounds the basin on its southwestern side, the role of this fault during accumulation of the Merced is uncertain. The sediment itself provides no evidence of an active fault at this location during deposition. Moreover, although the lower

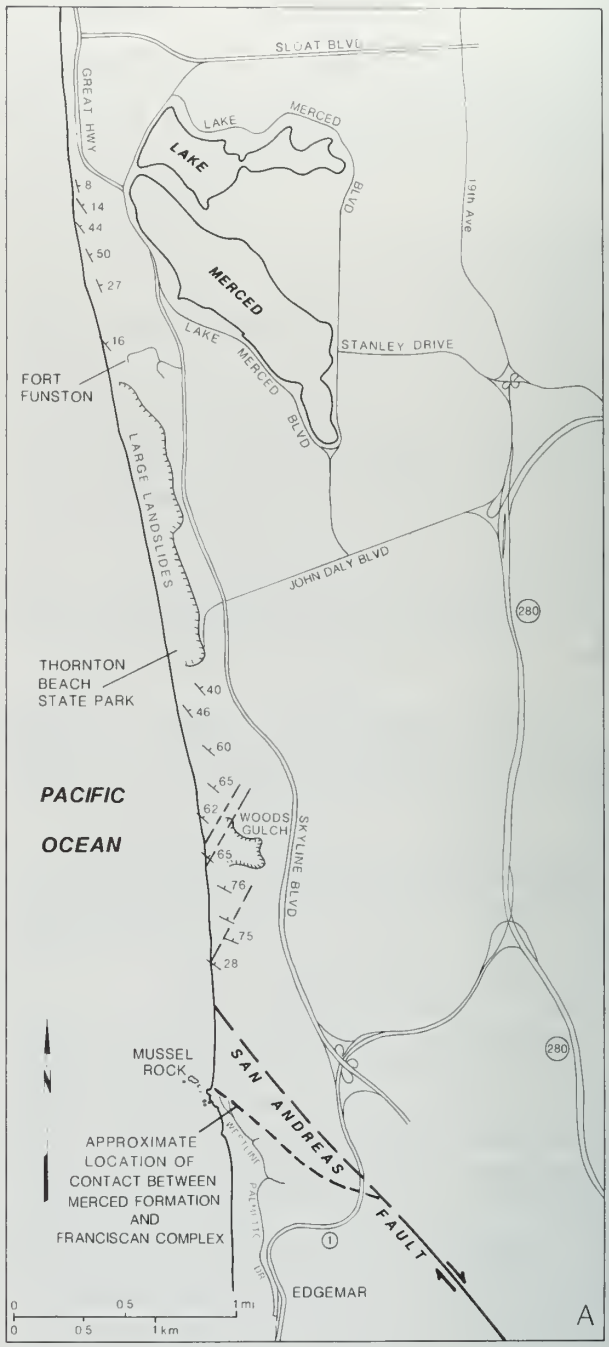

Figure 2. Geologic features of the Merced Formation in its sea cliff exposures south of San Francisco.

part of the section is cut by small, apparently right-lateral strike-slip faults that parallel the San Andreas, these faults seem to postdate the folding of the strata. The most recent deformation occurred prior to deposition of the Colma Formation, which rests in angular unconformity on strata of the underlying Merced Formation (Fig. 4).

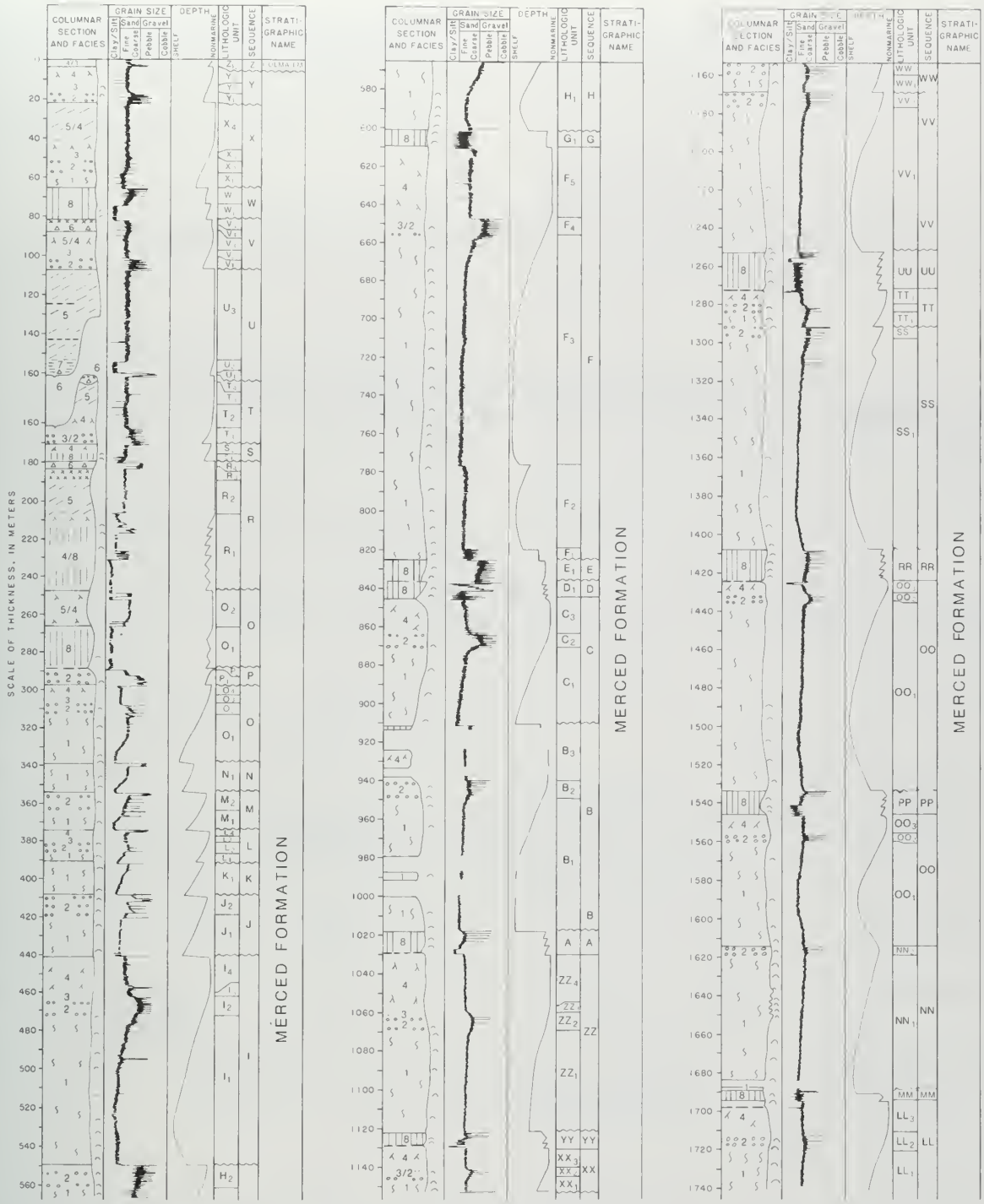

Figure 3. Part of the type section and depositional facies of the Merced and Colma formations exposed in sea cliffs north of the San Andreas fault, San Francisco Peninsula. Sequences and lithologic units as introduced by Hunter and others (1984). Facies identified by numbers in stratigraphic column and in Table 1 delineating their identifying characteristics: 1, shelf (including outer-shelf, mid-shelf, and inner-shelf facies); 2, nearshore (may include foreshore facies in some sequences); 3, foreshore; 4, backshore; 5, eolian dune; 6, alluvial; 7, freshwater pond/swamp/marsh; 8, embayment. Combinations of facies shown with slanted lines. Heavy horizontal dashed lines in the stratigraphic column indicate locations of lignitic layers; x's mark well-developed paleosols. Occurrence of mollusks shown schematically by symbols to right of column. Predominant grain sizes as estimated visually in the field. Wavy lines between sequences indicate erosional surfaces; gaps in section reflect covered intervals. All thicknesses in meters.

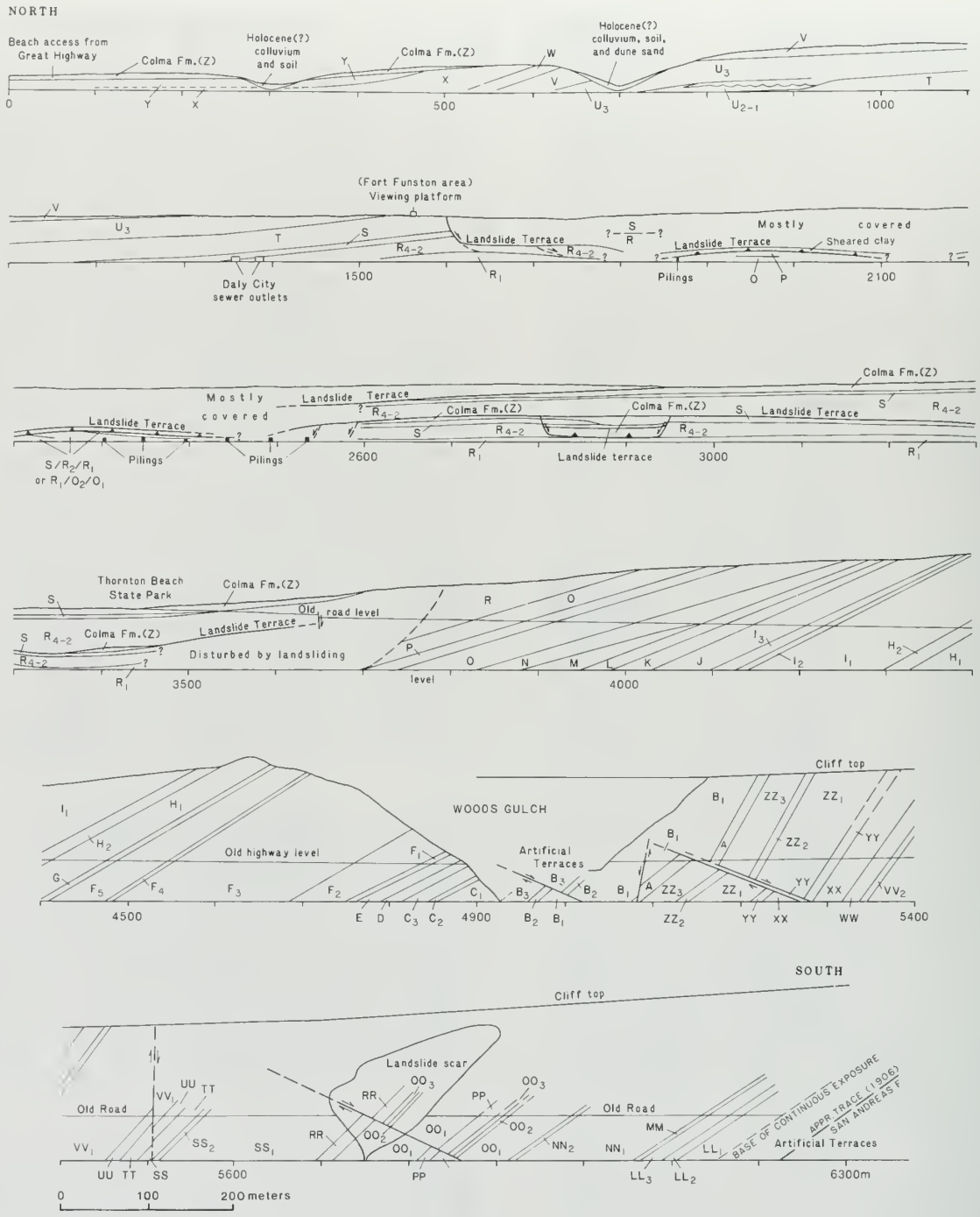

Figure 4. Generalized cross section of exposures of the Merced and Colma formations on the sea cliffs between Lake Merced and Mussel Rock, San Francisco Peninsula (southern end of section about 0.3 mi (500 m) north of Mussel Rock, Fig. 2). Letters and numeral subscripts refer to sequences and lithologic units in stratigraphic column (Fig. 3). Sections tie together end-to-end from northernmost section (top) to southernmost section (bottom). Scale in meters; no vertical exaggeration.

FEATURES

The sea cliff exposures of the Merced Formation contain many interesting sedimentologic features (see, for example, Table 1 and previous publications on the section). Here we focus on a few that we find to be of particular note, including transgressive-regressive cycles, trace fossils, a high-relief disconformity and associated giant load structures, a distinctive volcanic ash bed, evidence of tidal influences, features possibly generated by ancient earthquakes, and a large active landslide.

The features are identified both by position within the stratigraphic section (Fig. 3) and by location along the cross section of the sea cliffs (Fig. 4). Annotations (e.g., 0_3, 3750 m) indicate sequence or subsequence as shown on Figs. 3 and 4 and location along the sea cliff exposure as shown in Fig. 4.

Transgressive-regressive cycles: The facies in the Merced Formation are arranged in sequences that indicate alternate transgression and regression of the sea (Fig. 3). In the lower 1300 m of section (below sequence J), the pattern of transgression and regression is of generally larger scale than that in the upper 440 m. The lower 1300 m is dominated by shelf facies (Fig. 3), and the presence of a shoreline seems to occur mostly at or near relative low stands of the sea. In contrast, the upper 300 m is dominated by nonmarine facies, and the presence of a shoreline seems to be associated with relative high stands of the sea. This change coincides with the change in provenance that occurs in sequence P, 290 m below the top of the section. It may result from a seaward shift in average shoreline position caused by an increased rate of sedimentation. The origin of the transgressive-regressive cycles in the Merced is uncertain; although they appear generally similar in scale and duration to the known Pleistocene glacioeustatic sea level fluctuations (Clifton and others, 1988), tectonic and sedimentologic influences cannot be precluded.

The Merced section in the sea cliffs is dominated by shallowing-upward regressive sequences formed by a prograding shoreline, possibly in conjunction with a falling sea level. Complete progradational sequences in the sea cliff exposures have a basal facies of bioturbated shelf siltstone estimated to have accumulated in water depths on

Table 1. Characteristics and inferred origin of facies in sea cliff exposures of the Merced Fm., San Francisco, California

Inferred origin	Texture	Biota	Physical structures	Biogenic structures
Outer shelf	Sandy silt	Mollusks (*in situ* and scattered shells)	None	Intense bioturbation
Mid shelf	Sandy silt	Mollusks	Shell lags Parallel lamination Hummocky cross-stratification	Sharp-topped bioturbated intervals between sets of laminae
Inner shelf	Very fine sand Scattered small pebbles near top	Mollusks Echinoids	Shell lags Parallel lamination Hummocky cross-stratification	Locally intense bioturbation
Nearshore	Fine to coarse sand and gravel	Mollusks Echinoids	Lenticular sand and gravel beds High and low angle crossbedding Parallel lamination	Vertical burrows *Macaronichnus* (near top)
Foreshore	Fine to coarse sand and gravel Upward fining	Mollusks Echinoids	Parallel lamination Heavy mineral layers near top	*Macaronichnus* (near base)
Backshore	Fine sand	None	Parallel stratification Low angle crossbedding Climbing adhesion ripples Ripple lamination	Root/rhizome structures Vertebrate footprints Vertical burrows
Eolian dune	Fine sand	None	Medium- to large-scale crossbedding	Intense bioturbation and root structure in paleosols
Alluvial	Pebbly sand and gravel	None	Indistinct stratification Lenticular bedding Medium- to small-scale trough crossbedding	Intense bioturbation in paleosols
Pond/swamp/ marsh	Mud Peat Lignite	Freshwater diatoms Insect wings Terrestrial vertebrate bones	Flat-bedded (mud) Giant load casts	Root structures Burrows Intrastratal trails
Embayment	Mud, sand and gravel Upward-fining cycles	Mollusks Ostracods	Fine sand-silt-clay lamination Ripples and ripple-bedding Crossbedding Shell lags	Bioturbation Root/rhizome structures

the order of 300 ft (100 m) deep (Clifton, 1988). The successively overlying facies indicate deposition in progressively shallower water: bioturbated or bedded shelf sandstone, cross-stratified nearshore sand and gravel, planar-bedded foreshore deposits, and nonmarine backshore or eolian dune facies. Incomplete sequences show a similar transition but have one or more facies missing at the top or bottom of the sequence. A few display only an upward transition from shelf siltstone to shelf sandstone, and several consist of the filling of a coastal embayment. Fig. 5 indicates the range in facies of each of the progradational sequences in the sea cliff exposures of the Merced.

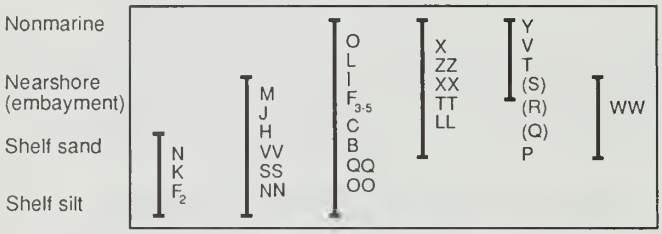

Figure 5. Range of facies in progradational sequences of the Merced Formation. Sequence designation as in Fig. 3.

The transgressive intervals in the section are not simple inversions of the regressive sequences for two reasons. First, the landward translation of a shoreface tends to cause the nearshore, foreshore and any nonmarine deposits associated with the retreating beach to be eroded (Bruun, 1962; Ryer, 1977). The hiatus thereby produced is generally marked by a lag deposit of pebbles and/or shells and an abrupt upward change to deeper water facies. Nearly all of the transgressive intervals in the Merced Formation show such a transgressive surface of erosion, and the facies involved in the upward deepening differ among the cycles (Fig. 6).

A second factor in the difference between regressive and transgressive sequences is that the nature of the regressive shoreline seems commonly to have differed from that produced by transgression. During regression, the dominant coastal morphology seems to have been a prograding strand plain without significant embayment; neither bay deposits nor tidal influence has been recognized within the progradational sequences. In contrast, the transgressions seem consistently to have produced a barrier coastline with extensive back-barrier lagoons or estuaries. Nearly half of

shelf silt ~ shelf sand	shelf silt ~ nearshore	shelf silt ~ nonmarine	shelf sand ~ nearshore	shelf sand ~ nonmarine	nearshore ~ nonmarine	shelf sand ~ embayment nonmarine	nonmarine embayment nonmarine
N→O K→L	M→N J→K	L→M I→J	H→I WW→XX VV→WW SS→TT NN→OO		X→Y U→V S→T Q→P	V→W→X F→G→H C→DE→F B→C ZZ→A→B XX→YY→ZZ TT→UU→VV QQ→RR→SS QQ→PP→QQ LL→MM→NN	R→S Q→R P→Q

Figure 6. Facies transitions in transgressive intervals of the Merced Formation. Wavy line indicates transgressive surface of erosion. Sequence designation as in Fig. 3.

the transgressive intervals in the section begin with a depositional transition from well-sorted nonmarine deposits containing root structures or other evidence of subaerial exposure to muddy sediment that contains marine mollusks (Fig. 6). In many of these transitions, a thin lignitic or peaty layer separates the sand and the mud. Typically, the muddy sediment becomes progressively coarser upsection, culminating in crossbedded sand and gravel that contain numerous shells and shell fragments. An erosional surface, marked by a shell and pebble lag, and abruptly overlain by shelf sand, caps these coarsening-upward sequences. Generally, this shelf sand grades upsection through an interval as much as 60 ft (20 m) thick into silt.

Such successions are interpreted to mean that the initial phase of marine transgression occurred at the landward margin of a coastal lagoon, where it encroached over an adjacent nonmarine coastal plain. The progressive upward coarsening of the inferred lagoonal deposits suggests an approaching barrier, and the crossbedded sand and gravel can be attributed to migrating tidal inlets. Fining-upward sequences several feet (decimeters to a few meters) thick are common in many of the embayment successions. Many of these have a basal layer of disarticulated and broken shells, beneath which numerous bivalves lie in growth position. These sequences probably reflect migrating tidal channels, of which only the lowermost part is preserved. The erosional surface that caps the inferred tidal inlet deposits can be attributed to a transgressive surface of erosion produced by the landward migration of the barrier. The upward fining of the overlying shelf sediment reflects progressive deepening as the transgression continues. Excellent examples of transgressive embayment deposits are represented by sequences RR (most fully exposed on cliffs above beach level), PP (5830 m), UU (5450 m), YY (5225 m), A (5080 m), D and E

combined, (4800 m), and W (530 m). The beach level exposure of sequences PP, YY, and A are complicated by faulting (Fig. 4).

Four of the transgressive intervals in the section lack a transgressive surface of erosion. In each case, it appears that the locality of the exposure was never crossed by a landward-migrating open-coast shoreline. Three of the examples (sequences Q, R, and S) represent embayments at the point of maximum transgression. The fourth, at the transition between subsequences F_2 and F_3, accumulated on the shelf seaward of the initiation of shoreface erosion. It is likely that other small, upward-deepening sequences are unrecognized elsewhere in the shelf facies.

One transgressive-regressive cycle may be recorded entirely in nonmarine deposits. The interval that encompasses sequences T and U records dissection of an exposed land surface followed by the back-filling of the valleys. The dissection suggests a lowering of base level (i.e., a drop in relative sea level), and the back-filling may reflect deposition associated with an ensuing sea level rise, at a location landward from the transgressing sea.

Trace fossils: The Merced Formation contains a diverse invertebrate fossil assemblage (Glen, 1959) and a number of vertebrate remains (Hall, 1965, 1966). The past activity of these organisms is recorded by abundant bioturbation and numerous trace fossils within the sediment. Our purpose here is not to provide a complete listing of the trace fossils, but to focus on some of the more distinctive ones, particularly those with paleo-environmental significance.

Fine sand in many of the upper nearshore and lower foreshore deposits contains concentrations of sinuous, subhorizontal circular tubes, a few millimeters in diameter, filled with sand lighter in color than the enclosing sand. Such trace fossils, named *Macaronichnus segregatis* by Clifton and Thompson (1978), are best seen when the outcrops are slightly damp. Several feet (decimeters) below the sediment-water interface similar traces are produced today by sediment-feeding polychaetes. *Macaronichnus* seems consistently to occur in very shallow-water deposits, and those in the Merced are no exception. Their restriction to the surf-swash transition may be due to elevated oxygen levels in the sediment caused by aeration of the water, low organic content, or a combination of the two. Good examples of *Macaronichnus* are present in sequences V, O, ZZ, and WW.

The traces of burrowing bivalves are present in several of the Merced facies. Muddy sediment immediately beneath tidal channel sand in sequences R (3150 m) and S (1370 m) contains irregular pockets up to 8 in (20 cm) wide and 12 in (30 cm) deep filled with sand from the overlying bed. In S, molds of large articulated clams were found in a few of these pockets (Császár and others, 1985). In R, bivalve shells or molds are not evident, but stratification in the overlying channel fill is disrupted by pipes, more than an inch (several centimeters) across and as much as 3 ft (1 m) long, that extend upward from the pockets. Laminae immediately adjacent to the pipes are drawn downward into them, and the pipes are interpreted to be the siphon tracks of large clams, probably *Panope*, that lived in the substrate below a partly filled tidal channel. Similar pipes in nearshore sand of sequences Y (100 m) and P (3720 m) probably represent the siphon tracks of other burrowing bivalves, such as *Siliqua*, whose remains have been leached from the sediment. Body fossils of the burrowing clam, *Schizotherus*, lie in living position in the shelf sand of sequence O (3800 m). There the vertical movements of the clams are recorded by concentrations, above and below the body fossil, of the small bivalve, *Psephidia*, whose disarticulated valves apparently were washed into the hole created by the clam.

Another distinctive trace occurs at the base of tidal channel deposits in sequence R (3250 m). There circular tubes, less than an inch (1.5 to 2.0 cm) in diameter, filled with shell fragments extend downward several feet (decimeters) from shell lag deposits into underlying mud. These traces appear to be borings, probably the living chambers of decapods that lived beneath the channel floor. Similar traces are common beneath other ancient tidal channel deposits (Clifton, 1983) and have been observed beneath modern tidal channels in Willapa Bay, Washington. The presence of the borings indicates that the mud into which the channel was cut was cohesive. The fact that many of the shells are stacked in near-vertical orientation within the borings suggests that the occupant actively back-filled its chambers.

Penecontemporaneous deformational structures that we interpret as vertebrate trace fossils

are locally common in the backshore facies (especially in subsequences R_4, S_2, T_2, and Y_3). Isolated structures, probably footprints, range from less than a foot to several feet (5 to 50 cm) in vertical and horizontal dimensions. Downbowed laminae in the centers of these structures indicate a vertically applied load, and upturned laminae around the lateral margins of the structures indicate outward and upward squeezing of sediment. The central downbowed parts of some structures stood as open holes for some time before being filled by sediment. Bedding-surface exposures of presumed footprints are rare, but a formerly well-exposed, now eroded, bedding surface in subsequence S_3 contained bilobate depressions probably made by split-hoofed ungulates and excellently preserved pawprints probably made by canids. The largest structures were probably formed by proboscideans such as *Mammuthus*, whose bones have been found in the Merced.

Where the structures are closely spaced, the interval in which they are found is convolutely laminated, and a footprint origin might seem doubtful were it not for the presence of associated isolated structures. The most intensely deformed beds are about 1 ft (30 cm) thick and are associated with thin mud layers near the base of the deformed zone. We interpret these beds to have been intensely trampled by large mammals, including mammoths, while the sediment was water-saturated; such beds might be called "tramplites."

High-relief disconformity and giant load structures: Beds in the vicinity of the contact between sequences T and U have many unusual features. The contact itself has the highest relief, about 100 ft (30 m), of any of the sequence-bounding disconformities in the Merced Formation. Exposures of the disconformity at the level of the present beach (at 800 m to 900 m on Fig. 4) are in a paleovalley of the disconformity surface, whereas exposures in the bluff to the south are on a former upland flat underlain by a series of stacked paleosols that make up subsequence T_4, the uppermost part of sequence T. Downslope slumping of beds in sequence T is evident on the south side of the paleovalley.

The paleovalley is filled by fluvial gravel, dark gray mud and peat deposited in a pond, marsh, or swamp, and eolian and pond-fill sand (subsequences U_1, U_2, and the lower part of subsequence U_3). The mud and peat, about 30 ft (9 m) thick, were deformed into giant load structures when eolian dune or pond-fill sand was deposited in the form of large-scale foresets that built out over the mud and peat. The loading of the mud and peat produced elongate synclinal lobes and intervening anticlinal ridges spaced about 50 ft (15 m) apart and having a structural relief of about 10 ft (3-4 m). Bedding in the sand overlying the mud and peat became intensely contorted during the loading. The giant load structures are well exposed only during winter periods when the beach is eroded.

Volcanic ash bed: A white vitric ash bed about 1 ft (0.3 m) thick near the top of subsequence S_3 provides the only closely constrained age data for the Merced. This bed has been assigned to the Rockland ash bed, an approximately 400,000-year-old ash bed found at numerous localities in northern and central California (Sarna-Wojcicki and others, 1985). An air-fall origin of the ash exposed in the bluff at Fort Funston (between 1300 m and 1600 m on Fig. 4) is indicated by the absence of locally derived grains except in its reworked upper part and by evidence that the ash was deposited on a subaerial surface, where it was reworked by wind. Eolian sedimentary structures, including stratification formed by climbing wind ripples and adhesion ripples, are found in a 3-ft (1-m) thick sand interval underlying the ash bed and in the reworked upper part of the ash bed itself. The source of the ash was near Lassen Peak, about 185 mi (300 km) to the northeast, and the relation of ash thickness to distance from the source suggests that the eruption was very large, at least as large as that responsible for the Mazama ash from Crater Lake, Oregon (Sarna-Wojcicki and others, 1985).

Evidence of tidal influences: The Pleistocene shorelines represented by these deposits almost certainly experienced tides similar to those of today. Evidence of these Pleistocene tides, however, is relatively rare in the seacliff exposures. As noted, the progradational sequences probably record deposition on a relatively unembayed advancing strand plain, where tidal currents would be of very local significance and where the main tidal effect would likely be raising and lowering the depth of different wave influences. During transgressive episodes, when embayments were a common feature of the shoreline, tides should have

contributed more directly to the character of the sediment, and it is in the transgressive or high-stand embayment deposits that tidal influences can be found in the Merced Formation.

In sequence D (4800 m), a sandy interval about 6 ft (2 m) below the top of the sequence contains rhythmic stratification in which sets of 10-14 organic-rich laminae 0.1-0.3 in (2-5 mm) thick alternate with a similarly thick set of laminae that contain little organic matter. Similar sets of organic-rich and organic-poor laminae have been cored on the accretionary banks of small intertidal channels in Willapa Bay, Washington, where the individual laminae are deposited by separate tides and the alternation of organic content reflects alternating spring and neap tides. The rhythmic strata in sequence D, which lie depositionally about 5 ft (1.5 m) above a shelly and pebbly channel floor lag, seem to have formed in a similar environment.

Tidal effects can also be seen in subsequence R_1. Crossbedded sand in the upper part of this subsequence (3200 m) contains rhythmically-spaced layers of mud on the foresets that strongly resemble neap-spring tidal bundles. Small channels about 4 in (10 cm) deep and several feet (decimeters) wide filled with laminated sediment and cut into bioturbated sediment (in subsequence R_1 at 1600 m) resemble the small runoff channels that cross modern intertidal flats (Clifton, 1983). Good examples of tidal channel sequences (Clifton, 1982) or parts of sequences occur in subsequence R_1 (1600 and 3100 m) as well as in subsequence S_1 (1370 m).

Features of possible earthquake origin in shelf siltstone: A curious sedimentary feature, possibly produced by ancient earthquakes, appears in fresh, wave-washed exposures of shelf siltstone in and below sequence O. The feature is manifested by intervals inches to feet (cm to dm) thick in which depositional and biogenic structures are obliterated and replaced by millimeter-thick lenses of sand, silt, and clay. In some intervals, these "laminar lenses" take the form of flattened rods that are aligned toward the north-northeast. A few of the intervals are marked by a basal concentration of concave-up bivalve shells, and many smaller shells and shell fragments lie normal to stratification and are aligned parallel to the rods. Tiny sandstone dikes, extending downward from master surfaces in many of the intervals, show a similar alignment. Deformed balls of stratified sediment lie encased within undeformed laminar lenses in some of the intervals. In thicker intervals, the laminar lenses may be folded or faulted, and a few intervals appear to be sites of mass failure that involved an immediately overlying bed.

The cause and mechanism of formation of these features are currently unknown. They clearly seem to be deformational in origin and can possibly be explained by the effects of liquefaction under alternating compressive and extensional stresses combined with a change in sediment response from fluid to brittle behavior. The distribution of the intervals seems to be unrelated to that of the storm-induced features that are also common in this facies. The persistent, north-northeast alignment of sand-rods, shells and sand dikes through more than 3280 ft (1000 m) of section suggests a tectonic or topographic influence. Their trend, however, seems unrelated to either paleoslope or to the dip direction of the strata. It does parallel the strike of extensional fractures that offset the strata and appear to reflect stresses accompanying the opening of the basin. The laminar-lensed intervals accordingly are attributed to earthquakes generated by movements on faults that bounded the subsiding Merced depositional basin.

Large active landslide: A landslide mass 1.3 mi (2.2 km) long and with a head scarp 100 ft (30 m) high occupies the stretch of coast between Fort Funston and Thornton Beach (1600 m to 3800 m on Fig. 4). Although the landslide existed in essentially its present form as early as topographic mapping of 1892, slow seaward movement along subhorizontal slip surfaces at or near the sole of the landslide mass continues at the present during wet winters. Several of these slip surfaces are exposed in the coastal bluffs, where the sliding causes a nearly continuous spalling of small blocks from the bluffs above the surfaces at times of maximum activity. Other slip surfaces cross the present beach, where movement along them produces scarps a few inches (centimeters) high that are planed off when the beach is next inundated. Large-scale landsliding in the Fort Funston-Thornton Beach area was favored by the presence of thick, relatively incompetent, subhorizontal mud beds of sequences Q and R at or near beach level in this stretch of coast (Fig. 4).

REFERENCES CITED

Bruun, P., 1962, Sea level rise as a cause of shoreline erosion: American Association of Civil Engineers Proceedings, *Journal of Waterways and Harbors*, v. 88, p. 117-130.

Chiocci, F.L., and Clifton, H.E., in press, Gravel-filled gutter casts in nearshore facies— indicators of ancient shoreline trend, *in* Osborne, R.H., ed., From Shoreline to Abyss, Contributions in Marine Geology Honoring Francis Parker Shepard: *Society of Economic Paleontologists and Mineralogists Special Publication.*

Clifton, H.E., 1982, Estuarine deposits: *in* Scholle, P.A., and Spearing, D., *Sandstone Depositional Environments*: American Association of Petroleum Geologists, Tulsa, OK, p. 179-189.

Clifton, H.E., 1983, Discrimination of subtidal and intertidal facies in Pleistocene deposits, Willapa Bay, Washington: *Journal of Sedimentary Petrology*, v. 53, p. 353-369.

Clifton, H.E., 1988, Sedimentologic approaches to paleobathymetry, with applications to the Merced Formation of central California: *PALAIOS*, v. 3, p. 507-522.

Clifton, H.E., 1989, The Merced Basin: *in* Wahrhaftig, C., and Sloan, D., eds., *Geology of San Francisco and vicinity*: Field Trip Guidebook T 105, 28th International Geological Congress, American Geophysical Union, Washington, D.C., p. 32-33.

Clifton, H.E., and Hunter, R.E., 1987, The Merced Formation and related beds - a mile-thick succession of late Cenozoic coastal and shelf deposits in the sea cliffs of San Francisco, California, *in* Hill, M.L., ed., *Cordilleran Section of the Geological Society of America Centennial Field Guide Volume 1*: Boulder, CO, Geological Society of America, p. 257-262.

Clifton, H.E. and Thompson, J.K., 1978, *Macaronichnus segregatis*, a feeding structure of shallow marine polychaetes: *Journal of Sedimentary Petrology*, v. 48, p. 1293-1302.

Clifton, H.E., Hunter, R.E., and Gardner, J.V., 1988, Analysis of eustatic, tectonic, and sedimentologic influences on transgressive and regressive cycles in the late Cenozoic Merced Formation, San Francisco, California, *in* Paola, C., and Kleinspehn, K.L., eds., *New Perspectives in Basin Analysis*: New York, Springer-Verlag, p. 109-128.

Császár, Geza, Clifton, H.E., and Hunter, R.E., 1985, Details of a Pleistocene coastal succession, Golden Gate National Recreation Area, California: *Eotvos Lorand Geophysical Institute of Hungary Geophysical Transactions*, v. 31, p. 169-189.

Glen, W., 1959, Pliocene and lower Pleistocene of the western part of the San Francisco Peninsula: *University of California Publications in Geological Science*, v. 36, p. 147-198.

Hall, N.T., 1965, *Petrology of the type Merced Group, San Francisco Peninsula, California*, MA thesis, University of California, Berkeley, 127 p.

Hall, N.T., 1966, Fleishacker Zoo to Mussel Rock (Merced Formation)—a Plio- Pleistocene nature walk: *California Division of Mines and Geology Mineral Information Service*, v. 19, p. S22-S25.

Hunter, R.E., Clifton, H.E., Hall, N.T., Császár, G., Richmond, B.M., and Chin, J.L., 1984, *Pliocene and Pleistocene coastal and shelf deposits of the Merced Formation and associated beds, northwestern San Francisco Peninsula, California*: Society of Economic Paleontologists and Mineralogists Field Trip Guidebook 3, 1984 Midyear Meeting, p. 1-29.

Ryer, T.A., 1977, Patterns of Cretaceous shallow-marine sedimentation, Coalville and Rockport areas, Utah: *Geological Society of America Bulletin*, v. 88, p. 177-188.

Sarna-Wojcicki, A.M., Meyer, C.E., Bowman, H.R., Hall, N.T., Russell, P.C., Woodward, M.J., and Slate, J.L., 1985, Correlation of the Rockland ash bed, a 400,000-year-old stratigraphic marker in northern California and western Nevada, and implications for middle Pleistocene paleogeography of central California: *Quaternary Research*, v. 23, p. 236-257.

Wagner, D.L., Bortugno, E.J., and McJunkin, R.D., (in press), Geologic map of the San Francisco-San Jose Quadrangle, California: Sacramento, California Division of Mines and Geology Map, scale 1:250,000.

Tectonic Framework of the Loma Prieta Area

R.J. McLaughlin, W.P. Elder, and Kristin McDougall[1]

INTRODUCTION

This field trip will focus on rocks in a major fault block along the northeast side of the San Andreas fault near Loma Prieta. This fault block, here referred to as the Sierra Azul block, is bounded on the southwest by the steeply dipping San Andreas fault, and to the northeast, by southwest-dipping segments of the Sargent, Berrocal, Sierra Azul, and Soda Springs faults (Fig. 1). The Sierra Azul block is at least 28 mi (45 km) long and about 4 mi (6 km) wide, and is composed of as much as 3600-5600 ft (1100-1700 m) of Coast Range ophiolite, overlain by 8200-9800 ft (2500-3000 m) of marine clastic rocks of Late Jurassic through early Miocene age. The strike-slip and reverse-motion Berrocal-Sargent fault system juxtaposes this fault block against shallow marine, early Miocene and younger rocks that rest depositionally on the Franciscan Complex. The field trip will look at the field relations of rocks in the Sierra Azul block and to the northeast, with emphasis on the timing of major Tertiary faulting, relationships of rocks across these faults, and possible long-term displacement history of the Sierra Azul block by large-scale movement on the Calaveras-Hayward-San Andreas fault system or precursor faults.

STRATIGRAPHY[2]

The following paragraphs summarize and discuss the stratigraphy and depositional settings of rocks in the field trip area.

Franciscan Complex (Upper Cretaceous to Lower Jurassic): Rocks north of the Soda Spring-Sierra Azul-Berrocal fault system, and structurally beneath the Sierra Azul block are assigned to the Central belt of the Franciscan Complex. Two separate terranes of the Central belt are present:

Permanente terrane (Upper to Lower Cretaceous): The Permanente terrane of Blake and others (1984) consists of 1) basaltic flows, breccias and tuffs; 2) radiolarian-bearing siliceous tuff; 3) foraminiferal, bioclastic and oolitic limestone, and radiolarian chert; and 4) metasandstone and argillite locally overlying the limestone section (Sliter and others, 1991).

Bald Mountain-El Sombroso terrane (Lower Cretaceous to Lower Jurassic or older): This name is informally applied here to the chert section of Bald Mountain and El Sombroso ridge. The unit structurally overlies the Permanente terrane and consists of 1) basaltic pillow flows, flow breccias, and aquagene tuff, overlain by 2) thin to thick lenses of radiolarian chert that are depositionally overlain by 3) volcanic-rich metasandstone and argillite.

Slate and phyllite of Loma Prieta Peak (Jurassic or older?): At Loma Prieta Peak, a thin sliver of slate and phyllite occurs above the sole of a thrust fault juxtaposing ophiolite with Eocene sandstone (Figs. 1, 2). The depositional and metamorphic ages of these rocks are unknown. However, this unit is similar to Jurassic rocks metamorphosed during the Nevadan orogeny in the western Sierra Nevada (i.e. the Mariposa Slate) and in the Klamath Mountains (i.e., the Galice Fm.).

Coast Range ophiolite (Jurassic): A 5200-5600 ft (1600-1700 m) thick slab of predominantly mafic to ultramafic igneous rocks in the Sierra Azul block is correlative with the Coast Range ophiolite. The best-exposed ophiolite sections in the Loma Prieta and Mount Umunhum areas (Fig. 1) are broken internally by attenuation and compressional faults. A composite section of the ophiolite includes a lower ultramafic and gabbro cumulate section, a middle dike and sill

[1] U.S. Geological Survey, 345 Middlefield Rd., Menlo Park, CA 94025

[2] The stratigraphic nomenclature and unit age assignments used in this report may not necessarily conform to current usage by the U.S. Geological Survey.

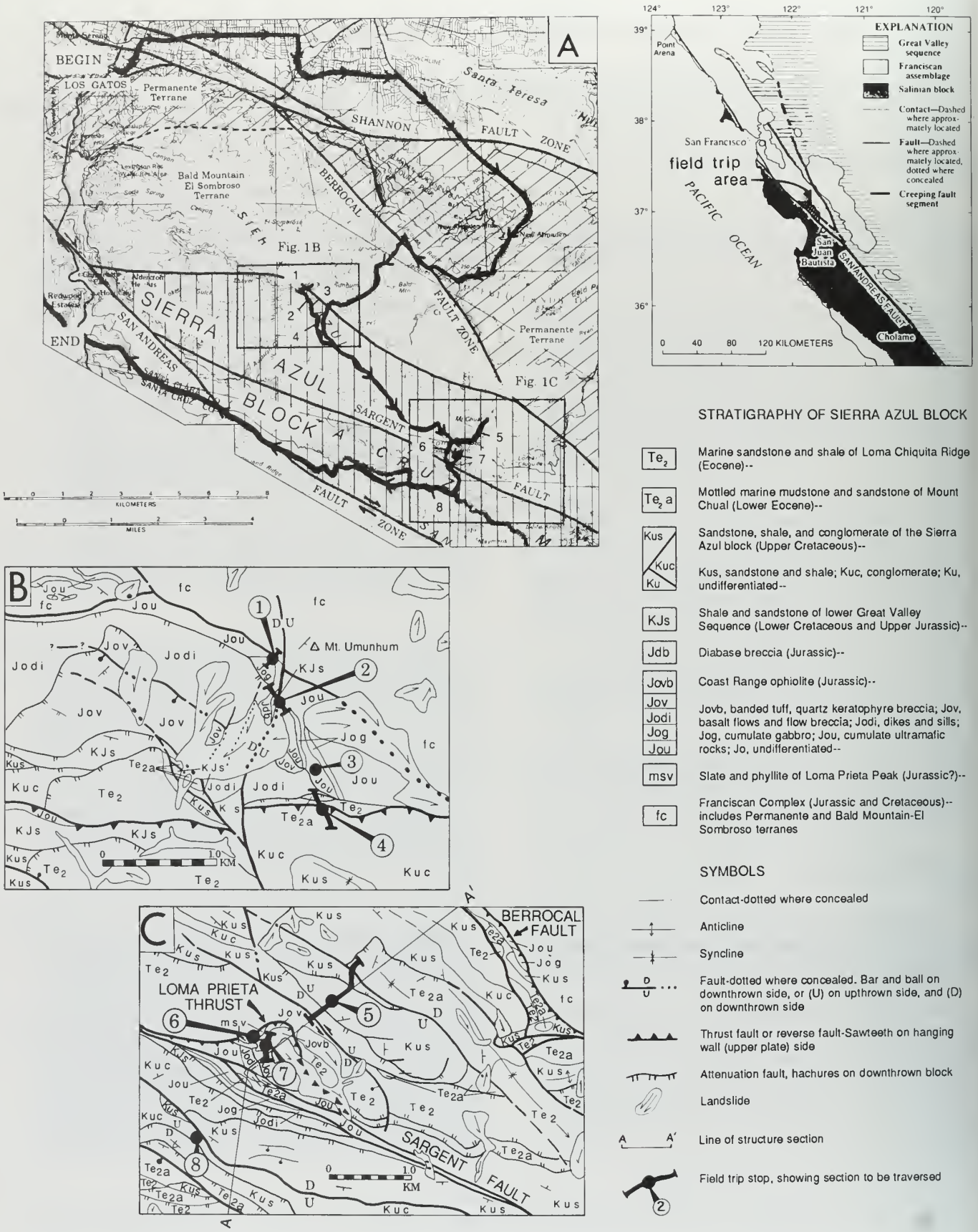

Figure 1A. Road map showing location of the Loma Prieta area and field trip stops; 1B. Geologic map of the Mount Umunhum area; 1C. Geologic map of the Loma Prieta Peak area, showing line of structure section in Figure 2A.

A

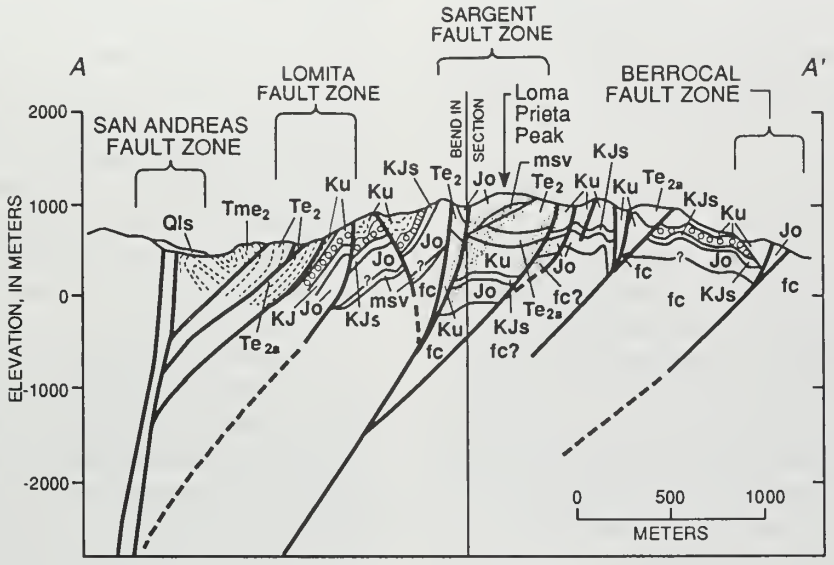

Comparative tectonostratigraphy north and south of Sargent-Berrocal fault zone

B

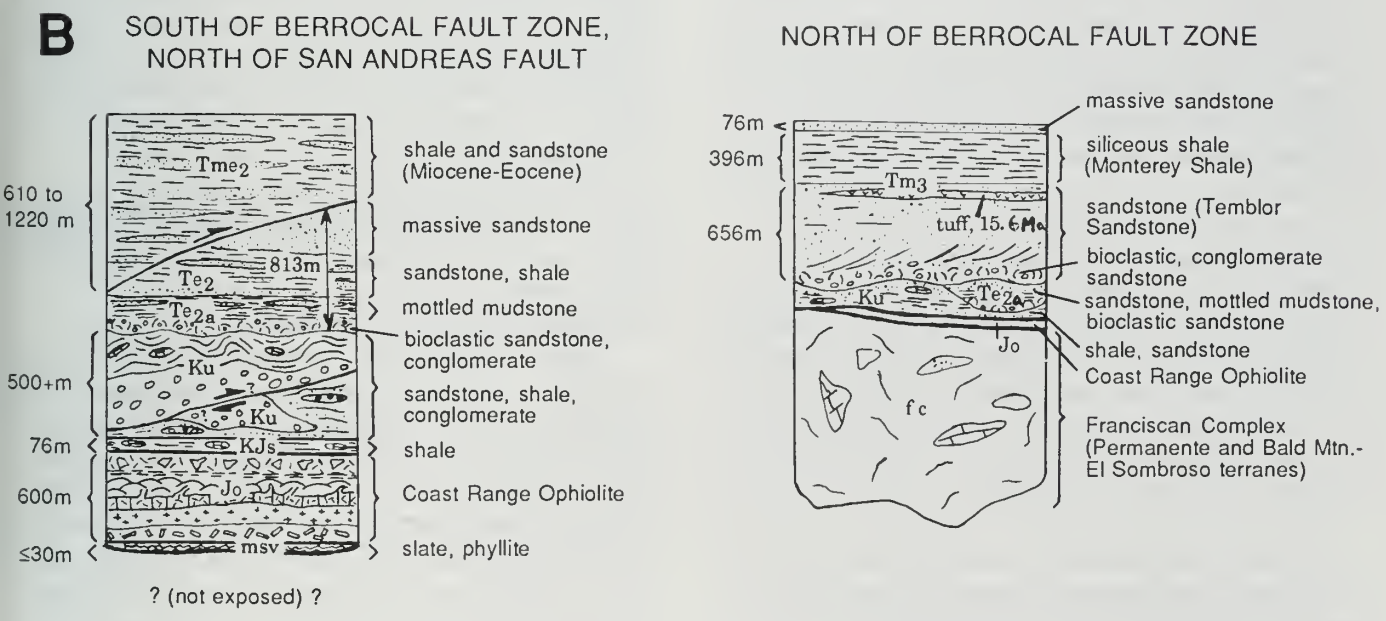

Figure 2A. Structure section through the Loma Prieta area. Section line is shown on Figure 1C; 2B. Comparative tectonostratigraphic relations across the Berrocal fault.

complex, and an upper volcanic and pelagic section.

No age data are available for the ophiolitic rocks of the Sierra Azul block, although Pb-U and K-Ar dating is in progress. Poorly preserved radiolarians from cherts in the volcanic unit suggest a Jurassic age (B. Murchey, written commun., 1989).

Shale and sandstone of lower Great Valley sequence (Lower Cretaceous and Upper Jurassic): Thin fault-bounded slices of hard shale, cherty arkosic wacke, and radiolarian tuff intervene between the Coast Range ophiolite and overlying rocks. This extensively sheared unit crops out along three narrow belts in the area and is up to 1000 ft (300 m) thick (Fig. 1). A Late Jurassic (Tithonian) to Early Cretaceous (Valanginian) age is indicated for this unit by several species of *Buchia* bivalves that occur in hard silicified carbonate beds and nodular shale.

Sandstone, shale and conglomerate of the Sierra Azul block (Upper Cretaceous): A thick section of Upper Cretaceous clastic rocks is bounded above and below by bedding-parallel faults and is laumontized and deformed by folding and faulting that predates the Eocene. The lower part of this unit consists predominantly of coarse pebble to boulder conglomerate with up to 84 percent rounded volcanic and plutonic clasts. The top of the conglomeratic interval locally contains channel-fill sequences with abundant transported shallow marine bioclastic debris of late Campanian age. Many of the fossils in this oyster-rich bioclastic sequence are extremely rare in California, being taxa that required a hard substrate for habitation (Elder, 1991). The conglomerate is overlain by flysch-like arkosic wacke and argillite. The argillite contains scattered carbonate concretions yielding late Campanian mollusks that appear to have been transported from a shelf setting. The Upper Cretaceous sequence largely reflects a westward-flowing submarine fan system fed by a nearshore source area.

Mottled marine mudstone and sandstone of Mount Chual (lower Eocene): This approximately 2600 ft (800 m) thick sequence is composed in ascending order of 1) a thin discontinuous conglomerate; 2) a discontinuous glauconite bed; 3) mottled red and green mudstone; and 4) interbedded quartzofeldspathic sandstone and mudstone (Fig. 2b). The base of this unit is a bedding-parallel fault at most localities. Where present, a conglomerate in the lowest exposed beds contains significant amounts of detritus derived from sources in the Franciscan Complex and Coast Range ophiolite, reflecting earliest unroofing of basement rocks in this region. The conglomerate locally exhibits tangential cross-bedding, is well sorted, and contains discocyclinnid foraminifers and red algae, indicative of a nearshore depositional setting.

The overlying mudstone is a distinctive olive green or mottled red and green color, and contains abundant foraminifers that are easily visible with a hand lens. Foraminifers and nannofossils support an early Eocene (Penutian, planktic zones P8 to P9 and nannoplankton zone CP11) age for the mudstone (McDougall, 1989, 1991). Benthic faunas suggest bathymetric ranges from lower bathyal to abyssal depths (> 6600 ft, 2000 m). The upward transition from conglomerate to mottled mudstone delineates a rapid transgression which occurred during or prior to foraminiferal zone P8.

Marine sandstone and shale of Loma Chiquita ridge (Eocene): As much as 2600 ft (800 m) of section is assignable to this unit of thick-bedded quartzofeldspathic sandstone overlain by rhythmically interbedded micaceous sandstone and carbonaceous shale, and by cavernous weathering quartzofeldspathic sandstone with minor semi-siliceous mudstone intercalations. An early to late Eocene age is indicated by molds of *Turritella buwaldana* in the middle part of the section, and by *Parvanussium stanfordensis* (identified by C. Powell, U.S. Geological Survey, 1988) in the upper part of the unit.

Marine shale and sandstone of Highland Way (lower Miocene to lower Eocene): This unit consists of up to 3900 ft (1200 m) of hard carbonaceous to cherty shale and minor interbeds of locally glauconitic quartzofeldspathic sandstone. Microfossils indicate early Eocene planktic zones P8 to P9 and nannofossil zone CP11 in the lower part of this unit, and a late Oligocene to early Miocene age (Zemorrian to Saucesian

stages) for the upper part of the unit (McDougall, 1989; Bukry, unpublished data). Benthic foraminifers indicate deposition at bathyal or greater depths. The upper part of this unit overlaps in age with the Temblor Sandstone northeast of the Berrocal-Sargent fault zone, but accumulated in a deeper water setting.

Temblor Sandstone (Oligocene to middle Miocene): The Temblor Sandstone consists of a basal conglomerate overlain by arkosic sandstone and by as much as 200 ft (61 m) of dacitic tuff and breccia (Fig. 2b; Bailey and Everhart, 1964). The Temblor conglomerate locally includes nearshore molluscan fossils and fragmental fossil material near the base. The conglomerate rests unconformably on the Franciscan Complex and Coast Range ophiolite. Fossils indicate deposition in a moderately shallow marine setting and an Oligocene or lower Miocene age for the lower part of the unit. Plagioclase from dacite tuff in the upper part of the Temblor yielded a K-Ar date of about 15.6 Ma (P. Russel and D. Sorg, written commun., 1990).

Monterey Shale (middle Miocene): The Monterey shale is exposed along the Shannon and Berrocal faults (Fig. 1) and depositionally overlies the Temblor Sandstone (Bailey and Everhart, 1964). Microfossils suggest a middle Miocene age (Luisian Stage, nannofossil zone CN3-CN4) and deposition at upper bathyal depths (1650-4950 ft, 500-1500 m) in an area of upwelling and high silica productivity (McDougall, 1989, and Bukry, unpublished data).

STRUCTURE AND ITS REGIONAL SIGNIFICANCE

Extension, contraction, and strike-slip: The Mesozoic through lower Miocene rock units of the Sierra Azul block are cut by contact- and bedding-parallel faults that emplace younger over older rocks, in many places with the loss of stratigraphic section. These faults are interpreted as attenuation faults. Major contractional faulting (thrusting), accompanied by strike-slip motion, has also occurred across the Berrocal-Sargent fault zone in the Sierra Azul structural block since about the early Miocene. This timing of earliest thrusting is slightly younger than, or may overlap, the latest attenuation faulting. Initiation of this thrusting is constrained by 1) the uplift and erosion of Eocene and older rocks northeast of the Berrocal-Sargent fault zone prior to and coeval with deposition of the early Miocene Temblor Sandstone (Fig. 2) 10 to 17 Ma K-Ar ages from hydrothermal K-feldspar (adularia) associated with alteration along the northeast directed Sargent thrust (McLaughlin and others, manuscript in review).

Based on 118 mi (190 km) of right-slip restoration across the Hayward-Calaveras fault system, the early Miocene (ca. 20 Ma) position of the Sierra Azul block was near Chalome, along the southwest side of the Diablo Range (McLaughlin and others, 1990). This location is close to the 20-24 Ma position of the Mendocino triple junction (Engebretson and others, 1985). Thus it can be argued that the contractional faulting was initiated near the propagating end of the San Andreas transform.

Crustal Shortening, uplift, and tectonic wedging: The widespread presence of laumontite in the Mesozoic clastic section is indicative of burial to 2-6 mi (3-10 km). Its absence in the overlying Eocene or younger rocks, suggests that the Mesozoic section was uplifted above 2 mi (3 km) prior to the early Eocene during early unroofing of the Coast Ranges. Further uplift of the Mesozoic section along the Sargent and Berrocal faults, and its northeastward emplacement over the Eocene section, must have accompanied and followed initiation of the San Andreas fault system.

The abrupt transition from shallow marine to bathyal or deeper Miocene deposits, and a lack of evidence for more than 2 mi (3 km) of right-slip across the Sargent-Berrocal fault system, suggests that as much as 31 mi (50 km) of the lower Miocene margin has been tectonically removed through fault-normal shortening. However, it is unlikely that this much shortening could be taken up in the 4 mi (6 km) between the Berrocal and San Andreas faults, unless at depth these faults are shallow-dipping or root into a nearly flat zone of uncoupling. Alternatively, some of the Miocene margin overridden by the Sargent and Berrocal

faults may have been subsequently cut off and right-laterally displaced along the San Andreas fault.

Deep crustal models for this region based on seismic refraction and reflection data may provide a mechanism for uplift and crustal shortening linked to the San Andreas fault and to a deep zone of uncoupling (Fuis and Mooney, 1990; Wentworth and Zoback, 1990). These models propose that a tectonic wedge composed of Franciscan Complex rocks extends eastward from the San Andreas fault to the Great Valley (Fig. 3). The west-dipping basal thrust of this hypothetical wedge displaces the Franciscan Complex eastward over Sierran basement. If this model is

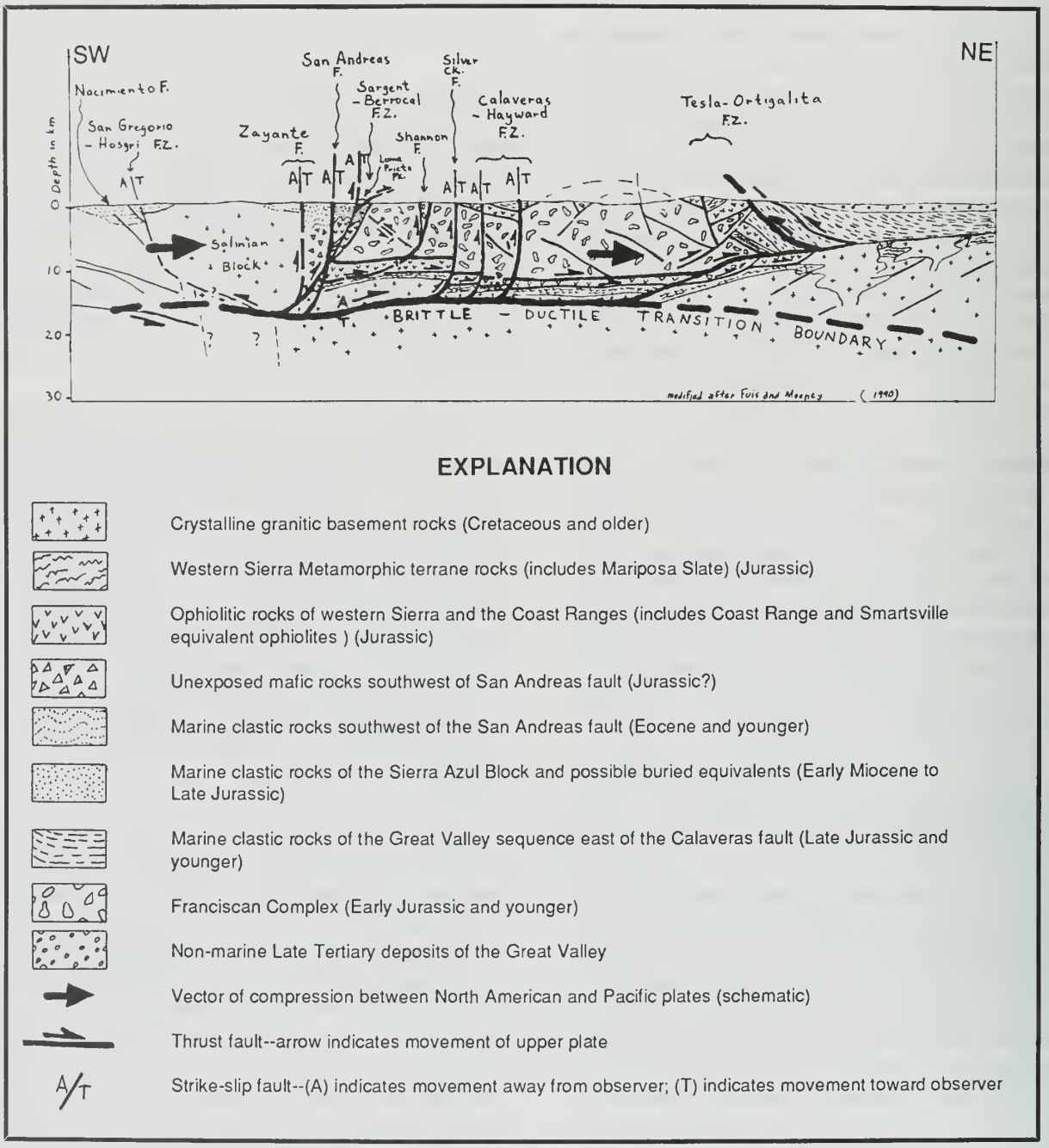

Figure 3. Hypothetical deep crustal structure along a northeast-southwest-oriented seismic refraction line through the field trip area. Modified after Fuis and Mooney, 1990.

valid, substantial episodic uplift and shortening since the early Tertiary would have been taken up on the basal thrust of the wedge and across faults that root into it.

ROAD LOG

The field trip area is reached by taking Hwy. 17 southwestward towards Santa Cruz from either I-280 or Hwy. 101. The road log begins at the Hwy. 9 (east) exit from Hwy. 17 at Los Gatos. Those using this field trip road log should note that several locked gates are encountered in the field trip area, beginning midway up Mount Umunhum Rd. Permission and access through these gates must be secured through numerous private land owners and the Mid-Peninsula Regional Open Space District. Distances are in miles.

0.0 At junction of Hwys. 17 and 9, take Hwy. 9-east exit and then left on Los Gatos Rd.

1.3 Turn right on Blossom Hill Rd.

4.6 Turn right on Camden Blvd.

7.7 Turn right on Almaden Blvd.

9.4 Turn right on Old Almaden Rd.

12.2 Historic town of New Almaden.

13.9 Turn right on Hicks Rd.

15.0 Basal Temblor conglomerate containing molluscan fragments and Franciscan detritus in depositional contact with underlying Franciscan basalts.

15.6 Turn left on Mount Umunhum Rd., leaving Berrocal fault zone and traversing through melange of Franciscan Bald Mountain-El Sombroso terrane.

16.9 Large composite block of radiolarian chert overlying metabasalt in Bald Mountain-El Sombroso terrane. Radiolarian biogeography and paleomagnetics indicate chert was translated north from near Early Jurassic paleoequator (Hagstrum and Murchey, 1991).

17.4 First locked gate. Pebbly Franciscan sandstone with green chert clasts to right.

17.7 Cut exposing well-bedded flysch-like metasandstone and argillite.

18.3 Faulted contact of Franciscan Complex with Coast Range ophiolite; obscured by large-scale landsliding.

20.5 Cross into Upper Cretaceous conglomerate.

20.7 Turn right on Loma Prieta Rd. Continue through two gates into abandoned Mount Umunhum Air Force Base; turn right on paved road to top of mountain and drive to locked gate.

22.1 **STOP 1** At this stop (Fig. 1B) we will inspect the fault contact of sheared Franciscan metasandstone with the Coast Range ophiolite. The ophiolite here is composed of coarse clinopyroxene-, olivine-, and hornblende-bearing cumulate gabbros cut by finer-grained dikes.

22.3 Return through gate at base entrance, driving through ophiolite section consisting of highly altered, weathered, and sheared dikes and sills of gabbroic to dioritic composition. These rocks are structurally high in the ophiolite, and some of the deeply weathered, fine-grained rocks appear to be stratified and may represent altered tuffs and flows.

22.5 **STOP 2** Here we will look at a north-northeast-trending fault that cuts through the ophiolite section (Fig. 1B). This fault juxtaposes the relatively upfaulted ultramafic and gabbroic cumulates of the ophiolite (to east) with the uppermost dike and sill rocks of the ophiolite (to west). The dike and sill rocks are overlain by a thin unit of brecciated diabase (sedimentary or tectonic brecciation?) that is subsequently overlain by sheared black mudstone considered to be part of the basal (Tithonian-Valanginian) Great Valley sequence. Continue driving east through

alternating ultramafic and gabbroic cumulates cut by gabbroic dikes.

22.9 **STOP 3** At this stop we inspect ultramafic cumulate rocks cut by discordant dikes and dikelets that are altered to rodingite assemblages. Note outcrop-scale faults offsetting dikelets.

Continue driving through cumulate section and through gate.

23.3 **STOP 4** From this stop, we will walk through a sheared and deformed interval adjacent to the contact of the ophiolite with the overlying sedimentary section. Here we can observe early Eocene red and green foraminifer-bearing shale (planktic foraminifer zones P7-P9) and quartzofeldspathic sandstone faulted above weathered dike rocks of the ophiolite. These Eocene rocks are then in fault contact with an overlying Late Cretaceous arkosic wacke and polymictic pebble to boulder conglomerate. The conglomerate contains abundant intermediate to silicic plutonic and volcanic clasts. Note extensive penetrative deformation, evidence of sheared-out transposed fold hinges, and boudinage in Eocene and Cretaceous rocks.

23.4 From intersection of paved road and east-trending gravel road, head east on gravel road through locked gate and along crest of Sierra Azul Mountains. The road passes through Late Cretaceous (Campanian) conglomerate, arkosic wacke, and interbedded shale of the Sierra Azul area. Older rocks of middle to early Late Cretaceous age are missing from the Great Valley section, and an attenuated section of *Buchia*-bearing shale (Tithonian-Valanginian) intervenes between the Coast Range ophiolite and Late Cretaceous rocks.

24.7 At road junction bear left on lower road.

26.0 Cross up-section from Late Cretaceous rocks across sheared and extensively hydrothermally altered zone of quartz-veined Eocene sandstone and shale of Loma Chiquita Ridge.

26.5 Views to southwest of Sargent fault trace forming prominent topographic notches.

28.1 Bear left at intersection taking road around north side of Loma Prieta Peak. Hydrothermally altered Eocene sandstone exposed in cuts below Loma Prieta thrust.

28.6 Topographic saddle formed by fault between Eocene (to southwest) and Cretaceous rocks (to northeast).

28.7 **STOP 5** Park at the junction of road to top of Crystal Peak. Here we will first inspect a well-exposed fault in Late Cretaceous sandstone.

Walk on road northward towards Mount Chual.

28.9 Observe broken and folded Late Cretaceous arkosic wacke and conglomerate.

29.0 Interval of flysch-like, thinly interbedded arkosic wacke and argillite.

29.1 Overlying massive argillite containing concretions, some of which yield macrofossils. Cross saddle and fault contact with Eocene on east flank of Mount Chual. Observe complex structural and stratigraphic relations in lower part of lower Eocene section just northeast of fault contact with Cretaceous rocks. The prominent outcrop southeast of the road is a well-sorted (slump-folded ?) conglomerate in the Eocene section, containing Franciscan and ophiolitic detritus, abundant shallow-marine bioclastics, and large foraminifers. This unit is overlain by a thin bed of glauconite sandstone and then by a distinctive unit comprised of mottled red and green foraminifer-bearing mudstone and quartzofeldspathic sandstone.

Return to vehicles and backtrack to junction of Loma Prieta Rd.

30.3 Turn left on Loma Prieta Rd. and drive along west flank of Loma Prieta Peak toward Sargent fault.

30.6 **STOP 6** Here we will look at a thin slice of slate and phyllite tentatively correlated with the Mariposa Slate of the western Sierra foothills. This slate and phyllite is intercalated between the Coast Range ophiolite in the hanging wall and Eocene sandstone in the footwall of the Loma Prieta thrust.

Drive southward to Sargent fault, traversing basalt and diabase in upper part of Coast Range ophiolite.

31.0 Turn left on road to Loma Prieta Peak and drive through gate. Active trace of Sargent fault crosses divide between Uvas Creek to east and Los Gatos Creek to west. Cumulate ultramafic and gabbroic rocks are exposed along Loma Prieta Rd. and on lower part of ridge south of Sargent fault. Broken and sheared pillow basalt flows and flow breccias are exposed in cuts along road to peak.

31.4 Crossing large landslide.

31.5 Turn left and drive through locked gate.

31.7 **STOP 7** Park at road intersection on southwest side of Loma Prieta Peak. Note pillow basalt in cuts at road juncture. Walk on lower road around northwest side of peak. Here we can observe a depositional contact between the basalt and an overlying arc sequence of banded water-laid andesitic tuff interbedded with black radiolarian chert and quartz keratophyre breccia having clasts up to boulder size. These rocks are cross-cut by fine quartz veins, and the keratophyre breccia is locally permeated with secondary potassic hydrothermal alteration (quartz-adularia).

Return to vehicles and drive back to Loma Prieta Rd.

32.5 Turn left on Loma Prieta Rd., crossing Sargent fault zone.

32.8 Crossing fault contact of ophiolite (to north) and attenuated section of Tithonian lower Great Valley sequence (to south).

32.9 Crossing faulted concordant contact of lower Great Valley sequence with overlying south-dipping Campanian conglomerate.

33.1 Contact of Late Cretaceous thinly bedded flysch overlying conglomerate.

33.3 Intersection of Mount Madonna Rd. Flysch section in roadcuts to left is complexly folded and downdropped along steeply dipping normal faults that are sub-parallel to bedding strike. Cross fault and pass back downsection into Campanian conglomerate.

34.0 **STOP 8** At this stop we will look at an interval lying near the top of the Campanian conglomerate and the base of the overlying massive arkosic wacke. The conglomerate represents a turbidite channel-fill deposit containing clasts up to boulder size. Here the conglomerate includes a channel-fill sequence containing transported oyster-rich bioclastic debris of shallow-water origin. Many rare nearshore taxa that required a hard substrate for habitation are present in this sequence. Note the large inoceramid bivalve cut by a small scale right-lateral fault.

Resume driving south toward the San Andreas fault. Drive down Mount Bach Rd. through fault-repeated Late Cretaceous and Eocene sections.

37.1 Turn right (northwest) on Highland Way and drive along active rift valley of San Andreas fault.

42.2 Passing Summit Ridge area along southwest side of San Andreas fault where major extensional and sinistral surface cracking occurred during Loma Prieta earthquake and in the earthquake of 1906. This deformation is well west of the main trace of the San Andreas fault.

44.1 Junction of Hwy. 17; end of road log.

REFERENCES CITED

Bailey, E.H., and Everhart, D.L., 1964, Geology and quicksilver deposits of the New Almaden District, Santa Clara County, California: *U.S. Geological Survey Professional Paper 360*, 206p.

Blake, M.C., Jr., Howell, D.G., and Jayko, A.S., 1984, Tectonostratigraphic terranes of the San Francisco Bay region, *in* Blake, M.C., Jr., ed., *Franciscan geology of northern California:* Pacific Section, Society of Economic Paleontologists and Mineralogists, v. 43, p. 5-22.

Elder, W.P., 1991, An unusual Late Cretaceous fauna from an oyster-rich interval in the Santa Cruz Mountains of California: *U.S. Geological Survey Bulletin 1394-E*, in press.

Engebretson, D.C., Cox, A., and Gordon, R.G., 1985, Relative motions between oceanic and continental plates in the Pacific basin: *Geological Society of America Special Paper 206*, 59p.

Fuis, G.S., and Mooney, W.D., 1990, Lithospheric structure and tectonics from seismic-refraction and other data, *in* R.E. Wallace, ed., The San Andreas fault system, *U.S. Geological Survey Professional Paper 1515*, p. 207-236.

Hagstrum, J.T., and Murchey, B.L., 1991, Paleomagnetism of Lower Jurassic chert within the Franciscan Complex, northern California, indicates deposition at the paleoequator and accretion near 7° north paleolatitude (abs.): *Geological Society of America Abstracts with Programs*, v. 23.

McDougall, Kristin, 1989, Paleogene benthic foraminifers from the Loma Prieta Quadrangle, California: *U.S. Geological Survey Open-File Report 89-649*, 91p.

McDougall, Kristin, 1991, Benthic foraminifers from the Laurel Quadrangle, California: *U.S. Geological Survey Open-File Report 91-13*, 66p.

McLaughlin, R.J., Sliter, W.V., Elder, W.P., McDougall, K., Russell, P.C., Sorg, D.H., Sims, J.D., and Blake, M.C., Jr., 1990, 190 km post-Middle Miocene offset on the Tolay-Hayward-Calaveras fault system superposed on large-scale Late Cretaceous to early Eocene translation (abs.): *Geological Society of America Abstracts with Programs*, v. 22, no. 3, p. 67.

McLaughlin, R.J., Blake, M.C., Jr., Griscom, A., Blome, C. D., and Murchey, B., 1988, Tectonics of formation, translation, and dispersal of the Coast Range ophiolite of California: *Tectonics*, v. 7, no. 5, p. 1033-1056.

Sliter, W.V., Murchey, B.L., McLaughlin, R.J., and Kistler, R.W., 1991, Permanente terrane: history of Early Cretaceous seamount formation in the eastern Pacific (abs.): *Geological Society of America Abstracts with Programs*, v. 23.

Wentworth, C.M., and Zoback, M.D., 1990, Structure of the Coalinga area and thrust origin of the earthquake, *in* Rymer, M.J., and W.L. Ellsworth, eds., The Coalinga, California, earthquake of May 2, 1983: *U.S. Geological Survey Professional Paper 1487*, p. 41-68.

Field Trip Guide to the Geology of Sonoma County

Terry Wright[1]

INTRODUCTION

Our field excursion into Sonoma County is a journey into an unique area. We will tour the scenic coastline, the Russian River valley and rolling interior hills that are the setting of world-famous wine and cuisine. Our route is over terranes of the Franciscan Complex, across the San Andreas fault to the Salinian block at Bodega Head. We continue up the coast through Central belt melange of the Franciscan Complex. We conclude by driving through the Russian River wine country and up the flank of Mount St. Helena to the Petrified Forest, where we can see 100 ft (30 m) logs of redwood preserved in ash of the Sonoma Volcanics. We will sample the bounty of this area with a Sonoma County wine and food tasting in the Petrified Forest Visitor Center.

OVERVIEW OF SONOMA COUNTY GEOLOGY

Geologically, Sonoma County is divided by the San Andreas fault (Figs. 1, 2). To the west on the tip of Bodega Head, is the Salinian terrane: ancient continental rocks formed far to the south and moved north at least 195 mi (315 km) by the fault. To the east of the fault is the Franciscan Complex; oceanic rocks mixed by faulting in an accretionary wedge as the ocean floor slid east under the edge of the continent. Both areas are covered by a thin mantle of younger rocks formed in shallow seas, beaches, volcanoes, and in present rivers.

***West of the San Andreas fault*:** Bedrock west of the fault (Fig. 2) is beautifully exposed on the ocean side of Bodega Head at Windmill Beach (Stop 1). The Bodega Head diorite of Cretaceous age contains inclusions of older gneiss, schist, marble and quartzite. These rocks are cut by pinkish stripes of coarse-grained granite pegmatite and aplite dikes, and are fractured by faults and joints related to the San Andreas fault system. Orange, layered sands of marine terrace deposits overlie the diorite, and modern quartz-rich sand forms the beach.

***East of the San Andreas fault*:** Bedrock east of the San Andreas fault is the Franciscan Complex (Fig. 2), a group of rocks formed on the ocean floor, in part many thousands of miles from here, and accreted as different terranes. These rocks were then mixed together in the subduction zone. Some rocks were faulted deep into the earth where they were affected by high pressure, but fairly low temperatures, giving rise to blueschist. The California state rock, serpentinite, is also typical. Examples of these rocks are beautifully exposed at Shell Beach on the coast south of Jenner (Stop 2).

A mountain range was formed here during the Tertiary and later was eroded into a hilly plain. A thin mantle of younger sedimentary and volcanic rocks then was deposited on the Franciscan Complex. The fine silica-rich sediments of the Monterey Formation and silt and mudstones of the Petaluma Formation were deposited in a shallow sea. In the late Tertiary volcanoes began erupting in southern Sonoma County. Magma was generated from the opening of a slab window associated with northward migration of the Mendocino triple junction and/or pulling apart along faults related to the San Andreas fault system (Hearn and others, 1981). Lava flows, ash falls and ash flows blasted out of a series of volcanoes and covered the area from Santa Rosa to Napa County with volcanic rocks. A forest of towering

[1] Geology Department, Sonoma State University, Rohnert Park, CA 94928; Visiting professor, Wellesley College, Wellesley, MA 02181

redwoods was felled by one of these blasts and buried under tons of ash (Mattison, 1990). This became the Petrified Forest (Stop 3). The volcanic rocks are collectively known as the Sonoma Volcanics.

To the west, sand and debris from the eruptions and erosion of the volcanoes collected in a shallow sea to form the Wilson Grove Formation. Light-colored smooth sandy outcrops with occasional fossil shells represent the Wilson Grove Formation in the hills around Sebastopol and Forestville.

Uplift from the plates grinding together along the San Andreas fault pushed the Franciscan Complex and overlying rocks upward. The Russian River established its present course to the sea before uplift. It then sliced down through the underlying hard rocks of the Coast Range during uplift and cut a canyon to the sea (Howard, 1979).

As the modern Coast Ranges grew, river erosion wore them down and filled valleys between ranges with sand and gravel. This formed the plain where Santa Rosa, Rohnert Park and Cotati are now located. The rugged mountains to the east are underlain by Franciscan Complex and Sonoma Volcanics. The low hills around Sebastopol are carved on the Wilson Grove sands and provide excellent drainage for growing apples and grapes. The rugged north coastal mountains are formed on the hard rocks of the Franciscan Complex. Sheared shale in fault zones make some areas very weak and susceptible to landsliding.

The San Andreas fault is the plate boundary between the continental North American plate and

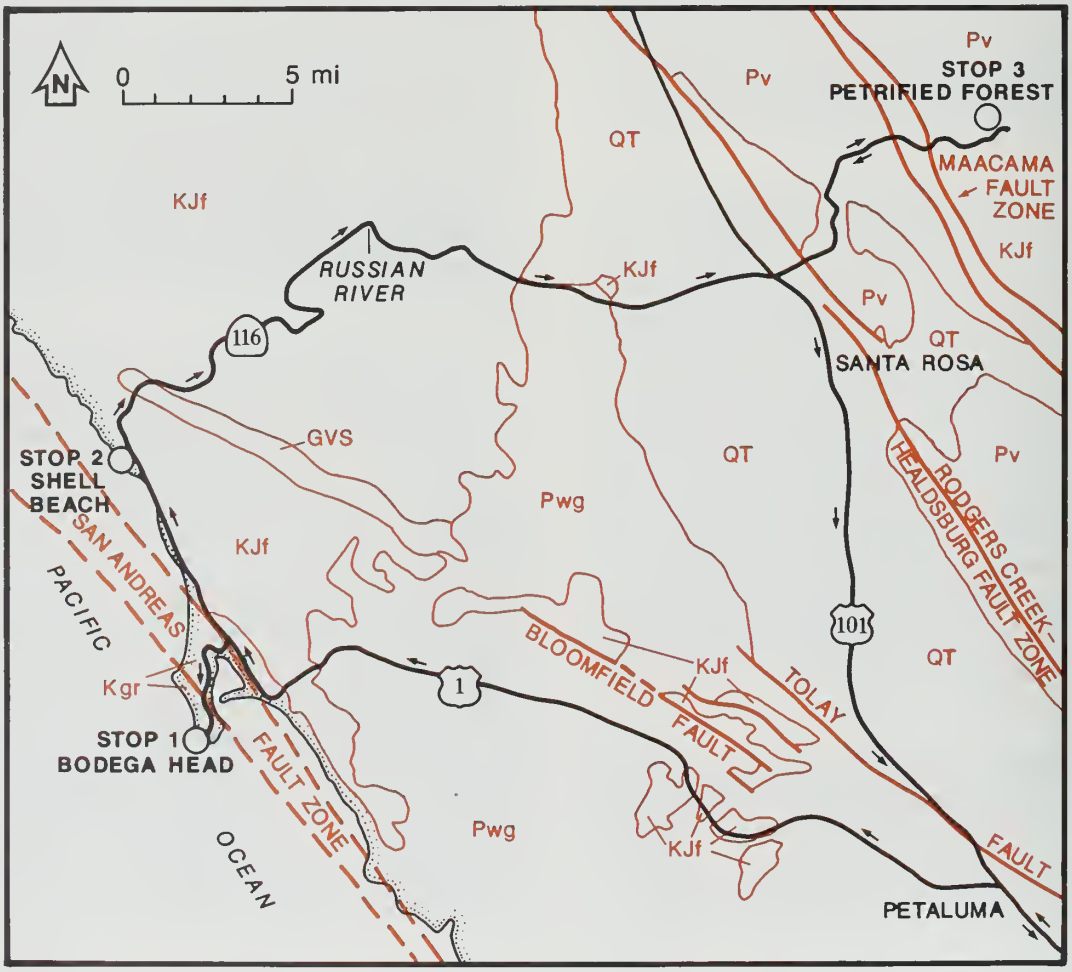

Figure 1. Map of field trip area showing major units. KJf, Franciscan Complex (n, Novato terrane; rn, Rio Nido terrane); GVS, Great Valley sequence; Pwg, Wilson Grove Formation; Pv, Sonoma Volcanics; QT, alluvium. Base map from Wagner and Bortugno, 1982.

the Pacific Ocean plate. It has displaced rocks on the west side to the north in a right-lateral sense. It stretches 650 mi (1046 km) from Shelter Cove in Humboldt County south to the Salton Sea. Bodega Head and the stretch of the coast from Fort Ross to Point Arena have moved at least 195 mi (315 km) from the south in the last 20 Ma. Diorite and granite seen at Bodega Head to the west of the fault have been displaced at least from the Tehachapi Mountains of southern California.

Movement continues today along the fault at the average rate of 1 in (2.5 cm) per year. However, it can occur suddenly with as much as 20 ft (6.5 m) of horizontal movement and 3 ft (1 m) of vertical movement, as it did during the 1906 earthquake. Damage in 1906 per capita was greater in Santa Rosa than in San Francisco because of thick alluvium in the Santa Rosa plain.

Minor earthquakes occur along the faults that parallel the San Andreas in Sonoma County. These are evidence of continued movement. Today most earthquakes occur on an eastern branch of the San Andreas fault, the Rodgers Creek-Healdsburg fault. In 1969, two moderate earthquakes rattled Santa Rosa, causing $8.35 million in damage (Alfors and others, 1973). Several small earthquakes occur in Sonoma County every month, mainly centered along the Maacama or Rodgers Creek-Healdsburg faults or in the Geysers geothermal area.

FIELD TRIP LOG

From the Cathedral Hill Hotel, follow Van Ness Ave. north to Lombard, turn left and follow Hwy. 101 and signs to the Golden Gate Bridge. Continue north across the bridge and up the steep hill (Waldo Grade). Road cuts on the Waldo Grade are in the Marin Headlands terrane (Blake and others, 1984). This terrane is a sequence of pillow lava overlain by bedded chert, which is in turn overlain by turbidites. This sequence formed in open ocean, travelled to the trench and then was accreted to the margin of the continent. During accretion, a series of thrust slices and folds formed (Wahrhaftig, 1984). Beautiful exposures of folds, faults and chert are on the road to the west into the Marin Headlands (Golden Gate National Recreational Area) at the north end of

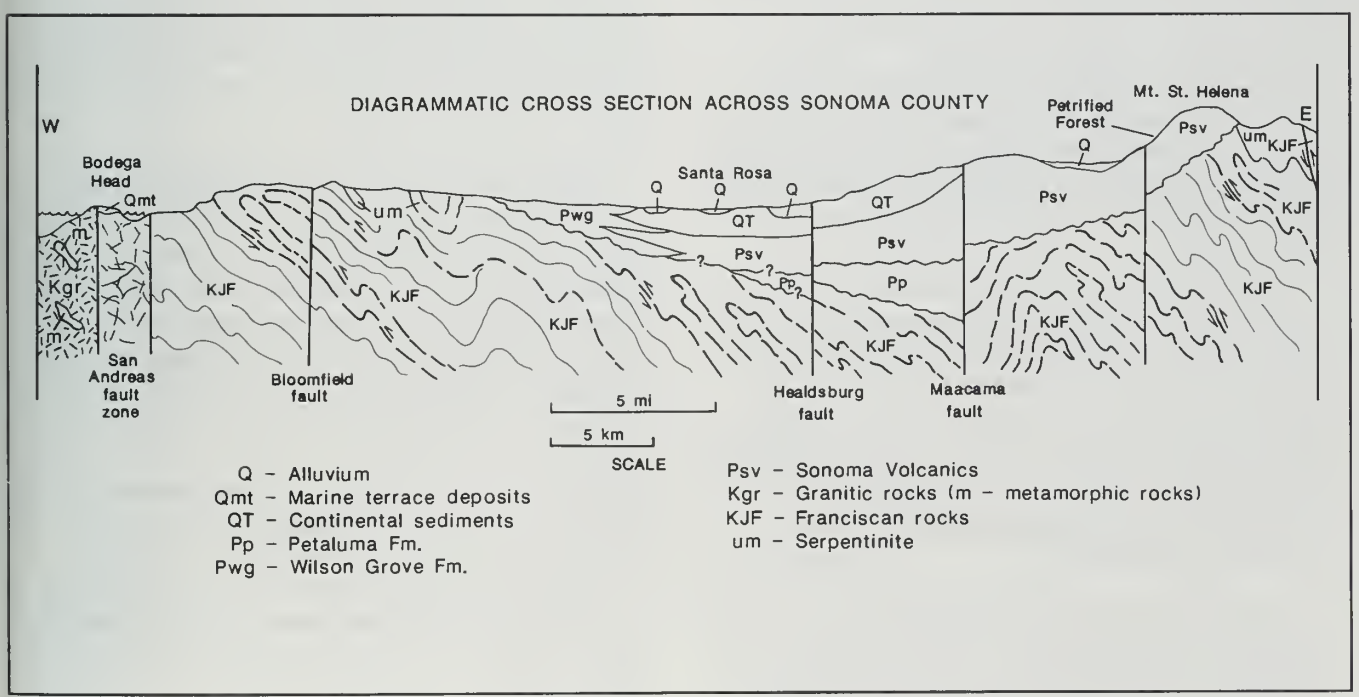

Figure 2. Geologic cross section across Sonoma County.

the Golden Gate Bridge. Uphill on Hwy. 101 we see beds of turbidites in a roadcut on both sides and then pillow lavas and chert on the left at the north side of the tunnel.

Continue on Hwy. 101 through Mill Valley, Corte Madera and San Rafael. Roadcuts here are mainly in melange of the Franciscan Central belt. Mt. Tamalpais is the high peak to the left (west). Its resistant peak is a quartzite unit that contains tourmaline. The notch north of San Rafael has good exposures of melange with a serpentinite matrix.

North of Novato, the Sonoma Mountains are to the right in the distance. The Rodgers Creek fault runs along the crest of the ridge. This is part of the San Andreas fault system and may be the northward continuation of the Hayward fault. On a clear day you can see side-hill ridges near the summit east of Petaluma. The Santa Rosa earthquakes of 1969 (M 5.6, 5.7) occurred along this fault to the north. Trenching studies across the fault east of Petaluma by the U.S. Geological Survey have resulted in an estimated 250-year recurrence interval for magnitude 7 earthquakes (Budding and others, 1989). The last major earthquake in this area was in 1808. There is no surface creep, and earthquake patterns display a seismic gap in this area. The U.S.G.S. considers this fault a prime suspect for future large earthquakes.

Drive north to Petaluma and take the Washington Street-Central Petaluma exit and then take a left (west) towards town. **Start odometer at the first stop light past the bridge**. Continue through town on Bodega Ave. toward Bodega Bay. Road log is in miles.

9.3 Two Rock. The town name comes from two resistant blocks of graywacke west of town. This is the Central terrane of the Franciscan Complex (Jurassic to Cretaceous in age). Typical melange topography occurs throughout this area with resistant blocks of graywacke and chert forming outcrops and sheared matrix forming smooth slopes.

15.5 Light-colored smooth outcrops on right are sandstones of the Wilson Grove Formation (late Miocene to Pliocene). These rocks formed in a shallow sea that covered the area between Petaluma and the coast and north to the Russian River. Some horizons contain fossil hash of pelecypods and gastropods.

Small landslides on the left are in sand of the Wilson Grove Formation. These are scars left from a disastrous storm that hit this area on January 2, 1982. Flooding and landslides caused major damage at Point Reyes and in this area.

The rounded hills and lack of trees made this the ideal location for Cristo's "Running Fence" art project. In 1976, a curtain of white nylon panels 10 ft (3 m) high was erected 15 mi (24 km) to the ocean from Hwy. 101, creating a beautiful interaction with the topography.

17.5 Continue straight west on Hwy. 1.

19.0 Entering Valley Ford. Watch for llamas on the right. A mural of the Running Fence is on the front of the store.

24.4 Hagemann Quarry (optional stop).

Vertical turbidite sequence exposed in quarry on the right. Watch for truck-crossing sign and pull over to the left side of the road carefully into large shoulder area. These rocks are mapped as the Novato Quarry terrane of the Franciscan Complex by Blake and others (1984). This is a homoclinal sequence of rhythmically bedded graywacke and shale, visible as gray and black vertical bands in the quarry wall.

A perfect exposure of an angular unconformity is in the overhang to the right of the main quarry. Vertical turbidite layers are overlain by horizontal massive beds of the Wilson Grove Formation sandstone. The sandstone appears as a rounded bluff. The contact is very sharp, and there is a basal conglomerate composed mainly of chert pebbles.

26.8 Town of Bodega Bay. This tourist and fishing town is on the east side of the bay. Erosion and perhaps some vertical movement along the San Andreas fault zone cause the low elevation here. The east side of the bay parallel to the highway is along the active trace of the fault.

28.2 Turn left onto East Shore Rd. (sign for Bodega Head). At the bottom of the hill, turn right on Bay Flat Rd. and drive across the active trace of the fault. Yes, the fault does run under the new houses here.

Sharp right turn. Note the "Hole in the Head" to the left. This large excavation was for the foundation of a proposed nuclear power plant. Pacific Gas and Electric Co., the local utility company, abandoned plans for this plant in 1964 after excavation revealed recent faulting.

STOP 1 - BODEGA HEAD

32.1 Bear right to Bodega Head parking lot. Take in the view and watch for whales offshore. A trail to the right of the parking lot leads to a gully and a rough descent to the beach below.

Grey outcrops rising from the beach are the Bodega Head diorite. The radiometric age of these rocks is 94.3 Ma (Wagner and Bortugno, 1982). Schlieren are prominent in outcrops on the ridge to the north. These rocks are the northernmost exposure of granitic rocks in the Coast Ranges. Similar rocks are exposed to the south on Point Reyes and south of San Francisco. Inclusions of older schist, gneiss, marble and quartzite in the diorite appear to be metamorphosed continental shelf deposits. They contain fragments of crinoids in the type area, so are probably pre-Cretaceous in age.

Granite pegmatite dikes cut the diorite and are probably late-stage differentiates of the diorite. All bedrock units are cut by faults and joint systems. These structures are related to the San Andreas fault. Pulver and Norwick (1977) studied their fracture geometry and determined that they are in simple Reidel shear relationship to the main San Andreas fault. The Windmill Cove fault is exposed in outcrops on the north side of the beach. A fault gouge zone parallel to a pegmatite dike and overlying fault breccia indicate shallow movement along this fault.

Stratigraphically overlying the diorite are layers of angular, coarse sandstone. These contain erosional debris from the diorite with a basal breccia layer of diorite, pegmatite, and schist and gneiss fragments. This sequence is a marine terrace deposit, formed at sea level and subsequently uplifted to present elevation. Radiocarbon age dates of at least 40,000 yrs on carbonized wood indicate uplift rates of about 0.1 mm/yr. Faults and folds in layers on the bluff north of the beach may have been caused by major earthquakes along the San Andreas fault. A fault that cuts this unit was uncovered during excavation of the foundation for the nuclear power plant in 1964. This ended plans for the plant.

White shells in dark organic soil at the top of the section are from Indian shell middens. A Miwok village site existed on Bodega Head until the 1950s.

36.0 Return to Hwy. 1, turn left (north). The road parallels the eastern edge of the San Andreas fault zone, with sand dunes filling the eroded and downwarped trace.

37.7 Salmon Creek Beach. We traverse into the Franciscan Complex Central belt melange here, with many sea stacks and isolated outcrops of resistant blocks surrounded by smooth slopes formed on the sheared shale matrix.

STOP 2 - SHELL BEACH

43.0 Turn off to left (west) into parking lot. This is an excellent place to look at classic exposures of melange. Fresh wave-cut exposures of matrix and a wide variety of lithologies make this an ideal study area. A rough trail descends to the beach with outcrops along the way. The questions we often ask here are: What is the origin of the melange: sedimentary or tectonic? What is the origin of the matrix? We will have time to look at field evidence and to discuss these and other aspects of melange. At low tide there are tidepools teeming with life.

Return to Hwy. 1, turn left (north). Cross the Russian River.

45.2 Turn right (east) onto Hwy. 116 toward Guerneville.

45.8 Outcrops on left cliffs are in Healdsburg terrane of the Great Valley sequence. Conglomerates contain granitic cobbles, in sharp contrast to surrounding oceanic rocks of the Franciscan

Complex. Perhaps these cobbles were eroded from the Sierra Nevada granitic rocks. The conglomerates are in the upper plate of a west-directed regional thrust fault.

We cross back into the Franciscan Complex quickly and continue along the Russian River.

52.8 Monte Rio. Continue straight on Hwy. 116.

55.3 Rio Nido terrane forms steep slopes on Late Cretaceous graywacke.

The Russian River canyon was formed by uplift and erosion in the last 3 my. The river established its course after the Wilson Grove sea withdrew to the west. Subsequent rapid uplift formed this part of the Coast Range, and the river was superposed on the bedrock.

56.9 Guerneville. Continue straight at stop sign on River Rd.

59.3 Enter Russian River Valley appellation wine area. The cool afternoon sea breezes in this area and excellent soils on terraces near the Russian River have fostered some world class wines. Korbel Winery on left.

62.5 Hacienda Bridge. During the flood of 1986, water was 10 ft (3 m) deep in this community. River discharge was 102,000 cfs.

67.2 At crest of hill we pass an outcrop of Wilson Grove Formation on the left. White fossil clam shells are scattered around the surface. The Trenton fault forms the eastern boundary of this outcrop and thrusts Franciscan Complex graywackes to the west over the Wilson Grove Formation. This may be an active fault.

72.5 Cross Hwy. 101; continue straight on Mark West Springs Rd.

73.4 Roadcuts on right (south) are the Sonoma Volcanics. This is a late Miocene-Pliocene volcanic field (6-2.9 Ma). It is composed of rhyolite and andesite lavas and tuff, welded tuff, stream gravels, diatomaceous sediments and basalt flows. Volcanic activity coincided with deposition of the Wilson Grove Formation in a shallow sea to the west. Ash and breccia beds in the Wilson Grove are attributed to eruptions of these volcanoes.

Origin of the volcanics is controversial. Hearn and others (1981) suggest that the area passed over a hot spot in the mantle or that deeply propagating faults lowered pressure at depth and generated basaltic magma, which rose to melt the crust and cause silicic magma to form.

The Rodgers Creek-Healdsburg fault crosses the road here and is displayed as a closely fractured area about 6.5 ft (2 m) wide in the steep outcrops on the right.

78.7 Bedding in ash deposits along the road is tilted, and many large-scale folds can be mapped in this sequence. Fox (1983) has studied this deformation and notes that it is related to stress along the San Andreas fault system.

79.9 Serpentinite on right in landslide area is Franciscan Complex exposed in the Maacama fault zone. This fault is active with many small earthquakes. It runs north 60 mi (97 km) to Willits and caused a M 5 earthquake there in 1978.

82.7 Turn left on Petrified Forest Rd.

83.5 Petrified Forest on left. We will take a short walk to view the excavated petrified logs. These *Sequoia langsdorfii* were ancestors of present-day redwoods (*Sequoia sempervirens*). The tree tops all point to the southwest and are surrounded by tuff. It seems likely that they were knocked over by a volcanic explosion. The presence of intact leaves and bark on the trees and unbroken glass shards in the adjacent tuff indicates that the trees were first felled by a volcanic blast and subsequently buried by an ash fall similar to the forests around Mt. St. Helens (Mattison, 1990).

After the hike, we will partake of Sonoma County wine and cuisine in the Petrified Forest Visitor Center. Return to Hwy. 101 by retracing the route; go south on Hwy. 101 to the Golden Gate Bridge and San Francisco.

REFERENCES CITED

Alfors, J.T., Burnett, J.L., and Gay, T.E., Jr., 1973, *Urban Geology Master Plan for California*: California Division of Mines and Geology, 112p.

Blake, M.C., Jr., Howell, D.G., and Jayko, A.S., 1984, Tectonostratigraphic terranes of the San Francisco Bay region: *in* Blake, M.C. Jr., ed., *Franciscan geology of northern California*: Pacific Section, Society of Economic Paleontologists and Mineralogists, v. 43, p. 5-22.

Budding, K.E., Schwarz, D.P., Ostergren, C.L., and Hoirup, D.F., Jr., 1989, Preliminary slip rate and earthquake recurrence on the Rodgers Creek fault zone, northern California (abs.): *EOS, Transactions*, v. 70, no. 43, p. 1211.

Fox, K.F., Jr., 1983, Tectonic setting of Late Miocene, Pliocene, and Pleistocene rocks in part of the Coast Ranges north of San Francisco, California: *U.S. Geological Survey Professional Paper 1239*, 33p.

Hearn, B.L., Jr., Donnelly-Nolan, J.M., and Goff, F., 1981, The Clear Lake Volcanics: tectonic setting and magma sources, *in* McLaughlin, R.J., and Donnelly-Nolan, J.M., eds., 1981, Research in the Geysers-Clear Lake geothermal area, Northern California: *U.S. Geological Survey Professional Paper 1141*, pp. 25-45.

Howard, A.D., 1979, *Geologic history of middle California*: University of California Press, Berkeley, CA, 113p.

Mattison, Elise, 1990, California's fossil forest: Sonoma County: *California Geology*, v. 44, no. 9, p. 195-202.

Pulver, B., and Norwick, S., 1977, The brittle features associated with the San Andreas fault zone; Marin and Sonoma counties, California (abs.): *Geological Society of America Abstracts with Programs*, v. 9:4, p. 484-485.

Wagner, D.L., and Bortugno, E.J., 1982, Geologic map of the Santa Rosa quadrangle: *California Division of Mines and Geology Regional Geologic Map Series, Map 2A*, scale 1:250,000.

Wahrhaftig, Clyde, 1984, Structure of the Marin Headlands block, California: a progress report: *in* Blake, M.C., Jr., ed., *Franciscan geology of northern California*: Pacific Section, Society of Economic Paleontologists and Mineralogists, v. 43, p. 31-50.

A fault zone on Grizzly Peak Boulevard 0.2 of a mile west of the Fish Ranch Road intersection. Shale, sandstone, and chert of the Claremont member of the Monterey group have been crushed and badly dislocated in a zone several hundred feet wide.

Guide to the Geology of the Berkeley Hills, Central Coast Ranges, California

David L. Jones and Garniss Curtis[1]

INTRODUCTION

Upper Mesozoic strata of the Great Valley sequence (GVS), igneous rocks of the Coast Range ophiolite (CRO), and overlying Cenozoic strata in the central Coast Ranges of California east of the Hayward fault are distributed in five fault-bounded stratigraphic assemblages (subterranes) that exhibit significant differences in their sedimentologic, volcanic, and structural histories (Fig. 1, Table 1). These five assemblages are best developed in a transect extending from the Berkeley Hills eastward to the edge of the Great Valley east of Mount Diablo. Other subterranes occur both to the north and south of this transect.

Development of these subterranes is the cumulative effect of a long and complex tectonic history involving a) differential sedimentation in basins formed by Cenozoic crustal extension; b) juxtaposition of once-separated basins by strike-slip fault movements; and c) eastward-directed oblique displacements on east-vergent folds and thrust faults, and west-vergent tectonic wedges ("blind thrusts"). During the past 4-5 my, both strike-slip faulting and thrusting have been active concurrently, but the initial onset of either kind of fault movement is not yet clear.

The existence of similar fault-bounded assemblages was recognized long ago, particularly by Clark (1930), who discriminated several structural "blocks" in the central Coast Ranges based on differences in their sedimentary and structural histories. Clark attributed these differences to vertical movements on steep faults, most of which he believed originated in pre-Cretaceous time. Later regional studies (e.g., Nilsen and Clarke, 1975; Dickinson and others, 1979) have concentrated more on the distribution and character of strata in the Great Valley than in the Coast Ranges to the west. Important interpretations concerning tectonic development of the East Bay Hills were published by Graham and others (1984), who recognized several structural blocks (Caldecott, Lafayette, and Diablo), that are comparable to some of the subterranes defined in this report.

Inappropriate stratigraphic nomenclature still remains as a persistent impediment to furthering

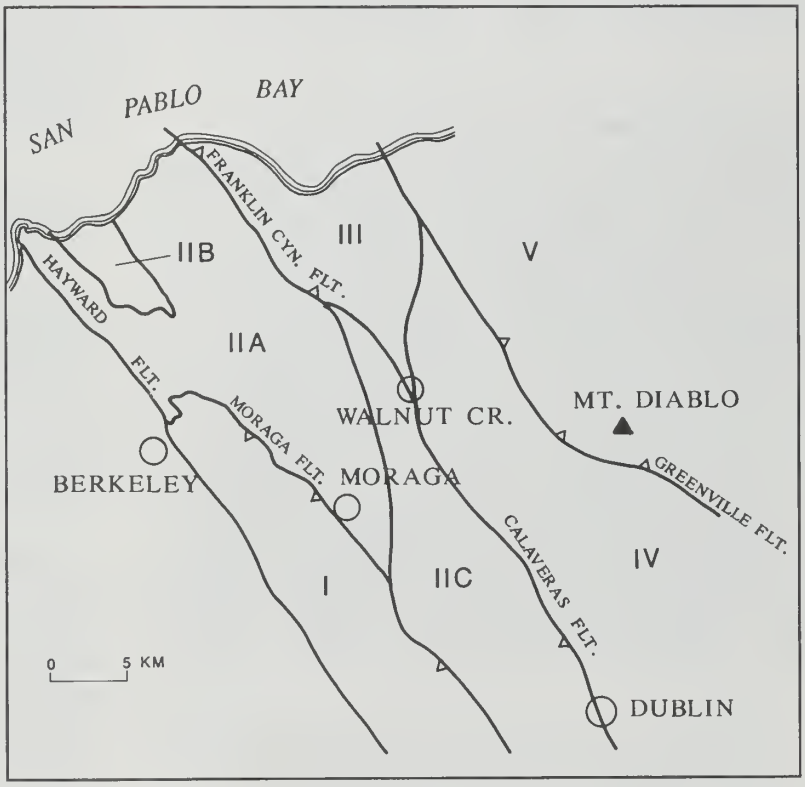

Figure 1. Index map showing distribution of subterranes in the East Bay Hills. Subterrane boundaries are major faults; barbs on upper plate of faults with significant component of thrust displacement.

[1] Department of Geology and Geophysics, University of California, Berkeley, CA 94720

Table 1. Comparative stratigraphic columns for East Bay subterranes.

I	IIA	IIB	IIC	III
Bald Peak Fm. Siesta Fm. Moraga Fm. Orinda Fm. Claremont Shale Sobrante? Fm. Eocene ss, sh GVS CRO	Mulholland Fm. Contra Costa Gp. Pinole Tuff Neroly Fm. Cierbo Fm. Briones Fm. Hercules Shale Rodeo Shale Hambre Sandstone Tice Shale "Claremont" Shale Sobrante Sandstone Kirker Tuff San Ramon Fm. "Markley" ss & sh	Pinole Tuff diatomite sandstone diatomite	Contra Costa Gp. Lafayette Tuff Briones Fm. Rodeo Shale sandstone "Claremont" Shale GVS	Briones Fm. "Sobrante" Sandstone San Ramon Fm. Markley Fm. Nortonville Shale Escobar Sandstone Muir Sandstone Las Juntas Shale Vine Hills Sandstone GVS

our understanding of central California regional tectonics. In some cases "formational" names are still applied to rocks of similar age but differing lithology (e.g., "Domengine Sandstone" includes coal-bearing non-marine deposits north and east of Mt. Diablo, and deep marine turbidites west of Mt. Diablo), or generalized terms, such as "Miocene sandstone" and "Orinda Formation," have been applied to a number of different units of differing age.

Previous estimates of the magnitude of cumulative strike-slip displacements on major faults (Calaveras, Greenville, Concord) east of the Hayward fault range from about 14 to 21 mi (23 to 33 km) (Page and Wahrhaftig, 1989). These estimates are based on displacements that have occurred during the past 3.5 my or less. Palinspastic reconstructions based on these estimates fail to unify Miocene and older stratigraphic assemblages now separated by faults, implying either that young fault displacements are much larger than suggested, or that important displacements have occurred that are older than ~3 Ma. No estimates have been published concerning the total amount of shortening produced during folding and thrust faulting, so quantifying these displacements through time remains an important goal.

Based on our analysis of regional stratigraphic patterns and the presence of tectonically juxtaposed subterranes, we suggest that published estimates of the amount of movement on East Bay faults are overly conservative and may be low by at least an order of magnitude. In addition, seismic hazard investigations have not given adequate attention to hazards associated with thrust faults and have failed to identify as potential seismic risks several faults that appear to exhibit large amounts of Neogene offset and which are likely candidates for secondary reactivation during major seismic events on known active faults. Furthermore, analyses of recent fault activity and estimates of seismic hazards have been concentrated in areas where ground breakage or fault creep can be observed. Potential hazards due to seismic activity and associated ground shaking on faults that do not intersect the ground surface need further evaluation.

EAST BAY SUBTERRANE

Distribution of subterranes in the central Coast Ranges east of the Hayward fault is shown on Fig. 1. Terrane boundaries are faults whose distribution and character are portrayed on an unpublished geologic map at a scale of 1:62,500 (Jones and Brabb, 1991). Stratigraphic columns for each subterrane are shown on Table 1.

Subterrane I (Berkeley and Oakland Hills): Subterrane I, the focus of this field trip, extends from north Berkeley south to at least the Calaveras Reservoir; its southern terminus is uncertain. Boundary faults include the Hayward, Mission, Calaveras, Palomares, Miller Creek, Moraga, and Pinole faults. This subterrane may be composite, in as much as three distinctive fault-bounded stratigraphic packages are present whose original paleogeographic relations cannot be readily established (Fig. 1). The northern package is the Caldecott block of Graham and others (1984).

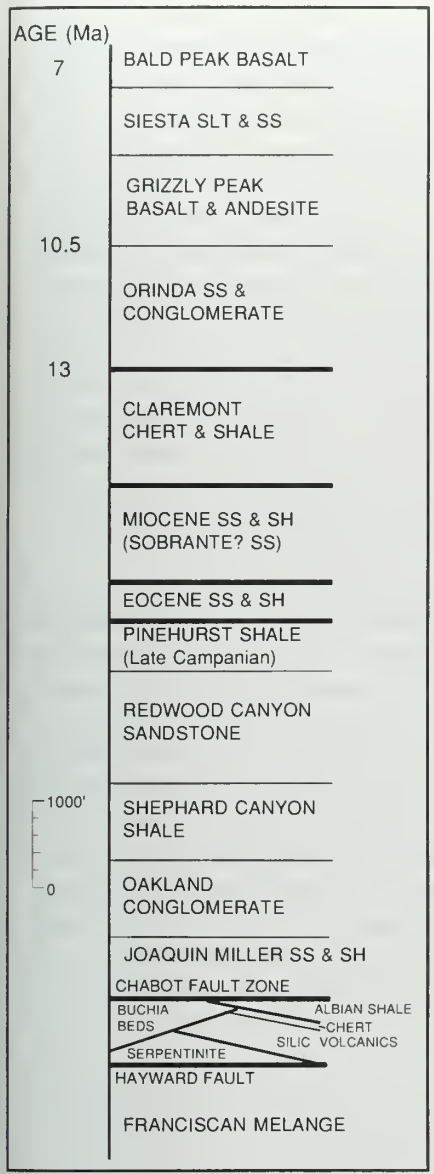

Figure 2. Composite columnar section of subterrane I (Caldecott block) in the Berkeley and Oakland Hills, showing characteristic stratigraphic sequence. Faults are shown by heavy horizontal lines.

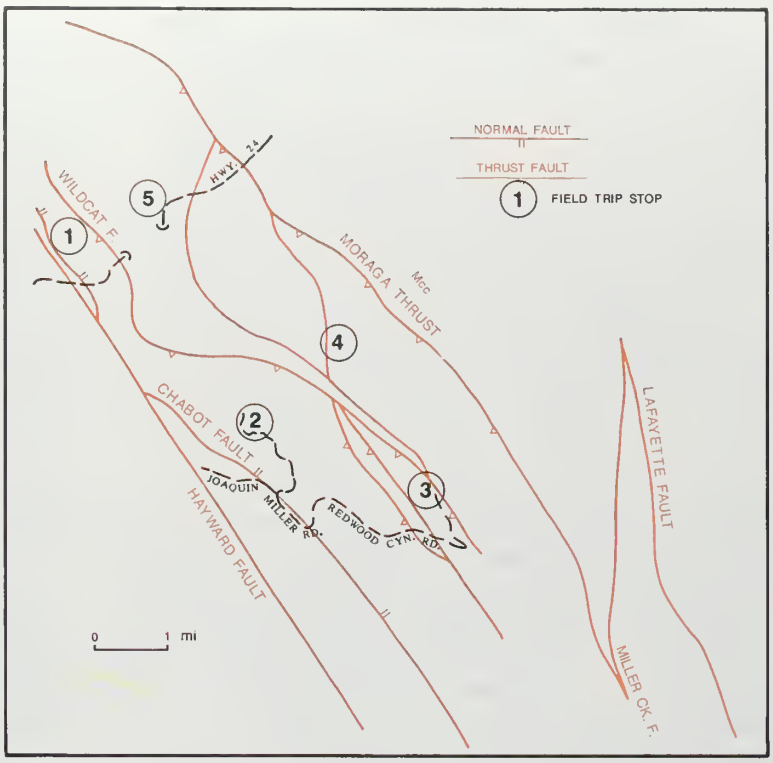

Figure 3. Sketch map of the Berkeley and Oakland Hills showing distribution of major faults and field trip stops.

The stratigraphy of the Caldecott block in the Berkeley and Oakland Hills is shown on Fig. 2. Field trip stops are shown on Fig. 3. The basal unit consists of a diverse suite of igneous rocks belonging to the CRO of early Late Jurassic age. Characteristic rocks present include sheared serpentinite, pillowed and intrusive keratophyre and quartz keratophyre, and bedded tuff containing Jurassic radiolarians. The siliceous volcanic rocks have long been designated as the Leona Rhyolite and Northbrae Rhyolite of supposed Pleistocene age, but these highly altered rocks are unlike any Neogene volcanic rocks present nearby and are clearly much older. A depositional contact of chert and Upper Jurassic radiolarian-bearing siliceous argillite on keratophyre at Stop 1 proves the Mesozoic age of these rocks. In addition, K-Ar radiometric ages indicate that these rocks are more than 125 Ma old. The original ophiolitic sequence has been strongly disrupted, and most of the cumulate ultramafic and gabbroic rocks are missing. Rocks of the upper part of the ophiolite are now distributed as blocks within a serpentinite-matrix melange similar to other serpentinite melanges found along the Coast Range fault. Krueger and Jones (1989) believe these melanges formed as a result of early Cenozoic extensional faulting. Keratophyric volcanic rocks and bedded tuff within the melange are similar to siliceous volcanic and volcaniclastic rocks (Lotta Creek Tuff) that typify the CRO of the Del Puerto terrane, and differ strongly from basaltic ophiolitic rocks of the Elder Creek terrane as exposed on the north side of Mt. Diablo (Williams, 1983).

Great Valley Sequence: Upper Jurassic and Lower Cretaceous *Buchia*-bearing clastic sedimentary rocks of the GVS also occur as slabs and blocks within the serpentinite melange. None of these rocks occur east of the Chabot fault, which, at Stop 1, is an east-dipping normal fault that separates younger strata of the GVS from *Buchia*-bearing rocks and from the serpentinite melange.

Depositional contacts of basal Great Valley strata on volcanic rocks of the CRO were first documented by Robinson (1956) from a quarry in the Hayward quadrangle, where Upper Jurassic shale with belemnites overlies pillowed greenstone. Another depositional contact occurs in the Berkeley Hills, where keratophyre is overlain by a few inches (centimeters) of chert and siliceous argillite followed by a few feet (meters) of brown-weathering silty shale. Pyritized radiolarians extracted from the siliceous argillite include *Parvicingula santabarbaraensis* Pessagno, *Hsuum cuestaensis* Pessagno, *Paronella(?) exotica* Pessagno, and other forms characteristic of the upper part of Radiolarian Zone 2 (Kimmeridgian or older) as defined by Pessagno and others (1984). Because the brown-weathering silty shale was deposited on the radiolarian-bearing strata, and because it resembles *Buchia*-bearing strata occurring elsewhere in the Berkeley Hills, a Late Jurassic age is assumed for these rocks.

Structurally overlying and separated from the Jurassic strata by an east-dipping shear zone (=Chabot fault?) is a 16-ft (5-m) thick section of dark gray silty shale with abundant calcareous concretions. This grades up into 33 ft (10 m) of thin-bedded carbonaceous sandstone and interbedded siltstone which lacks calcareous concretions. A small scrap of an ammonite in a small calcareous concretion was found in float near the base of the siltstone exposure. This ammonite is identified as *Brewericeras hulenense* of early Albian age and constitutes the only evidence for the presence of Albian rocks within the East Bay Hills. It also demonstrates that attenuation faulting has occurred within the GVS, as Lower Cretaceous (pre-Albian) strata have been excised along the east-dipping fault that bounds the base of the concretionary shale.

To the south in the East Bay Hills, the Chabot fault consistently shows the same structural relations seen at Stop 1, in that it separates Middle to Upper Cretaceous sandstone, conglomerate, and shale units of the GVS on the east side of the fault from *Buchia*-bearing strata and dismembered fragments of the CRO on the west side of the fault. Perkins (1974) also interprets the Chabot fault to be a bedding-parallel, east-dipping structure along which his petrofacies B and Cl locally have been cut out and younger rocks of his petrofacies C2 have been juxtaposed against CRO. The Chabot fault is thus equivalent to attenuation faults at the top of the CRO described by Jones (1987), Krueger and Jones (1989), and Jayko and others (1987) from elsewhere in the Coast Ranges and thought to have formed during a major period of crustal extension with attendant uplift of Franciscan blueschists during the early Cenozoic.

Compilation of recent earthquake epicenters indicate that the Chabot fault south of Hayward is seismically active, suggesting that the older extensional fault has now been reactivated as a strike-slip strand of the Calaveras-Hayward fault system. The Hayward fault, which forms the west boundary of subterrane 1, separates rocks of the CRO and GVS on the east from Franciscan rocks on the west. Thus, this active strike-slip fault occupies precisely the older Coast Range fault that throughout the California Coast Ranges always intervenes between the CRO and various terranes of the structurally lower Franciscan Complex.

Rocks of the GVS have been subdivided into formations in the hills east of Oakland (Case, 1963, 1968; Radbruch, 1969; see Fig. 2). Elsewhere in the East Bay Hills, no consistent nomenclature has been applied to these rocks because of poor exposure, structural complexities, and a general paucity of fossils necessary for detailed age correlations. Even in the Oakland Hills where the most detailed studies have been carried out, the stratigraphic sequence is poorly dated, and correlation with named units of the GVS elsewhere is difficult. The Oakland Conglomerate (Stop 2) constitutes one of the more distinctive clastic units within the Oakland Hills, in that it is composed dominantly of rounded pebbles and cobbles of quartz porphyry, granite and quartz monzonite, dacite, rhyodacite, and rhyolite with abundant quartzite in a turbidite sandstone matrix (Table 1, from Perkins, 1974) with abundant K-feldspar (mean=16 percent). Similar conglomerates are

reported by Perkins (1974) from a number of localities within the East Bay Hills in strata of early Late Cretaceous age. The provenance of these siliceous volcanic, granitic, and quartzite cobbles is uncertain; some (e.g., Seiders and Blome, 1988) claim a Sierran source, but the East Bay Hills strata are richer in K-feldspar, quartzite, siliceous volcanics and granitic clasts, and poorer in chert, than are coeval strata on the east side of the Diablo Range (Mansfield, 1972). Perkins (1974) also emphasized that the mid-Cretaceous Sacramento Valley petrofacies (Boxer and Cortina) of Dickinson and Rich (1972) cannot be recognized within the East Bay Hills.

Stratigraphically above the Oakland Conglomerate are the undated Shephard Creek Formation (mainly shale) and the Redwood Canyon Formation (thick-bedded turbidites - Stop 3). Foraminifers from an unnamed unit of variegated green and minor red shale with calcareous concretions that overlies the Redwood Canyon Formation are Late Campanian in age. This unit grades up into the Pinehurst Shale (Stop 3), consisting of siliceous shale, mudstone, and minor sandstone. Although originally considered to be Paleocene in age (Case, 1968) based on benthic foraminifers, analysis of abundant and beautifully preserved radiolarians extracted from siliceous shale indicates that this unit also is late Campanian in age (Silk and Jones, 1991). The Pinehurst Shale is folded and repeated at least three times by imbricate thrust faults that are part of a Neogene east-vergent thrust system that places Cretaceous strata on top of Cenozoic rocks along the east front of the Oakland Hills.

Cenozoic Stratigraphy: Cenozoic deposits of the Berkeley and Oakland Hills commence with a poorly exposed unnamed unit of Eocene sandstone and shale. Based on Case's map (1968), this unit is faulted against Cretaceous strata on the southwest and Miocene strata on the northeast. Radbruch (1969) shows the former contact as mostly faulted and the latter as depositional. According to Case (1968), strata within this unit may range in age from early Paleocene (Ynezian) to middle Eocene ("Domengine"). Preliminary studies of this unit by Jones and Brabb (1991) suggest that massive sandstone with occasional shelly conglomeratic beds constitutes a lower member, with green foraminiferal claystone forming an upper member. Where observed along Skyline Blvd., the contact between these two members is a fault.

Miocene rocks comprise, in ascending order, the Sobrante(?) Formation, Claremont Shale, Orinda Formation, Moraga Formation, Siesta Formation, and Bald Peak Basalt (Fig. 2). None of these rock units can be recognized with confidence east of the Moraga thrust, although the name "Claremont Shale" has been widely and inappropriately applied to siliceous shale and very minor chert occurring east of the fault.

The so-called Sobrante(?) Sandstone of the East Bay Hills consists dominantly of massive brownish-grey organic-rich sandy siltstone in which bedding is poorly developed, with lesser amounts of glauconitic sandstone and minor conglomerate present locally. The siltstone unit has not been recognized north of Strawberry Canyon nor south of the Upper San Leandro Reservoir. A Miocene (or older?) age is based on foraminifers from numerous localities (see Radbruch, 1969).

The contact of the Sobrante(?) Formation and the Claremont Shale is faulted throughout the extent of these two units, and no unequivocal depositional contact has yet been documented. Along Skyline Blvd. and Tunnel Rd., the lower part of the Claremont consists of brown siltstone and porcellanite interbedded(?) with massive white, fine-to-medium-grained sandstone. This sandstone unit is neither continuous nor everywhere at the same stratigraphic level. The upper beds of the Claremont Shale are mainly chert with minor brown siltstone interbeds that are strongly folded, generally overturned to the east, and are probably repeated several times by faulting and folding. Underlying strata do not exhibit a comparable style of deformation, so significant faults may occur at or near the base of the cherty sequence and also at the base of the formation.

Typical exposures of the Claremont Shale consist mainly of alternating thin bands of diatomaceous chert and brown shale (black when fresh), with occasional beds of orange-weathering dolomitic limestone. The alternation of chert and shale is believed by some (e.g., Murray and others, 1990) to be the result of diagenesis, rather than being a primary sedimentologic feature.

Whatever the origin of this "bedding," it is found only in Claremont chert occurring west of the Moraga fault. Exposures of "Claremont Shale" east of the Moraga fault consist of massive diatomite and siliceous shale with very minor lenses of chert that lack the rhythmic alternation shown by the type Claremont. The age of the type Claremont is generally accepted as Luisian (middle Miocene - 13-16 Ma) based on foraminifers reported by Kleinpell (1938, Table 13, loc. DC-1). Of the six species reported from this locality, however, all extend down to at least the Relizian (lower Miocene), and none are reported by Kleinpell to occur in the supposed equivalent "Claremont Shale" of Contra Costa County (Bear Creek anticline) which does indeed contain Luisian forms. The age span of the type Claremont Shale thus remains uncertain, as does the age of the underlying "Sobrante Sandstone," which is probably no younger than early Miocene.

The Orinda Formation discordantly overlies the Claremont Shale; where exposed, the contact is faulted. Locally (e.g., near Roundtop), a few feet (meters) of fossiliferous fine-grained marine sandstone and conglomerate with clasts of Claremont chert occur between typical Orinda sandy conglomerate and Claremont chert. The restricted distribution of these rocks as well as the general lack of transitional beds between the deep marine Claremont and the fluvial Orinda, suggest that a detachment fault separates the Orinda from the Claremont, as first proposed by Wagner (1978). Other evidence cited by Wagner for detachment along this contact includes shearing of the upper part of the Claremont and truncation of lamprophyric dikes that intrude the Orinda but do not cross into the Claremont. A tectonic rather than an erosional contact is also supported by the absence of Claremont clasts in the Orinda. Instead, clasts of graywacke from both the Franciscan and GVS are abundant, along with clasts of Franciscan red chert and blueschist. Red chert clasts contain Jurassic radiolarians similar to those in chert widely dispersed in melange of the Franciscan Central terrane (Murchey and Jones, 1984), which is also the home of blueschist knockers. A small exposure of Orinda Formation west of the Wildcat fault lacks blueschist clasts, contains rare red chert, and is characterized by abundant pebbles and cobbles of black chert. A different provenance is clearly indicated. Preliminary study of poorly preserved radiolarians extracted from these black cherts indicates that they probably are Cretaceous in age, and are unlike any cherts known from the Central terrane. The Franciscan Permanente terrane, which contains abundant limestone and some interbedded black chert beds and nodules, is a possible, but unproven, source for these unusual clasts. Additional study of Orinda clast composition and distribution is warranted as a possible aid in establishing offset on the Wildcat fault.

The lower several hundred feet (meters) of the Orinda consists mainly of fine sand and siltstone with thin beds of pebble conglomerate. Clast size and abundance of conglomerate increases upward; in the upper 500 ft (150 m) clasts of biotite-bearing Cretaceous sandstone up to 12 in (30 cm) in diameter are common (Stop 5). Pebble and cobble imbrication indicates sediment transport from the west. This part of the Orinda consists of interbedded massive conglomerate beds as much as 30-45 ft (10-15 m) thick, alternating with units of similar thickness composed of green and red sandstone and siltstone in which mammalian fossils of Clarendonian age are locally abundant. At Caldecott Tunnel the Orinda is about 2000 ft (600 m) thick; it thins markedly both to the north and south.

The age of the Orinda Formation is generally accepted as Mohnian, ranging from 13 to 10.5 Ma (Curtis, 1989). The top of the Claremont is believed to be no older than 14 Ma (Curtis, 1989), so the change from deposition at bathyal depths to subaerial conditions (estimated maximum uplift ~4920 ft, 1500 m; Hill, 1979) occurred within 1 my at an uplift rate of .06 in/yr (1.5 mm/yr). This rapid uplift is not recorded in the coeval sedimentary record in the nearby Bear Creek anticline sequence, where both the Tice Shale and Rodeo Shale remained at bathyal depths throughout this time interval. This supports our interpretation that these unlike sequences have been tectonically juxtaposed from widely separated areas of deposition.

The Orinda Formation is overlain by the Moraga Volcanics (Stop 5), consisting of a basal member of five basalt flows capped by a distinctive crystal-lithic rhyolite tuff, a middle

sedimentary member of conglomerate and sandstone with a thin titanaugite basalt flow at the top, and an upper member of five basaltic to andesitic flows. These volcanic rocks are overlain by the Siesta Formation, consisting mainly of silt and clay with fine sand and local beds and lenses of freshwater limestone. To the north, the Siesta interfingers with the Bald Peak Basalt, which is the youngest unit exposed in the Berkeley Hills stratigraphic section. Volcanism extended over a period of less than 2 my, with the base of the Moraga yielding K-Ar dates of ~10.2 Ma, the rhyolite tuff 9.6 Ma, and the Bald Peak Basalt, 8.5-8.4 Ma (Curtis, 1989). This volcanic sequence, which is about 2300 ft (700 m) thick, does not occur east of the Moraga thrust, although small bodies of younger basalt of latest Miocene or Pliocene age occur near Lafayette on the east side of the Moraga fault.

STRUCTURE

The structure of the Berkeley Hills subterrane remains poorly understood, even though rock distribution is now fairly well-known. All the rocks are strongly folded and cut by numerous faults, including extensional faults, late Neogene to Holocene? thrust faults, and active strike-slip faults. Prominent structural features include the Hayward fault on the west and the Moraga-Miller Creek-Palomares fault system on the east. In between are numerous subsidiary faults that are splays of the major faults, and which have had a complex structural history. Much remains to be learned concerning the history and magnitude of both normal and thrust faulting in the East Bay Hills.

Normal Faults: The presence of low angle normal faults (=attenuation faults) within the Coast Ranges is a concept introduced only a few years ago (Jones, 1987; Krueger and Jones, 1989), and little agreement exists concerning the age, distribution, and amount of displacement that may have occurred on this class of faults. Evidence for attenuation faulting on the Chabot fault and also higher in the GVS can be seen at Stop 1. Additional attenuation faulting may have occurred between Cretaceous and Eocene strata, and between the Eocene and Miocene, but all of these contacts have been modified by younger thrust and strike-slip faults, so their original character is now obscured by later tectonic events.

Thrust faults: The region between the Hayward fault on the west and the Calaveras fault on the east is characterized by the presence of a young east-verging fold and thrust belt (Aydin, 1982). The Moraga thrust is the best known and most obvious strand of this thrust system, but other major strands include, from east to west, the Las Trampas fault, Bollinger Ridge thrust, San Leandro Creek fault of Case (1968), an unnamed fault along Redwood Creek, and western splays of the Wildcat fault. Strata throughout this belt are strongly folded with direction of overturning consistently to the east. Aydin (1982) interprets these compressional structures to be the result of interaction between the left-stepping Calaveras and Hayward-Rodgers Creek fault zones. This explanation is too simple, however, because a west-directed coeval fold and thrust system exists on the east side of the Calaveras fault (Crane, 1988) that is related to westward overturning of the Altamont anticline and overthrusting along the Greenville-Concord fault systems. Thus, the entire eastern part of the central Coast Ranges, all the way from the Hayward fault to the eastern edge of the Great Valley, shows evidence of major Neogene and younger compression that is broader in scale than can be attributed to left-stepping on the Calaveras-Hayward fault systems.

Important structures east of the Calaveras fault that appear to have significant west-directed thrust displacements include the Greenville fault, the Franklin Canyon fault, the Verona and Williams faults, and postulated faults in the Sycamore and Green Valleys (Crane, 1988). Miocene and Pliocene strata west of the Greenville fault are overturned to the west for a distance of nearly 25 mi (40 km) extending southeastward from Walnut Creek. Crane (1988) attributed this overturning and related thrust faults to continuing upward movement of the Mt. Diablo "serpentinitic diapiric mass," but no direct relation exists between overturning, thrusting, and proximity to Mt. Diablo. Rather than being serpentinite-cored diapirs, both Mt. Diablo and the Sulphur Springs Mountains to the north appear to represent structural culminations of arched low-angle attenuation

faults along which significant crustal thinning had occurred in Paleogene time. In the case of Mt. Diablo, folding of the Altamont anticline and uplift due to thrusting on the Greenville fault have elevated and exposed these earlier extensional faults. The core of Mt. Diablo itself appears to be a rotated block with anomalous east-west structural trends with southeast-directed thrust-faulting along its southern margin. Present structural relief across the Greenville fault may be as much as 6.2 mi (10 km), presuming that a full sequence of GVS is buried beneath Cenozoic rocks of the Livermore Valley.

The change in vergence of folds and thrusts across the Calaveras fault suggests that this fault separates two blocks whose structural behavior is quite different. All the thrusts east of the Calaveras trend to the northwest and apparently terminate as blind structures; they can be interpreted as roof faults of tectonic wedges similar to those described by Wentworth and others (1984). Thrust faults related to tectonic wedges are known, or suspected, to occur along the entire eastern margin of the Coast Ranges (Wentworth and others, 1984, Wentworth and Zoback, 1989; Namson and Davis, 1988), where they have given rise to damaging earthquakes at Winters and Coalinga.

Because none of the western thrusts involve the CRO or underlying Franciscan rocks, they can best be interpreted as thin-skinned structures that probably root in a basal decollement. Anticlines, such as the Glorietta anticline that folds the Moraga Formation, appear to develop on ramps where the thrusts cut up-section.

Minimum age of thrusting in the East Bay Hills is not well constrained. The Moraga thrust displaces rocks as old as 8.4 Ma, and overrides strata of the Mulholland Formation, which may be as young as 6 Ma (Creely and others, 1982). Holocene sediments are not known with certainty to be displaced, although preliminary mapping by Curtis (unpublished data) suggests that recent landslides may be truncated and buried by this fault.

Strike-slip faults: Although the location of major active strike-slip faults in the East Bay Hills has long been established, total displacements and offset rates through time remain poorly constrained. The Hayward-Rodgers Creek fault system has an estimated offset of 27 mi (43 km) based on separation of the coeval Tolay Volcanics and the Donnell Ranch Volcanics of Youngman (1989) of Sonoma County and the Moraga Formation of the Berkeley Hills (Fox and others, 1985). Palinspastic realignment of these rocks, however, fails to unite pre-Moraga and pre-Tolay units, suggesting that pre-10 Ma movement occurred along this fault. Despite the general similarity of ages, strong lithic contrasts between the Moraga and the Tolay-Donnell Ranch Volcanics casts doubt on the correlation of these supposed offset units.

Fox and others (1985) estimate 17 mi (28 km) of displacement on the Calaveras-Franklin Canyon-Carneros fault system, based on a possible separation of Oligocene and Miocene strata in the Carneros district and Mt. Veeder on the west side of the fault from equivalent strata near Martinez (Fox, 1983). This measurement is suspect, however, in that the connection of the Franklin Canyon fault with the Carneros fault is not proven, and the lithology of correlated Miocene rocks is dissimilar. In any case, this presumed displacement must have occurred before formation of the lower member of the Sonoma volcanics (~7.2 Ma), which overlies the Neroly Formation at Carneros Creek but does not occur near Martinez. The upper age limit of the Neroly is ~8 Ma, so the postulated rate of displacement was ~1.2 in/yr (3 cm/yr).

Page (1982) and Page and Wahrhaftig (1989) have summarized geologic evidence for displacement along the Calaveras fault and conclude the most likely offset is ~12 mi (~20 km) during the past 3.6 my, for an average slip rate of 0.22 in/yr (0.56 cm/yr). This estimate for offset on the main strand of the Calaveras fault is clearly incompatible with Fox's estimate of displacement on the Carneros fault, so further work is indicated on the connection of faults north of the Bay with those to the south.

Regional analysis of Miocene strata shows that rocks east of the Calaveras fault in the Sunol Park-Pleasanton area are most like coeval strata occurring west of Dublin in the southern part of

the "Contra Costa basin." The minimum separation of these two sequences across the Calaveras fault is about 6.2 mi (10 km). A direct connection is difficult to achieve, however, because post-Briones sediments are markedly different; near Dublin, coarse sandstone and conglomerate of the Contra Costa Group rests on the Briones, whereas a thick unit of non-clastic freshwater limestone and chert caps the Briones east of the fault. In any case, remapping (Jones, unpublished data) has demonstrated that this assemblage of Miocene strata in the Sunol Park region is itself fault-bounded and overlies volcanic-rich Neroly strata along a west-dipping thrust fault. Miocene strata underneath this thrust rest depositionally on Franciscan rocks that form the core of the Diablo antiform.

Estimates of much larger displacements along the Hayward-Calaveras fault system have been suggested, based on offset volcanic rocks (Curtis, 1989) and on offset hydrothermal vein systems (McLaughlin and others, 1990). Curtis (1989, p. 33) points out that the Quien Sabe Volcanics east of Hollister and the Tolay Volcanics of Sonoma County (Fig. 4) are similar in age and composition, and he suggests that they once may have been contiguous. If true, this would imply an offset of 120 mi (190 km) along the Calaveras-Hayward-Rodgers Creek fault system. McLaughlin and others (1990) arrived at a similar interpretation based on the present distribution of Neogene adularia-bearing hydrothermal veins that decrease in age northward in the same manner as Neogene volcanic rocks. They postulate 28 mi (45 km) of displacement on the Hayward-Rodgers Creek fault system and 90 mi (145 km) on the Calaveras. It should be emphasized that simple palinspastic reconstructions based on restoring these postulated strike-slip displacements fail to unite pre-Late Miocene stratigraphy across either the restored Hayward fault or the Calaveras fault, and provide no explanation for the presence of the coeval, but lithically distinct assemblage, of Moraga volcanic rocks. This fact fortifies our belief that: a) significant pre-San Andreas strike-slip movements occurred, and/or; b) Neogene displacements include such a large component of convergent movement on thrusts and blind thrusts that large lateral tracts have been tectonically buried.

ROAD LOG

STOP 1 - Old quarry near intersection of Hiller Rd. and Tunnel Rd., north of Hwy. 24. CRO with depositional contact of chert on keratophyre overlain by Knoxville shale; attenuation faults between Knoxville and Albian concretionary shale and Albian shale and Campanian(?) sandstone.

STOP 2 - Skyline Blvd. in Redwood Regional Park, Oakland, about 2 mi south of the intersection with Redwood Rd. Siliceous volcanic clasts in mid-Cretaceous Oakland Conglomerate.

STOP 3 - Pinehurst Rd. (southern end) - at locked fire road 1.2 mi east of intersection with Redwood Rd. Type locality of Pinehurst Shale, originally dated as Paleocene, but abundant radiolarians establish a Late Cretaceous (late Campanian) age. This unit is repeated several

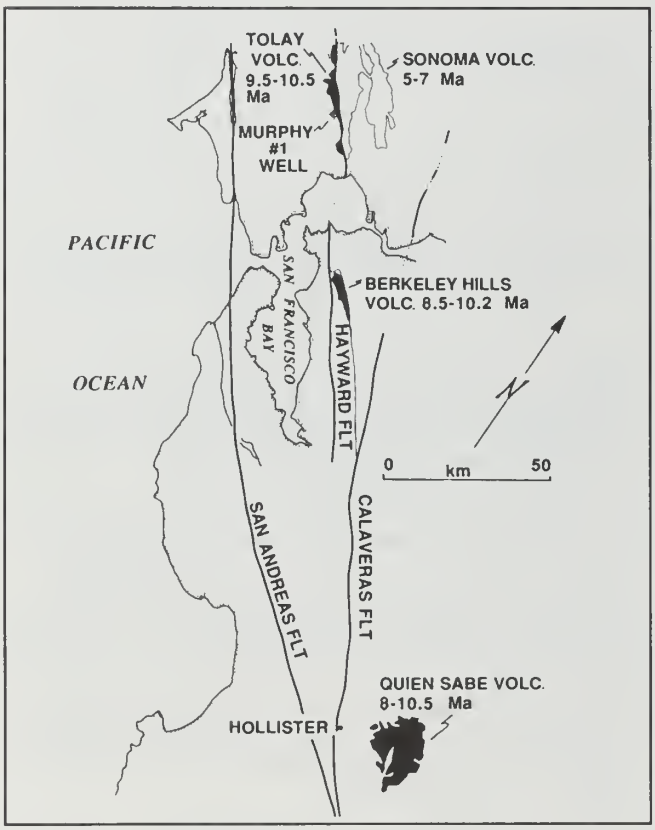

Figure 4. Sketch map showing distribution and age of Miocene volcanic rocks in central California that may have been displaced by movements along the Calaveras and Hayward faults.

times by imbricate thrust faults. Underlying units are calcareous shale and thick turbidites of the Redwood Canyon Formation.

STOP 4 - Pinehurst Rd. (northern end) - Continue north on Pinehurst Rd. about 4 mi around first hairpin turn (3/4 mi east of Skyline Rd. Chert of the Miocene Claremont Shale overturned to the east; Sobrante(?) Sandstone and obscured fault contact with massive Miocene mudstone mapped as part of Sobrante(?) Sandstone.

STOP 5 - Fish Ranch Rd. exit from Hwy. 24 (north side of highway). Interbedded sandstone and conglomerate of the Orinda Formation overlain by basalt flows of the Moraga Formation.

REFERENCES CITED

Aydin, Atilla, 1982, The East Bay hills, a compressional domain resulting from interaction between the Calaveras and Hayward-Rodgers Creek faults, *in* Hart, E.W., Hirschfeld, S.E., and Schulz, S.S., eds., Proceedings conference on earthquake hazards in the eastern San Francisco Bay area: *California Division of Mines and Geology Special Publication 62*, p. 11-22.

Case, J.E., 1963, *Geology of parts of the Berkeley Hills and San Leandro Hills*: Ph.D. thesis, University of California, Berkeley, 1216p.

Case, J.E., 1968, Upper Cretaceous and lower Tertiary rocks, Berkeley and San Leandro Hills, California: *U.S. Geological Survey Bulletin 1251-J*, p. Jl-J29.

Clark, B.L., 1930, Tectonics of the Coast Ranges of middle California. *Geological Society of America Bulletin*, v. 41, p. 747-828.

Crane, R.C., 1988, Field trip guide to the geology of the San Ramon valley and environs: Northern California Geological Society, p. 1-13.

Creely, Scott, Savage, D.E., and Ogle, B.A., 1982, Stratigraphy of upper Tertiary nonmarine rocks of central Contra Costa basin, California, *in* Ingersoll, R.V., and Woodburne, M.W., eds, *Cenozoic nonmarine deposits of California and Arizona*, Pacific Section, Society of Economic Paleontologists and Mineralogists, p. 11-22.

Curtis, G.H., 1989, Berkeley Hills, *in* Wahrhaftig, C., and Sloan, D., eds., *Geology of San Francisco and vicinity*. Field Trip Guidebook T105, 28th International Geological Congress, American Geophysical Union, Washington, D.C., p. 47-52.

Dickinson, W.R., and Rich, E.I., 1972, Petrographic intervals and petrofacies in the Great Valley sequence, Sacramento Valley, California: *Geological Society of America Bulletin*, v. 83, p. 3007-3024.

Dickinson, W.R., Ingersoll, R V., and Graham, S.A., 1979, Paleogene sediment dispersal and paleotectonics in northern California: *Geological Society of America Bulletin*, v. 90, pt. II, p. 1458-1528.

Fox, D.F., Jr., 1983, Tectonic setting of late Miocene, Pliocene, and Pleistocene rocks in part of the Coast Ranges north of San Francisco, California: *U.S. Geological Survey Professional Paper 1239*, 33p.

Fox, K.F., Jr., Fleck, R.J., Curtis, G.H., and others, 1985, Implications of the northwestwardly younger age of the volcanic rocks of west-central California: *Geological Society of America Bulletin*, v. 96, p. 647-654.

Graham, S.A., McCloy, C., Hitzman, M., Ward, R., and Turner, R., 1984, Basin evolution during change from convergent to transform continental margin in central California: *American Association of Petroleum Geologists Bulletin*, v. 68, p. 233-249.

Hill, J.M., 1979, Stratigraphy and paleoenvironment of Miocene phosphatic rocks in the east San Francisco Bay region, California: *U.S. Geological Survey Open-File Report 79-1570*, 70p.

Jayko, A.S., Blake, M.C. Jr., and Harms, Tekla, 1987. Attenuation of the Coast Range ophiolite by extensional faulting, and nature of the Coast Range "thrust," California: *Tectonics*, v. 6, no. 4, p. 475-488.

Jones, D.L., 1987, Extensional faults in collisional settings: comparison of California and Japan (abs.): *Geological Society of America Abstracts with Programs*, v. 19, no. 7, p. 720.

Jones, D.L., and Brabb, E.E., 1991, New geologic map of Contra Costa and Alameda counties, California (abs.): *Geological Society of America Abstracts with Programs,* in press.

Kleinpell, R.M., 1938, *Miocene stratigraphy of California:* American Association of Petroleum Geologists, Tulsa, OK, 450p.

Krueger, S.W., and Jones, D.L., 1989, Extensional fault uplift of regional Franciscan blueschists due to subduction shallowing during the Laramide orogeny: *Geology*, v. 17, p. 1157-1159.

Mansfield, C.F., 1972, Petrofacies units and sedimentary facies of the late Mesozoic strata west of Coalinga, California, *in Cretaceous of the Coalinga area*: Pacific Section, Society of Economic Paleontologists and Mineralogists guidebook, p. 19-26.

McLaughlin, R.J., Sliter, W.V., Elder, W.P., McDougall, K., Russell, P.C., 1990, 190-km post-middle Miocene offset on the Tolay-Hayward-Calaveras fault system superposed on large-scale Late Cretaceous to early Eocene translation (abs.): *Geological Society of America Abstracts with Programs*, v. 22, no. 3, p. 67.

Murchey, B.L., and Jones, D.L., 1984, Age and significance of chert in the Franciscan Complex in the San Francisco Bay region, *in* Blake, M.C. Jr., ed., *Franciscan geology of northern California:* Pacific Section, Society of Economic Paleontologists and Mineralogists, v. 83, p. 23-30.

Murray, R.W., Jones, D.L., ten Brink, M.R.B., Gerlach, D.C., and Russ, G.P., III, 1990, Diagenetic formation of bedded chert inferred from rare earth, major, and trace element chemistry of the Franciscan Complex, Monterey Group and DSDP cores: *EOS, Transactions*, v. 71, no. 43, p. 1392.

Namson, J.S., and Davis, T.L., 1988, Seismically active fold and thrust belt in the San Joaquin Valley, central California: *Geological Society of America Bulletin*, v. 100, p. 257-273.

Nilsen, T.H., and Clarke, S.H., 1975, Sedimentation and tectonics in the early Tertiary continental borderland of central California: *U.S. Geological Survey Professional Paper 925*, p. 1-64.

Page, B.M., 1982, Modes of Quaternary tectonic movement in the San Francisco Bay region, California, *in* Hart, E.W., Hirschfeld, S.E., and Schulz, S.S., eds., Proceedings conference on earthquake hazards in the eastern San Francisco Bay area: *California Division of Mines and Geology Special Publication 62*, p.1-10.

Page, B.M., 1984, The Calaveras fault zone of California—an active plate boundary element, *in* Burnett, J.H., and Sherburne, R.W., eds., The 1984 Morgan Hill, California earthquake: *California Division of Mines and Geology Special Publication 68*, p. 109-122.

Page, B.M., and Wahrhaftig, Clyde, 1989, San Andreas fault and other features of the transform regime, *in* Wahrhaftig, C., and Sloan, D., eds., *Geology of San Francisco and vicinity*. Field trip guidebook T105, 28th International Geological Congress, American Geophysical Union, Washington, D.C., p. 22-27.

Perkins, M.E., 1974, *Geology and petrology of the East Bay outlier of the late Mesozoic Great Valley sequence, Alameda County, California*: MS thesis, University of California, Berkeley, 120p.

Pessagno, E.A., Jr., Blome, C.D., and Longoria, J.F., 1984, A revised radiolarian zonation for the Upper Jurassic of western North America: Paleontological Research Institute, *Bulletin American Paleontology*, v. 87, no. 320, 51p.

Radbruch, Dorothy, 1969, Areal and engineering geology of the Oakland East quadrangle, California: *U.S. Geological Survey Map GQ-769*, scale 1:24,000.

Robinson, 1956, Geologic map of the Hayward quadrangle, California: *U.S. Geological Survey Map GQ-88; scale 1:24,000.*

Seiders, V.M., and Blome, C.D., 1988, Implications of upper Mesozoic conglomerate for suspect terrane in western California and adjacent areas: *Geological Society of America Bulletin*, v. 100, p. 374-391.

Silk, Michelle, and Jones, D.L., 1991, Age and tectonic setting of the Pinehurst Shale in the Berkeley Hills, California Coast Ranges (abs.): *Geological Society of America Abstracts with Programs*, in press.

Wagner, J.R., 1978, *Late Cenozoic history of the Coast Ranges east of San Francisco Bay*: Ph.D. thesis, Univerity of California, Berkeley CA, 160p.

Wentworth, C.M., Blake, M.C. Jr., Jones, D.L., Walter, A.W., and Zoback, M.D., 1984, Tectonic wedging associated with emplacement of the Franciscan assemblage, California Coast Ranges: *in* Blake, M.C., Jr., ed., *Franciscan geology of northern California:* Pacific Section, Society of Economic Paleontologists and Mineralogists, v. 43, p. 163-173.

Wentworth, C.M., and Zoback, M.D., 1989, The style of late Cenozoic deformation at the eastern front of the California Coast Ranges: *Tectonics*, v. 8, no. 2, p. 237-246.

Williams, K.M., 1983. *The Mount Diablo ophiolite, Contra Costa County, California*: MS Thesis, San Jose State University, 156p.

Youngman, M.A., 1989, *K-Ar and $^{40}Ar/^{30}Ar$ geochronology, geochemistry, and structural reinterpretation of the southern Sonoma volcanic field, Sonoma County, California*: MS Thesis, University of California, Berkeley, CA, 92p.

Soils, Paleosols, and Quaternary Sediments Offset Along the Hayward Fault at Point Pinole Regional Shoreline, Richmond, California

Glenn Borchardt[1] and Kimberley A. Seelig[2]

INTRODUCTION

This full-day field trip entails a 4.2-mi (7-km) hike around the shoreline at Point Pinole. We will examine the tectonic geomorphology of the Hayward fault during the first half of the trip, emphasizing the results of our recent work on the paleoseismology of the fault. Features along the fault include a prominent fault scarp, side-hill benches, linear troughs, active and offset landslides, and USGS monuments offset by fault movement. Holocene features demonstrating great crustal stability and the effects of increasing sea level include bay mud cliffs and a 1.3-ka peat layer found at the 24-in (60-cm) depth in a tidal marsh. Quaternary features include a Sangamon terrace with an associated wave-cut platform buried by beach sand, showing that the Bay was once 20-26 ft (6-8 m) higher than at present. Among the highlights of the trip are outstanding exposures of the Tertiary "Garrity member " of the Contra Costa Group and Wisconsin paleosols developed in beach sand and in alluvium.

FIELD TRIP LOG

Leave San Francisco via the Bay Bridge and proceed north on I-80 toward Richmond. Exit at Hilltop Dr., go west to its end at San Pablo Ave., turn right onto San Pablo Ave. and left onto Atlas Rd. at the first stoplight. Follow signs to Point Pinole Regional Shoreline (Figs. 1 and 2). Park in the lot and walk across the field south of the parking lot to Stop 1.

This semi-wilderness park is over 2000 acres, being about 1.5 mi (2.5 km) from the parking lot to the fishing pier at Pinole Point. From 1881 to 1960 the land was used to manufacture explosives. It was purchased from U.S. Steel in 1972 and is now being "undeveloped." The park is especially important for soil tectonics and paleoseismology because it contains one of the last relatively undeveloped stretches of the Berkeley segment of the Hayward fault.

Since 1984 we have been describing paleosols in the rapidly eroding cliffs along the shoreline,

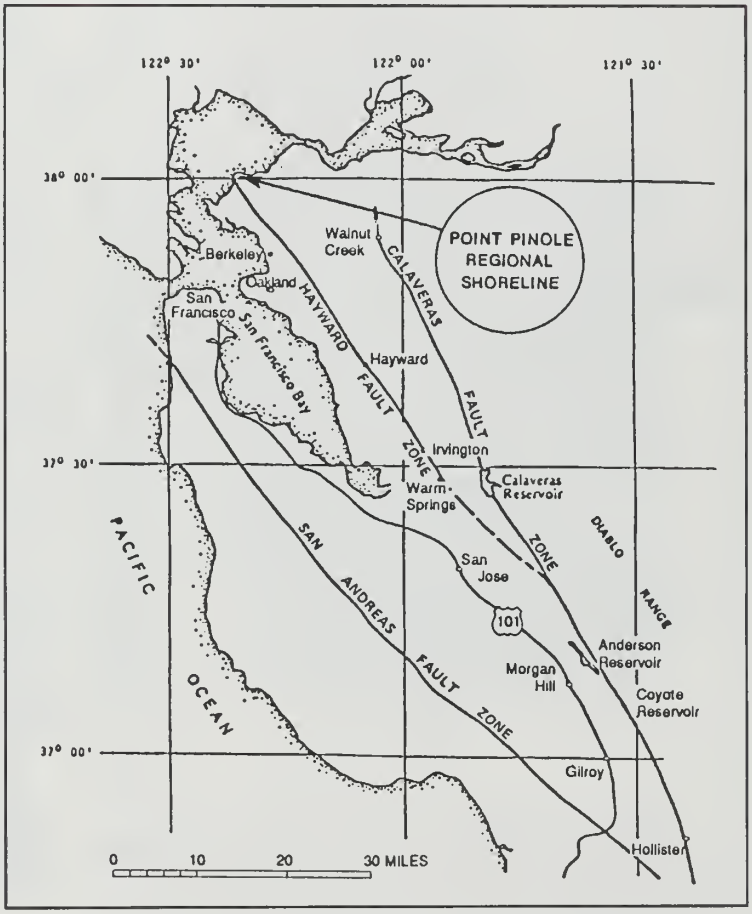

Figure 1. Point Pinole Regional Shoreline at the northwestern end of the Hayward fault (modified from Cotton and others, 1986).

[1]California Division of Mines and Geology, Pleasant Hill, CA 94523, and Soil Tectonics, Berkeley, CA 94705-0335
[2] John Carollo Engineers, Walnut Creek, CA 94598

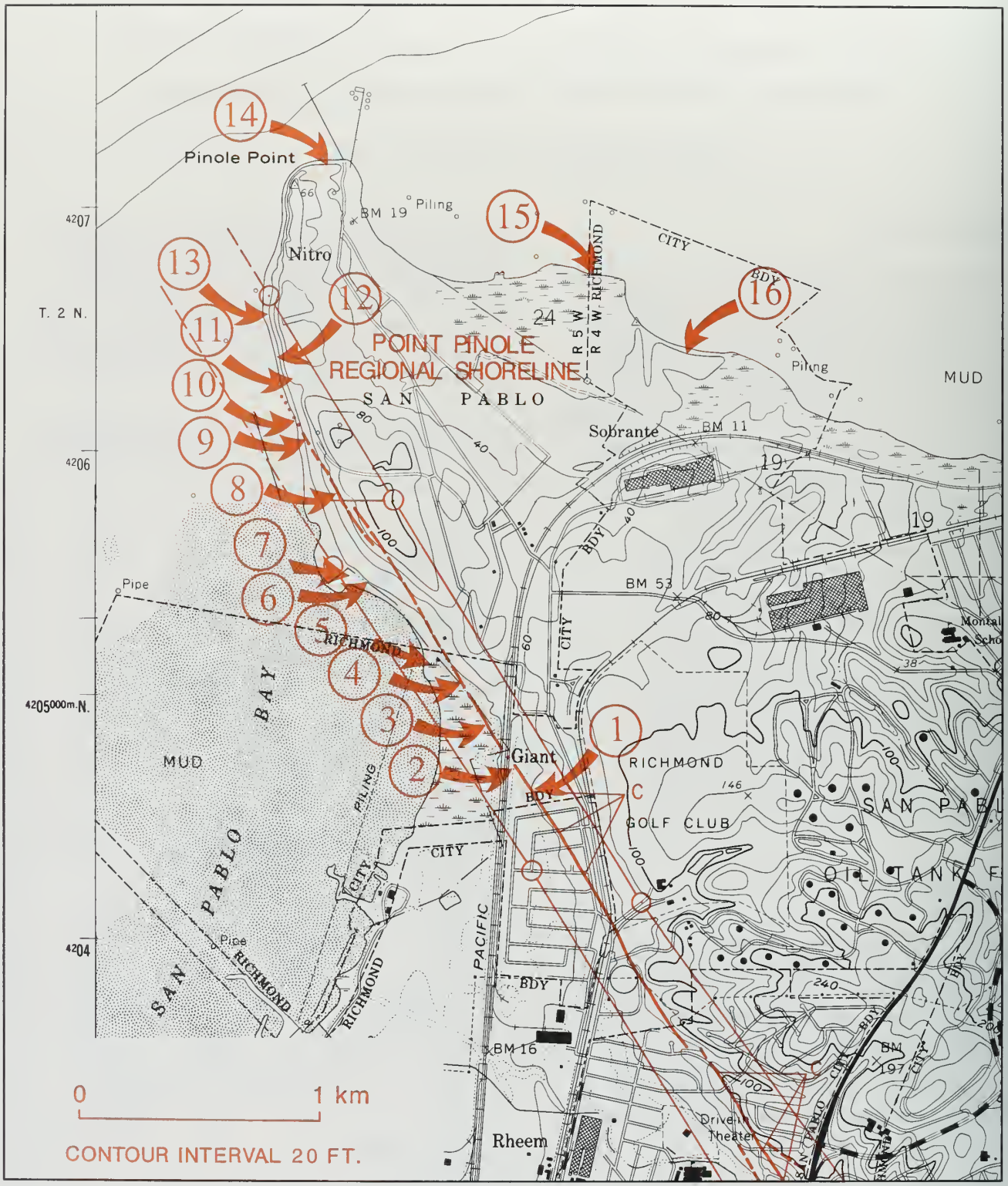

Figure 2. Point Pinole Regional Shoreline showing the Hayward fault, the Special Studies Zone (California Division of Mines and Geology, 1982), and the stops to be discussed on the trip. C indicates creeping section of the fault. Lines with circles designate the Special Studies Zone.

digging trenches, and placing boring transects across the fault. For those interested in the details see Borchardt (1988a, 1988b) and Borchardt and others (1988).

STOP 1 - USGS ALINEMENT ARRAY

The Hayward fault is delineated here by a southwest-facing scarp associated with a prominent white lineament on 1939 air photos. A series of benchmarks placed perpendicular to the fault by the USGS in 1968 underwent 2.6 in (65 mm) of aseismic displacement between 1968 and 1980 (0.2 in/yr, 5.3 mm/yr), Harsh and Burford, 1982.

STOP 2 - OFFSET WAVE-CUT PLATFORM(?)

The Hayward fault generally forms the boundary between the East Bay Hills and the alluvial plain formed along San Francisco Bay (Fig. 1). But at this site, the fault is up to 650 ft (200 m) from the range front (Fig. 2). Borchardt (1988a) speculated that the Bay waters reached elevations up to 13 ft (4 m) higher than this point during the Sangamon highstand dated at 122 ka (Edwards and others, 1987). A trench across the fault here disclosed a southwest-dipping, thinly bedded Plio-Pleistocene unit on the southwest side of the fault and a flat-lying Pleistocene colluvial unit on the northeast side of the fault. A well-developed residual soil formed across the exposed ends of the Plio-Pleistocene beds, demonstrating that the present surface has been neither degraded nor aggraded since the bedrock was planated. The nearest significant sources of degradation or aggradation include an intermittent stream 2260 ft (690 m) and a steep hillside 3150 ft (960 m) to the southeast. If the planation was indeed a result of the Sangamon highstand, then the slip rate here was 0.2-0.3 in/yr (5.7-7.9 mm/yr) during the last 122 ka.

STOP 3 - TIDAL MARSH AND FAULT SCARP

A prominent southwest-facing scarp forms an abrupt boundary between the tidal marsh and the uplands north of the railroad tracks. This linear scarp strikes N30°W, on trend with the Hayward fault seen on air photos and in seismic excavations to the southeast. We studied a small embayment here that contains late Holocene surficial estuarine deposits overlying the projection of the fault.

A landform in the shape of an alluvial fan exists in the tidal marsh to the south. An auger boring here revealed a well-developed, clayey soil judged to be of early Wisconsin age (Borchardt and others, 1988; P1 on Fig. 3). The nearest significant source of aggradation is the intermittent stream about 2750 ft (840 m) to the southeast (Fig. 2). If this landform is indeed an alluvial fan deposited from that stream, it could not have formed until the Sangamon sea retreated below this level after 114 ka, a minimum slip rate of 0.3 in/yr (7.4 mm/yr).

STOP 4 - PEAT AND CRUSTAL STABILITY

A black sedimentary peat containing sand-size flakes of vermiculite is buried in the bay mud at this site (Fig. 4). The peat gave a radiocarbon age of 1.36 ± 0.08 ka (dendro-corrected to 1.30 ka). Examination of the salt marsh cliff (Stop 5) and probings throughout the marsh revealed that the base of this distinctive peat layer exists at depths between 14 and 30 in (36-75 cm) and that it ranges in thickness from 4 to 10.5 in (10-27 cm). Its depth and age (Fig. 5) are what would be expected in a crustally stable part of the world such as Florida or Micronesia. Global eustatic sea level rise has been about 0.015 in/yr (0.4 mm/yr) during the last 4 ka, but measurements at the Golden Gate show a rise of 0.08 in/yr (2 mm/yr) between 1857 and 1975.

STOP 5 - BAY MUD CLIFF

Modern plant remains of the type found in the dated peat layer may be seen here mixed with vermiculite particles at the edge of the mud flat. At low tide the dated peat layer may be seen within the bay mud deposits along the full length of the salt marsh cliff. This is an ideal exposure of bay mud, which is of mixed clay mineralogy and normally contains only clay and silt. Sand, if any, is brought in locally from nearby upland drainages.

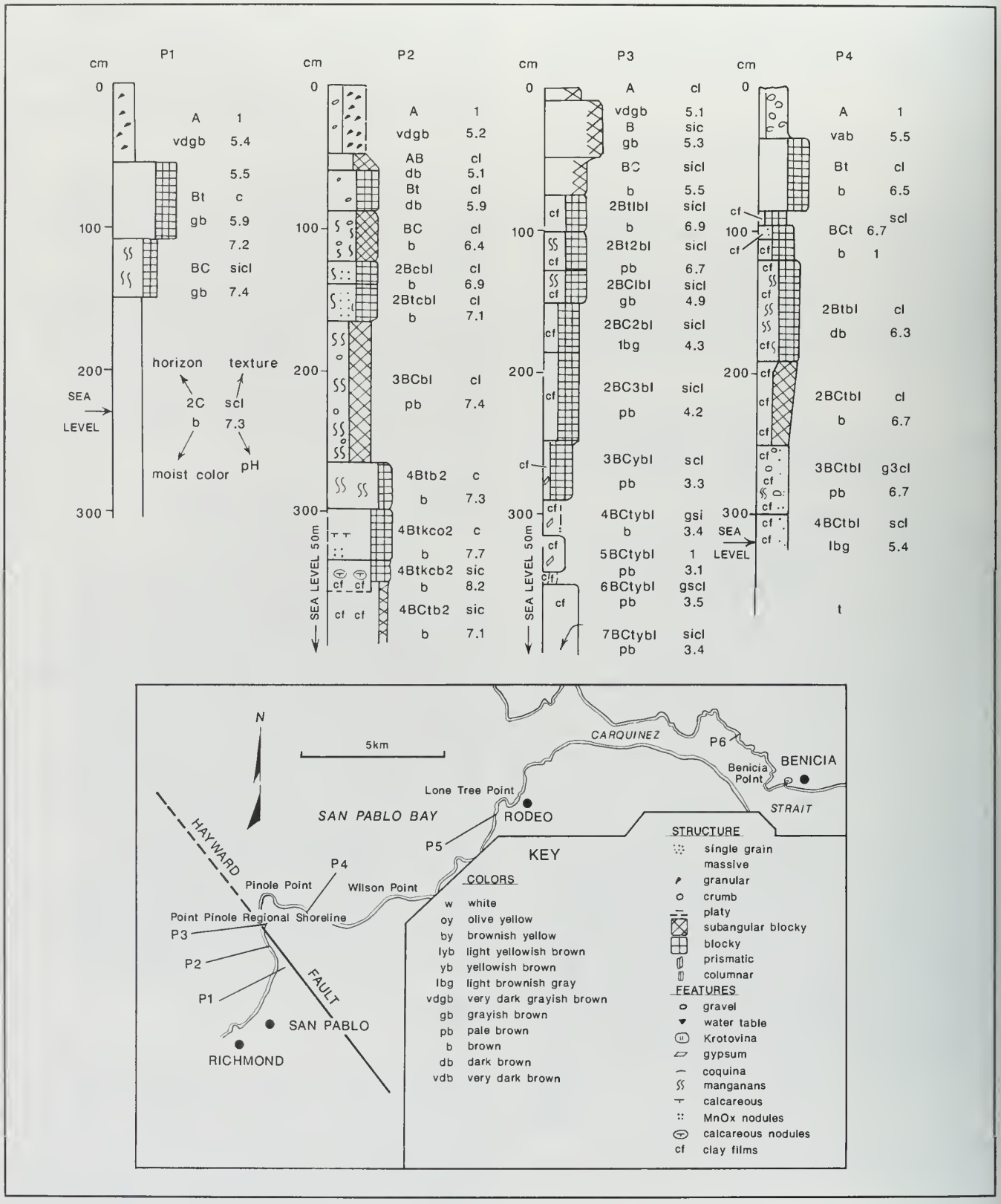

Figure 3. Paleosol sections studied at Point Pinole Regional Shoreline (modified from Borchardt and others, 1988, which describes the nomenclature).

STOP 6 - PALEOSOL SECTION P2

This paleosol section, like most of the others along the shoreline (Fig. 3), was exposed as a result of erosion produced by rising sea level in San Pablo Bay. Note that the young trees at the shoreline are being rapidly undermined. The modern soil has traces of gravel and a moderately developed B horizon overlying a zone of manganan (manganese oxide coating) development. The first paleosol is moderately well developed and contains manganese concretions in the B horizon. The second paleosol has manganese concretions above and calcite nodules beneath the base of a strongly developed B horizon.

The development in the lower paleosol here is particularly striking. This paleosol has a 35-in (88-cm) thick B horizon with strong blocky structure and clay films that extend into the BC horizon for at least another 18 in (45 cm). At a depth of 131 to 140 in (333-355 cm) the base of the paleosol contains moderately dense, 2 in (5 cm) diameter calcite nodules. The mechanism by which lime nodules could form in soils and paleosols of the Bay Area is not well understood. In California, most calcareous soil horizons are found in the semiarid and arid regions. Calcium carbonate nodules, however, have been reported in borings in east-west cross sections across southern San Francisco Bay (Atwater and others, 1977). Recent ^{230}Th-^{234}U analysis of two of these nodules, however, resulted in an age of 26 ka. This was confirmed by a ^{14}C date of 21 ka coral-corrected to 26 ka. The modern wave-cut platform about 330 ft (100 m) northwest of this site is presently cutting through a zone of calcite nodules that dips southwest.

STOP 7 - LANDSLIDE TOE

Modern as well as ancient landslides occur along the Hayward fault as it crosses the southwest side of the ridge-line. A water pipeline has been displaced approximately 33 ft (10 m) downslope by a major landslide that crosses the Hayward fault. Landslide deposits "rumple" the landscape, producing closed depressions as well as raised topography. The soils within such deposits are typically multicolored, having both oxidized and reduced zones that are indicated by changes in iron mineralogy. The yellow to

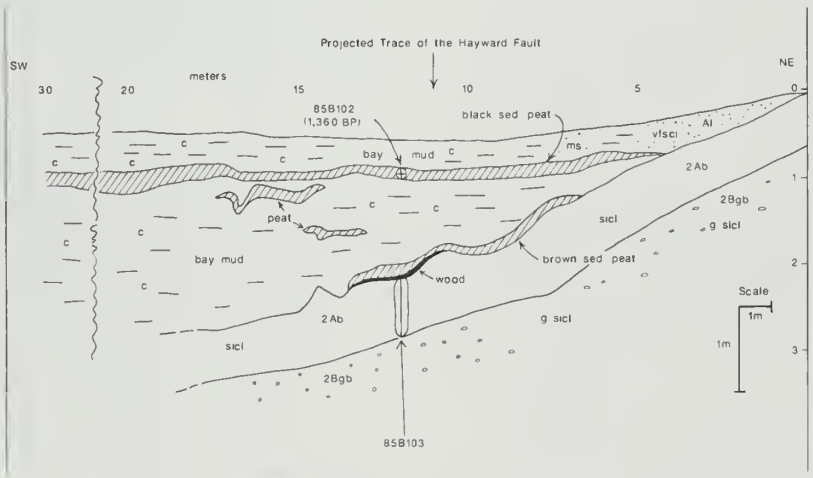

Figure 4. Cross section prepared from a core transect at Stop 4 showing the peat, bay mud deposits, and the paleosol overlying the projected trace of the Hayward fault (from Borchardt, 1988b, which describes the nomenclature).

yellow-brown colors are generally produced by goethite, whereas the reddish colors are produced by hematite.

As we head uphill, we will cross a series of side-hill benches and linear depressions that are parallel to the Hayward fault. It is likely that some of the downslope depressions are the oldest and were produced during early Holocene earthquakes. These may contain "faults" that are no longer active.

STOP 8 - LANDSLIDE/FAULT COMPLEX

A trench was dug here across this prominent linear depression in a side-hill bench along the mapped trace of the fault. The trench exposed a cross section through a block of northeast-dipping Tertiary bedrock that had slid across the fault and was subsequently displaced. The soil southwest of the fault is only 3 ft (1 m) thick, whereas the soil northeast of the fault is up to 13 ft (4 m) thick. The lower 3 ft (1 m) of the deep soil was devoid of modern rootlets and yielded a soil carbon age of 3.69 ± 0.22 ka.

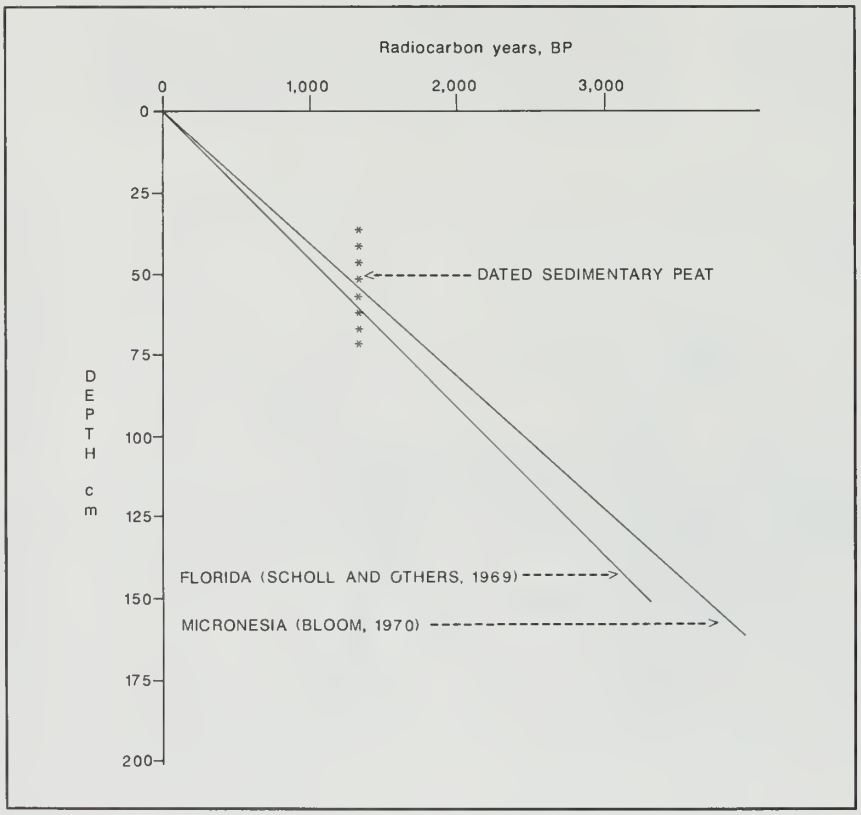

Figure 5. Age and depth to the base of the sedimentary peat layer in relation to global submergence curves (from Borchardt, 1988b).

STOP 9 - DEVITRIFIED TUFF OUTCROP

This tuff unit is exposed only on the southwest side of the fault. It contains much detritus reworked from older Tertiary rocks. No exposure east of the fault was located. The significance of this tuff is not yet known, and it cannot be correlated with the Wilson Grove or Pinole Tuff because of faulting and folding between the two outcrops.

STOP 10 - LANDSLIDE COMPLEX-LANDWARD TERMINUS OF THE FAULT

Evidence of modern landslide movement abounds on the beach just southwest of the trace of the Hayward fault. Bricks and debris from a turn-of-the-century gunpowder factory have been carried down to the beach and have been partially buried by the toe of a landslide that was triggered by wave erosion. The slide plane contains well-developed slickensides where it meets the shoreline angle.

Because of the great complexity and current activity of the landslides here, we have been unable to find positive evidence for movement of the Hayward fault. The suspect fault zones here are extremely high in smectite, but no one has ever found slickensides or other evidence of fault movement. A shallow trench within the surf zone here had mudstone in contact with polished and sheared serpentinite.

STOP 11 - PALEOSOL SECTION P3

The modern surface here consists of a weakly- to moderately-developed Holocene soil overlying a zone of manganan development at a depth of 3.3 ft (1 m) (Fig. 3). The underlying paleosol is moderately well-developed, having clay films that extend to the base of the section at a depth of 16 ft (5 m). Below the paleosol the pH drops to less than 3.5 and numerous gypsum needles are present. The abnormally low pH is a result of the oxidative dissolution of pyrite that may have formed here when sea level was higher.

STOP 12 - PLEISTOCENE DEPOSITS

The Quaternary sequence at Point Pinole lies unconformably upon the Tertiary bedrock which dips steeply to the northeast. The Quaternary cover varies from 10 to 26 ft (3 - 8 m) thick, being composed of sandstone, siltstone, mudstone, and conglomerate with clasts similar to those in the Tertiary sequence (Table 1).

STOP 13 - TERTIARY "GARRITY MEMBER"

The Tertiary sequence at Point Pinole appears to be an extension of the "Garrity member" of the Contra Costa Group as mapped by Wagner (1978). The total thickness of this unit is unknown due to faulting and erosion, but a tilted section at least 0.75 mi (1.2 km) thick is exposed along this part of the shoreline.

The "Garrity member" in these bluffs consists of conglomerate, cross-bedded and massive sandstone, siltstone, and mudstone. The conglomerate is generally matrix-supported and is composed of clasts derived from Tertiary volcanics, Franciscan rocks, Monterey Shale, other Tertiary marine formations, and clasts from the Great Valley sequence (Table 1; Borchardt and others, 1988). The presence of clasts reworked from the Claremont shale distinguishes the "Garrity member" from other formations in the Contra Costa Group. It is clearly younger than the Orinda Formation in the Berkeley Hills. For instance, the "Garrity member" contains deeply weathered volcanic clasts derived from the 9-Ma Moraga and Bald Peak formations which overlie the Orinda Formation at its type locality. A bed near the base of the "Garrity member" along San Pablo Ave. was mapped as Pinole Tuff by Wagner

Table 1. Composition of conglomerates at Pinole Point. One hundred points taken for each sample with a 1-m square grid.

PROVENANCE	TERT. %	QUAT. %
Franciscan Clasts		
Blueschist	3	2
Metagraywacke	7	4
Red and green chert	5	10
Serpentinite	4	5
Subtotal	19	21
Great Valley Sequence Clasts		
Sandstone	3	8
Subtotal	3	8
Franciscan and/or Great Valley Sequence Clasts		
Chert	18	11
Conglomerate	4	0
Granitic	0	4
Greenstone	1	3
Metavolcanic	17	7
Porphyritic volcanic	3	8
Quartzite	3	6
Subtotal	46	39
Tertiary Clasts		
Sandstone	7	9
Schist	1	2
Shale		
Claremont	4	6
Other	3	3
Siltstone	4	1
Volcanic	6	3
Subtotal	25	24
Matrix:	7	8
Subtotal	7	8
TOTAL	100	100

(1978) and Dibblee (1980), but has been correlated with the tuff of the Wilson Grove Formation (Sarna, written comm., 1988) which has been dated at about 6 Ma.

STOP 14 - ANCIENT WAVE-CUT PLATFORM AT PINOLE PT.

As we saw at Stop 5, Point Pinole seems to have a high degree of crustal stability despite the presence of the Hayward fault. Subsidence in San Francisco Bay generally decreases from south to north (Atwater and others, 1977). Sangamon coquinas have been found 16 ft (5 m) above sea level along the Carquinez Strait (Atwater and others, 1981; Borchardt and others, 1988; P5 and P6, Fig. 3) and thus the Pinole area is one of the few places along the Bay where one might expect to see evidence for a sea level higher than the present. This exposure affords a rare opportunity to view a cross section through an ancient wave-cut platform produced during the last time such a global highstand occurred - during isotope stage 5e of the Sangamon interglacial at about 122 ka. The beach here once faced east and was formed in an environment similar to that of the modern beach which now faces north. As you examine the outcrop, look for paleosols, poorly sorted alluvium, well-sorted beach sand, lag gravel with well-rounded clasts, a planated surface, and the shoreline angle.

Continue to the fishing pier where the view to the southeast includes the gently sloping surface and broad expanse of the Sangamon terrace that overlies the ancient wave-cut platform.

STOP 15 - WHITTELL MARSH

The prominent salt marsh cliffs here are a result of erosion produced by the ongoing rise in sea level. The tidal marsh nearest the bay is being destroyed, whereas the tidal marsh farthest from the Bay invades the upland. Between 1939 and 1983 the shoreline retreated by 108 ft (33 m), while the marsh advanced landward by 226 ft (69 m)—a gain of 118 ft (36 m) (Borchardt, 1988b). The shoreline on the other side of Point Pinole retreated by 85 ft (26 m), whereas the marsh advanced landward by 164 ft (50 m) during the same period.

STOP 16 - COOK'S POINT, PALEOSOL SECTION P4

Here coastal erosion provides us a magnificent northwest-southeast cross section through an alluvial fan which is part of the Sangamon terrace. After the highstand at 122 ka, the shoreline began to advance. By 114 ka, sea level had dropped to an elevation corresponding to present sea level, whereupon aggradation could begin here (Borchardt and others, 1988). Continued progradation resulted in the deposition of the upward-fining alluvial units that formed the parent material of the lowermost paleosol at this site (P4, Fig. 3). Soil development proceeded apace during the early Wisconsin, being interrupted by aggradation probably during the mid-Wisconsin interglacial period around 50 ka. The modern surface, therefore, consists of a late Wisconsin relict paleosol having a moderately developed B horizon that overlies a striking zone of manganan development at a depth of 3 ft (1 m).

Return to the parking lot at 4.2 mi (7.0 km). Turn left onto Giant Hwy. and retrace the route to San Francisco.

ACKNOWLEDGEMENTS

The manuscript was kindly reviewed by Chris J. Wills. This work was performed in cooperation with the East Bay Regional Park District, and with funds supplied by the California Division of Mines and Geology and the U.S. Geological Survey.

REFERENCES

Atwater, B.F., Hedel, C.W., and Helley, E.J., 1977, Late Quaternary depositional history, Holocene sea level changes, and vertical crustal movement, southern San Francisco Bay, California: *U.S. Geological Survey Professional Paper 1014*, 15p.

Atwater, B.F., Ross, B.E., and Wehmiller, J.F., 1981, Stratigraphy of Late Quaternary estuarine deposits and amino acid stereochemistry of oyster shells beneath San Francisco Bay, California: *Quaternary Research*, v. 16, p. 181-200.

Bloom, A.L., 1970, Paludal stratigraphy of Truk, Ponape, and Kusaie, Eastern Caroline Islands: *Geological Society of America Bulletin*, v. 81, p. 1895-1904.

Borchardt, Glenn, 1988a, Soil development and displacement along the Hayward fault, Point Pinole Regional Shoreline, Richmond, California, *in* Borchardt, Glenn, ed., Soil development and displacement along the Hayward fault (Volume II): Point Pinole, California: Final technical report for the U.S. Geological Survey National Earthquake Hazards Reduction Program, *California Division of Mines and Geology Open-File Report DMG OFR 88-13*, p. 95-161.

Borchardt, Glenn, 1988b, Estuarine deposition and its relationship to the Hayward fault, Point Pinole Regional Shoreline, Richmond, California, *in* Borchardt, Glenn, ed., Soil development and displacement along the Hayward fault (Volume II): Point Pinole, California: Final technical report for the U.S. Geological Survey National Earthquake Hazards Reduction Program, *California Division of Mines and Geology Open-File Report DMG OFR 88-13*, p. 163-220.

Borchardt, Glenn, Seelig, K.A., and Wagner, D.L., 1988, Geology, paleosols, and crustal stability at Point Pinole Regional Shoreline, Contra Costa County, California, *in* Borchardt, Glenn, ed., Soil development and displacement along the Hayward fault (Volume II): Point Pinole, California: Final technical report for the U.S. Geological Survey National Earthquake Hazards Reduction Program, *California Division of Mines and Geology Open-File Report DMG OFR 88-13*, p. 3-94.

California Division of Mines and Geology, 1982, Mare Island and Richmond quadrangles: State of California Special Studies Zones, Revised Official Maps, scale 1:24,000.

Cotton, W.R., Hall, N.T., and Hay, E.A., 1986, *Holocene behavior of the Hayward-Calaveras fault system, San Francisco Bay area, California*: Final Technical Report to the U.S. Geological Survey (Contract No. 14-08-0001-20555), Foothill-De Anza Community College District, Los Altos Hills, CA, 15p.

Dibblee, T.W., Jr., 1980, Preliminary geologic map of the Richmond quadrangle, Alameda and Contra Costa counties: *U.S. Geological Survey Open-File Report 80-1100*, scale 1:24,000.

Edwards, R.L., Chen, J.H., Ku, T -L., and Wasserburg, G. J., 1987, Precise timing of the last interglacial period from mass spectrometric determination of Thorium-230 in corals: *Science*, v. 236, p. 1547-1553.

Harsh, P.W., and Burford, R.O., 1982, Alinement-array measurements of fault slip in the eastern San Francisco Bay area, California, *in* Hart, E.W., Hirschfeld, S.E., and Schulz, S.S., eds., Proceedings of the conference on earthquake hazards in the eastern San Francisco Bay Area: *California Division of Mines and Geology Special Publication 62*, p. 251-260.

Scholl, D.W., Craighead, F.C., Sr., and Stuiver, Minze, 1969, Florida submergence curve revised: Its relation to coastal sedimentation rates: *Science*, v. 163, p. 562-564.

Wagner, J.R., 1978, *Late Cenozoic history of the Coast Ranges east of San Francisco Bay:* Ph.D. Dissertation, University of California, Berkeley, CA, 161p.

Franciscan Complex, Coast Range Ophiolite and Great Valley Sequence: Pacheco Pass to Del Puerto Canyon, California[1]

A.P. Bennison,[2] M.C. Blake, Jr.,[3] B.F. Cox,[3]
W.P. Elder,[3] W.G. Ernst,[4] Tekla Harms,[5] and T.H. Nilsen[6]

INTRODUCTION

This field trip covers part of the Diablo Range and adjacent San Joaquin Valley of central California (Fig. 1). The core of the range is made up of rocks of the Franciscan Complex, flanked by Coast Range ophiolite (CRO) and Great Valley sequence (GVS). The Franciscan Complex in this area consists of deformed and metamorphosed sedimentary and volcanic rocks containing fossils of Late Jurassic to Late Cretaceous age. These rocks are believed to represent an accretionary wedge that was subducted to depths of 12-20 mi (20-30 km). The Middle to Late Jurassic CRO represents a slab of oceanic upper mantle and crust that was trapped between the Sierran magmatic arc and the Franciscan trench. The Upper Jurassic to Upper Cretaceous GVS is a thick accumulation of mudstone, sandstone, and conglomerate that was deposited on the ophiolite in a forearc-basin setting. The objectives of this field trip are to examine good exposures of these three major units in order to better understand their sedimentary, igneous, and metamorphic histories, to examine some of the major faults bounding the units, and to gain an understanding of the tectonic history of this portion of the Coast Ranges.

REGIONAL GEOLOGY

Franciscan Complex: Previous workers subdivided the Franciscan Complex of the Diablo Range into several mappable units (Cotton, 1972; Cowan, 1974; Crawford, 1975, 1976; Blake, 1981; Ernst, 1987). Two tectonostratigraphic terranes have been recognized. The first, the Eylar Mountain, comprises intercalated zones of coherent metagraywacke and disrupted melange. The origin of the melange units is controversial. Cotton (1972) interpreted them as mudstone-rich units disrupted by shearing, whereas Crawford (1975) interpreted them to represent submarine landslide deposits (olistostromes). Several facts have emerged regarding these melanges: (1) according to Jacobson (1978), graywacke from melanges and metagraywacke units have similar sandstone compositions, although those from the melanges on the average are slightly more lithic ($Q_{28}F_{42}L_{30}$ vs $Q_{29}F_{48}L_{23}$); (2) blocks of high-grade blueschist, amphibolite, and eclogite are restricted to the melange zones; (3) the metamorphic grade of melange graywacke is usually lawsonite-albite, whereas that of the metagraywacke units is often jadeitic pyroxene-quartz; and (4) melanges appear to possess a higher mudstone/sandstone ratio than the coherent units.

Within the coherent metagraywacke units of the Eylar Mountain terrane, there is locally a succession of metabasalt overlain by metachert that is, in turn, overlain by slaty mudstone and metagraywacke. The radiolarian chert and basalt may represent layers 1 and 2 of oceanic crust, upon which the continent-derived graywacke and mudstone were deposited. Radiolarians of Late Jurassic age are present in melange blocks and in chert below coherent metagraywacke, and a single *Buchia fischeriana* of Late Jurassic (Tithonian) age was found in a coherent metagraywacke unit (Crawford, 1976).

---

[1] The stratigraphic nomenclature and unit age assignments used in this report may not necessarily conform to current usage by the U.S. Geological Survey.

[2] Consultant, Tulsa, OK; volunteer, U.S. Geological Survey, 345 Middlefield Rd., Menlo Park, CA 94025
[3] U.S. Geological Survey, 345 Middlefield Rd., Menlo Park, CA 94025
[4] Stanford University, Stanford, CA 94305
[5] Amherst College, Amherst, MA 01002
[6] 133 Madera Ave., San Carlos, CA 94070

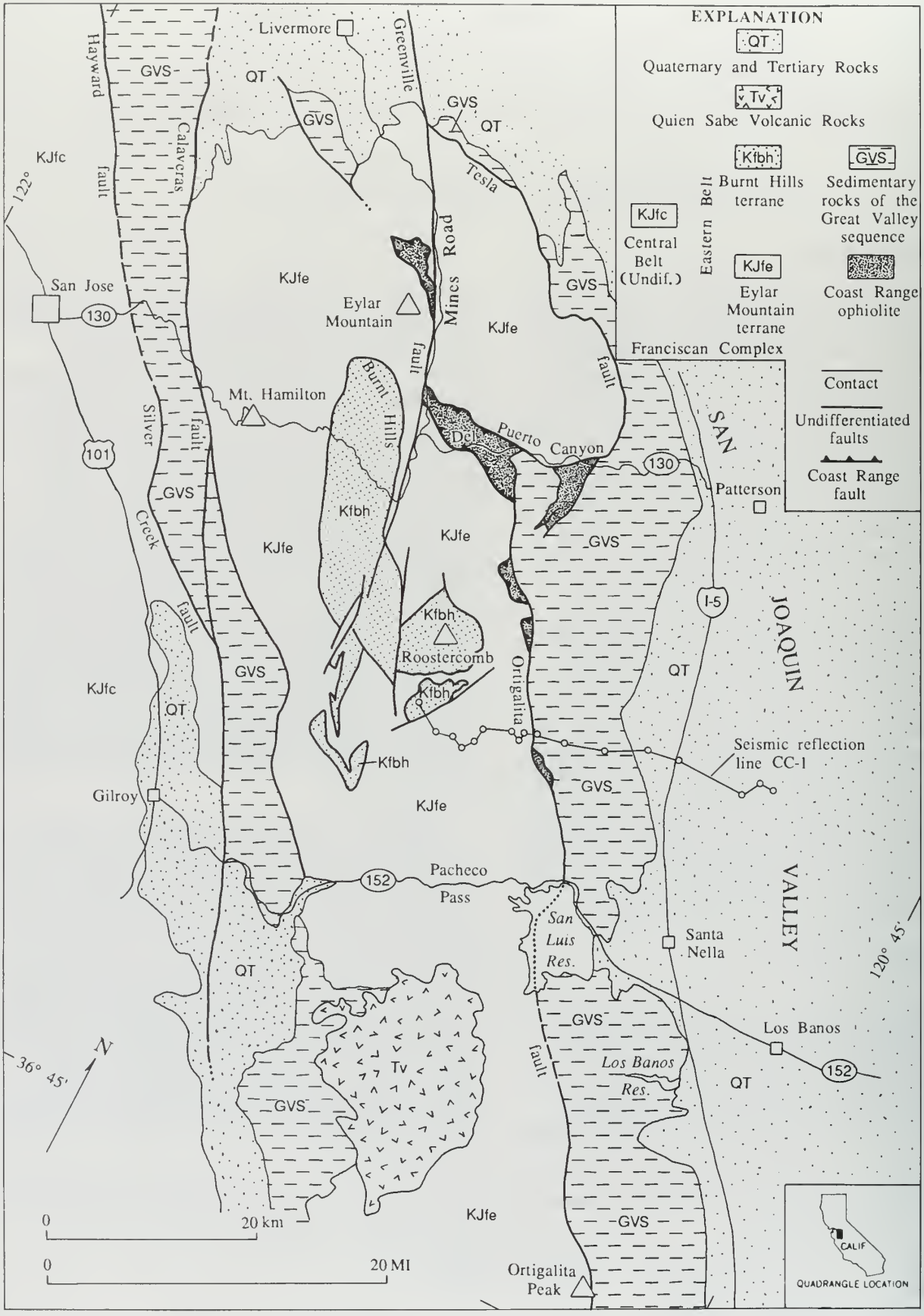

Figure 1. Simplified geologic map of the northern Diablo Range and adjacent areas showing region covered by field trip.

The metamorphic petrology of the Eylar Mountain terrane has received considerable attention (see Ernst, 1987, for a review). Much of this work has focused on the Pacheco Pass traverse, which will be examined in several stops of the field trip. Metagraywackes of the Eylar Mountain terrane contain rather abundant coarse-grained (1-2 mm) detrital fragments of intergrown lawsonite and white mica, attesting to at least two episodes of blueschist facies metamorphism (Crawford, 1975).

The second terrane, the Burnt Hills (Blake, 1981; Blake and others, 1990), also consists of metabasalt-metachert-metagraywacke, but it differs from the Eylar Mountain terrane in age and sandstone composition. These rocks have yielded Early Cretaceous radiolarians and the megafossils *Inoceramus (Sphenoceramus) nagaoi* and *Bostrychoceras* sp. of Late Cretaceous (late Santonian-early Campanian) age. According to Jacobson (1978), the average sandstone composition is $Q_{38}F_{52}L_{10}$. Burnt Hills terrane sandstones contain coarse-grained detrital biotite and white mica, myrmekite, sphene, allanite, apatite, zircon, garnet, and tourmaline, suggesting a predominantly granitic source. Curiously, hornblende, a common mineral in Sierran plutons, has not been identified. The sandstones also contain detrital grains of white mica-lawsonite identical to fragments in the Eylar Mountain terrane.

Cowan (1974) and Morrell (1978) documented a remarkably narrow, about 0.6 mi (1 km) zonation of metamorphic minerals in metagraywacke of the Burnt Hills terrane near the Roostercomb, about 12 mi (20 km) north of Pacheco Pass (Fig. 1). Our field studies (Blake and others, 1990; Blake and Showalter, 1991) indicate that this zonation is interrupted such that there are three thrust sheets (nappes) each consisting of discontinuous basal basalt overlain by chert and arkosic metagraywacke and slaty mudstone. Within the lowest nappe, progressive metamorphism is characterized by the disappearance of pumpellyite and the growth of glaucophane and jadeitic pyroxene. Fossils in these rocks require that the metamorphism was younger than about 83 Ma.

The structural relations between the two Franciscan terranes remain unclear. In the Roostercomb area (Fig. 1), the Burnt Hills terrane structurally overlies the Eylar Mountain terrane. To the southwest, however, melange correlated with the Eylar Mountain terrane structurally overlies the Burnt Hills terrane. The two terranes may form a series of imbricate slices (Cowan, 1974).

Coast Range ophiolite: Rocks correlated with the CRO are present at several localities in the Diablo Range. The most complete and accessible section is along Del Puerto Canyon (Fig. 1). Here, detailed mapping by Evarts (1977, 1978) has documented a faulted but nearly complete sequence of mantle harzburgite and dunite, layered ultramafic rocks, layered gabbro, intrusive gabbro, pillow basalt, and flows and sills of keratophyre and quartz keratophyre. Hornblende from plagioclase peridotite and gabbro yielded K-Ar mineral ages of 163 and 161 Ma (Lanphere, 1971). Overlying the ophiolite is the Lotta Creek Tuff which consists of volcanogenic sandstone, siltstone, conglomerate, and fine-grained radiolarian tuff.

Great Valley sequence: The stratigraphy of the GVS in the eastern Diablo Range and adjacent northern San Joaquin Valley was recently reviewed by Bartow and Nilsen (1990). Fig. 2 is a generalized correlation chart modified from their Figs. 3 and 5.

Within the Del Puerto-Pacheco Pass area, the basal unit of the GVS, the Hawk shale of Schilling (1962), consists of 150-500 ft (50-150 m) of dark mudstone that locally contains *Buchia* species of Late Jurassic (Tithonian) to Early Cretaceous (Valanginian) age, indicating a condensed sequence relative to the thick Upper Cretaceous section. The Hawk shale is overlain locally by additional shaly deposits of Early Cretaceous age. Shale at Del Puerto Canyon has yielded early Albian fossils (Bartow and others, 1983; Elder and Miller, 1990). Farther south, near Quinto and Romero creeks, a post-Valanginian shale unit (Fig. 3, unit 1) has yielded sparse molluscan fossils that may be older than Albian, possibly as old as Hauterivian (Bennison, unpublished data).

In the Pacheco Pass area, most of the GVS about 26,000 ft (8000 m) consists of Upper Cretaceous marine sandstone, mudstone and conglomerate generally assigned to the Panoche Formation and overlying Moreno Formation. The Panoche

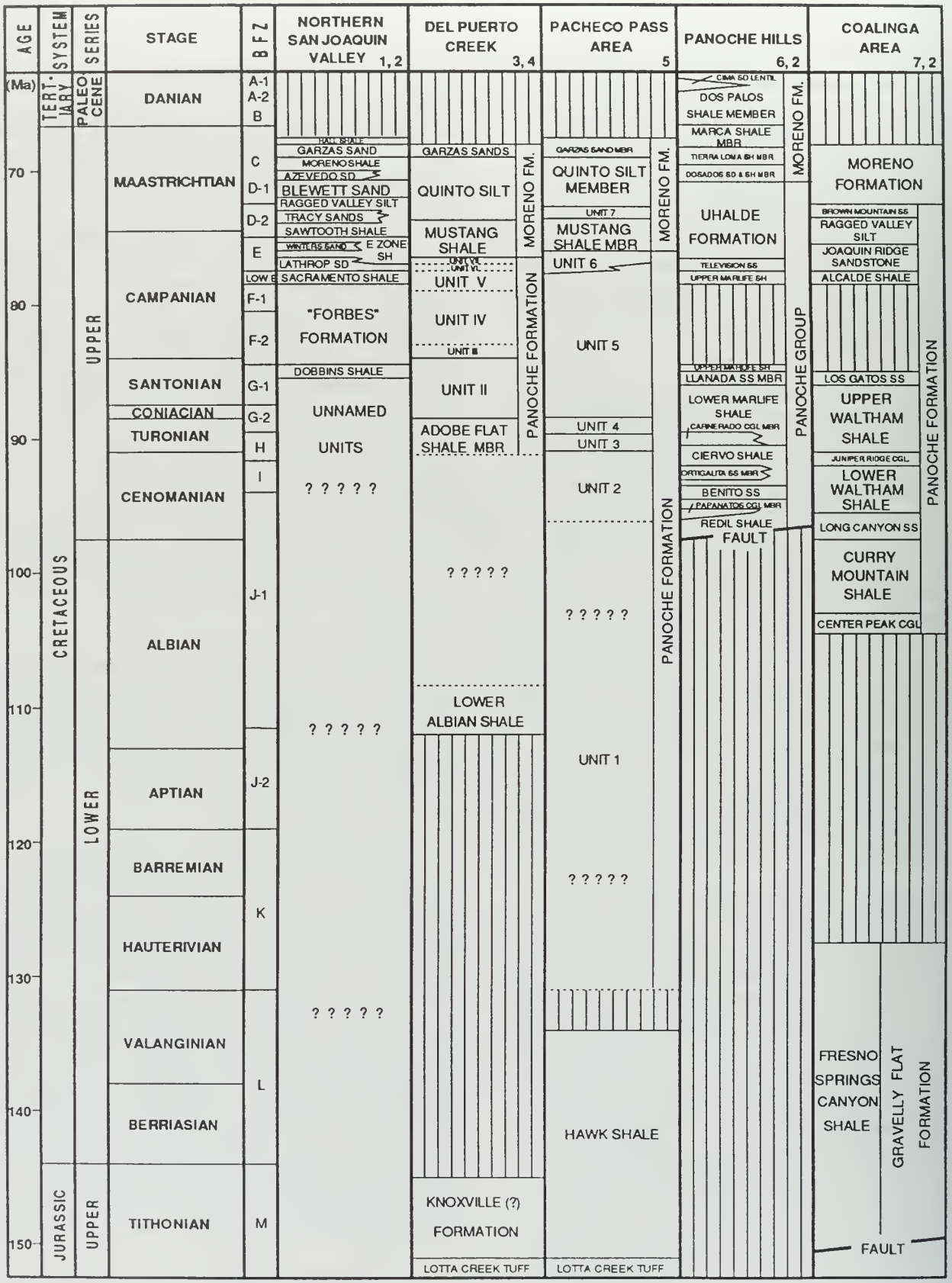

Figure 2. Correlation chart for GVS of the eastern Diablo Range (modified from Bartow and Nilsen, 1990, Figs. 3 and 5). The numbers adjacent to the column headings indicate the following sources of age and nomenclature: 1, Edmonson and others (1964); 2, Almgren (1986); 3, Bishop (1970); 4, Maddock (1964); 5, A.P. Bennison (unpublished data); Schilling (1962); 6, Payne (1951, 1960, 1962); 7, Anderson (1972). Benthic foraminiferal zones (BFZ) from Goudkoff (1945) and Berry (1974).

Formation consists mainly of turbidites and related deposits of submarine fan origin. It exhibits major facies changes and extreme lensing of rock units (Fig. 3). Consequently, the sequence of lithostratigraphic units recognized by Payne (1960) 19-25 mi (30-40 km) to the south in the Panoche Hills is only partly recognizable near San Luis and Los Banos Reservoirs. One of us (A.P. Bennison) believes that three of Payne's units are mappable into the Pacheco Pass area. In ascending order, these units are the Papanatas Conglomerate Member of the Redil Shale, Benito Sandstone, and Ciervo Shale (Figs. 2, 3; units 2, 3, and 4). These units are Cenomanian to Turonian in age and appear to become older to the south (Fig. 2). Additional overlying units of sandstone,

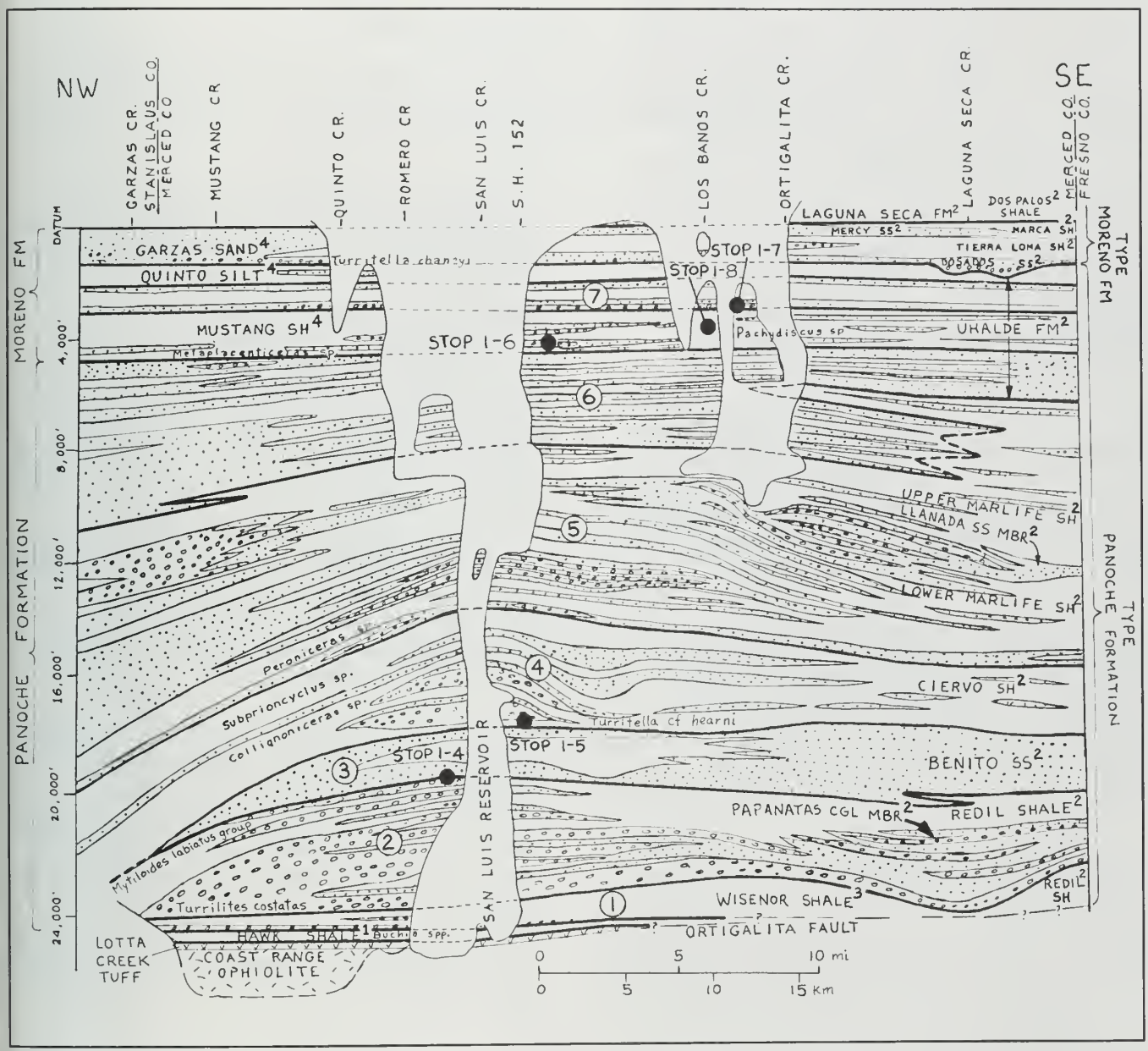

Figure 3. Interpretive stratigraphic diagram of GVS near San Luis and Los Banos reservoirs, showing approximate stratigraphic locations of field trip stops 1-4 to 1-8. Based on unpublished mapping of A.P. Bennison. Lithologic patterns are as follows: random dashes, ultramafic and mafic igneous rocks; vees, volcaniclastic rocks; circles, conglomerate; dots, sandstone; unpatterned, mudstone. Superscripts indicate the following sources of stratigraphic nomenclature: 1, Schilling (1962), Pacheco Pass quadrangle; 2, Payne (1951, 1960, 1962), Panoche Hills; 3, Briggs (1953), Ortigalita Peak quadrangle; 4, Bennison (cited in Bishop, 1970). Encircled numbers represent unnamed units of A.P. Bennison (unpublished mapping).

conglomerate, and mudstone in the Panoche Formation range in age from Coniacian to Campanian or early Maastrichtian. Bennison believes that a thick sandstone-rich interval near the top of the Panoche succession (Fig. 3, unit 6) is the lithostratigraphic equivalent of Anderson's (1972) Joaquin Ridge Sandstone near Coalinga.

The Moreno Formation consists of mudstone and sandstone that form the upper, mainly Maastrichtian, part of the GVS. It is generally distinguished from the underlying Panoche Formation by a greater abundance of mudstone, less conglomerate, and by locally abundant megafossils. Cherven and Fischer (1984) portray a broad coarsening-upward sequence within the Moreno in the Mt. Diablo area, which they attribute to a change from slope shale to delta-front and delta-plain sandy paleoenvironments. Most of the known fossil reptiles in California, including dinosaurs, plesiosaurs, and mosasaurs have been discovered within the Moreno of the eastern Diablo Range.

REGIONAL TECTONIC HISTORY

Integration of the previously described geologic data with plate-tectonic models suggests the following speculative sequence of events:

(1) During the Late Jurassic and again during the Late Cretaceous, Franciscan clastic rocks derived from a continental source area were deposited in a trench on a subducting oceanic plate composed of basalt and overlying radiolarian chert. At the same time, strata of the GVS were deposited to the east in a forearc basin floored by the CRO.

(2) Concurrent with sedimentation, the Franciscan rocks were either continuously or episodically subducted eastward to depths great enough to form lawsonite, aragonite, and jadeitic pyroxene. Blueschist radiometric ages suggest metamorphism occurred during about 122-76 Ma.

(3) Following their subduction, the Franciscan rocks were tectonically uplifted some 12-20 mi (20-30 km) along virtually the same P-T path where they were subducted, thereby preserving metamorphic aragonite. Uplift was apparently accompanied by extensional faulting along the Coast Range fault (Platt, 1986; Jayko and others, 1987; Harms and others, 1987).

(4) During the Cenozoic, the Franciscan rocks were thrust eastward onto CRO and GVS along the Tesla-Ortigalita fault system. This process may be going on today, as evidenced by the 1983 Coalinga earthquake that resulted from deep, east-directed thrusting (Wentworth and Zoback, 1990).

ROAD LOG DAY 1

From San Francisco travel south on Hwy. 101 to Gilroy and west on Hwy. 152 to Pacheco Pass. Road log is in miles.

0.0 Pacheco Pass. Intersection State Hwy. 152 and Dinosaur Point Rd. (old highway). The first three stops (Fig. 4) are modified from an earlier field trip guidebook (Ernst, 1987) based on geologic and mineral-assemblage maps of the Pacheco Pass area by Ernst and others (1970). Units dip predominantly to the east. The dominantly clastic section of locally graded Franciscan metagraywacke and shale appears stratally coherent, as indicated by lateral continuity of interbedded cherty units (Fig. 4). Nevertheless, pods of greenstone, blueschist, and minor serpentinite occur in the stratigraphically lowest part of the metaclastic sequence, unit D, suggesting that this unit in part represents a melange. Mafic meta-igneous rocks intrude the stratigraphically higher units. Metamorphic mineral assemblages are shown on inset box of Fig. 4.

0.9 **STOP 1-1** An exposure of relatively coarse-grained metagraywacke of unit B crops out along the former highway east of the road junction with Hwy. 152 near Pacheco Pass. This is the so-called "jadeite pegmatite" locality. Sprays of sodic pyroxene are faintly visible with the aid of a good hand lens, forming about 40 volume percent of the rock. The pyroxene has overgrown and completely replaced albitized detrital plagioclase grains. Return to Hwy. 152 and proceed east.

2.3 **STOP 1-2** Well-bedded coherent metagraywacke and interlayered metashale of unit D crop out in a right-side-up, gently east-dipping sequence along Hwy. 152 approximately 0.5 mi

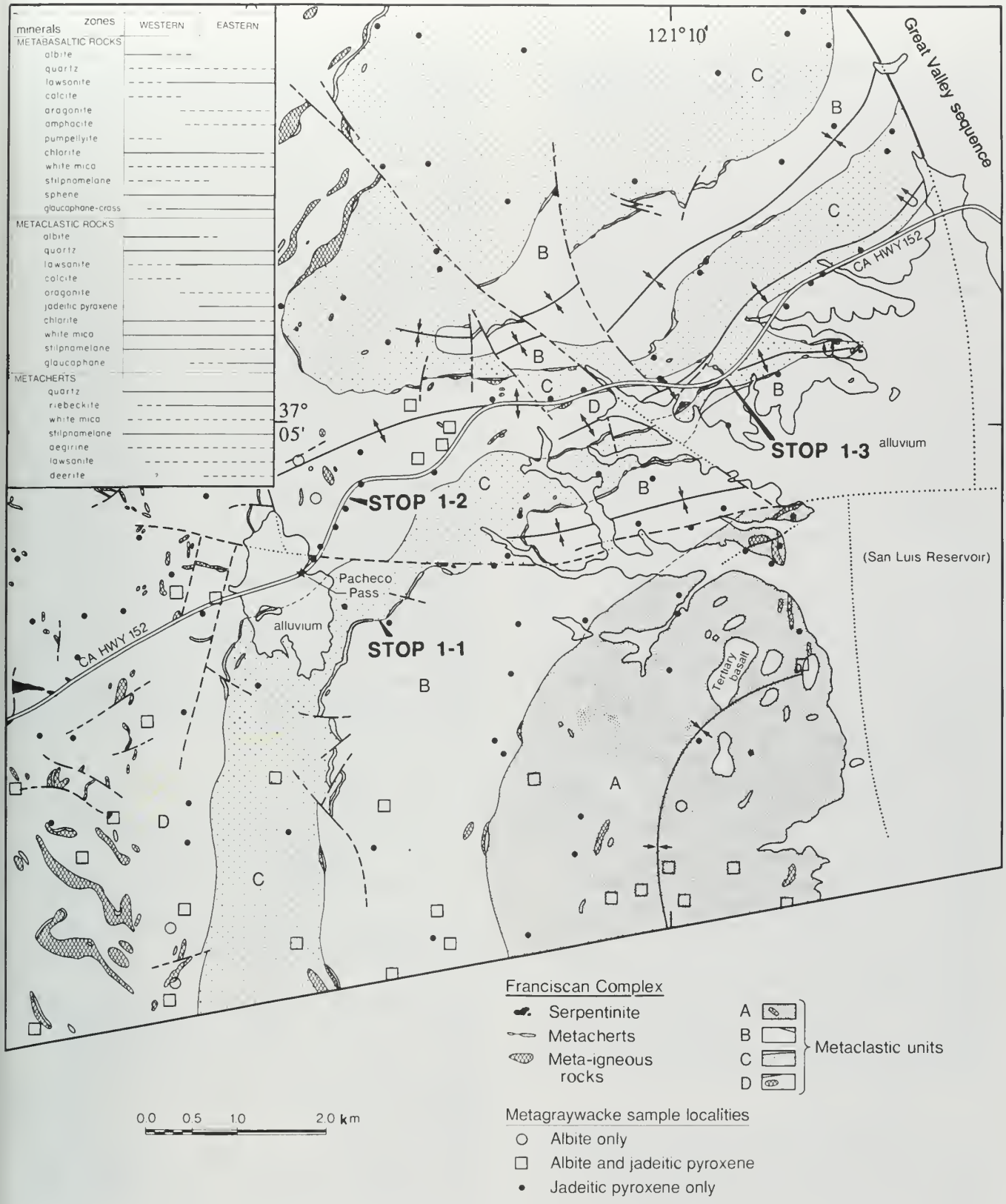

Figure 4. Interpretive geology and mineral assemblages of the Pacheco Pass area (after Ernst and others, 1970, and new mapping). Geologic map shows field trip stops 1-1 to 1-3 described in the text. Four metaclastic units of the Franciscan Complex in this area, referred to as units A-D, are distinguished. These are continuous with rocks mapped as Eylar Mountain terrane to the north. Inset box shows presumably synchronous mineral parageneses in the principal Franciscan rock types proceeding eastward across the Diablo Range in the vicinity of Pacheco Pass (after Seki and others, 1969; Ernst and others, 1970; and Maruyama and others, 1985), assuming a more or less autochthonous section.

(0.8 km) northeast of the summit. Graded bedding is distinct. Some metaclastic rocks contain jadeitic pyroxene ± aragonite, whereas others carry relict albite.

4.8 **STOP 1-3** About 1.5 mi (2.4 km) to the east, Hwy. 152 crosses the axial trace of a small, east-plunging anticline within metachert and siliceous red metashale near the base of unit C. These pelagic rocks are clearly interstratified with the dominantly sandy metaclastic Franciscan units both here and throughout the mapped area. Beneath the siliceous horizon, pods of greenstone and metagabbro occur within the metagraywackes of unit D. Contrasting phase assemblages in these *in situ* rock types reflect the influence of original bulk composition on blueschist-facies mineralogy. The quartzose metacherts contain 0-10 volume percent of riebeckitic amphibole, stilpnomelane and aegirine, as well as trace amounts of lawsonite. The mafic meta-igneous rocks are rich in chlorite+lawsonite and contain variable amounts of relict clinopyroxene, neoblastic omphacite and glaucophane-crossite ± aragonite. The sodic pyroxene formed relatively early as a groundmass phase, or as a replacement of igneous titanaugite, whereas the sodic amphibole formed later within stringers and fracture-related patches. Associated metagraywackes are similar to those previously described, except that some specimens contain abundant relict albite grains and little or no new jadeitic pyroxene. White mica and glaucophane-crossite from a metabasaltic block directly beneath the meta-chert horizon just south of the highway yielded K-Ar radiometric mineral ages of 115 ± 3 and 122 ± 3 Ma, respectively (Suppe and Armstrong, 1972). These ages are 20 my older than U-Pb mineral ages from metagabbroic samples obtained about 20 mi (32 km) to the southeast at Ortigalita Peak by Mattinson and Echeverria (1980).

7.4 Long bridge across inlet of San Luis Reservoir straddles the Ortigalita fault zone, separating Franciscan Complex from Cenomanian conglomerate and thin-bedded turbidites of the GVS.

9.8 Turn off California Hwy. 152 for the Romero Visitor Center, San Luis Reservoir.

10.0 **STOP 1-4** Descend from parking lot into a small bay of the San Luis Reservoir (Fig. 5). A thick unit of stacked sandstone deposits is well exposed along the lakeshore directly adjacent to the Romero Visitor Center (Fig. 5, unit K_3). Bennison (unpublished mapping) has traced this sandstone (unit 3, Figs. 2, 3) 25 mi (40 km) southeastward to Little Panoche Creek, where it was mapped as the Benito Sandstone Member of the Panoche Formation by Payne (1962). This unit is underlain by an interval of Cenomanian cobble conglomerate (unit 2, Figs. 2, 3; Fig. 5, unit K_2) more than 1000 ft (300 m) thick that Bennison correlates with Payne's (1962) Papanatas Conglomerate Member of the Redil Shale. The sequence appears to form a large inner-fan channel or submarine-canyon fill dominated by Mutti and Ricci Lucchi (1972) Facies A conglomerate, Facies B sandstone, and Facies E thin-bedded turbidites. Cobble imbrication and rare sole structures indicate paleocurrents flowed southward or southeastward approximately parallel to the strike of the conglomerate beds. Abundant clasts of pink granite that are present here near the top of the thick conglomeratic unit apparently represent the earliest occurrence of potassium-rich plutonic rock detritus in the local succession of the GVS (Cox and Seiders, 1991).

10.3 Return to Hwy. 152 and turn right.

13.2 Turn right for Basalt Recreation Area.

15.2 Stop for toll gate.

16.0 Turn right off paved road and follow dirt road a short distance eastward.

16.2 **STOP 1-5** Wave-cut outcrops at this stop expose a sequence of thin-bedded turbidites (Fig. 5, unit K_4). Bennison (unpublished mapping) correlates these rocks with the Ciervo Shale of Payne (1962) (unit 4, Figs. 2, 3). The sequence appears to consist mostly of Mutti and Ricci Lucchi (1972) Facies B and E middle-fan-channel and channel-margin deposits, with the direction of sediment transport toward the south. One thin sandstone layer contains abundant small clay rip-up clasts and a dwarf molluscan fauna, possibly reflecting a size-sorted assemblage. *Turritella* in several beds have a

northeast to southwest current orientation. The following fauna of Turonian aspect were found at this locality: *Turritella* cf. *hearni* (Anderson), *Pachycardium? ramondianum* Gabb, *Carycorbula* aff. *parilis* (Gabb), scaphopod.

19.2 Return to Hwy. 152 and turn right.

21.6 Stop for Hwy. 33; continue on Hwy. 152.

22.6 Turn right at Hilldale Ave.

23.1 **STOP 1-6** Here we see large blocks of conglomerate or breccia that have been excavated from the Mustang Shale member near the base of the Moreno Formation (Fig. 5, unit K_m). Bennison (unpublished mapping) has found that similar conglomeratic lenses crop out discontinuously at about this stratigraphic level from Romero Creek to south of Los Banos Creek. These lenses contain abundant angular limestone clasts that have been bored by bivalves

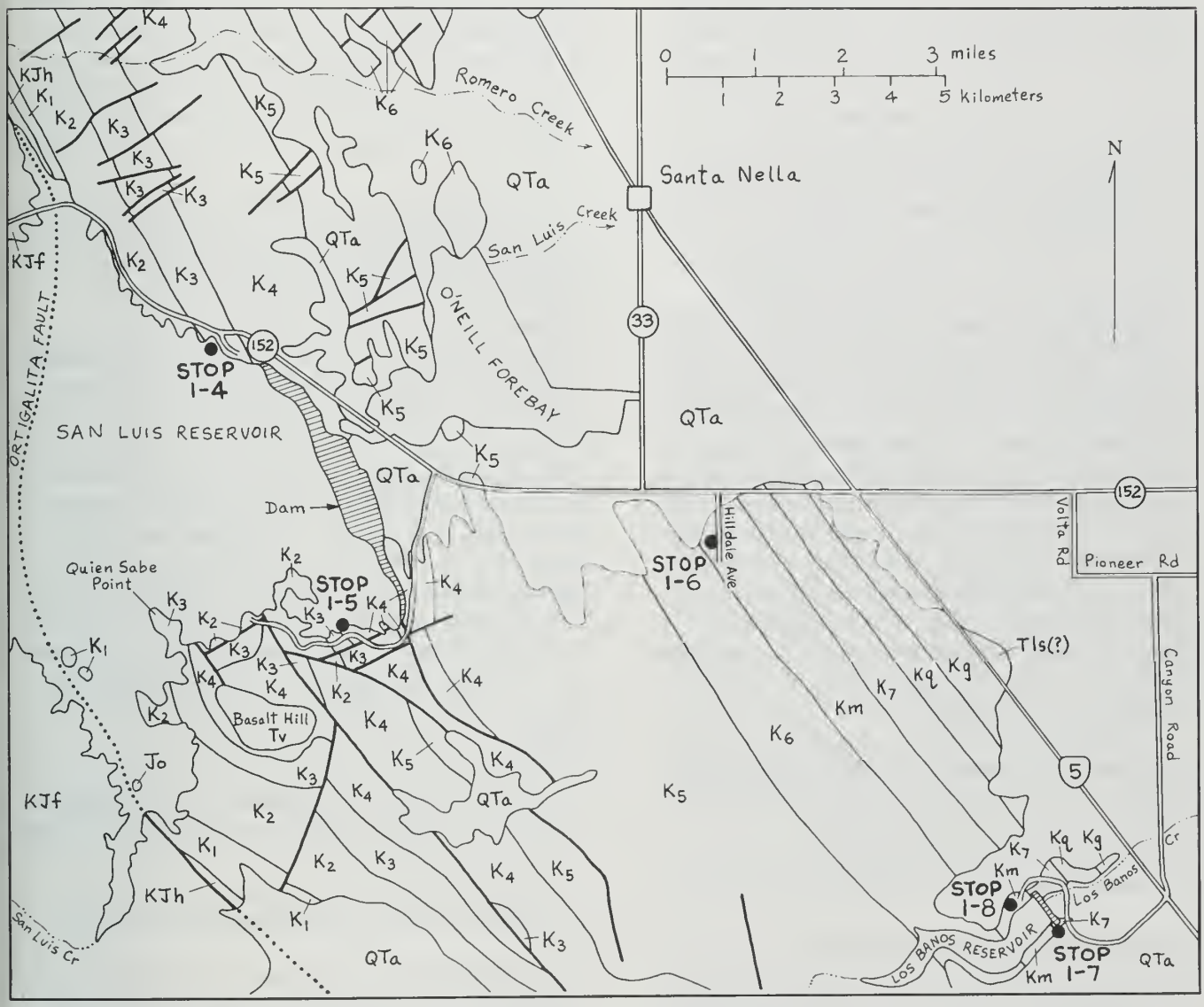

Figure 5. Simplified geologic map of eastern Diablo Range near San Luis and Los Banos reservoirs showing field trip Stops 1-4 to 1-8 in GVS. Geology from unpublished mapping of A.P. Bennison. Unit symbols are as follows: KJf, Franciscan Complex, undifferentiated; Jo, Coast Range ophiolite; KJh, Hawk shale of Schilling (1962); K_1-K_7, unnamed units of GVS (A.P. Bennison, unpublished mapping) that are equivalent to units 1-7 on Fig. 3. Units K_m, K_q, and K_g represent the Mustang shale, Quinto silt, and Garzas sand members of the Moreno Formation, respectively. Cenozoic units include: Tls, Paleocene Laguna Seca Formation; Tv, Miocene basalt; QTa, upper Cenozoic alluvial deposits. Sources of stratigraphic nomenclature are indicated in caption of Fig. 3.

from all directions and that contain inoceramid bivalve fragments and the lucinid bivalve *Thyasiracretacea* (Whiteaves). To the north at Romero Creek a similar conglomerate lens lies about 650 ft (200 m) upsection from a large bedded limestone lens. The latter contains a similar fauna, but with the addition of large *Solemya* bivalves and the late Campanian ammonite *Metaplacenticeras pacificum* Smith. The lucinid and solemyid bivalves are chemotrophic feeders characteristic of spring vent communities, suggesting that the limestone clasts and associated iron-rich nodules seen at this stop reflect submarine spring deposits.

23.6 Return to Hwy. 152 and turn right.

24.6 Here, on both sides of Hwy. 152, blocks of fossiliferous sandstone have been excavated from the basal Garzas sand member of the Moreno Formation. Bennison (unpublished mapping) correlates this bed with Payne's (1962) Dosados Sandstone, which is the basal member of the type Moreno Formation (Fig. 3). This correlation is based on molluscan fossils, including *Turritella chaneyi*, that are found in both units. Payne concluded that the Moreno Formation pinches out north of San Luis Reservoir owing to an erosional unconformity at the base of the overlying Paleocene Laguna Seca Formation. In contrast, A.S. Huey and A.P. Bennison have long maintained that the type Moreno Formation disappears northward through facies changes from shale to sandstone.

Continue on Hwy. 152.

27.5 Turn right (south) on Volta Rd., left (east) on Pioneer Rd., then right (south) on Canyon Rd. toward Los Banos Reservoir.

35.6 Turn left at Y intersection.

35.8 Turn left on dirt road and park.

36.0 **STOP 1-7** This stop provides a panoramic overview of the Los Banos Reservoir area. Buttresses for the dam consist of massive fossiliferous sandstone and conglomerate (Fig. 5, unit K_7). Bennison (unpublished mapping) correlates these deposits with Anderson's (1972) Brown Mountain Sandstone of the Coalinga area. The latter unit forms the uppermost part of the Panoche Formation near Coalinga, whereas the deposits here at Los Banos Reservoir are more reasonably assigned to the Moreno Formation. This difference reflects the diachronous nature of the Panoche-Moreno boundary (Figs. 2, 3).

Descend west along trail to observe one of the best fossil collecting localities in the Diablo Range. A sequence of stacked, thickening-upward deltaic distributary-mouth-bar deposits characterizes the section. Abundant molluscan fossils and hummocky cross-stratification in the upper parts of the thickening-upward megasequences indicate a shallow-water origin.

The conglomerate has yielded well-preserved mollusks that are housed at the California Academy of Sciences, University of California at Berkeley, and Stanford University. The more common species in this diverse early Maastrichtian fauna include: *Glycymeris (Glycymerita) banosensis* Anderson, *Cymbophora triangulata* (Waring), *Opis pacifica* (Anderson), *Calva* sp., *Ostrea* sp., and *Phasianella garzana* Anderson. The dominant fossil is *G. (Glycymerita) banosensis,* which is also known (A.P. Bennison, unpublished data) from pebbly calcareous sandstones about 1800 ft (550 m) stratigraphically below the Garzas sand between Quinto and Garzas Creeks (Fig. 3, unit 7; several miles north of Fig. 5). The Garzas sand also contains abundant large *Glycymeris*, but these are identified as *G. (Glycymerita)* aff. *veatchii major* Smith (Elder and Miller, 1990).

36.5 Return to intersection and turn left downhill to cross Los Banos Creek and continue on paved road past toll station.

37.8 Turn left downhill toward parking area.

38.0 **STOP 1-8** On the north side of Los Banos Reservoir we examine the basal mudstone unit of the Moreno Formation, which directly underlies the unit of fossiliferous sandstone and conglomerate that we studied at the preceding stop. This fine-grained unit consists predominantly of maroon or violet-gray to brown-gray

shaly mudstone. It was informally named the Mustang shale member by Bennison (cited in Bishop, 1970). Foraminifers belonging to Goudkoff's (1945) D zone are common throughout the unit. Bennison now favors establishing the stratotype for the Mustang shale member here at Los Banos Reservoir, where it is bounded below by a thick sandstone unit of the uppermost Panoche Formation (Figs. 3, 5). The Mustang shale typically is 1650-2000 ft (500-600 m) thick and probably correlates with the Ragged Valley Silt of the Coalinga district (Figs. 2, 3). *Inoceramus, Pachydiscus* and other molluscan species occur locally in the Mustang shale.

49.1 Return to Hwy. 152.

51.0 Turn right onto I-5.

55.6 Enter Santa Nella (end of Day 1).

ROAD LOG DAY 2

0.0 Leave Santa Nella on I-5 north.

26.6 Patterson exit. Take Del Puerto Canyon Rd. west. Geology and stops for today's field trip are shown on Fig. 6.

28.5 **STOP 2-1** Overview of upper part of GVS and overlying Tertiary rocks. Exposures of sandstone of Moreno Formation are visible on north side of canyon, behind windmill.

29.1 Large landslide disrupts Moreno Formation on north side of canyon. A.P. Bennison and others collected remains of a mosasaur here in 1937.

29.7 Contact between Moreno and Panoche Formations as mapped by previous workers.

30.0 **STOP 2-2** Outcrops of upper Panoche Formation on north side of road. Thin- to thick-bedded turbidites are of Facies B and E of Mutti and Ricci Lucchi (1972). Time-equivalent sand-rich submarine-fan deposits of the upper Lathrop sand form good reservoirs in the subsurface of the northern San Joaquin basin.

31.1 Shale in upper Panoche Formation (= Sacramento shale of the northern San Joaquin Valley). Foraminifers here are of mid-Campanian age and indicate bathyal water depths.

31.9 Shale unit, probably equivalent to Santonian Dobbins shale of the northern San Joaquin Valley (Fig. 2).

34.1 **STOP 2-3** Conglomerate of Panoche Formation cropping out in road cuts. One of us (Elder) recently found the Coniacian to Santonian ammonite (*Kossmaticeras* aff. *japonicum* Matsumoto) in pebbly sandstone here. Outcrop contains faults of several orientations, pebbly mudstone, and rounded pebble- to boulder-size clasts composed predominantly of silicic volcanic rocks. Lack of cross-stratification and absence of shallow-water fossils suggest a submarine canyon or inner-fan channel environment.

36.5 **STOP 2-4** Fault separating CRO and GVS. To east is shale containing Early Albian *Leconteites leconteii* (Anderson). To west is keratophyre and quartz kerotophyre (Del Puerto volcanics of Maddock, 1964). Kinematic indicators show down-to-the-east sense of offset (normal) along fault. At least 1000 ft (300 m) of Lotta Creek Tuff and about 500 ft (150 m) of Upper Jurassic-Lower Cretaceous Hawk shale have been removed along this fault. Previous workers (Maddock, 1964; Bartow and others, 1983) show this lower Albian shale to be disconformable(?) beneath strata of the Panoche Formation. An old USGS fossil locality near here is of Turonian age (Elder and Miller, 1990), which suggests that the top of the shale unit is also faulted.

Walk west along road to see keratophyre and quartz keratophyre sills with columnar joints.

36.9 Here is another normal(?) fault that drops the keratophyre down against intrusive gabbro and plagiogranite. A U-Pb date on plagiogranite near here of 154 ± 2 Ma (Hopson and others, 1981) is noticeably younger than the previously-mentioned K-Ar dates (161-163 Ma).

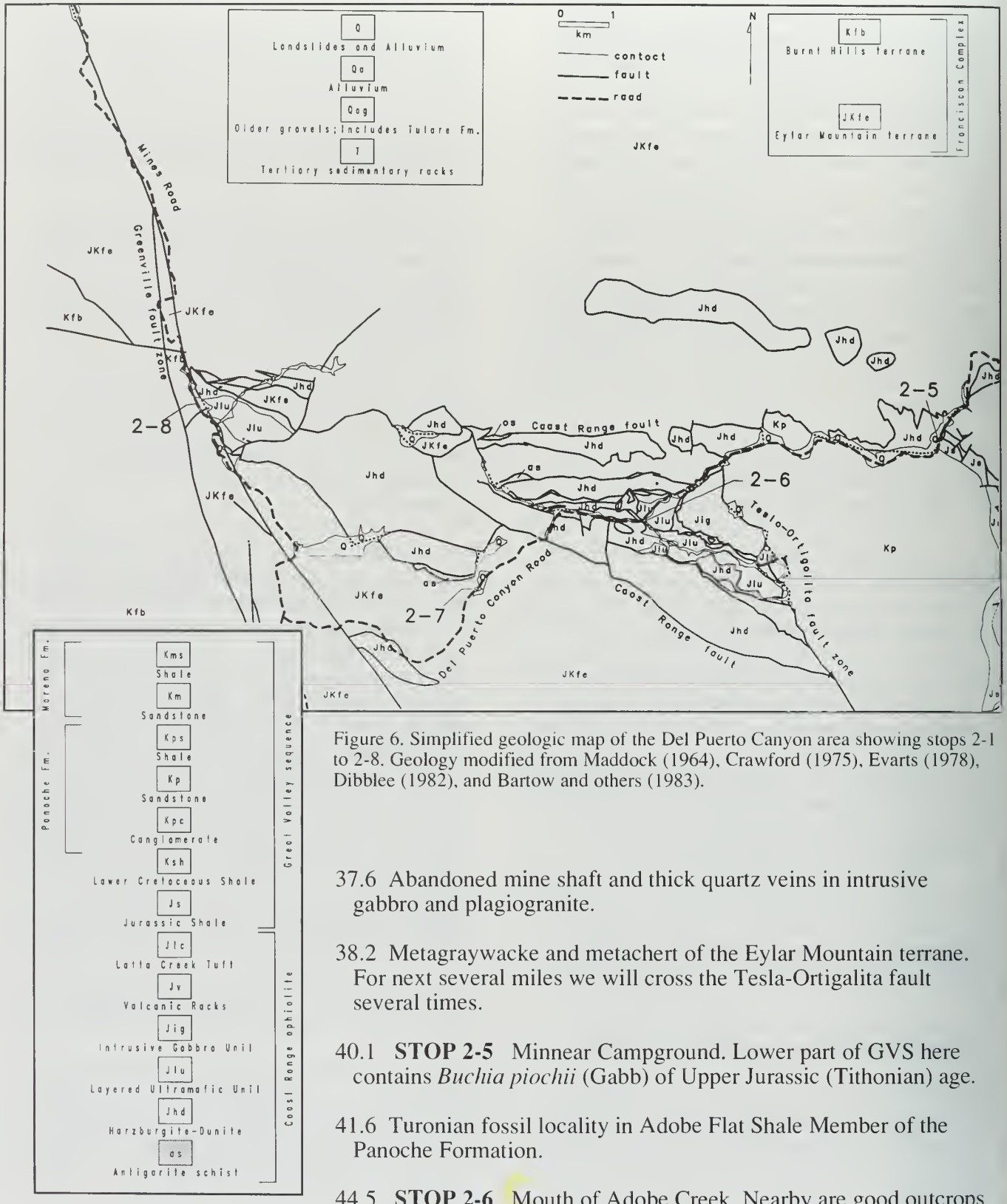

Figure 6. Simplified geologic map of the Del Puerto Canyon area showing stops 2-1 to 2-8. Geology modified from Maddock (1964), Crawford (1975), Evarts (1978), Dibblee (1982), and Bartow and others (1983).

37.6 Abandoned mine shaft and thick quartz veins in intrusive gabbro and plagiogranite.

38.2 Metagraywacke and metachert of the Eylar Mountain terrane. For next several miles we will cross the Tesla-Ortigalita fault several times.

40.1 **STOP 2-5** Minnear Campground. Lower part of GVS here contains *Buchia piochii* (Gabb) of Upper Jurassic (Tithonian) age.

41.6 Turonian fossil locality in Adobe Flat Shale Member of the Panoche Formation.

44.5 **STOP 2-6** Mouth of Adobe Creek. Nearby are good outcrops of wehrlite and dunite representing the layered ultramafic portion of CRO. Chromite was mined and milled here during World Wars I and II.

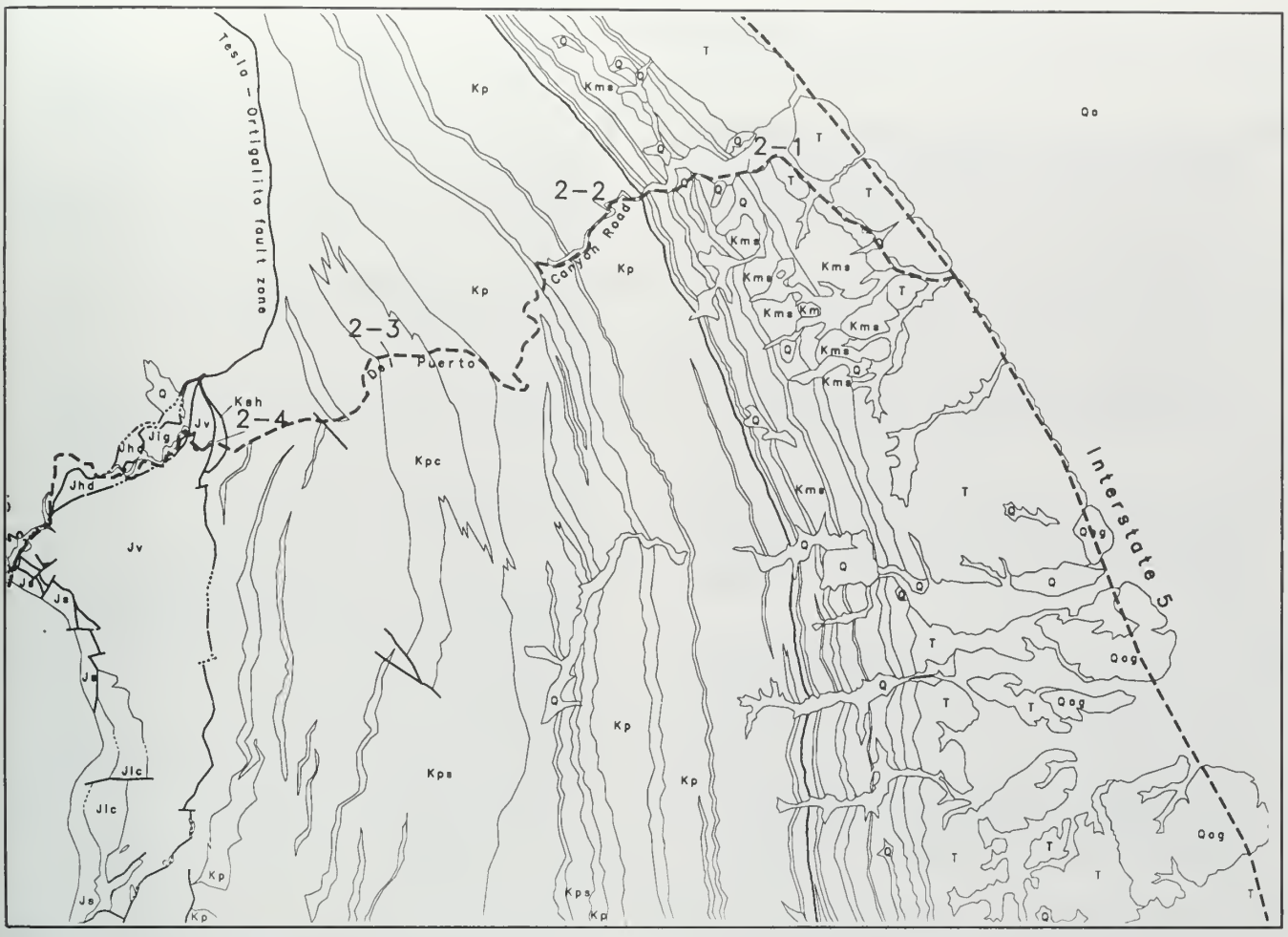

47.0 **STOP 2-7** Short hike to see Coast Range fault. Although many different faults with varying orientations form the present boundary between the Franciscan Complex and overlying CRO and GVS in the Del Puerto Canyon area, the most significant fault is preserved here. Eylar Mountain metagraywacke below the subhorizontal fault is textural zone (TZ) 1 or 2A (Jayko and Blake, 1989) and grades upward within 30 ft (10 m) to mylonite of TZ-2B+. The mylonitic metagraywacke contains the metamorphic mineral assemblage quartz-albite-lawsonite-jadeitic pyroxene-phengite and is believed to have formed under P-T conditions of 9-12 kb and 300-400°C (Harms and Dunlap, 1991). Overlying the metagraywacke is antigorite schist formed from serpentinized harzburgite of the CRO (Evarts, 1978) (Figure 6). Kinematic interpretation of the mylonites indicates predominantly eastward displacement of the overlying CRO, but includes top-to-the-west offset along a few short segments of the fault. These results are consistent with low-angle normal faulting along the Coast Range fault with at least 9-15 mi (14-24 km) of tectonic overburden removed by extension in order to account for the inferred metamorphic pressures.

47.6 Boundary between Stanislaus and Santa Clara counties.

50.4 Junction with Mines Rd. Proceed north toward Livermore.

53.0 **STOP 2-8** Outcrops of TZ-2A sandstone and mudstone of the Burnt Hills terrane.

Last stop of day. Continue on Mines Rd. to Livermore; then west to San Francisco on I-580 and Bay Bridge.

REFERENCES CITED

Almgren, A.A., 1986, Benthic foraminiferal zonation and correlations of Upper Cretaceous strata of the Great Valley of California—a modification, *in* Abbott, P.L., ed., *Cretaceous stratigraphy western North America*: Pacific Section, Society of Economic Paleontologists and Mineralogists, v. 46, p. 137-152.

Anderson, J.Q., 1972, Cretaceous subdivisions of the Coalinga District, Fresno County, California, *in Cretaceous of the Coalinga area*: Society of Economic Paleontologists and Mineralogists, Pacific Section, 1972 Fall Field Trip Guidebook, p. 11-18.

Bartow, J.A., Lettis, W.R., Sonneman, H.S., and Switzer, J.R., Jr., 1983, Geologic map of the east flank of the Diablo Range from Hospital Creek to Poverty Flat, San Joaquin, Stanislaus, and Merced counties, California: *U.S. Geological Survey Miscellaneous Investigations Map I-1656*, scale 1:62,500.

Bartow, J.A., and Nilsen, T.H., 1990, Review of the Great Valley sequence, eastern Diablo Range and northern San Joaquin Valley, central California: *in* Kuespert, J.G., and Reid, S.A., eds., *Structure, stratigraphy and hydrocarbon occurrences of the San Joaquin Basin, California*: Pacific Sections, Society of Economic Paleontologists and Mineralogists and American Association of Petroleum Geologists, p. 253-265.

Berry, K.D., 1974, *Mesozoic foraminiferal zonation, Turonian to Tithonian stages, Pacific Coast Province:* Society of Economic Paleontologists and Mineralogists, Pacific Section, Annual Meeting, April, 1974, San Diego, CA, Preprints, p. 1-29.

Bishop, C.C., 1970, Upper Cretaceous stratigraphy on the west side of the northern San Joaquin Valley, Stanislaus and San Joaquin counties, California: *California Division of Mines and Geology Special Report 104*, 29p.

Blake, M.C., Jr., 1981, Geologic transect of the northern Diablo Range, California, *in* Frizzell, Virgil, ed., *Upper Mesozoic Franciscan rocks and Great Valley sequence, central Coast Ranges, California*: Pacific Section, Society of Economic Paleontologists and Mineralogists, Annual Meeting Guidebook, San Francisco, 1981, p. 35-43.

Blake, M.C., Jr., Fisher, G.R., Sorg, D.H., Murchey, B.L., and Elder, W.P., 1990, Complex metamorphic and structural history of two Franciscan terranes in the northern Diablo Range, California (abs.): *Geological Society of America Abstracts with Programs*, v. 22, no. 3, p. 8.

Blake, M.C., Jr., and Showalter, P.K., 1991, Preliminary tectonic synthesis of the northern Diablo Range, California (abs.): *Geological Society of America Abstracts with Programs*, Cordilleran Section meeting (in press).

Briggs, L.I., Jr., 1953, Geology of the Ortigalita Peak quadrangle, California: *California Division of Mines and Geology Bulletin 167*, 61p.

Cherven, V.B. and Fischer, J.F., 1984, *Latest Cretaceous and early Tertiary depositional systems of the northern Diablo Range, California, in* Pacific Section, Society of Economic Paleontologists and Mineralogists Field Trip Guidebook no. 2, 1984 mid-year meeting, San Jose, California, p. 31-72.

Cotton, W.R., 1972, Preliminary geologic map of the Franciscan rocks in the central part of the Diablo Range, Santa Clara and Alameda counties, California: *U.S. Geological Survey Miscellaneous Investigations Map I-343*, scale 1:62,500.

Cowan, D.S., 1974, Deformation and metamorphism of the Franciscan subduction zone complex northwest of Pacheco Pass, California: *Geological Society of America Bulletin*, v. 85, p. 1623-1634.

Cox, B.F., and Seiders, V.M., 1991, Paleogeographic significance of conglomerate clast assemblages in the Great Valley sequence, central California (abs.): *Geological Society of America Abstracts with Programs*, Cordilleran Section meeting (in press).

Crawford, K.E., 1975, *The geology of the Franciscan tectonic assemblage near Mt. Hamilton, California*: Unpublished Ph.D. dissertation, University of California, Los Angeles, 137p.

Crawford, K.E., 1976, Reconnaisance geologic map of the Eylar Mountain quadrangle, Santa Clara and Alameda counties, California: *U.S. Geological Survey Miscellaneous Field Studies Map MF-764*, scale 1:24,000.

Dibblee, T.W., Jr., 1982, Preliminary geologic map of the Patterson quadrangle, Stanislaus County, California: *U.S. Geological Survey Open-File Report 82-394*.

Edmonson, W.F., Callaway, D.C., Hoffman, R.D., and Teitsworth, R.A., 1964, Stratigraphic units of northern San Joaquin Valley and southern Sacramento Valley: *San Joaquin Geological Society Selected Papers*, v. 2, p. 4.

Elder, W.P., and Miller, J.W., 1990, Checklists of Jurassic and Cretaceous macrofauna from U.S. Geological Survey collections within the San Jose 1:100,000 map sheet, California: *U.S. Geological Survey Open-File Report 90-534*.

Ernst, W.G., 1987, Jadeitized Franciscan metamorphic rocks of the Pacheco Pass-San Luis Reservoir area, central California Coast Ranges, *in* Hill, M.L., ed., *Cordilleran Section of the Geological Society of America Centennial Field Guide Volume 1*, p. 245-250.

Ernst, W.G., Seki, Y., Onuki, H., and Gilbert, M.C., 1970, Comparative study of low-grade metamorphism in the California Coast Ranges and the outer metamorphic belt of Japan: *Geological Society of America Memoir 124*, 276p.

Evarts, R.C., 1977, The geology and petrology of the Del Puerto ophiolite, Diablo Range, central California Coast Ranges, *in* Coleman, R.G., and Irwin, W.P., eds., North American ophiolites: *Oregon Department of Geology and Mineral Industries Bulletin 95*, p. 121-140.

Evarts, R.C., 1978, *The Del Puerto ophiolite complex, California: A structural and petrologic investigation*: Ph.D. dissertation, Stanford University, Stanford, CA, 409p.

Goudkoff, P.P., 1945, Stratigraphic relations of Upper Cretaceous in Great Valley, California: *American Association of Petroleum Geologists Bulletin*, v. 29, p. 956-1007.

Harms, T.A., Jayko, A.S., and Blake, M.C., Jr., 1987, Kinematic evidence of extensional unroofing of the Franciscan Complex along the Coast Range fault, northern Diablo Range, California (abs.): *Geological Society of America Abstracts with Programs*, v. 19, no. 7, p. 694.

Harms, T.A., and Dunlap, C.E., 1991, Extensional faulting along the base of the Coast Range ophiolite at the Del Puerto outlier, northern Diablo Range, California (abs.): *Geological Society of America Abstracts with Programs*, Cordilleran Section (in press).

Hopson, C.A., Mattinson, J.M., and Pessagno, E.A., Jr., 1981, Coast Range ophiolite, western California, *in* Ernst, W.G., ed., *The geotectonic development of California, Rubey Volume 1*: Englewood Cliffs, N.J., Prentice Hall, p. 418-510.

Jacobson, M.I., 1978, Petrologic variations in Franciscan sandstone from the Diablo Range, California, *in* Howell, D.G., and McDougall, K.A., eds., *Mesozoic paleogeography of the western United States:* Pacific Section, Society of Economic Paleontologists and Mineralogists, Pacific Coast Paleogeography Symposium 2, p. 401-417.

Jayko, A.S., and Blake, M.C. Jr., 1989, Deformation of the eastern Franciscan belt, northern California: *Journal of Structural Geology*, v. 11, p. 375-390.

Jayko, A.S., Blake, M.C. Jr., and Harms, Tekla, 1987, Attenuation of the Coast Range ophiolite by extensional faulting and nature of the Coast Range "thrust," California: *Tectonics*, v. 6, p. 475-488.

Lanphere, M.A., 1971, Age of the Mesozoic oceanic crust in the California Coast Ranges: *Geological Society of America Bulletin*, v. 82, p. 3209-3212.

Maddock, M.E., 1964, Geology of the Mt. Boardman quadrangle, Santa Clara and Stanislaus counties, California: *California Division of Mines and Geology Map Sheet 3*, scale 1: 62,500.

Maruyama, S., Liou, J.G., and Sasakura, Y., 1985, Low-temperature recrystallization of Franciscan graywackes from Pacheco Pass, California: *Mineralogical Magazine*, v. 49, p. 345-355.

Mattinson, J.M., and Echeverria, L.M., 1980, Ortigalita Peak gabbro, Franciscan complex: U-Pb date of intrusion and high-pressure-low temperature metamorphism: *Geology*, v. 8, p. 589-593.

Morrell, R.P., 1978, *Geology and mineral paragenesis of Franciscan metagraywacke near Paradise Flat, northwest of Pacheco Pass, California*: Unpublished MS thesis, Stanford University, Stanford, CA, 73p.

Mutti, E., and Ricci Lucchi, F., 1972, *Le torbiditi dell' - Appennir settentrionale: introduzione all'analisi di facies. Memoria della Societá Geologica Italiana, VII*, p. 161-199; English translation, by T.H. Nilsen, 1978, International Geologic Review, v. 20, p. 125-166, *AGI Reprint Series 3*.

Payne, M.B., 1951, Type Moreno Formation and overlying Eocene strata on the west side of the San Joaquin Valley, Fresno and Merced counties, California: *California Division of Mines and Geology Special Report 9*, 29p.

Payne, M.B , 1960, *Type Panoche, Panoche Hills area, Fresno County, California*: Pacific Section, Society of Economic Paleontologists and Mineralogists Spring Field Trip 1960 Guidebook, p. 1-12.

Payne, M.B., 1962, Type Panoche Group (Upper Cretaceous) and overlying Moreno and Tertiary strata on the west side of the San Joaquin Valley, *in* Bowen, O.E., ed., Geologic guide to the gas and oil fields of northern California: *California Division of Mines and Geology Special Bulletin 181*, p. 165-175.

Platt, J.P., 1986, Dynamics of orogenic wedges and the uplift of high-pressure metamorphic rocks: *Geological Society of America Bulletin*, v. 81, p. 1037-1053.

Schilling, F.A., Jr., 1962, The Upper Cretaceous stratigraphy of the Pacheco Pass quadrangle, California: Ph.D. dissertation, Stanford University, Stanford, CA, 153p.

Seki, Y., Ernst, W.G., and Onuki, H., 1969, *Phase proportions and physical properties of minerals and rocks from the Franciscan and Sanbagawa metamorphic terranes*, a supplement to Geological Society of America Memoir No. 124: Japan Society for Promotion of Science, Tokyo, Japan, 85p.

Suppe, J., and Armstrong, R.L., 1972, Potassium-argon dating of Franciscan metamorphic rocks: *American Journal of Science*, v. 272, p. 217-233.

Wentworth, C.M., and Zoback, M.D., 1990, Structure of the Coalinga area and thrust origin of the earthquake, *in* Rymer, M.J., and Ellsworth, W.L., eds., The Coalinga, California, earthquake of May 2, 1983: *U.S. Geological Survey Professional Paper 1487*, p. 41-68.

Jadeitized metagraywacke near Stop 1-2, Pacheco Pass, California. *Photo by Edgar Bailey.*

Sutter Buttes Field Trip Guide

Brian P. Hausback[1] and Tor H. Nilsen[2]

INTRODUCTION

The Sutter Buttes form a strangely isolated knobby extrusive center in the middle of the Sacramento Valley, 6 mi (10 km) northwest of Yuba City (Fig. 1). Geologist, traveler, rancher, and Indian alike have pondered the significance of this enigmatic topographic blemish.

This is a guide to the igneous, sedimentary, and structural framework of the Sutter Buttes volcano. Field trip stops include exposures of Mesozoic and Tertiary sedimentary rocks of the Sacramento basin as well as of the igneous and fragmental deposits produced during Quaternary magmatism. We will attempt to summarize many of these aspects of the Buttes during the field trip. We also refer you to Anderson (1983) for a short summary of the geologic evolution of the Sutter Buttes area.

The **Sutter Buttes are entirely under private ownership and permission must be obtained before entering any land.** Entrance can be obtained through two organizations that offer guided walks into the Buttes: the Middle Mountain Foundation (Phone: 916-343-6614) and the West Butte Sanctuary Co. (Phone: 916-668-1913).

PREVIOUS WORK

Williams (1929) described the Sutter Buttes as a deeply dissected huge central laccolithic intrusion with attendant extrusions. This work was reinterpreted by Williams and Curtis (1977) as a complex of smaller extrusive and intrusive domes. The domes pushed up and erupted through the surrounding pre-volcanic Sacramento basin sedimentary section and resulted in a surrounding volcaniclastic apron. Geologic maps of the Sutter Buttes have been published by Lindgren and Turner (1895), Williams (1929), Johnson (1943), Garrison (1962b), and Williams and Curtis (1977) (Fig. 2).

GEOLOGIC OVERVIEW

Williams and Curtis (1977) gave prosaic names to the important geologic features of the Sutter Buttes. The circular Sutter Buttes were formed during the early Pleistocene by piercement intrusions and extrusions of rhyolite and andesite. The central mass of spiny domes was called the Castellated Core. Previously deposited Upper Cretaceous, Eocene, and Miocene to Pliocene strata were warped, folded, and faulted by the intrusions and form a lowland circular ring of outcrops, called the Moat, that flanks the volcanic core of the Buttes. Tuff and breccia, largely reworked by fluvial processes, form the Rampart outer ring that slopes away from the volcanic center and overlaps the uparched Moat sedimentary rocks.

REGIONAL STRATIGRAPHY

Pre-volcanic sedimentary rocks of the Sacramento basin are exposed in the Moat of the Sutter Buttes and have been divided in various ways by different workers, resulting in some major differences in age and formation assignments.

Cretaceous Depositional Systems: The oldest strata exposed are generally fine-grained and have been assigned to the Forbes Formation ("Forbes Shale"); overlying beds of sandstone are the Kione Formation ("Kione Sands," "Kione Sand," or "white sand marker bed") (Johnson, 1943; Thamer, 1961; Garrison, 1962a (Fig. 3); Williams

[1] Geology Department, California State University, Sacramento, CA 95819
[2] 133 Madera Ave., San Carlos, CA 94070

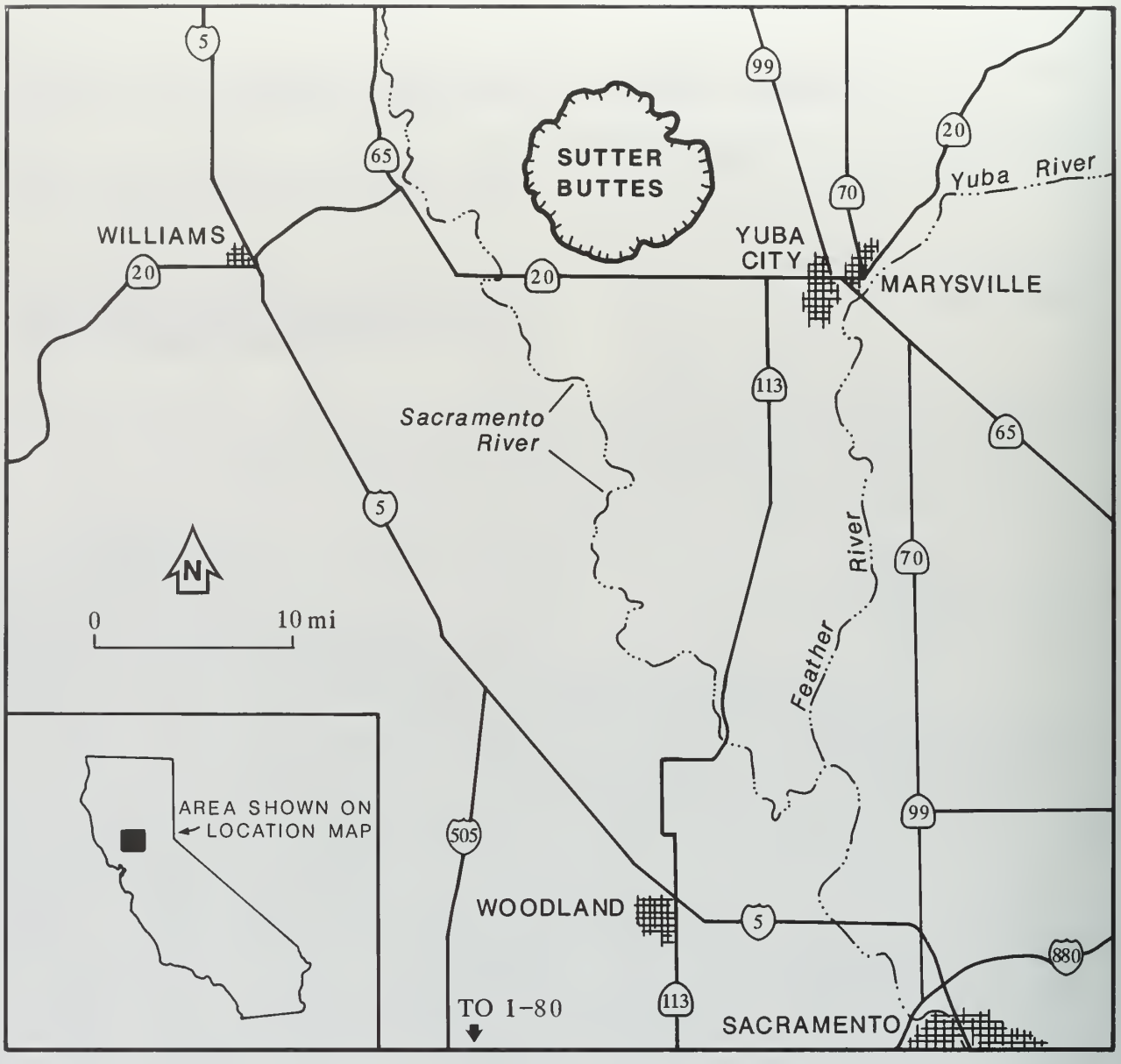

Figure 1. Map of the central Sacramento basin showing location of the Sutter Buttes and related outcrop areas.

and Curtis, 1977). Nilsen (1990) provides a summary of the subsurface geology of the Upper Cretaceous units, and Nilsen and Imperato (1990) prepared a field guide to these units around the margins of the Sacramento valley.

Because previous geologic maps generally emphasized the geology of Tertiary volcanic and plutonic units, the exact distribution of the Forbes and Kione formations in the Buttes area remains unclear. The structural framework of the Upper Cretaceous units in and near the Sutter Buttes area is also very complex. Strata adjacent to the piercement intrusions are vertical to overturned and complexly faulted. Quaternary units that dip radially away from the Buttes have covered important flanking folds and faults.

The Forbes and Kione formations crop out along the western, southern, and eastern flanks of the Sutter Buttes. Because outcrops on the western and eastern flanks are largely covered by landslides or are involved in landsliding, much of the stratigraphic emphasis here is on the southern flank. The Forbes Formation in subsurface is reportedly underlain by a thick shale unit, the Funks Shale, which rests conformably on granitic basement rocks; although the Funks does not crop

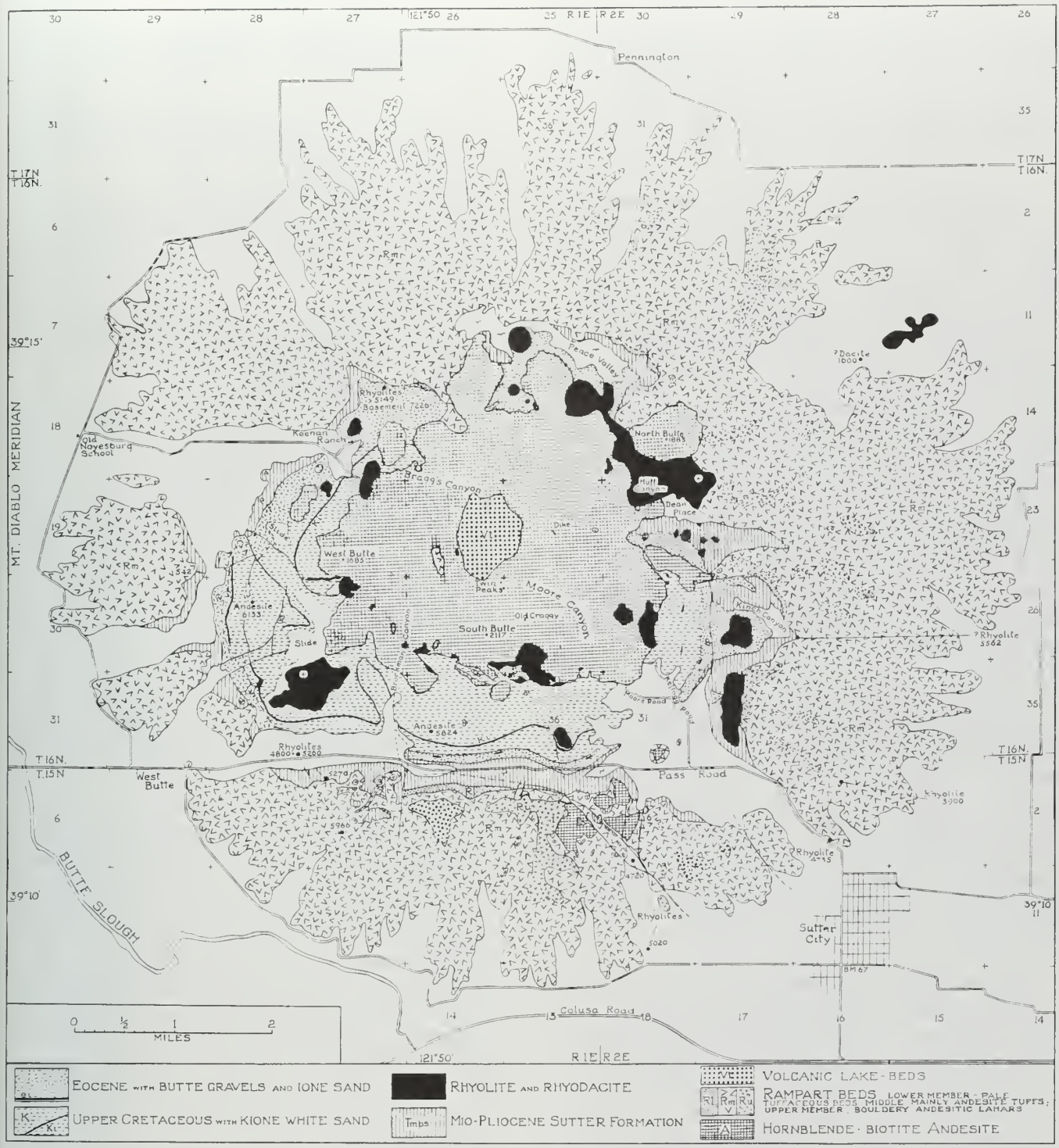

Figure 2. Geologic map of the Sutter Buttes area (Williams and Curtis, 1977).

out in the Buttes area, it does crop out to the west in the Coast Ranges. Neither the Dobbins Shale Member of the Forbes Formation nor the Guinda Formation, which overlie the Funks Formation in the Coast Ranges to the west, have been recognized in the Sutter Buttes area.

Because the base of the Forbes Formation cannot be observed in outcrop, its true stratigraphic thickness is not known. Johnson (1943) indicated a maximum exposed thickness of 2750-4350 ft (840-1325 m) for the Forbes Formation on the south flank of the Buttes, and Garrison (1962a) proposed a thickness of 2700-4000 ft (823-1220 m). The basal exposed part of the Forbes Formation generally consists of baked shale, hardened and resistant from contact with volcanic necks. Most of the directly overlying strata that are less resistant do not crop out well and are subject to massive slope failures. Field mapping and hiking along ridges that appear not to have failed suggests that most of the Forbes Formation consists of shale; although this shale is rarely exposed, it does appear to underlie smooth, grass-covered slopes in much of the area.

Contrary to most published descriptions of the Forbes Formation which describe it as massive shale, it contains prominent conglomerate and sandstone units within its upper part. These beds appear to consist of laterally discontinuous bundles of coarse-grained strata that crop out locally but do not form laterally continuous ridges such as those within the overlying Kione and Ione formations. Only a few of the coarse-grained beds are well exposed.

The bundles of conglomerate and sandstone are about 10-40 ft (3-12 m) thick, and generally form sequences that appear to fine and thin upward. The conglomerate contains a variety of lithic clasts, most commonly fine-grained metavolcanic clasts that are as large as 1 in (2.5 cm) in diameter. Rip-up clasts of shale and clasts of ferruginous concretions are also present in these beds. Scattered carbonaceous fragments are present along some bedding surfaces, and abraded molluscan fragments have been observed locally.

The bundles of conglomerate and sandstone in the Forbes Formation are generally massive to parallel-stratified and do not contain cross-

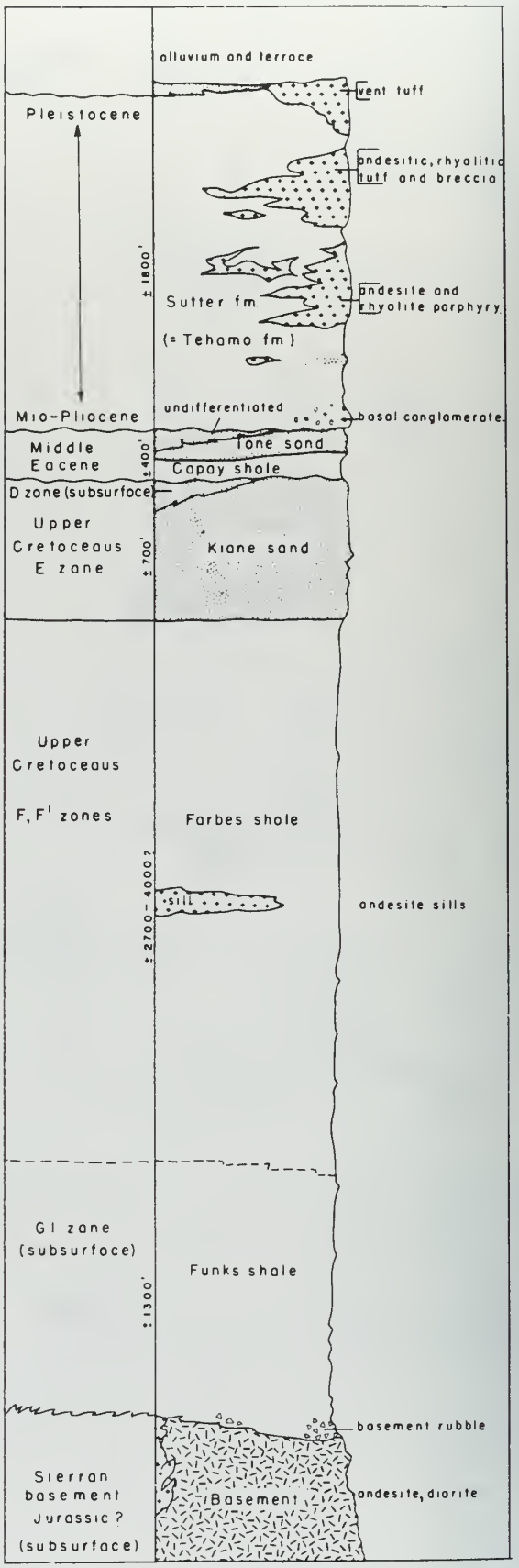

Figure 3. Generalized stratigraphic column for the Sutter Buttes area (from Garrison, 1962a).

bedding, *in situ* molluscan fossils, or other features indicative of shallow-marine conditions. However, upsection toward the base of the overlying Kione Formation, hummocky cross-stratification in the uppermost bundles of conglomerate and sandstone can be observed. This feature forms broad, wavy stratification in fine- to medium-grained sandstone, and is interbedded with bioturbated fine-grained sandstone and mudstone containing molluscan fossils. The upper part of the Forbes Formation in the Sutter Buttes area was probably deposited in shoaling conditions by redeposition of sands from storm waves.

The overlying Kione Formation has many features characteristic of deposition in a complex of deltaic, fluvial, and shallow-marine environments. It locally contains abundant molluscan fossils, particularly oyster fragments, cross-stratified conglomerate and sandstone, plant fossils, rip-up clasts of shale and ferruginous concretions, and lithic pebbles as large as 1 in (2.5 cm) in diameter. A few measurements of clast imbrication and cross bedding suggest sediment transport generally toward the west and south. Outcrops of the conglomerate and sandstone of the Kione Formation are more abundant and closely spaced, suggesting that there is less interbedded shale than in the Forbes Formation.

Tertiary Depositional Systems: Eocene strata of the Capay Formation ("Capay Shale") and the Ione Formation (Ione "sand") unconformably overlie the Cretaceous units. The Capay Formation is about 250 ft (76 m) thick in most of the area but may be as thick as 400 ft (122 m) on the western flank of the Buttes. It consists chiefly of greenish-gray shale and claystone with interbedded buff-colored sandstone that is locally rich in ferruginous concretions. Glauconite is common, and carbonaceous layers are reported by Williams and Curtis (1977) from the northern and eastern flanks of the Buttes. Abundant benthic foraminifers and ostracodes indicate a Penutian (early Eocene) to Ulatisian (early middle Eocene) age and deposition in generally shallow-marine conditions (Stipp, 1926; Merriam and Turner, 1937; Israelsky, 1940; Marianos and Valentine, 1958; Olson, 1961).

The overlying Ione Formation is approximately 150 ft (46 m) thick (Thamer, 1961; Garrison, 1962a) and consists chiefly of friable, white-weathering, quartzose sandstone of middle Eocene age. The Ione Formation is regionally as thick as 900 ft (275 m), crops out along the west flank of the Sierra Nevada, and consists of deltaic, lagoonal, and fluviatile deposits (Creely, 1965; Gillam, 1974). Its lower member rests on a deeply weathered lateritic surface and consists of quartzose and anauxitic sandstone, claystone, and local coals.

The Ione Formation grades laterally southward and eastward into the Domengine Formation, a shelf sandstone widespread in the Sacramento basin, that records westward progradation of a tide- and wave-dominated deltaic system (Bodden, 1983; Cherven, 1983). Williams and Curtis (1977) report the presence of anauxite in quartzose sandstone of the Ione Formation, and noted the presence of numerous conglomeratic layers within and above the Ione Formation that they assign to the Butte Gravels; they also reported Eocene megafossils from a prominent conglomeratic bed 700 ft (215 m) above the top of the Kione Formation on the south flank of the Buttes. Williams and Curtis (1977, p. 12) indicate a maximum thickness of about 1200 ft (365 m) for the Butte Gravels, whereas previous workers assigned much of this sequence to the Sutter Formation (Thamer, 1961; Garrison, 1962a).

The Eocene deposits are overlain by the nonmarine Sutter Formation (Dickerson, 1913), which consists chiefly of fine-grained sandstone, siltstone, tuff, and minor amounts of gravel. A prominent conglomerate forms the base of the unit. The stratigraphy and age assignments of the Sutter Formation have been particularly complex and varied. Williams and Curtis (1977, p. 13-14) concluded that the Sutter Formation ranged in age from Oligocene to Pliocene and that it generally rested conformably on Eocene strata, although locally the contact was unconformable. Most other workers have equated the Sutter Formation or Sutter "beds" with the Tehama Formation, a widespread Miocene, Pliocene, and Pleistocene unit in the Sacramento basin (Thamer, 1961; Garrison, 1962a). Williams and Curtis (1977) argue that the Sutter Formation was derived from the Sierra Nevada rather than the Coast Ranges and Cascade Range, the chief source area for the Tehama Formation. They also contend that the

Sutter Formation is 600-1000 ft (183-305 m) thick in the Sutter Buttes area, rather than the 1800 ft (550 m) proposed by other workers.

VOLCANIC GEOLOGY

Williams and Curtis (1977) divided the magmatic episode at the Sutter Buttes into a prevolcanic period of intrusion, uplift and erosion, followed by a period of volcanic dome extrusion with attendant explosive eruptions. The following discussion summarizes and adds to their account.

The magmatic episode appears to have occurred in Early to Middle Pleistocene. Williams and Curtis report K-Ar dates ranging from 2.4 to 1.4 Ma for the volcanic activity. However, more recent $^{40}Ar/^{39}Ar$ dating (Hausback and others, 1990) on single crystals of sanidine extracted from the oldest erupted volcanic deposits at the Sutter Buttes indicates that volcanism began about 1.59 Ma. Dated samples were derived from a rhyolite pyroclastic breccia in the lower Rampart beds on the south side of Pass Rd. in the Sutter Buttes. These beds directly overlie the prevolcanic Sutter Formation and record the earliest, explosive eruptions at the Sutter Buttes volcano. These new dates are approximately 0.8 my younger than the previously reported K-Ar date from this same site (Hausback and others, 1990).

Although the upper age limit of volcanism has not yet been determined, preliminary $^{40}Ar/^{39}Ar$ results from biotite crystals derived from several of the volcanic domes from the core of the Sutter Buttes yield ages from 1.56 to 1.36 Ma.

Prevolcanic Intrusion: Necks of Sutter Buttes magmas began intruding some time before the initial volcanic ejections. These initial intrusions were largely rhyolitic and caused substantial tilting and uplift of the pre-volcanic Cretaceous through Tertiary section. The Rampart volcaniclastic beds lie unconformably atop the tilted Moat section, suggesting that substantial deformation and erosional stripping of the pre-volcanic Cretaceous and Tertiary section had already taken place before volcanic eruptions began.

***Volcanic Episode*:** Intrusion and uplift continued as volcanic eruptions began, resulting in further deformation of the Moat rocks. Williams and Curtis (1977, p. 37) state, "No other volcanic region that we know of exhibits stronger or more extensive deformation of overlying beds by rising magmas than can be seen in the Sutter Buttes."

Extrusives at the Sutter Buttes range from 55-71 percent SiO_2 (mafic andesite to rhyolite), all of which form viscous domes with the exception of some tabular lavas that erupted at a satellite vent in the southeast sector of the Buttes. The silicic domes are biotite rhyolites and hornblende-biotite rhyodacites, which form a discontinuous outer ring of the Castellated Core. This distribution is probably structurally controlled by a circular fracture network formed during the prevolcanic intrusion and uplift. The crude circular vent distribution of the rhyolites is concentric with an outer network of arcuate high-angle reverse faults that underlie the Moat and Rampart along the north, east, and south sides of the Buttes (Williams and Curtis, 1977; Harwood and Helley, 1987). These faults may be the result of central uplift and domal flexure caused by multiple injection of intrusive necks into the central Sutter Buttes area before any magmas had reached the surface. Later, andesite domes invaded and extruded into the interior of the ring of rhyolite domes, forming the high, spiny peaks so characteristic of the core of the Sutter Buttes (Fig. 4).

Fragmental deposits were continually shed from the growing assemblage of volcanic domes.

Figure 4. View of the Sutter Buttes from near Williams, 20 mi (32 km) to the west (Williams, 1929).

Volcanic activity at the Sutter Buttes coincides with the Nebraskan glacial period (1.6-1.3 Ma, Chorley and others, 1984). Eruptions during this wet climatic period may explain the thorough reworking of the pyroclastics of the Rampart and central lacustrine deposits (mentioned below). Early silicic eruptions gave rise to rhyolite tuffs and lithic breccias deposited unconformably on the Sutter Formation as the lower Rampart. These fragmental rhyolite deposits were also locally tilted as the extrusive domes continued to rise. Andesite eruptions followed and, in part, may have been contemporaneous with rhyolitic extrusions. Resultant andesitic middle Rampart deposits overlie, locally in distinct angular unconformity, the lower Rampart. The final stage of deposition consisted of coarse blocky andesite diamicts of the upper Rampart. These units were deposited as both lahars and pyroclastic flows probably derived by dome collapse. The upper Rampart deposits record the final stages of volcanism; hence, they show little or no deformation from dome intrusion and form the gently inclined slopes, so characteristic of the Rampart apron.

In the center of the Castellated Core of andesite domes is a small oval-shaped deposit of lacustrine beds. These sediments were deposited in a deep crater lake during the explosive eruption phase of volcanism and have since been intruded and deformed by the surrounding andesite domes. The lakebeds form a 1000-ft (305-m) thick section of reworked lapilli tuff and tuff breccia deposited as a sequence of turbidites (Zaffran, 1988).

FIELD TRIP LOG - DAY ONE

Leave San Francisco by taking Hwy. 101 north over the Golden Gate Bridge. Connect with Hwy. 37 and east to Vallejo. Take I-80 northeast to just beyond Vacaville and then north on I-505 to I-5. As you approach I-5 you should have a nice view of the Sutter Buttes on a reasonably clear day. Go north on I-5 for 24 mi, passing through the towns of Dunnigan, Arbuckle, and Williams. On the north side of Williams take the Hwy. 20 exit east towards Colusa. Set your odometer at the exit; the following mileage is in cumulative miles.

2.5 Photo opportunity. Pull off on right shoulder of road.

8.7 Turn right at the stop sign and continue on Hwy. 20.

9.4 Turn left on Bridge St. at "T" intersection; cross bridge over the Sacramento River.

9.7 Turn right on Butte Slough Rd., immediately past bridge.

15.3 Turn left onto Pass Rd. at the stop sign.

18.4 Pass roadcut in the Rampart beds.

21.4 Park on the right near steel corral. Both hikes for Stop 1 begin here.

Please do not trespass on any of the private lands of the Sutter Buttes without prior permission from the owners!!!!

STOP 1 - SOUTH MOAT AREA (Fig. 5)

Hike A - northward into the south flank of Sutter Buttes adjacent to South Butte. The traverse begins on Quaternary alluvial fan deposits and progresses downsection through the Ione, Capay, Kione, and Forbes formations. The walk is approximately 2 mi (3.2 km), from an elevation of about 270 ft (82 m) to about 750 ft (230 m), and takes about 2-3 hrs to view the entire sequence. On the return, walk upsection from the Forbes Formation to the Ione Formation, to observe bundles of conglomerate and sandstone within the Forbes Formation, which are best exposed on the south-trending ridge in the center of section 35, T.16N., R.1E., Sutter Buttes 7.5 minute quadrangle.

The section is generally steeply dipping to overturned; beds closest to the intrusive rocks are overturned toward the south, whereas strata farther to the south, adjacent to Pass Rd., dip steeply southward away from the Buttes. Several outlying intrusive bodies in sections 33, 34, 35, and 36 underlie hills to the south of South Butte and have complicated the regionally simple arcuate structure of the Cretaceous and Tertiary strata. On the traverse, you will see representative

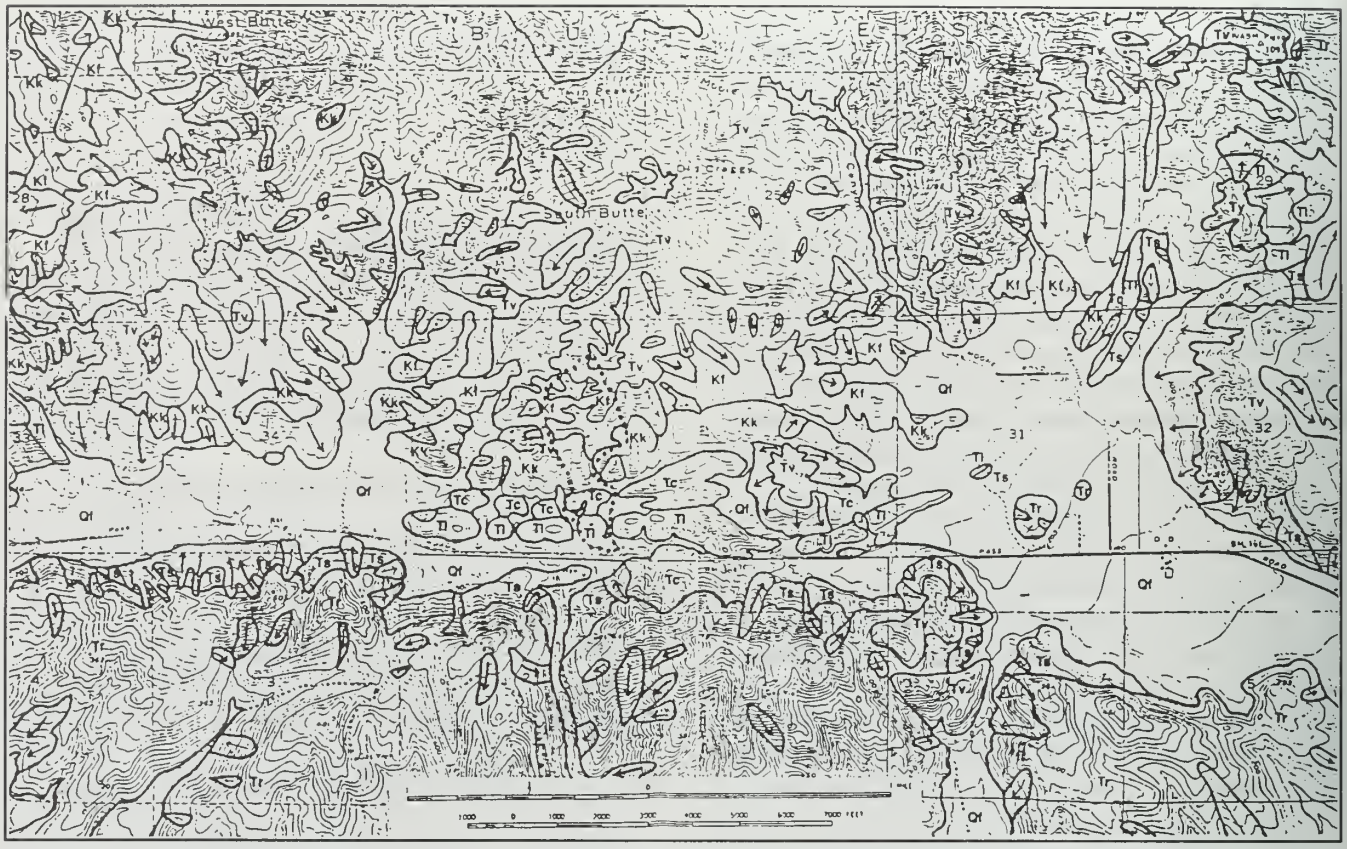

Figure 5. Simplified geologic map of the area of Stop 1 of the Sutter Buttes field trip (modified from Thamer, 1961; Garrison, 1962b; Williams and Curtis, 1977; Nilsen and Imperato, 1990).

outcrops of each Cretaceous and lower Tertiary unit exposed in the Sutter Buttes.

Hike B - on the other side of Pass Rd. Hike to the south of Pass Rd. through exposures of the Sutter Formation, lower Rampart, and middle Rampart. The hike takes approximately 1-2 hrs and is over gently inclined terrain. The Sutter Formation is composed of tan tuffaceous siltstones and sandstones that are steeply dipping to the south. The unit displays cross bedding and channel cut-and-fill structures. Locally, the Sutter contains pebble conglomerate lenses and layers up to 16 ft (5 m) thick; clasts are composed of well-rounded, hard, metamorphic lithologies. The dip of the sequence shallows upsection away from Pass Rd. The contact with the lower Rampart is not exposed here. The lower Rampart is composed of bedded biotite rhyolite pebble breccia and tuff. The deposits are mostly water reworked, but contain local primary volcanic tuff beds. These deposits were probably produced by the initial explosive eruptions at the Sutter Buttes and have been dated at 1.59 Ma (Hausback and others, 1990). The middle Rampart consists of blocky diamict layers of mixed andesite and rhyolite, with the proportion of rhyolite diminishing upsection. The middle Rampart layers are channeled into the upper tuffs of the lower Rampart.

Return to the vans and continue east on Pass Rd. and then south through the town of Sutter to Hwy. 20. Turn left (east) on Hwy. 20 and continue to Yuba City.

DAY 2 - SOUTHEAST PART OF THE BUTTES

As we approach the Buttes, we cross flat rice fields to the abrupt topographic edge of the Rampart beds. The Ramparts form gently inclined bouldery slopes. Stratigraphically, this is the upper part of the Rampart.

Please do not trespass on any of the private lands of the Sutter Buttes without prior permission from the owners!!!!

0.0 Enter the Sutter Buttes at green locked gate (set the odometer here) off Butte House Rd. We enter the Buttes along one of the many large radial valleys. Up the valley we see North Butte, one of the largest and youngest of the extrusive andesite domes; also ahead and to the left is another more eroded andesite dome, called Old Man.

0.6 On the Rampart notice that many of the surfaces near the roads are unnaturally boulder-free. The rocks have been collected for decorative stone and used in the local communities as well as in Sacramento.

Pass under the first set of powerlines. On the right are outcrops of diamicts of the Rampart.

1.1 Double set of gates. Notice the old, well-constructed boulder fencelines, built by Chinese and American Indian laborers (Hendrix, 1980).

2. 8 Pass through another gate and park immediately on the left.

STOP 2

A very short walk to the top of the low hill to the right of the road. Overview of the northeastern Sutter Buttes and hikes to be taken at Stop 3. We will hike later to exposures of the upper Rampart and then to the base of North Butte, the large spiny, rounded dome dominating the skyline to the northwest.

3.4 Blue locked gate.

4.0 **STOP 3 (Fig. 6)**

Park at the pond. The pond is stocked with goldfish; no fishing please! We will hike for about 6 hrs from here.

Hike A: Walk up valley to the south. Poor exposures of lower Rampart ("rhyolitic Rampart" in Fig. 6) and Sutter Formation along the stream. Continue to the left as the valley broadens toward the top.

The major outcrop on this leg of the hike is the middle and upper Rampart (of Williams and Curtis, 1977; here designated "andesitic Rampart" in Fig. 6) at Pigeon Peak. This exposure is an erosional remnant of Rampart beds capped by a 26-40 ft (8-12 m) thick blocky diamict layer. The Pigeon Peak diamict is monolithologic porphyritic andesite, similar to the majority of the domes in the central core. The unit is massive but slightly coarser at the top, with blocks up to 10 ft (3 m) in diameter. Many blocks show excellent prismatic cooling fractures, suggesting that the blocks were deposited while hot, then cracked after deposition. Locally, blocks are indented into adjacent clasts, suggesting that the blocks reacted plastically upon deposition. The hot emplacement of this layer is corroborated by the alignment of the magnetic orientation (NRM) of nine clasts measured by flux gate magnetometer (reversed polarity). This coarse unit was probably deposited from a block and ash pyroclastic flow resulting from a dome collapse event. The blocky deposit overlies, with erosional unconformity, typical middle Rampart andesitic pumiceous-lithic tuff breccias, probably lahars, minor pyroclastic flow deposits, and reworked tephras. The outcrop is pervasively broken by a northeast-striking fault and fracture system that cuts many of the clasts and stratigraphic contacts. The offsets are normal, down to the southeast. This deformation could be the result of late intrusion of andesite stocks.

Retrace steps to the west and then toward the high craggy Old Man andesite dome. Note the recently active earthflows on some of the slopes underlain by the Sutter Formation or possibly older units. At the saddle on the east side of Old Man is a view of many of the domes of the Castellated Core and the Moat to the south. Hike along a circuitous route to the northwest and back to the main access dirt road, returning to the vehicles past the main buildings of the Dean Ranch. The long barn was built in 1860 by the Union Lumber Company; this was their winter range for oxen. Cross the valley to Hike B.

Hike B: Walk to the west along the north side of the valley toward North Butte. On this leg, we will look at a variety of exposures of the lower Rampart, adjacent silicic domes, overlying middle Rampart, and North Butte andesite dome. This area provides many examples of the silicic domes that surround the igneous core of the Sutter Buttes.

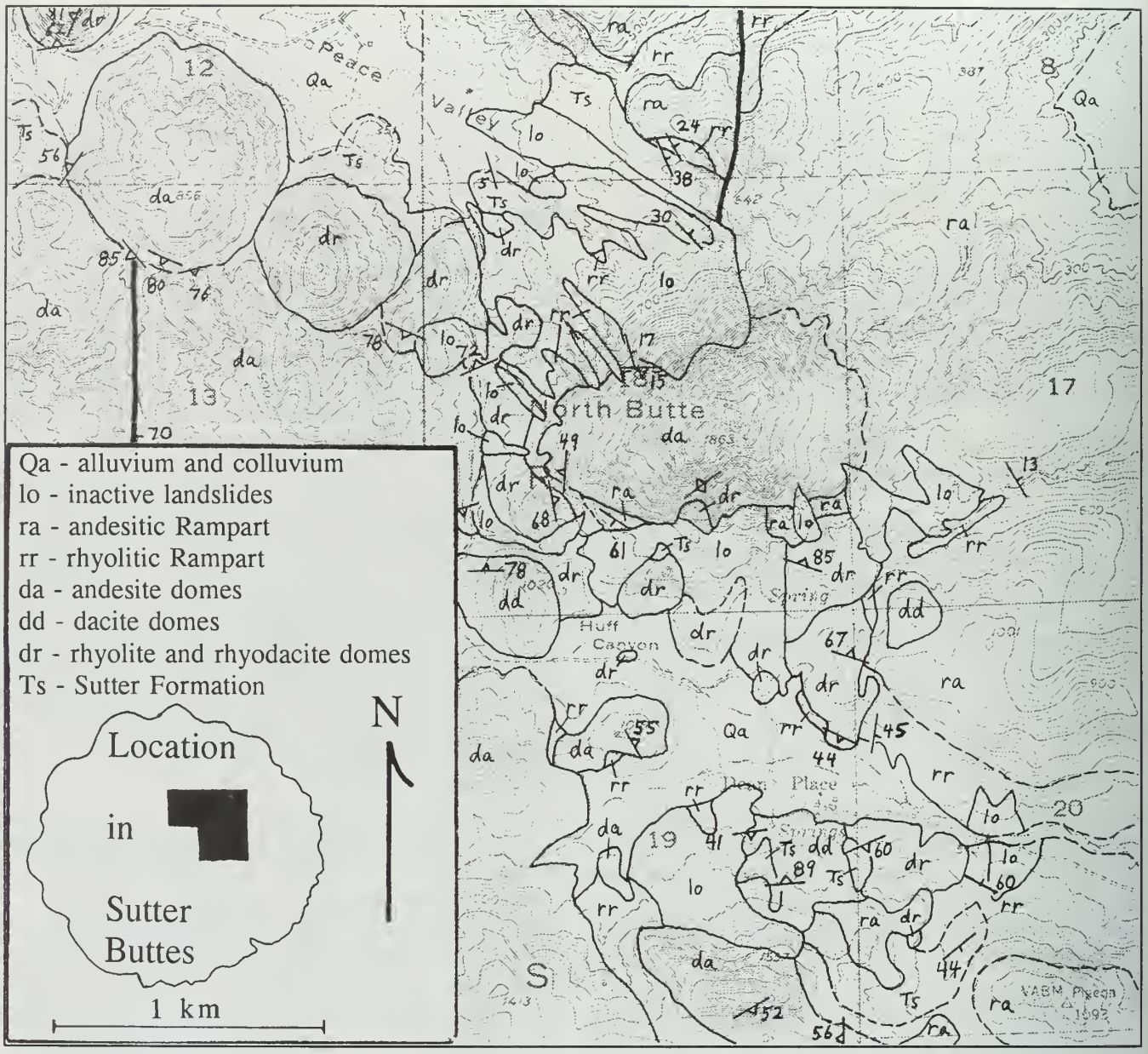

Figure 6. Preliminary geologic map of a portion of the northeastern Sutter Buttes volcano; for use with Stop 3.

ACKNOWLEDGEMENTS

Brian Hausback's studies have been partially supported by grants from the Research Award Program at California State University, Sacramento. Special thanks to Garniss Curtis and Carl Swisher of the Geochronology Center at the Institute of Human Origins for assistance with radiometric dates and for lengthy discussions which have greatly contributed to understanding this volcano.

Tor Nilsen's work in the Sutter Buttes and surrounding area has been part of a series of multidisciplinary regional subsurface studies conducted by RPI Pacific, Inc., and Applied Earth Technology Inc.; both organizations contributed considerable support for the outcrop studies.

We greatly appreciate the generosity of George and Mardel Meyers, Randy and Shirley Schnabel, Bob and Julie Steidlmayer, Mr. and Mrs. Jack Sheppard, and Dr. Ray Libby for access to their properties and permission to take this field trip into the area.

REFERENCES CITED

Anderson, W., 1983, *The Sutter Buttes: a naturalist's view*: Chico, CA, The Natural Selection Publishers, 326p.

Bodden, W.R., III, 1983, Depositional environments of the Eocene Domengine Formation outcrop on the north side of Mt. Diablo, California, *in* Cherven, V.B., and Graham, S.A., eds., *Geology and sedimentology of the southwestern Sacramento Basin and East Bay Hills*: Pacific Section, Society of Economic Paleontologists and Mineralogists, v. 29, p. 43-57.

Cherven, V.B., 1983, Stratigraphy, facies, and depositional provinces of the middle Eocene Domengine Formation, southern Sacramento Basin, *in* Cherven, V.B., and Graham, S.A., eds., *Geology and sedimentology of the southwestern Sacramento Basin and East Bay Hills*: Pacific Section, Society of Economic Paleontologists and Mineralogists, v. 29, p. 59-72.

Chorley, R.J., Schumm, S.A., and Sugden, D.E., 1984, *Geomorphology*: London, Methuen and Co., Ltd., 605p.

Creely, R.S., 1965, Geology of the Oroville (15') quadrangle, Butte County, California: *California Division of Mines and Geology Bulletin 184*, 86p.

Dickerson, R.E., 1913, Fauna of the Eocene at Marysville Buttes: *California University Department of Geological Sciences Bulletin*, v. 7. p. 257-298.

Garrison, L.E., 1962a, The Marysville (Sutter) Buttes, Sutter County, California: *California Division of Mines and Geology Bulletin 181*, p. 69-72.

Garrison, L.E., compiler, 1962b, Generalized geologic map of Marysville Buttes: *California Division of Mines and Geology Bulletin 181*, Plate 4, scale 1:62,500.

Gillam, M.L., 1974, *Contact relations of the Ione and Valley Springs Formations in the Buena Vista area, Amador County, California*: MS thesis, Stanford University, Stanford, CA, 180p.

Harwood, D.S., and Helley, E.J., 1987, Late Cenozoic tectonism of the Sacramento Valley, California: *U.S. Geological Survey Professional Paper 1359*, 46p.

Hausback, B.P., Swisher, C.C. III, and Curtis, G.H., 1990, New $^{40}Ar/^{39}Ar$ ages from the Sutter Buttes volcano, California: American Geophysical Union, *EOS, Transactions*, v. 71, no. 43, p. 1646.

Hendrix, L.B., 1980, *Sutter Buttes - Land of Histum Yani*: Marysville, CA, Normark Printing Co., 154p.

Israelsky, M.C., 1940, Notes on some Foraminifera from Marysville Buttes, California: *Sixth Pacific Science Congress*, v. 2, p. 569-580.

Johnson, H.R., 1943, Marysville Buttes (Sutter Buttes) gas field: *California Division of Mines Bulletin 118*, p. 610-615, scale 1:100,000.

Lindgren, W., and Turner, H.W., 1895, Marysville Folio: *U.S. Geological Survey Geologic Atlas of the United States*, Folio, v. 17.

Marianos, A.W., and Valentine, J.W., 1958, Eocene ostracode fauna from the Marysville Buttes, CA: *Micropaleontology*, v. 4, p. 363-372.

Merriam, C.W., and Turner, F.E., 1937, The Capay middle Eocene of northern California: *California University Department of Geological Sciences Bulletin*, v. 24, p. 91-114.

Nilsen, T.H., 1990, Santonian, Campanian, and Maestrichtian depositional systems, southern Sacramento basin, California, *in* Ingersoll, R.V., and Nilsen, T.H., eds., *Sacramento Valley Symposium and Guidebook*: Pacific Section, Society of Economic Paleontologists and Mineralogists, v. 65, p. 95-132.

Nilsen, T.H., and Imperato, D.P., 1990, Geologic field trip guidebook to Upper Cretaceous gas-producing strata, northern and central Sacramento basin, California, *in* Ingersoll, R.V., and Nilsen, T.H., eds., *Sacramento Valley Symposium and Guidebook*: Pacific Section, Society of Economic Paleontologists and Mineralogists, v. 65, p. 153-181.

Olson, R.E., 1961, Correlation of Eocene strata exposed in Fig Tree Gulch, Sutter County, California: *Report of the Annual Field Trip of the Geological Society of Sacramento*, p. 32-35.

Stipp, T.F., 1926, *The Eocene Foraminifera of the Marysville Buttes*: MA thesis, Stanford University, Stanford, CA, 70p.

Thamer, D.H., 1961, *Report of the annual field trip of the Geological Society of Sacramento*, p. 36-41, map scale 1:48,000.

Williams, H., 1929, Geology of the Marysville Buttes, California: *California University Department of Geological Sciences Bulletin*, v. 18. p. 103-220, map scale 1:62,500.

Williams, H., and Curtis, G.H., 1977, The Sutter Buttes of California: *University of California Publications in Geological Sciences*, v. 116, 56 p., map scale 1:62,500.

Zaffran, L.L., 1988, *The central lakebeds of the Sutter Buttes, California*: Senior thesis, Geology Department, California State University, Sacramento, CA, 31p.

Comparison of Structural and Metamorphic Histories of Terranes in the Western Metamorphic Belt, Sierra Nevada, California

Scott R. Paterson[1] and Warren D. Sharp[2]

INTRODUCTION

The Sierra Nevada batholith is bordered on its western margin by a series of metasedimentary, metavolcanic, and ocean-floor assemblages called the Western Metamorphic belt (WMB). These assemblages have been divided into a series of terranes separated by large ductile shear zones (Fig. 1). The extent of, and nomenclature for, different terranes is controversial. But most workers recognize, from east to west, a Northern Sierra terrane (Shoo Fly complex), Merced River terrane (Calaveras complex), and Foothills terrane. A complicated package of rocks between the Calaveras complex and Foothills terrane is sometimes separated from the above terranes and called the Sullivan Creek terrane (greenschist-phyllite belt). Major faults in this part of the WMB include the Calaveras-Shoo Fly thrust (separates the Shoo Fly and Calaveras complexes), a controversial fault called the Sonora fault (separates the Calaveras complex and phyllite-greenschist belt), the Melones fault zone (separates the greenschist-phyllite belt and Foothills terrane), and the Bear Mountains fault zone (BMFZ; separates eastern and western Foothills terrane).

There is still surprisingly little agreement about the extent of terranes, the significance or even existence of various fault zones, the generations and age(s) of structures and metamorphism in separate terranes, or about the mechanisms by which these structures and metamorphism developed (e.g., collision, thrust imbrication and burial in an accretionary wedge, pluton emplacement, ocean-floor processes, etc.).

This trip will focus on the nature and ages of structures, strains, and metamorphism in the Foothills, Sullivan Creek, and Merced River terranes. We will particularly emphasize an examination of these rocks between the Bear Mountains, Melones, and Sonora faults, as this region remains the most contentious in recent tectonic interpretations.

The following roadlog is in miles: the first number is the total mileage for each day, the second is the interval from the last entry. Measurements of planar data are in azimuthal format (strike/dip) with the strike direction to the left of the dip direction. Strain data are listed in the format X, Y, Z (SI=number, LP=number), where X, Y, and Z are the percent extensions along the x, y, and z axes of the strain ellipsoid, SI is the strain intensity, and LP is the Lode's parameter (see Paterson and others, 1989, for further discussion of strain parameters).

DAY 1 - TRANSECT ACROSS CENTRAL WMB

Leave downtown San Francisco by driving east over the Bay Bridge on I-80. Once across the bridge, take Hwy. 580 to Hayward and Livermore. Continue east on Hwy. 205 to Tracy and on Hwy. 120 to Oakdale (SF to Oakdale is about 107 mi). From the main junction in Oakdale (at stop light and Chevron station), travel east on Hwy. 120/108 approximately 14 mi to first large road cut on right after you reach the divided highway.

STOP 1-1 At this stop we will look at moderately deformed greenstones of the Gopher Ridge volcanic sequence (Clark, 1964). Farther south, this sequence is antiformal, going from subvolcanic Late Jurassic plutons and associated dikes and sills in the core of the antiform to lapilli tuffs, breccias, and flows, to fine-grained tuffs, and finally to overlying Late Jurassic slates and

[1] Department of Geological Sciences, University of Southern California, Los Angeles, CA 90089-0740
[2] Department of Earth and Space Sciences, State University of New York at Stony Brook, NY 11974-2100

graywackes (Tobisch and others, 1989). Here, only the lapilli tuffs and breccias, metamorphosed during low greenschist facies conditions, are common. A single cleavage (140/85) is associated with strains of 72, 13, -48 (SI = 0.87, LP = .31). Fold axes and stretching lineations are usually steep. These structures are Late Jurassic (early folding) to Cretaceous (cleavage development): the age of the volcanic rocks is unknown but is also thought to be Late Jurassic. Farther north, volcanic rocks similar to the Gopher Ridge volcanic sequence overlie the 160 Ma Smartsville ophiolite.

0.0, 0.0 Continue east on Hwy. 108/120. We will drive through more Gopher Ridge volcanics and then Late Jurassic slates and graywackes of the Salt Springs sequence (seen on Day 3).

7.0, 7.0 Turn right on J59 (La Grange Rd.).

7.8, 0.8 Cross Bear Mountains fault, from Mariposa Formation to greenstones of Peñon Blanco Formation.

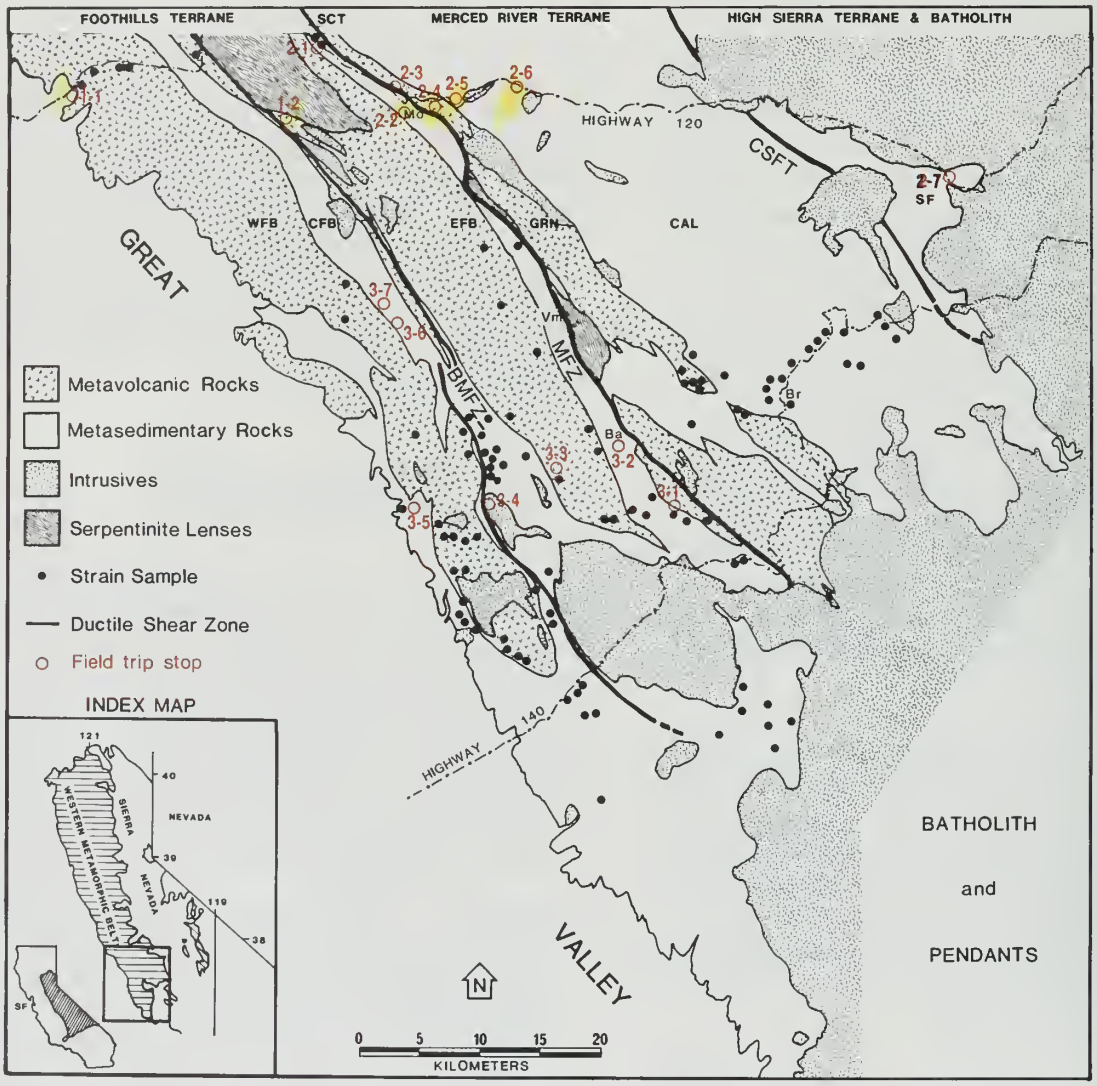

Figure 1. Generalized map of southern portions of the WMB, after Paterson and others (1989). SCT, Sullivan Creek terrane; Mo, Moccasin; Br, Briceburg; Ba, Bagby; WFB, CFB, EFB, western, central, and eastern Foothills belts, respectively; GRN, greenschist-phyllite belt; CAL, Calaveras complex; SF, Shoo Fly complex; BMFZ, Bear Mountains fault zone; MFZ, Melones fault zone; CSFT, Calaveras-Shoo Fly thrust. Trip stops shown with large numbers, except for stops near Standard pluton (see Fig. 4 for locations of these stops).

9.0, 1.2 Intersection with Red Hill Rd., bear right.

9.6, 0.6 Intersection with Old Don Pedro Rd., bear left. This road is mostly in the Peñon Blanco Formation, but locally skirts into serpentinite of the western edge of the Tuolumne ultramafic complex (TUM).

11.9, 2.3 Gated dirt road. This is Stop 1-2. Park on the shoulder, cross fence on left (east) side carefully, and proceed up the dirt road for about 0.3 mi to the (abandoned?) herder's cabin. The exposures of Fig. 2 are in the small creek to your left, both up and downstream from the cabin.

STOP 1-2 At this locality, we will examine the southwestern margin of dunite and harzburgite of the Tuolumne ultramafic complex (Morgan, 1976), where it is in fault contact with mafic tuff and breccia of the Lower Jurassic Peñon Blanco Formation (Figs. 1, 2). Along this contact, in a zone up to 1640 ft (500 m) wide, the ultramafic rock is converted to antigorite schist, talc-magnetite schist, and talc-tremolite schist. The general strike of the schistosity is west-northwest, parallel to the contact, with steep dips to the north-northeast, though in detail it is complexly folded. This intense fabric dies out gradually to the northwest, grading into less altered and sheared ultramafic rock. The southwestern contact with the Peñon Blanco Formation is sharp, with little-deformed greenstones 3-6 ft (1-2 m) from it (Fig. 2).

The central part of the schistose zone is a melange, consisting of blocks of hornblendite, garnet amphibolite, quartz-albite-amphibole schist, and quartzite in a matrix of ultramafic schist. The amphibole-rich rocks are derived from basic igneous parents and the quartz-rich rocks from impure cherts. Many of the blocks have complex internal schistosities. The typical mineralogy of metabasite blocks is amphibole-garnet (grossular-almandine)-clinozoisite-albite-rutile-sphene-apatite ± chlorite ± ilmenite. Geobarometry using the GRAIL assemblage (Bohlen and Liotta, 1986) yields a minimum pressure of crystallization of 6 ± 1 kb at an estimated minimum temperature of 500°C, corresponding to a depth of 12 mi (20 km).

In contrast, regional metamorphism in the Peñon Blanco Formation is prehnite-pumpellyite to lower greenschist facies (Morgan, 1976; Tobisch and others, 1989). Thus the assemblages of the melange blocks imply that the fault has a vertical component of displacement of several miles. As discussed below, the fault probably had a shallow initial dip, so the horizontal component of displacement may have been tens of miles. As suggested by previous workers (Schweickert and Bogen, 1983), the melange blocks are interpreted as fragments of a dynamic contact aureole formed by thrusting of hot ultramafic rock over arc or oceanic crustal rocks. Similar zones occur beneath the Oman ophiolite (Coleman, 1981), the Bay of Islands ophiolite (Jamieson, 1981), and other ultramafic sheets.

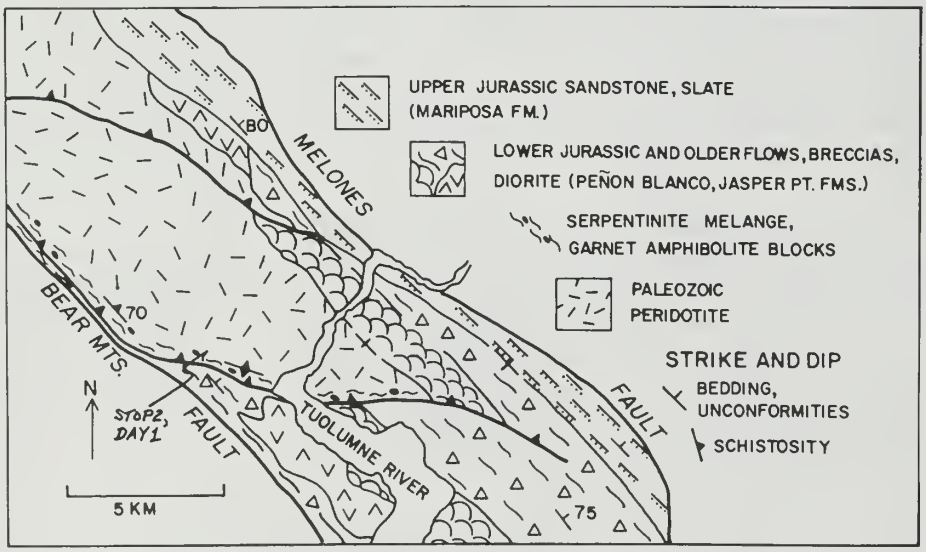

Figure 2. Map of Tuolumne ultramafic complex and associated rocks. Note the serpentinite-matrix melange along the southwest contact of the peridotite and the steep, uniform dips in the Jurassic Peñon Blanco and Mariposa formations. Modified after Morgan (1976), Schweickert and Bogen (1983), and unpublished mapping of C.W. Leighton and W.D. Sharp.

Cooling of the zone through about 500°C is dated by an Ar/Ar incremental heating analysis of amphibole from one of the blocks, which yields an age of 178 ± 1.4 Ma. Four other samples from along strike in this zone or in similar zones in the area of Fig. 1 yield ages of 176-181 Ma (Leighton, 1986). These ages are minimums for the crystallization of the blocks and are considered to approximate the age of faulting that emplaced the blocks against the relatively cool (<350°C) Peñon Blanco Formation.

The steep dips in the Upper Jurassic Mariposa Formation (Stop 2-1) and comparable dips in the Peñon Blanco Formation indicate that the region between the Bear Mountains and Melones faults has been strongly tilted, and that much of this tilting is post-Mariposa in age. Removal of this tilt from the fault at the base of the ultramafic massif allows its pre-Mariposa orientation to be assessed. This requires knowing the sense, magnitude, and axis of post-Mariposa body rotations. The overall eastward-facing of the tilted region and the lack of folding of the fault's trace suggests a simple clockwise rotation has occurred. Body rotations leading to dips of about 70° have recently been estimated in the vicinity by Paterson and others (1989). Axes of rotation plunge shallowly to moderately southeastward, based on the orientation of minor and map-scale fold axes in the area (Bogen, 1984; Paterson and others, 1989). After removal of appropriate tilting, the fault dips 20° to 40° to the northeast. If slip on the fault occurred parallel to the dip direction of its pre-Late Jurassic orientation, significant Middle Jurassic shortening in a northeast-southwest direction is indicated.

The fault is distinctly older than the folding and cleavage formation in the cover rocks of the Foothills terrane. It also predates that terrane's Late Jurassic age of accretion in some models (Ingersoll and Schweickert, 1986), yet the orientation of the fault is like that of potentially coeval structures in the Calaveras complex (Stop 1-4) and is most easily related to underplating at a west-facing convergent margin.

Turn around and retrace the route to the intersection with Red Hill Rd.

14.8, 2.9 Intersection with Red Hill Rd., turn right, crossing the serpentinized dunite of the TUM.

16.2, 1.4 Dry wash. Good spot to see tan-weathering, weakly foliated serpentinized dunite. Dark crystals are relict chrome spinel. Within similar dunite of the central part of the massif is a swarm of hornblende diorite dikes (Morgan, 1976). They dip steeply and strike east to northeast. Hornblende from one has yielded an Ar/Ar age of 167 ± 2 Ma. This is considered an igneous age for the dike swarm, based on retention of igneous Ar ages in hornblende from 196-200 Ma plutons in the massif. This age is significant because it shows that magmatism similar in age to that prevalent in the Sullivan Creek terrane and Calaveras complex also occurs in this massif.

17.5, 1.3 Bear right at the intersection.

18.8, 1.3 Town of Chinese Camp and intersection with Hwys. 49/120. Turn left onto Hwy. 49, then bear right at fork, staying with Hwy. 49. The route leaves the ultramafic complex. The outcrops around the fire station are diorite of Chinese Camp, dated at 199 ± 2 Ma (Saleeby, 1982) and considered coeval with the Peñon Blanco Formation.

22.4, 3.6 Junction with Hwy. 108, turn right.

25.3, 2.9 Entering Jamestown, turn right onto Main St., then right on Donovan St.

25.5, 0.2 Turn right on Seco St.

26.3, 0.8 Join Campo Seco Rd., and bear right. Stay to the right (straight) through the intersection on Jacksonville Rd.

26.7, 0.4 Stay on Jacksonville Rd. around sharp left turn.

28.1, 1.4 At the small village of Stent, bear right.

29.3, 1.2 High bridge over Sullivan Creek, Stop 1-3. Park on the far end of the bridge, walk back to the upstream side of the north end, and descend the steep slope to the creek.

STOP 1-3 This locality is about 2600 ft (800 m) east of the trace of the Melones fault, in strongly deformed greenstones (Fig. 3). They are derived principally from pillowed lava flows and lesser volcaniclastic rock. Massive, fine-grained, equigranular, plagioclase-rich rock occurs locally and may be hypabyssal intrusions. East of this locality, tuffs and tuff-breccias replace pillows as the dominant rock type. Similar greenstones extend southeastward to the Merced River, comprising the metavolcanic unit of the Sullivan Creek terrane (Sharp, 1988) or part of the phyllite-greenschist belt of Schweickert and Bogen (1983).

The volcaniclastic rocks probably were deposited in a basin adjacent to a volcanic arc. The thickness and extent of the flows suggests they may have formed at a spreading center. The stratigraphic age of the greenstones is unknown, but it must predate 169 ± 2 Ma, the Ar/Ar hornblende age of the Page Mountain pluton (Fig. 3). Two other dated plutons that intrude the Sullivan Creek terrane, the Cobb's Creek and the Dogtown, yield Ar/Ar ages of 168 and 165 Ma, respectively.

Structures downstream from the bridge are described by Schweickert and Bogen (1983) and Schweickert and others (1984).

Below the bridge, pillow lavas that have been strongly shortened in an east-west direction and elongated along steeply eastward-plunging axes are well exposed. Steeply-dipping, northwest-striking extension fissures filled with quartz cut the pillows and intra-pillow matrix. These are sub-perpendicular to the direction of maximum horizontal elongation of the pillows and may have formed during flattening of the pillows. Weak northeast-striking crenulations are also present, but the associated strain is minor. Strains similar to or greater than those of the main fabric of this locality are typical of pillow lavas along the western side of the Sullivan Creek terrane.

At locality A of Fig. 4, a hypabyssal intrusion has subtle centimeter-scale, mineral-ratio layering which is probably primary and a well-developed schistosity parallel to the flattening plane of the pillows. In thin section, this rock is a thoroughly recrystallized greenschist facies tectonite, consisting of albite, green amphibole, chlorite, epidote, white mica and sphene. Amphibole from this rock has yielded an Ar/Ar age of 163 ± 6 Ma. Because growth of this amphibole occurred under metamorphic conditions at or below its expected closure temperature for Ar loss, this age is considered to date its growth and the development of the flattening fabric. Three other widely distributed samples of Sullivan Creek greenstones have yielded similar Ar/Ar amphibole ages of 161-163 Ma. This suggests a uniform age of metamorphic crystallization and/or Ar retention as far south as the Merced River.

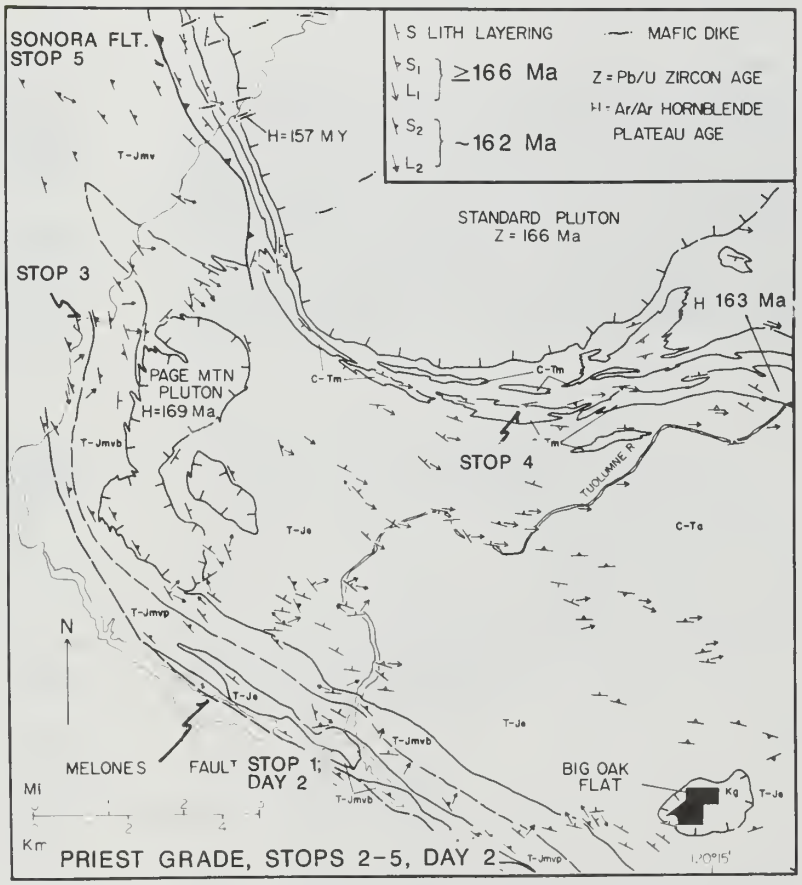

Figure 3. Map of the Sullivan Creek terrane and Calaveras complex in the Tuolumne River area (after Sharp, 1988, and references therein) showing Stops 1-3 to 1-5, and 2-1 to 2-5. Units are as follows: C-Ta, Calaveras complex argillite and chert; C-Tm, Calaveras complex marble and amphibolite; T-Je, Sullivan Creek epiclastic rocks; T-Jmvb and T-Jmvp, Sullivan Creek metavolcanic breccias and pillows; Jm, Mariposa Fm.

This age is significantly older than the main cleavage in Late Jurassic rocks west of the Melones fault, which developed between 145 and 123 Ma (Tobisch and others, 1989). The observed age span of 40 my for similarly oriented ductile fabrics in the region contrasts with the widely held concept of brief, contemporaneous fabric development in rocks on either side of the Melones fault (compare with Schweickert and others, 1984). Tobisch and others (1989) attributed diachronous localization of cleavage development west of the Melones fault to the effects of heat and fluids around intrusions. A similar explanation may apply to the Sullivan Creek terrane considering the close ages of plutons (169-165 Ma) and metamorphic recrystallization and cooling (161-163 Ma) observed there. If so, ductile deformation and metamorphism of regional scale may be more closely related to the age and distribution of magmatism than to the effects of crustal thickening resulting from accretion.

Evidence for polystage, nearly coaxial shortening is present at locality B (Fig. 4) where a folded ductile shear zone is exposed. Over several feet approaching the zone, the flattening strain in the pillows becomes increasingly intense until the pillow structures are obliterated and the zone grades into a banded biotite-chlorite schist. The zone is tightly folded about axes plunging 40° to the south-southeast, with axial surfaces oriented 350/80. A well-developed crenulation cleavage locally parallels the axial surface. In thin section, the rock is a crenulated greenschist consisting of albite, quartz, chlorite, white mica, carbonate, sphene, and pyrite. Crenulation cleavage domains are strongly enriched in white mica and pyrite. The zone initially developed as a thrust or reverse fault under greenschist facies conditions. This ductile fault was then folded and the fold flattened by additional east-west shortening. This structural sequence may have formed as a continuum based on the comparable metamorphic grade of the wall-rocks, the shear zone schistosity, and the crenulation cleavage, as well as the uniform direction of shortening. This coaxial superposition contrasts with the geometry of superposition observed in phyllites of the Sullivan Creek terrane which lie to the east (Stop 2-5).

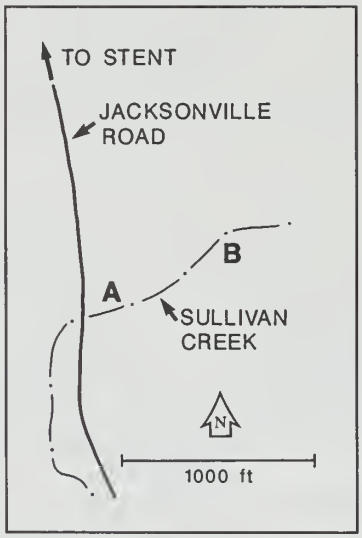

Figure 4. Location map for Stop 1-3 in the greenstones of the Sullivan Creek volcanics. A is the location of an hypabyssal intrusion in flattened pillow lavas. B is the location of a folded, crenulated ductile shear zone.

Turn around and drive north back to Stent.

30.6, 1.3 At Stent, bear right.

31.6, 1.0 T- intersection at Algerine Rd., turn right. Cross Sullivan Ck. (upstream of Stop 1-3).

32.9, 0.4 Cross Curtis Ck. The route passes into a narrow strip of Sullivan Ck. phyllite and then into the Page Mountain pluton dated at 169 Ma.

34.9, 2.0 Intersection with Twist Rd., turn left.

35.5, 0.6 Intersection with Lime Kiln Rd. Turn right, staying with the Algerine-Wards Ferry Rd. The route is now in the Calaveras complex.

36.9, 1.4 Cross Rough and Ready Ck.

38.9, 2.0 Intersection with Wards Ferry Rd., turn left.

39.1, 0.2 Sharp right turn in road, Stop 1-4. Park and walk back towards the last intersection, looking at the roadcuts.

STOP 1-4 At this locality, marble and interleaved amphibolite of the Calaveras complex is exposed (Fig. 3). Of interest here are both protolith and structural features. Fine-grained amphibolite and garnet-bearing mica schist (some of which contain clasts of calcite marble)

may be metamorphosed basaltic volcanic and volcaniclastic rocks. Coarser-grained amphibolite may be derived from gabbro. Some amphibolites have high contents of Ti, Zr and La relative to typical convergent margin or ocean ridge magma suites. Since these elements are relatively immobile during metamorphism and are not abundant in marble, their measured abundances probably reflect igneous values and indicate the parent rocks were in part alkalic basalts. The amphibolites are interleaved with coarse-grained, white to blue-gray marble and fine-grained buff to tan dolomitic marble. Breccias with clasts of dolomitic marble in a calcite marble matrix suggest penecontemporaneous dolomitization. Although not exposed here, gray ribbon chert occurs along strike. This lithologic association has been interpreted by several workers as seamount fragments scraped from the down-going oceanic plate into the accretionary wedge (Sharp, 1988).

The overall northwest trend of this marble-amphibolite unit at map-scale (Fig. 3), along with similar trending, fault-bounded lithologic packages (Schweickert and others, 1988), may result from accretion of the Calaveras complex at a northwest-striking convergent margin. Accretion must be post-Early Triassic, the age of the youngest known strata in the complex, but pre-Middle Jurassic, the age of the oldest dated crosscutting intrusions (Sharp, 1988).

The strong, east-striking, steeply-dipping schistosity and east-plunging stretching lineation visible at this locality are related to regionally developed east- to southeast-trending, upright folds superposed on the northwest-striking accretionary structures. The superposed folds have trends consistent with formation in a northwest-trending, dextral, simple shear zone (Saleeby and others, 1986). Their plunge may have initially been controlled by the dip of the earlier structures.

Additional tightening and reorientation of the cross folds took place during forcible emplacement of the Middle Jurassic Standard pluton (Schweickert and others, 1988), which has a diameter of 6.2 mi (10 km) and crops out 0.62 mi (1 km) to the north of this stop (Fig. 3). The age of the Standard pluton is 166 ± 2 Ma, based on U/Pb zircon analyses. The pluton consists of minor clinopyroxene-rich ultramafic rocks and voluminous gabbro, tonalite and granodiorite. Two smaller bodies to the northwest, the Parrot's Ferry and Vallecito plutons, yield similar isotopic ages.

Amphibolite is characterized by the mineral assemblages amphibole-clinozoisite-albite-sphene ± garnet ± biotite. Three similar amphibolites occurring eastward along strike at distances of 1.4 to 2.2 mi (2.3 to 3.5 km) from the Standard pluton yield Ar/Ar isochron ages of 161-163 Ma. These ages reflect crystallization or degassing of the amphiboles in the thermal aureole of the Standard pluton. Temperatures greater than 500°C would be required to degas the amphiboles, while growth of amphibole requires minimum temperatures of about 400°C. In either case, the Ar data show that the Standard pluton imposed a broad, hot thermal aureole on the Calaveras complex.

At a distance from the Standard pluton and other intrusions, the grade of the Calaveras complex appears to be lower greenschist facies (Paterson and Sample, 1988). This suggests that metamorphism to grades above lower greenschist facies, which characterizes the Calaveras complex over much of the area northward from the Tuolumne River to the Stanislaus River, may be related to the thermal effects of Middle Jurassic magmatism. This view contrasts with earlier concepts of Calaveras metamorphic history which related the higher grade metamorphism to a regional event of Triassic age (compare with Schweickert and others, 1988). Based on the existing isotopic age data, the age of metamorphism in the Calaveras complex and its relation to plutonism are directly analogous to those of the Sullivan Creek terrane. This shared thermo-magmatic history beginning at or before 169 Ma argues against the presence of a younger (Late Jurassic) suture between them.

Turn around and drive back to Algerine-Wards Ferry Rd.

39.3, 0.2 Intersection with Algerine-Wards Ferry Rd. Turn right, retracing route to Lime Kiln Rd.

42.7, 3.4 Intersection with Lime Kiln Rd. Turn right.

43.4, 0.7 Intersection, bear right (straight) on Lime Kiln Rd.

44.7, 1.3 Cross Curtis Ck., swinging briefly into altered diorite of the peripheral facies of the Standard pluton.

46.4, 1.7 Cross Sullivan Ck. Upstream from the road are water-polished exposures of Calaveras complex quartzite and mica schist in the inner aureole of the Standard pluton, which lies about 490 ft (150 m) to the east. The rocks contain cordierite, sillimanite (in thin section) and aplitic to pegmatitic dikes that may be the result of local partial melting.

47.4, 1.0 Intersection with Sonora bypass for Hwy. 108. Go through the light and park on the right for Stop 1-5. Cross Lime Kiln Rd. and examine the deep, fresh roadcuts on the north side of the bypass.

STOP 1-5 This relatively new outcrop has not been studied by us in detail, but it provides an opportunity to examine a fault that separates the Calaveras complex on the east from phyllite and greenstone of the Sullivan Creek terrane to the west (Fig. 3). This is presumably an exposure of the Sonora fault, which has been considered to be a potential Late Jurassic suture (Schweickert and others, 1984). Proceed west, beginning in siliceous argillite of the Calaveras complex that is hornfelsed by the Standard pluton which crops out about 2600 ft (800 m) to the east. The large mafic dike, rich in clinopyroxene phenocrysts, which intrudes argillite near the east end of the outcrop, is similar to mafic phases of the Standard pluton. It post-dates the northwest-striking, steeply-dipping penetrative structures in its wallrocks which are largely the result of reorientation of earlier structures during emplacement of the Standard pluton by outward expansion. The argillite is bounded to the west by a sheared and tightly folded zone containing a thin sliver of talc schist. To the west are similar argillaceous metasediments, though finer grained with white siltstone lenses, and then greenstones considered to be part of the Sullivan Creek terrane.

Proceed north on Lime Kiln Rd. to Sonora. End of Day 1.

DAY 2 - MELONES AND SONORA FAULTS

Drive west on Hwy. 108 past Jamestown. About 3 mi west of Jamestown turn south towards Chinese Camp and Hwy. 120. From the junction with Hwy. 120, drive south 3.8 mi to large road cuts on right side of road.

STOP 2-1 We are now east of the Peñon Blanco volcanics and TUM (Stop 1-2; Figs. 1, 3). Here we will examine tilted sandstones, shales, and conglomerates of the Oxfordian to Kimmeridgian Mariposa Formation, eastern Foothills terrane recrystallized during low greenschist to subgreenschist facies metamorphism (detrital chlorite grains in mudrocks and prehnite-pumpellyite assemblages in volcanics are found locally). The dominant cleavage (126/80) is roughly bedding parallel but refracts across some sandstone and conglomerate layers. This cleavage is associated with strains in conglomerate of 40, 6, -33 (SI=0.53, LP=.5). Local folds of bedding and bedding-parallel fissility have variable plunges. Later, we will contrast the well-bedded, fossiliferous, and weakly deformed and metamorphosed Mariposa Formation seen here with other slate-graywacke units in the Foothills terrane.

0.0, 0.0 Continue south on Hwy. 120.

3.7, 3.7 Junction with Hwy. 49.

4.4, 0.7 Continue on Hwy. 120 and take right turn towards Hetch Hetchy store immediately after crossing bridge.

4.5, 0.1 Stop near large drainage cut on right side of road.

STOP 2-2 Here we examine intensely deformed slates, sandstones, and local conglomerates (with Oxfordian-Kimmeridgian fossils found in the slates) near (or in?) the Melones fault zone (Fig. 5). Good sedimentary structures are preserved including cross-bedding, rip-up clasts, and soft-sediment folds: cross-bedding generally indicates younging to the east. These units have been metamorphosed during low greenschist facies metamorphism, under slightly higher conditions than the last stop probably due

to nearby small intrusive bodies in the Melones fault.

One dominant cleavage (293/83) is associated with strains in slate of 40, 25, -43 (SI=0.69, LP= .75), sandstone of 12, 8, -17 (SI=0.23, LP=.76), and grits of 12, 4, -14 (SI=O.19, LP=.41). These strains are still quite low compared to those immediately east of the MFZ (e.g., Fig. 6 and next few stops). Note also that in contrast to Stop 2-1, here bedding is boudinaged and rootless isoclinal fold hinges (with axes that fall along girdle parallel to cleavage) are common. The presence of syn-depositional structures (Bogen, 1984), isoclinal rootless fold hinges but low ductile strains, and the flattening strains in the mudrocks, suggest to us that most of these structures formed during deposition, that is, during the Late Jurassic.

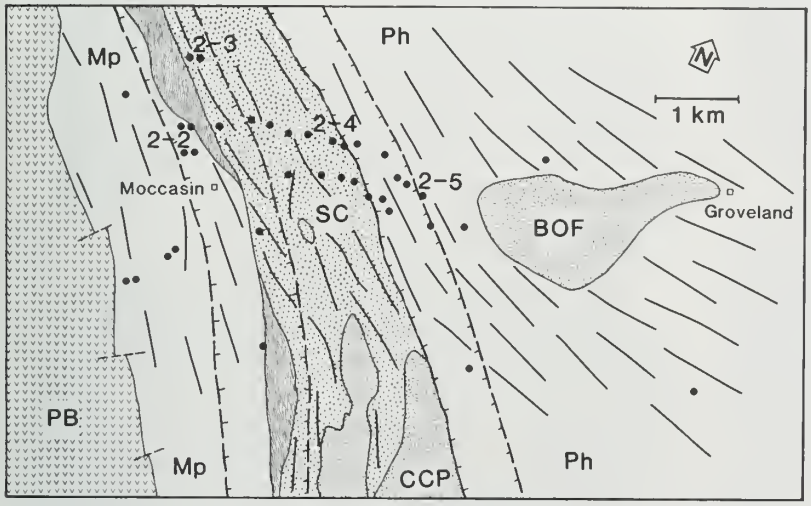

Figure 5. Map of the Moccasin-Priest Grade region showing Stops 2-2 to 2-5. PB, Peñon Blanco volcanics; Mp, Mariposa Fm.; SC, Sullivan Creek volcanic sequence; Ph, phyllite and Calaveras-type lithologies; CCP, Cobbs Creek pluton; BOF, Big Oak Flat pluton. Black dots, locations of strain samples, trend lines show average strike of steeply dipping pervasive cleavage. Zones of high strain outlined by T symbols.

4.6, 0.1 Return to Hwy. 120 and head east up New Priest Grade. We almost immediately cross the Melones fault and drive through greenschists in the Sullivan Creek terrane.

5.5, 0.9 Turn left on Grizzley Road.

6.0, 0.5 Stop at roadcuts of light-colored volcanic rocks on right.

STOP 2-3 We are now in the eastern and upper plate of the east-dipping MFZ and are again looking at the Sullivan Creek volcanic sequence seen at Stop 1-3 (Figs. 3, 5). Here

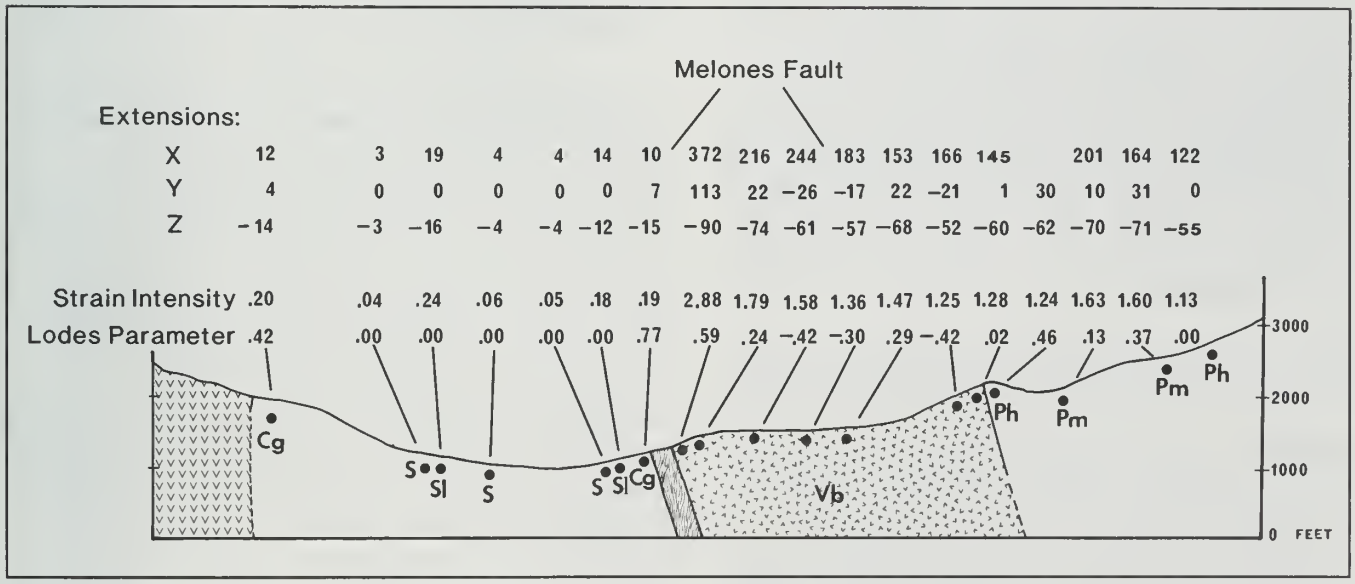

Figure 6. Strain profile of tectonic strains in transect through Moccasin-Groveland area (strains due to volume losses have been removed from slates and sandstones). Strain intensity and Lode's parameter defined by Hossack (1968). Type of marker used indicated by the following symbols: Cg, conglomerate; Ph, phyllite; Pm, pebbly mudstone; S, sandstone; Sl, slate; Vb, volcanic lapilli or breccia.

deformed pillows or breccia fragments record strains of 372, 113, -90 (SI=2.88, LP=.59), some of the highest strains we have measured in the WMB (Fig. 6). One penetrative and several nonpenetrative cleavages are present, along with local folds and a well-developed stretching lineation.

The structures and strain reflect a combination of older wall rock deformation and younger deformation in the MFZ. Thus, caution should be used when interpreting structures east of the fault as kinematic indicators. However, lineations and kinematic indicators in the western footwall indicate that the most recent history of fault movement is one of dip-slip.

6.5, 0.5 Return to Hwy. 120 and continue up New Priest Grade. We will drive through deformed breccias and pillows. Note the decrease in strain (represented by the decreasing axial ratios of these objects) as we travel away from the MFZ.

8.4, 1.9 Park in turnout on right side of road at sharp corner.

STOP 2-4 The sheared contact between Sullivan Creek volcanic rocks and the belt of argillaceous phyllites and graywackes is exposed immediately east of the sharp bend in the road (Fig. 5). The dominant cleavage, which has changed from northwest orientations near the MFZ to west-northwest orientations, is associated with strains in volcanic rocks of 145, 1, -60 (SI=1.28, LP=.02) and in phyllites of 85, 28, -58 (SI=1.41, LP=.29). Nonpervasive cleavage and locally developed folds of bedding and cleavage are also present.

9.0, 0.6 Continue up New Priest Grade to large turnout on left side of road in sharp road bend.

STOP 2-5 The rock here consists of strongly cleaved phyllite, often containing flattened clasts of sandstone and abundant late pyrite. Rocks like these form a strip along the east side of the greenstones of the Sullivan Creek terrane that extends to the southern end of the metamorphic belt. The phyllites are intruded by 169-165 Ma plutons and so are Middle Jurassic or older. In the Merced River area, they contain Early Triassic limestones interpreted as olistoliths (Bateman and others, 1985) and so are Early Triassic or younger. In the Merced River area, where strains are lower, an east-facing depositional contact between argillite of this unit and underlying greenstone is preserved (Herzig, 1985).

The older penetrative cleavage (281/60 where not folded) is associated with strains in pebbly mudstones of 210, 10, -70 (SI=1.6, LP=.13). The younger domainal cleavage (12/85) and associated folding indicate values of shortening between 0 percent (no folding) and 50 percent (tight folds) assuming that the folds formed by buckling and plane strain.

The younger open to tight folds have axial surfaces striking northeast to northwest, nearly perpendicular to the general strike of the folded surface. This geometry of superposition is typical of large areas of the Sullivan Creek terrane, especially at a distance from the Melones fault. It is distinct from that seen at Stop 1-3 in the Sullivan Creek greenstones and raises the possibility that the continuous cleavage at this locality is different in age from that of the greenstones. One possibility is that the continuous cleavage here is broadly correlative to that of similarly oriented, pre-Middle Jurassic crossfolds and cleavage in the Calaveras complex.

The relationship of the phyllite unit to the Calaveras complex is controversial. The contact has been considered lithologically gradational (Paterson and others, 1989), a Late Jurassic suture (Schweickert and others, 1984, 1988), or a pre-Middle Jurassic thrust modified by Late Jurassic or younger faulting (Sharp, 1988). Indirect evidence of the relationship includes the following. The Early Triassic limestone olistoliths in the phyllite unit are identical to Early Triassic limestones structurally interleaved with cherts of the Calaveras complex. Neodymium isotope compositions of the western Calaveras complex and the phyllite are the same, and their model ages of about 1.5 Ga reflect derivation, at least in part, from Proterozoic or older continental crustal sources (O.C. Evans and W.D. Sharp, unpublished data). An origin for the phyllite consistent with these data would be derivation by sedimentary reworking of Calaveras complex materials near

the toe of an accretionary wedge, followed by incorporation of the phyllite and underlying greenstones into the wedge by underplating.

11.0, 2.0 Continue east on Hwy. 120 to Big Oak Flat. We are now driving through the highly weathered Big Oak Flat pluton (Fig. 5). Probably Cretaceous in age, this pluton postdates all ductile structures seen at the last stop, does not visibly deform its wall rocks, has a small contact aureole with minor assimilation, and has no recognizable means of emplacement (Paterson, 1989). Because exposures are so poor we will not stop.

12.3, 1.3 Continue east to Groveland (this marks the eastern end of the Big Oak Flat pluton).

15.3, 3.0 Continue to new roadcuts on left side of road.

STOP 2-6 Presumably we have now crossed everyone's "Sonora fault" and are now looking at disrupted argillites, and metacherts or metasandstones in the Calaveras complex (Figs. 1, 3). Disrupted bedding and aligned metamorphic minerals (greenschist facies) define the main cleavage (125/80) which is locally overprinted by younger folds and cleavage. This is a good "quiz" stop: we have previously mentioned controversy about the generations of structures, grade of metamorphism, and continuity of features between the Calaveras complex and Sullivan Creek terrane. What do you think?

23.0, 7.7 Continue east on Hwy. 120 to Buck Meadows, and

36.5, 13.5 Yosemite National Park entrance.

43.3, 6.8 Continue to paved pullout on right.

STOP 2-7 Across the road, multiply deformed, isoclinally folded schists and quartzites of the Shoo Fly complex are exposed. If time allows, we will discuss the nature and interpretation of the largely Paleozoic deformation and metamorphism in this unit.

45.0, 1.2 Continue east to Crane Flat. Go straight at junction and head towards Yosemite Valley.

53.0, 9.0 Turn right (west) on Hwy. 140.

57.6, 4.6 Leave Yosemite Park.

57.9, 0.3 Stop in turnouts past the park entrance.

STOP 2-8 (Optional): El Portal Intrusive Suite. Aligned enclaves in tectonically nondeformed Cretaceous granodiorites. If time allows, we will examine magmatic structures (aligned enclaves, magmatic shear zone) and the nature and timing of emplacement of the Cretaceous Sierra Nevada batholith.

90.0, 30.1 Continue west on Hwy. 140 to Mariposa. This drive takes us along the Merced River across most of the units seen earlier today (Shoo Fly, Calaveras, Sullivan Creek). End of Day 2.

DAY 3 - FOOTHILLS TERRANE

Today, we will first examine the Melones fault and then examine different units along a transect across the Foothills terrane.

0.0, 0.0 From the junction of Hwys. 140 and 49, head north on Hwy. 49. We are initially in volcanic rocks and thin units of phyllite in the Sullivan Creek terrane.

2.2, 2.2 Between 2.2 and 3.2 miles we cross the Melones fault, here marked by lenses of serpentinite and other ultramafic blocks surrounded by the slate-graywacke sequences of the Mariposa Formation and volcanic rocks and phyllite to the east.

5.9, 3.7 Turn right on road to Mt. Bullion.

8.9, 3.0 Stop and look at the Melones fault.

STOP 3-1 We will make a brief stop in greenstones of the Bullion Mountain sequence (Herzig, 1985). This unit consists mostly of mafic tuff-breccia, much of which is rich in coarse clinopyroxene phenocrysts, as well as minor tuffs and pillows. Its oldest known rocks are at least Callovian, based on an Ar/Ar hornblende age of 169 ± 3 Ma for a shallow level clinopyroxene-hornblende gabbro. This may be a feeder for the volcaniclastic rocks based on its

local porphyritic texture and lack of contact aureole. The sequence also yielded an age of 167 ± 1 Ma for a plutonic clast from a tuff-breccia, and an Oxfordian-Kimmeridgian fossil (Clark, 1964). Thus the age range of the sequence corresponds to that of lithologically similar rocks interbedded with the Mariposa Formation, west of the Melones fault (e.g., the Logtown Ridge Formation). Extrusives of the sequence also overlap in age with the plutons that intrude the Sullivan Creek terrane and the Calaveras complex, leading to the suggestion that the Bullion Mountain sequence is, in a broad sense, their eruptive equivalent.

Compared to the greenstones of the Sullivan Creek terrane, this unit is notably less deformed (no widespread cleavage and strain ellipsoids close to spheres) and recrystallized (Herzig, 1985; Paterson and others, 1989). It is separated from the Sullivan Creek terrane by an incompletely understood, mappable high strain zone exposed in the Merced River canyon (perhaps a folded thrust or reverse fault, Herzig, 1985, and pers. comm., 1990). A possible explanation for these relations is that the Bullion Mountain sequence originated and remained at higher levels than the Sullivan Creek terrane within a single Middle to Late Jurassic arc. Such an arc is envisioned to have been built across a heterogeneous assemblage of basement rocks including the Calaveras complex, the Sullivan Creek terrane, and the Tuolumne ultramafic complex. These disparate basement rocks were probably assembled by offscraping and imbrication into an early Mesozoic accretionary wedge at a west-facing convergent margin.

11.9, 3.0 Return to Hwy. 49 and head north past Mt. Bullion. This section of road passes through the Mariposa Formation.

19.9, 8.0 Drive through Bear Valley.

29.4, 9.5 Pull into paved overlook on left side of road.

STOP 3-2 This stop provides an excellent overview of relationships on both sides of the Melones fault zone along the Merced River (Fig. 7). To the east is a complicated assemblage of rocks including the Sullivan Creek volcanic sequence, mixed volcaniclastic and metasedimentary rocks, the Late Jurassic Mt. Bullion sequence (last stop), and Calaveras-type rocks with argillaceous phyllites, pebbly mudstones, sandstones, metacherts, and limestones blocks with Late Triassic and Carboniferous fossils. West of the MFZ (and exposed at this stop) are slates, graywackes, and local conglomerates and volcaniclastic-rich units of the Mariposa Formation. The fault zone is marked by lenses of ultramafic material, local dike swarms and other intrusives, and deformed footwall and hanging wall rock types.

Across the road are exposures of folded and cleaved slates and graywackes. The penetrative cleavage (319/57) is associated with strains in sandstone of 18, 7, -21 (SI=.30, LP=.51) and in slates of 69, 28, -54 (SI=.97, LP=.54)(Fig. 8). Folds of bedding and bedding-parallel fissility have axes that show the usual scatter along a girdle parallel to cleavage. Steep down-dip lineations occur in these rocks near the MFZ and show variable orientations in the hanging wall. Strain intensities also show a large jump across the fault, except in the Mt. Bullion volcanic sequence (Fig. 8).

We might consider alternative models of the MFZ at this stop. Paterson and others (1989) have argued that the MFZ represents a sharp discontinuity in rock types, structures, strains, and age of deformation, and a small break in grade of metamorphism, and thus represents a significant boundary in the WMB. In contrast, Schweickert and others (1984) argue that similar rock types and structures occur on both sides of the MFZ, and thus downplay the significance of this fault (presumably in part because they interpret the Sonora fault as the important Late Jurassic suture between Foothills and Calaveras assemblages).

Another alternative is that the Melones fault may have a two-part history of dip-slip movement: early movement occurred along the high-strain zone east of the Mt. Bullion sequence and formed the high strains in much of the Sullivan Creek volcanic sequence. Later movement, along the fault cutting the Mt. Bullion sequence, occurred during the Late Jurassic deformation in the eastern Foothills terrane.

38.9, 9.5 Return to Bear Valley and turn right (west) on Hornitos Rd. (J-16). Drive west through Mariposa Formation (first mile) and underlying Peñon Blanco volcanics.

41.7, 2.8 Stop in turnouts near roadcuts on both sides of road.

STOP 3-3 We are now near the southern end of the Peñon Blanco volcanic sequence, last seen at Stop 1-2 (Figs. 1, 9). The greenstones here largely consist of breccia and lapilli tuffs, tuffs, and some flows. Bogen (1984) has interpreted this volcanic sequence to be a large submarine volcanic center constructed on an oceanic basement and now folded into a large upright, southeast-plunging anticline. Both the nature of basement and of the overall structure of this unit are controversial.

Cleavage is absent except in fine-grained units near the margins of the volcanic pile. The nearest measured strains in lapilli tuffs are 9, 0, -9 (SI=0.13, LP=.07). Facing directions (usually to east), minor folds, and intersection lineations do not support the existence of a southeast-plunging anticline. Instead, these structures are more consistent with a locally folded, east-facing homoclinal sequence, or with a complexly folded, overturned anticline.

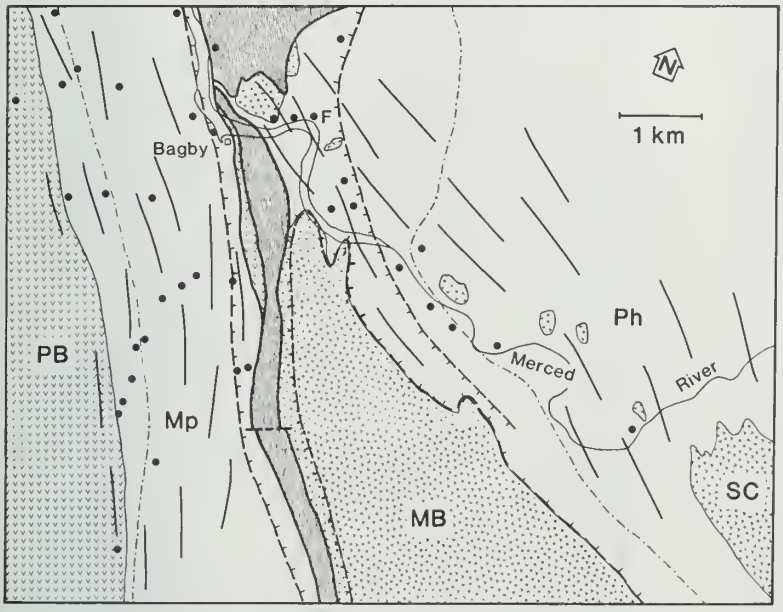

Figure 7. Bagby area; PB, Peñon Blanco volcanics; Mp, Mariposa Fm.; Um, ultramafic rocks; serpentinites, and other rock types along the Melones fault; MB, Mt. Bullion volcanic sequence; SC, Sullivan Creek volcanic sequence; Ph, phyllite and Calaveras-type lithologies. Black dots, locations of strain samples, trend lines show average strike of steep-dipping pervasive cleavage. Zone of high strain outlined by T symbols. F, locality of Late Triassic conodonts.

Continue west on Hornitos Rd. At base of hill (about 1.7 mi), we will pass into a compositionally and structurally heterogeneous group of rocks interpreted by us to be a melange belt subsequently deformed by movement in the BMFZ (Figs. 9, 10).

49.8, 7.9 This is the eastern edge of the highly deformed Hornitos Pluton.

51.5, 1.6 Stop on a small road that heads straight at sharp bend in main road.

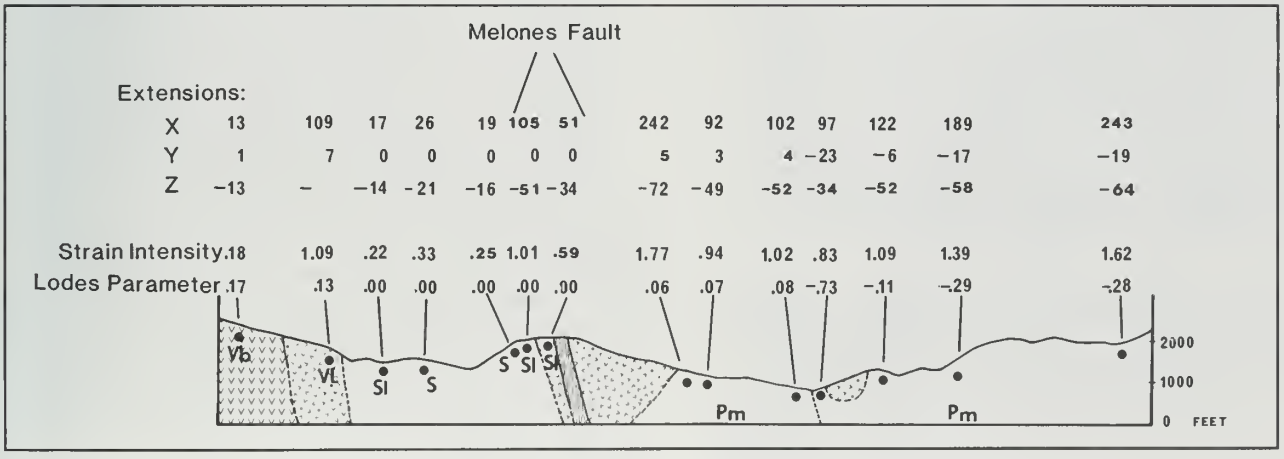

Figure 8. Strain profile of tectonic strains in Bagby area. Abbreviations and interpretations as in Fig. 6.

STOP 3-4 This stop is located in the northwest section of the Hornitos intrusive complex (HIC; Fig. 9). Nearby roadcuts and stream exposures show the compositional and structural heterogeneity displayed by this pluton. We will also examine highly deformed wall rocks exposed immediately to the west.

The HIC, located entirely within the BMFZ, is compositionally heterogeneous over short distances due to widespread mingling of magmas which produced elongate enclaves and discontinuous lensoid bodies. However, the western half of the pluton tends to be more felsic (tonalites to granites) than the eastern half (tonalites to gabbros). Where preserved, igneous structures and microstructures indicate that much of the pluton consists of numerous sills, some of which contained a magmatic foliation (aligned feldspars and mafic minerals). A U/Pb zircon age of 150 Ma and a $^{40}Ar/^{39}Ar$ age of 140 Ma from biotite were obtained for this pluton (Saleeby and others, 1989).

Most of the pluton is deformed, and particularly in the western half, displays folded mylonitic foliations and strong southeast-plunging stretching lineations. Metamorphic hornblende+ clinopyroxene is associated with this foliation, indicating initial high-temperature deformation. Conjugate shear zones occur sporadically in the Hornitos pluton and cut the older mylonitic foliation. These shear zones are associated with metamorphic assemblages indicating conditions of lower amphibolite to greenschist facies.

The mylonitic foliation is subparallel to the magmatic foliation and is typically continuous with foliations in the wall rock. No recognizable contact aureole is preserved around the HIC, although relict porphyroblasts do exist. These porphyroblasts show that cleavage developed both before, during, and after porphyroblast growth. We have interpreted the emplacement of this pluton as syntectonic with respect to cleavage development in the BMFZ.

Nearby wall rock structures are complex with several generations of folding visible. Pebbly mudstones record strains of 114, 12, -58 (SI=1.17, LP=.20). This strain and the multiple generations of structures are interpreted to reflect progressive deformation during movement along the BMFZ.

52.2, 0.7 Continue south on J-16 to Hornitos and turn right (west) on Merced Falls Rd. Hornitos is located on phyllites and graywackes in the BMFZ.

52.4, 0.4 Intensely cleaved greenschists of the Gopher Ridge volcanic sequence with local folds and crenulation cleavage.

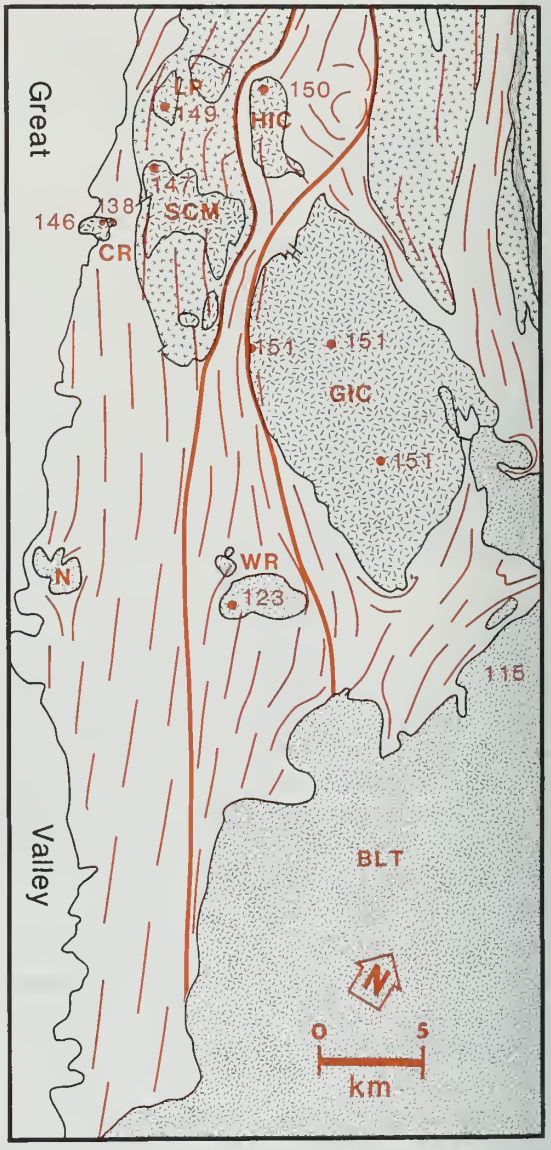

Figure 9. Generalized map of southern portions of the Foothills terrane. Random V pattern, volcanic rocks; clear area east of GVSe, Late Jurassic slate-graywacke sequences; thin dashes, average trend lines of pervasive cleavage; thick lines show borders of BMFZ. U/Pb zircon ages from Saleeby and others (1989) shown with black dots. Pluton abbreviations as follows: LP, La Paloma; HIC, Hornitos intrusive complex; SCM, Santa Cruz Mountain; CR, Courthouse Rock; N, Nora; GIC, Guadalupe igneous complex; WR, White Rock; BLT, Bass Lake tonalite.

55.2, 2.8 Here we enter the westernmost exposed slate-graywacke sequence, the Merced Falls slate of Clark (1964).

62.5, 7.3 Turn right towards McSwain Dam and Lake McClure and park near first road cuts.

STOP 3-5 This is the only exposure we will see of the westernmost exposed slate-graywacke belt, the Merced Falls slate of Clark (1964). The western contact of the Gopher Ridge sequence is about 0.5 mi east of here. Although the structures in these roadcuts look deceptively simple (one generation of folding and cleavage development), close inspection of these and nearby exposures show that multiple generations of folds do exist, similar to structures seen in the BMFZ. No fault has been mapped in this region. Instead, we suggest that shearing along the volcanic-metasedimentary contact caused the more complex structures seen here.

63, 0.5 Turn around and head west. Turn right on Merced Falls Rd.

74.2, 11.2 Turn left on Pepito Dr.

74.8, 0.6 Park near large rock to right of road.

STOP 3-6 At this stop and Stop 3-7, we will examine blocks of material in the BMFZ (Fig. 10; see also Miller and Paterson, 1991). Tectonic blocks within the BMFZ include metavolcanic rocks, ultramafic rocks, gabbros, diorites, amphibolites with uncertain protoliths, calc-silicate rocks, sandstones and sedimentary breccias. Sandstones, metavolcanic rocks, and many of the plutonic rocks in the fault zone may have counterparts in the adjacent eastern and western zones of the Foothills terrane, whereas the other blocks are exotic with respect to units presently exposed. Some of the exotic amphibolites are considerably higher grade than the sedimentary matrix in the central segment of the BMFZ.

Ultramafites, widely scattered throughout the BMFZ, range from a few meters to approximately 1.2 mi (2 km) in length. They are variably metamorphosed and commonly metasomatized; protoliths are thus difficult to ascertain. The ultramafic blocks vary considerably in fabric development,

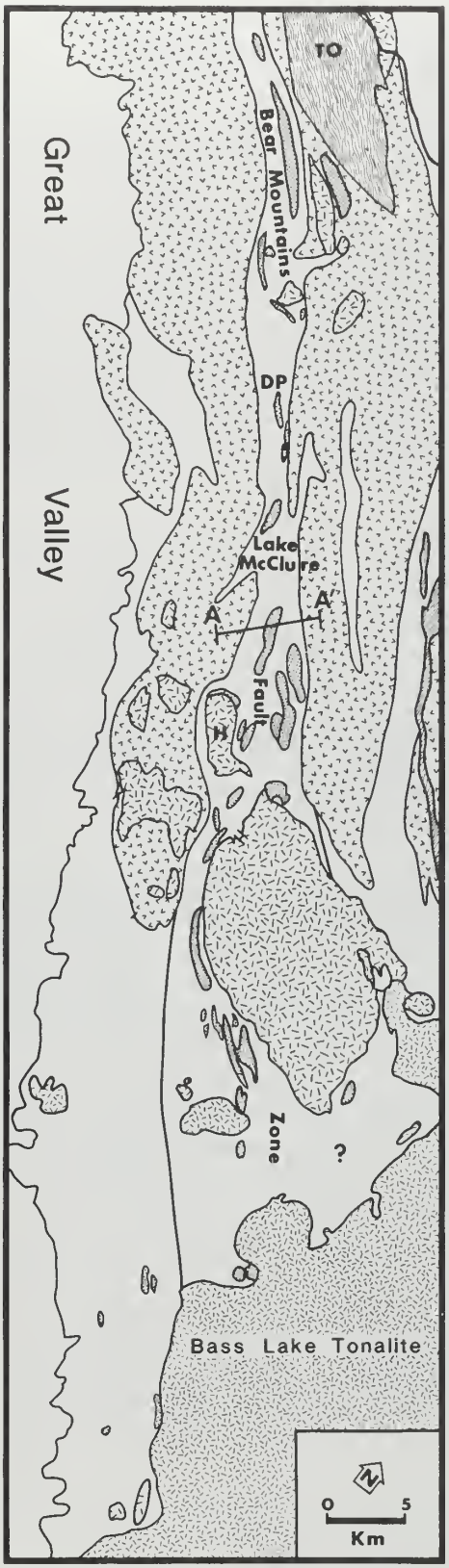

Figure 10. Distribution of blocks along the BMFZ. TO, Tuolumne ultramafic complex.

which in part reflect the changing metamorphic grade along strike within the BMFZ.

Clinopyroxene and hornblende gabbro blocks in the Pepito Dr. area occur as small (less than 33-ft, 10-m wide) pods within talc schists and serpentinites, which are themselves blocks within the fault zone. The gabbros are cut by numerous narrow (1 to 5 mm) cataclastic zones. Cleavage lamellae in clinopyroxenes have been spectacularly kinked and offset by microfaults. Low-temperature metamorphism accompanied this brittle deformation and is best marked by prehnite veins, uralitization of clinopyroxene and igneous hornblende, and saussuritization of plagioclase.

Distinctive volcaniclastic blocks in the Pepito Dr. area contain a variety of clasts which differ from those elsewhere in the fault zone. The most abundant clasts are diabases, displaying subophitic texture, and fine-grained gabbros. Other fragments include: trachytic volcanic rocks containing plagioclase and lesser clinopyroxene microphenocrysts; aphanitic basalts; rare felsite; and rare basalt showing variolitic texture suggestive of derivation from pillow lavas.

Amphibolites also are present in the northern fault where they show a sharp metamorphic break with the low-grade ultramafic, gabbro and metavolcanic blocks and the metasedimentary host rocks. The amphibolites, like the gabbros in this area, only occur as pods within the ultramafic blocks. These fine- to medium-grained amphibolites contain the assemblage blue-green (Z) hornblende-plagioclase-epidote-sphene ± garnet ± muscovite. Garnet is the only phase to form porphyroblasts. The amphibolites display a strong foliation marked by elongate hornblende, epidote, muscovite and sphene, and by compositional layering. Hornblende defines a lineation and also forms polygonal arcs in some samples. These microfolds include rounded crenulations and chevron structures. The amphibolites are well-recrystallized, but show retrograde alteration associated with widespread narrow cataclastic zones oriented at a high angle to foliation. Chloritization probably is synchronous with the veining in nearby gabbro blocks.

Several small (6-10 ft, 2-3 m wide) blocks of polymict sedimentary breccia are also encased in ultramafites in this area (Stop 3-7). Most clasts display foliation oriented at various angles to the foliation in the matrix, indicating that they were deformed prior to erosion. Amphibolite clasts dominate (>75 percent) and resemble the nearby tectonic blocks of amphibolite; most striking are distinctive micaceous amphibolites which occur both as clasts and tectonic blocks. Next in abundance are well-foliated impure quartzitic clasts which contain different combinations of garnet, hornblende and muscovite. Felsite is subordinate and chloritic schists and possible serpentinite are rare. The clastic matrix is dominated by amphibole.

Metamorphic assemblages and modes in the tectonic blocks provide evidence that these rocks were extensively infiltrated by metasomatic fluids. Most of the smaller ultramafic blocks were pervasively metasomatized. They commonly consist of the high-variance assemblage tremolite-chlorite, and nearly monomineralic tremolitic rocks are abundant in some blocks. Modes in some of the high-grade ultramafic blocks also suggest metasomatism. These include rocks which consist mainly of clinoamphibole and poikiloblastic enstatite, as well as significant amounts of aluminous green spinel and minor olivine. Furthermore, assemblages typical of isochemical amphibolite-facies metamorphism of ultramafites, such as forsterite-tremolite-talc, have not been recognized.

The Pepito Dr. area is perhaps best characterized as a slab of serpentinite melange enclosed within the metasedimentary matrix of the BMFZ. Overall, the blocks in this area comprise a broadly ophiolitic assemblage that is inferred to form the basement to the Foothills terrane according to Saleeby (1982) and Sharp (1988). The occurrence of ultramafites and gabbros is compatible with this suggestion, as is the presence of amphibolites. Amphibolite-facies metabasites in some of the ophiolite melanges are inferred to have formed in an oceanic fracture zone (Saleeby, 1982). Such a setting can explain the mixing of higher-grade rocks with weakly metamorphosed ones. The sandstones with abundant diabase clasts and the locally derived sedimentary breccias may have formed by deposition at the base of fault scarps in a fracture zone. This depositional setting accounts for the abundant amphibolite fragments and most

of the other clast types in the breccias. The impure quartzites are possibly siliceous sediments metamorphosed in the postulated transform zone.

Alternatively, the amphibolites which occur as tectonic blocks and the impure quartzites which were a source for the sedimentary breccias (see above) formed in a dynamothermal sole. This sole perhaps was correlative with that mapped beneath the Tuolumne ultramafic complex (Stop 1-2). In this interpretation, the sole subsequently was uplifted and eroded and then the entire assemblage was incorporated into serpentinite melange prior to the even later mixing with the sedimentary matrix in the BMFZ.

75.4, 0.6 Continue on Pepito Dr. to junction with Hwy. 132. Turn right and park immediately.

STOP 3-7 These low road cuts and nearby exposures show many of the metasedimentary breccias and blocks, and mafic and ultramafic materials described at the last stop. Given sufficient time, we will examine these materials and discuss possible scenarios for the BMFZ.

Turn around and head west on Hwy. 132. After about 2.1 mi, turn right on Bond's Flat Rd. Pass over Don Pedro Dam (5.9 mi) and turn right at junction with J-59 (8.1 mi). Go 19 mi and turn left on Hwy. 120/108. Return to San Francisco via Hwys 120 to Oakdale and Manteca, 205 to Livermore, 580 to Hayward and Oakland, and I-80 to SF.

REFERENCES CITED

Bateman, P.C., Harris, A.G., Kistler, R.W., and Krauskopf, K.B., 1985, Calaveras reversed: westward younging is indicated: *Geology*, v. 13, p. 338-341.

Bogen, N.L., 1984, Stratigraphic and sedimentologic evidence of a submarine island-arc volcano in the lower Mesozoic Peñon Blanco and Jasper Point Formations, Mariposa County, California: *Geological Society of America Bulletin*, v. 96, p. 1322-1331.

Bohlen, S.R., and Liotta, J.J., 1986, A barometer for garnet amphibolites and garnet granulites: *Journal of Petrology*, v. 27, p. 1025-1034.

Clark, L.D., 1964, Stratigraphy and structure of part of the western Sierra Nevada metamorphic belt, California: *U.S. Geological Survey Professional Paper 410*, 70p.

Coleman, R.G., 1981, Tectonic setting for ophiolite obduction in Oman: *Journal of Geophysical Research*, v. 86, p. 2497-2508.

Herzig, C.T., 1985, *Jurassic rocks east of the Melones fault zone, central Sierra Nevada foothills, California*: unpublished MS Thesis, State University of New York at Stony Brook, 88p.

Hossack, J.R., 1968, Pebble deformation and thrusting in the Bygdin area (Southern Norway): *Tectonophysics*, v. 5, p. 315-339.

Ingersoll, R.V., and Schweickert, R.A., 1986, A plate-tectonic model for ophiolite genesis, Nevadan orogeny, and forearc initiation, northern California: *Tectonics*, v. 5, p. 901-912.

Jamieson, R.A., 1981, Metamorphism during ophiolite emplacement-the petrology of the St. Anthony Complex: *Journal of Petrology*, v. 22, p. 397-449.

Leighton, C.W., 1986, *Geochronology and metamorphic petrology of amphibolite blocks, Sierra Nevada foothills, California:* unpublished MS Thesis, State University of New York at Stony Brook, 152p.

Miller, R.B. and Paterson, S.R., 1991, Geology and tectonic evolution of the Bear Mountains fault zone, Foothills terrane, central Sierra Nevada, CA: *Tectonics*, in press.

Morgan, B.A., 1976, Geologic map of the Chinese Camp and Moccasin quadrangles, Tuolumne County, California: *U.S. Geological Survey Miscellaneous Field Studies Map MF-840*, scale 1:24,000.

Paterson, S.R., 1989, Are syntectonic granites truly syntectonic? *EOS, Transactions*, American Geophysical Union, v. 70, p. 763-770.

Paterson, S.R., and Sample, J.C., 1988, The development of folds and cleavages in slate belts by underplating in accretionary complexes: a comparison of the Kodiak Formation Alaska, and the Calaveras Complex, California: *Tectonics*, v. 7, p. 859-874.

Paterson, S.R., Tobisch, O.T., and Bhattacharrya, T., 1989, Regional structural and strain analyses of terranes in the Western Metamorphic belt, central Sierra Nevada, California: *Journal of Structural Geology*, v. 11, p. 255-273.

Paterson, S.R., Tobisch, O.T., and
Emplacement and deformatio
volcanic arc construction in th
central Sierra Nevada, Califor
press.

Saleeby, Jason B., 1982, Polygenet
California Sierra Nevada: geoc
ostratigraphic development: *Jo*
Research, v. 87, no. B3, p. 180

Saleeby, J.B., and others, 1986, Exp
continent-ocean transect, Corri
nia offshore to Colorado platea
America Centennial Continent-

Saleeby, J.B., Geary, E.E., Paterson,
O.T., 1989, Isotopic systematics
$^{40}Ar/^{39}Ar$ (biotite/hornblende) fr
Foothills terrane, Sierra Nevada
Society of America Bulletin, v.

Schweickert, R.A., and Bogen, N.L.,
transect of Sierran Paleozoic thr
belts: Pacific Section, Society of
gists and Mineralogists Guidebo

...n, N.L., Girty, G.H., Hanson, R.E.,
..., 1984, Timing and expression of the
...ierra Nevada, California: *Geologi-*
...*ca Bulletin*, v. 95, p. 967-979.

...uerian, C., and Bogen, N.L., 1988,
...metamorphic history of Paleozoic
...nent terranes in the western Sierra
... Ernst, W.G., ed., *Metamorphism*
...*n of the western United States*:
York, p. 789-822.

...Cretaceous crustal evolution in the
..., California, in Ernst, W.G., ed.,
...*rustal evolution of the western*
...ce-Hall, New York, p. 823-864.

...C., Morgan, B.A., Newell, M.F.,
..., Isotopic U-Pb ages of zircon
...the central Sierra Nevada,
...*ogical Survey Professional Paper*

...S.R., Saleeby, J.B., and Geary, E.
...timing of deformation in the
...tral Sierra Nevada, California; its
...s: *Geological Society of America*
...1-413.